

**SYNTHESIS AND CHARACTERIZATION OF PHENYLENE-  
BASED DICATIONIC IONIC LIQUIDS**

**MUNIRAH SUFIYAH ABD RAHIM**

**DISSERTATION SUBMITTED IN FULFILMENT OF THE  
REQUIREMENTS FOR THE DEGREE OF MASTER OF  
SCIENCE**

**DEPARTMENT OF CHEMISTRY  
FACULTY OF SCIENCE  
UNIVERSITY OF MALAYA  
KUALA LUMPUR**

**2012**

## ABSTRACT

Dicationic ionic liquids are being developed and are found to have better properties than common room temperature ionic liquids. By comparison, they possess higher melting temperature, wider electrochemical window and stronger ionic conductivity rather than RTILs. Previous reports suggest that dicationic ionic liquids have potential applications as solvent in organic synthesis, dye sensitized solar cells, phase transfer catalyst, lubricants, surfactants and as a stationary phase in gas liquids chromatography column. Eight series of dicationic ionic liquids were successfully synthesized by reacting  $\alpha,\alpha$ -dibromo-p-xylene with tertiary amines (pyridine, 1-methylpyrrolidine, 1-butylpyrrolidine, triethylamine, 1-methylpiperidine, 1-methylmorpholine, *N,N*-dimethylethanoamine and *N,N*-diethylethanoamine) at the 1,4-position, forming symmetrical cations with bromide, hexafluorophosphate and bis(trifluoromethanesulfonyl)imide as the counter-anions. Dicationic ionic liquids were successfully synthesized with yield of more than 85%, through conventional methods (quaternization reaction followed by anion exchange). Counter-anion plays an important role in determining thermal properties of dicationic ionic liquids. Bromide moieties have poorer thermal stability compared with hexafluorophosphate moieties. On the other hand, bis(trifluoromethanesulfonyl)imide moieties are the most thermally stable dicationic ionic liquids while having the lowest melting point. Few bis(trifluoromethanesulfonyl)imide salts melt at temperature below 100°C which is in good agreement with the definition of ionic liquids. All dicationic ionic liquids appear as solid at ambient temperature and were purified through recrystallization with an appropriate solvent. Upon recrystallization, nine dicationic ionic liquids afforded single crystal suitable for X-ray crystallography.

measurement. The molecular structure of crystals are solved, refined, and found to be in good agreement with the expected structures. Based on the chromatographic analysis, hexafluorophosphate and bis(trifluoromethanesulfonyl)imide moieties have extremely low bromide and water content.

## ABSTRAK

Cecair ionik dwikation telah dikaji dan ia didapati mempunyai ciri-ciri yang lebih baik daripada cecair-cecair ionik yang biasa. Jika dibanding dengan cecair-cecair ionik monokation, cecair ionik dwikation mempunyai takat lebur yang lebih tinggi, keupayaan elektrokimia yang lebih lebar dan konduktiviti ion yang lebih kuat. Hasil penyelidikan yang terdahulu mendapati bahawa cecair ionik dwikation mempunyai potensi sebagai pelarut dalam sintesis organik, sel solar peka-pewarna, pemangkin fasa pemindahan, bahan pelincir, surfaktan dan sebagai fasa pegun dalam turus kromatografi cecair-gas. Lapan siri cecair ionik dwikation telah berjaya dihasilkan daripada tindakbalas kimia antara  $\alpha,\alpha$ -dibromo-p-xilena dan 3° amina seperti piridina, 1-metilpirolidina, 1-butilpirolidina, trietilamina, 1-metilpiperidina, 1-metilmorfolina, N,N-dimetiletanolamina dan N,N-dietiletanolamina pada posisi 1,4-, membentuk satu molekul kation yang simetri manakala ion-ion seperti bromida, heksafluorofosfat dan bis(trifluorometansulfonil)imida bertindak sebagai pasangan anion. Teknik konvensional telah digunakan untuk mensintesis cecair ionik dwikation dan berjaya menghasilkan garam organik yang sangat tulen dengan peratusan hasil melebihi 85 %. Anion memainkan peranan yang penting dalam menentukan sifat-sifat termal bagi cecair ionik dwikation. Rangkaian garam bromida mempunyai kestabilan terhadap haba yang paling rendah diikuti oleh rangkaian garam heksafluorofosfat. Sebaliknya, rangkaian garam bis(trifluorometansulfonil)imida pula mempunyai kestabilan terhadap haba yang paling baik di samping mempunyai takat lebur yang paling rendah berbanding dua rangkaian garam lain. Tambahan lagi, beberapa garam organik bis(trifluorometansulfonil)imida melebur pada suhu di bawah 100 °C justeru mematuhi ciri-ciri penting sebagai cecair ionik.



Kesemua cecair ionik dwikation ini wujud sebagai pepejal pada suhu bilik. Oleh itu, cara terbaik untuk menuliskan garam-garam organik ini ialah melalui penghabluran semula menggunakan pelarut organik yang sesuai. Berdasarkan keputusan analisa kromatografi, garam bis(trifluorometansulfonil)imida dan hexafluorofosfat mempunyai kandungan bromida dan air yang sangat rendah. Hasil dari proses penghabluran semula, sembilan garam telah berjaya membentuk hablur tunggal yang sesuai untuk analisa menggunakan teknik kristalografi sinar X. Hasil uji kaji telah mendapati bahawa hablur-hablur tersebut mempunyai struktur-struktur molekul seperti yang dijangka.

## ACKNOWLEDGEMENTS

First of all, I would like to express my greatest gratitude to The Almighty God for giving me the will to further my studies and for blessing me with good health throughout my research.

A special thank goes to my lovely parents and family for their warm support and understanding during the hardest time.

I wish to express my sincere thanks to Prof Yatimah Alias for her guidance and thoughtful supervision during the three years of my research and the completion of this thesis.

I would also like to thank Prof Urs Welz-Biermann for giving me the opportunity to work in China Ionic Liquids Laboratory (CHILL), Dalian for the duration of two months.

A warm thank also goes to my colleagues in D220 laboratory for providing me a good working atmosphere as well as their kind assistance throughout the duration of my study.

I would also like to acknowledge University of Malaya for providing the scholarship and funding from grant PPP 383/2010B.

Lastly, I wish to express my grateful thanks to all my dear friends for sharing their knowledge, advices as well as encouragement during the duration of my course. I will never forget the precious time we spent together during our joy and sorrow.

## Table of Contents

ABSTRACT .....	ii
ABSTRAK .....	iv
ACKNOWLEDGEMENT .....	vi
TABLE OF CONTENT .....	vii
LIST OF FIGURES .....	ix
LIST OF TABLES.....	xiv
LIST OF SYMBOLS AND ABBREVIATIONS.....	xvii
LIST OF SYNTHESIZED DICATIONIC IONIC LIQUIDS .....	xviii
CHAPTER 1: INTRODUCTION.....	1
1.1 Introduction to Ionic Liquids.....	1
1.2 The Importance of Study.....	3
1.3 The Scope of Research.....	5
1.4 The Objectives of Research.....	7
The Outline of Thesis.....	8
CHAPTER 2: LITERATURE REVIEWS .....	10
2.1 Introduction of Ionic Liquids.....	10
2.2 Synthesis of Ionic Liquids.....	15
2.3 Purification of Ionic Liquids .....	18
2.4 Functionalized Ionic Liquids.....	23
2.5 Introduction to Dicationic Ionic Liquids.....	24
2.6 Applications of Dicationic Ionic Liquids.....	25
2.6.1 Dicationic ionic liquids as a solvent .....	25
2.6.2 Dicationic ionic liquids as a surfactant .....	27
2.6.3 Dicationic ionic liquids as a lubricant.....	30
2.6.4 Dicationic ionic liquids in chemical separation and extraction.....	32
2.6.5 Dicationic ionic liquids as a catalyst.....	34
2.6.6 Dicationic ionic liquids in dye sensitized solar cell.....	36
2.6.7 Dicationic ionic liquids in self-assembly chemistry.....	38

CHAPTER 3 : EXPERIMENTAL PROCEDURES .....	40
3.1 Chemicals .....	40
3.2 Instrumentations.....	40
3.3 Synthesis Section .....	43
3.3.1 Preparation and characterization of bromide salts .....	43
3.3.2 Preparation and characterization of bis(trifluoromethanesulfonyl)imide salts (NTf <sub>2</sub> <sup>-</sup> ) .....	48
3.3.3 Preparation and characterization of hexafluorophosphate salts (PF <sub>6</sub> <sup>-</sup> ).....	53
 CHAPTER 4 : RESULTS AND DISCUSSIONS .....	 57
4.1 : <i>N,N'</i> -[1,4-Phenylenebis(methylene)]dipyridinium series .....	58
4.2: <i>N,N'</i> -[1,4-Phenylenebis(methylene)]bis( <i>N,N</i> -diethylethanaminium) series .....	69
4.3 : <i>N,N'</i> -[1,4-Phenylenebis(methylene)]bis( <i>N,N</i> -dimethylpyrrolinium) series .....	78
4.4 : <i>N,N'</i> -[1,4-Phenylenebis(methylene)]bis( <i>N,N</i> -dibutylpyrrolinium) series.....	89
4.5 : <i>N,N'</i> -[1,4-Phenylenebis(methylene)]bis( <i>N,N</i> -dimethylpiperidinium) series .....	98
4.6 : <i>N,N'</i> -[1,4-Phenylenebis(methylene)]bis( <i>N,N</i> -dimethylmorpholinium) series ..	109
4.7 : <i>N,N'</i> -[1,4-Phenylenebis(methylene)]bis( <i>N,N</i> -dimethyl-(2-hydroxy)ethanaminium) series .....	118
4.8 : <i>N,N'</i> -[1,4-Phenylenebis(methylene)]bis( <i>N,N</i> -dibutyl-(2-hydroxy) ethanaminium) series .....	124
4.9 : Thermal Properties of Dicationic Ionic Liquids .....	130
4.10 : Fourier-Transform Infra Red Spectroscopy .....	158
4.11 : Elemental Analyses .....	161
4.12 : Halides Analysis .....	164
4.13 : Solubility in Solvents .....	166
4.14 : Application : Self Assembly Chemistry of [Tea] <sup>2+</sup> .2[Br] with <i>p</i> -Sulfonatocalix[4]arene.....	169
 CHAPTER 5 : CONCLUSION .....	 172
REFERENCES .....	174
LIST OF PUBLICATIONS .....	182
CONFERENCES AND PROCEEDINGS .....	183
APPENDICES .....	184

## List of Figures:

Figure 2.01 : Common synthesis pathway for the preparation of ionic liquids exemplified for an ammonium salt .....	15
Figure 2.02 : The type of monocationic ionic liquids and analogous dicationic ionic liquids studied for analytes partitioning behavior and their critical micelle concentrations (CMC) values .....	28
Figure 4.01 : $^1\text{H}$ NMR spectrum of $[\text{Pyr}]^{2+}.2[\text{Br}]^-$ .....	59
Figure 4.02 : $^1\text{H}$ NMR spectrum of $[\text{Pyr}]^{2+}.2[\text{NTf}_2]^-$ .....	59
Figure 4.03 : $^1\text{H}$ NMR spectrum of $[\text{Pyr}]^+.2[\text{PF}_6]^-$ .....	60
Figure 4.04 : $^{13}\text{C}$ NMR spectrum of $[\text{Pyr}]^{2+}.2[\text{Br}]^-$ .....	62
Figure 4.05 : $^{13}\text{C}$ NMR spectrum of $[\text{Pyr}]^{2+}.2[\text{NTf}_2]^-$ .....	62
Figure 4.06 : $^{13}\text{C}$ NMR spectrum of $[\text{Pyr}]^{2+}.2[\text{PF}_6]^-$ .....	63
Figure 4.07 : Thermal ellipsoid plot of compound $[\text{Pyr}]^{2+}.2[\text{NTf}_2]^-$ at the 70% probability level; hydrogen atoms are drawn as spheres of arbitrary radius. Symmetry-related atoms are not labeled.....	64
Figure 4.08 : $[\text{Pyr}]$ cation moiety in compound $[\text{Pyr}]^{2+}.2[\text{NTf}_2]^-$ .....	65
Figure 4.10 : Thermal ellipsoid plot of compound $[\text{Pyr}]^{2+}.2[\text{PF}_6]^-$ at the 70% probability level, hydrogen atoms are drawn as spheres of arbitrary radius.....	66
Figure 4.11 : $[\text{Pyr}]$ cation moiety in compound $[\text{Pyr}]^{2+}.2[\text{PF}_6]^-$ .....	67
Figure 4.12 : $^1\text{H}$ NMR spectrum of $[\text{Tea}]^{2+}.2[\text{Br}]^-$ .....	70
Figure 4.13 : $^1\text{H}$ NMR spectrum of $[\text{Tea}]^{2+}.2[\text{NTf}_2]^-$ .....	70
Figure 4.14 : $^1\text{H}$ NMR spectrum of $[\text{Tea}]^{2+}.2[\text{PF}_6]^-$ .....	71
Figure 4.15 : $^{13}\text{C}$ NMR spectrum of $[\text{Tea}]^{2+}.2[\text{Br}]^-$ .....	72
Figure 4.16 : $^{13}\text{C}$ NMR spectrum of $[\text{Tea}]^{2+}.2[\text{NTf}_2]^-$ .....	73
Figure 4.17 : $^{13}\text{C}$ NMR spectrum of $[\text{Tea}]^{2+}.2[\text{PF}_6]^-$ .....	73
Figure 4.18 : Molecular structure of the compound $[\text{Tea}]^{2+}.2[\text{Br}]^-$ with displacement ellipsoids drawn at 50% probability level. Hydrogen atoms are drawn as spheres at arbitrary radius.....	75
Figure 4.19 : $[\text{TEA}]$ cation moiety in compound $[\text{Tea}]^{2+}.2[\text{Br}]^-$ .....	76
Figure 4.20 : $^1\text{H}$ NMR spectrum of $[\text{Mpyl}]^{2+}.2[\text{Br}]^-$ .....	79
Figure 4.21 : $^1\text{H}$ NMR spectrum of $[\text{Mpyl}]^{2+}.2[\text{NTf}_2]^-$ .....	79
Figure 4.22 : $^1\text{H}$ NMR spectrum of $[\text{Mpyl}]^{2+}.2[\text{PF}_6]^-$ .....	80
Figure 4.23 : $^{13}\text{C}$ NMR spectrum of $[\text{Mpyl}]^{2+}.2[\text{Br}]^-$ .....	82
Figure 4.24 : $^{13}\text{C}$ NMR spectrum of $[\text{Mpyl}]^{2+}.2[\text{NTf}_2]^-$ .....	82
Figure 4.25 : $^{13}\text{C}$ NMR spectrum of $[\text{Mpyl}]^{2+}.2[\text{PF}_6]^-$ .....	83

Figure 4.26 : Molecular structure of the compound $[\text{Mpyl}]^{2+}.2[\text{Br}]^-$ with displacement ellipsoids drawn at 50% probability level. Hydrogen atoms are drawn as spheres at arbitrary radius. ....	84
Figure 4. 27 : $[\text{Mpyl}]$ cation moiety in compound $[\text{Mpyl}]^{2+}.2[\text{Br}]^-$ .....	85
Figure 4.28 : Molecular structure of the compound $[\text{Mpyl}]^{2+}.2[\text{NTf}_2]^-$ with displacement ellipsoids drawn at 50% probability level. Hydrogen atoms are drawn as spheres at arbitrary radius. ....	86
Figure 4.29 : $[\text{Mpyl}]$ cation moiety in compound $[\text{Mpyl}]^{2+}.2[\text{NTf}_2]^-$ .....	87
Figure 4.30 : $^1\text{H}$ NMR spectrum of $[\text{Bpyl}]^{2+}.2[\text{Br}]^-$ .....	90
Figure 4.31 : $^1\text{H}$ NMR spectrum of $[\text{Bpyl}]^{2+}.2[\text{NTf}_2]^-$ .....	90
Figure 4.32 : $^1\text{H}$ NMR spectrum of $[\text{Bpyl}]^{2+}.2[\text{PF}_6]^-$ .....	91
Figure 4.33 : $^{13}\text{C}$ NMR spectrum of $[\text{Bpyl}]^{2+}.2[\text{Br}]^-$ .....	93
Figure 4.34 : $^{13}\text{C}$ NMR spectrum of $[\text{Bpyl}]^{2+}.2[\text{NTf}_2]^-$ .....	93
Figure 4.35 : $^{13}\text{C}$ NMR spectrum of $[\text{Bpyl}]^{2+}.2[\text{PF}_6]^-$ .....	94
Figure 4.36 : Molecular structure of the compound $[\text{Bpyl}]^{2+}.2[\text{PF}_6]^-$ with displacement ellipsoids drawn at 50% probability level. Hydrogen atoms are drawn as spheres at arbitrary radius.....	95
Figure 4.37 : $[\text{Bpyl}]$ cation moiety in compound $[\text{Bpyl}]^{2+}.2[\text{PF}_6]^-$ .....	96
Figure 4.38 : $^1\text{H}$ NMR spectrum of $[\text{Nmpp}]^{2+}.2[\text{Br}]^-$ .....	99
Figure 4.39 : $^1\text{H}$ NMR spectrum of $[\text{Nmpp}]^{2+}.2[\text{NTf}_2]^-$ .....	99
Figure 4.40 : $^1\text{H}$ NMR spectrum of $[\text{Nmpp}]^{2+}.2[\text{PF}_6]^-$ .....	100
Figure 4.41 : $^{13}\text{C}$ NMR spectrum of $[\text{Nmpp}]^{2+}.2[\text{Br}]^-$ .....	102
Figure 4.42 : $^{13}\text{C}$ NMR spectrum of $[\text{Nmpp}]^{2+}.2[\text{NTf}_2]^-$ .....	102
Figure 4.43 : $^{13}\text{C}$ NMR spectrum of $[\text{NMPP}]^{2+}.2[\text{PF}_6]^-$ .....	103
Figure 4.44 : Molecular structure of the compound $[\text{Nmpp}]^{2+}.2[\text{Br}]^-$ with displacement ellipsoids drawn at 50% probability level. Hydrogen atoms are drawn as spheres at arbitrary radius. ....	104
Figure 4. 45 : $[\text{Nmpp}]$ cation moiety in compound $[\text{Nmpp}]^{2+}.2[\text{Br}]^-$ .....	105
Figure 4.46 : Molecular structure of the compound $[\text{Nmpp}]^{2+}.2[\text{NTf}_2]^-$ with displacement ellipsoids drawn at 50% probability level. Hydrogen atoms are drawn as spheres at arbitrary radius .....	106
Figure 4.47 : $[\text{Nmpp}]$ cation moiety in compound $[\text{Nmpp}]^{2+}.2[\text{NTf}_2]^-$ .....	107
Figure 4.48 : $^1\text{H}$ NMR spectrum of $[\text{Mmorp}]^{2+}.2[\text{Br}]^-$ .....	110
Figure 4.49 : $^1\text{H}$ NMR spectrum of $[\text{Mmorp}]^{2+}.2[\text{NTf}_2]^-$ .....	110
Figure 4.50 : $^1\text{H}$ NMR spectrum of $[\text{Mmorp}]^{2+}.2[\text{PF}_6]^-$ .....	111
Figure 4.51 : $^{13}\text{C}$ NMR spectrum of $[\text{Mmorp}]^{2+}.2[\text{Br}]^-$ .....	113

Figure 4.52 : $^{13}\text{C}$ NMR spectrum of $[\text{Mmorp}]^{2+} \cdot 2[\text{NTf}_2]^-$ .....	113
Figure 4.53 : $^{13}\text{C}$ NMR spectrum of $[\text{Mmorp}]^{2+} \cdot 2[\text{PF}_6]^-$ .....	114
Figure 4.54 : Molecular structure of the compound $[\text{Mmorp}]^{2+} \cdot 2[\text{NTf}_2]^-$ with displacement ellipsoids drawn at 50% probability level. Hydrogen atoms are drawn as spheres at arbitrary radius. ....	115
Figure 4. 55 : $[\text{Mmorp}]$ cation moiety in compound $[\text{Mmorp}]^{2+} \cdot 2[\text{NTf}_2]^-$ .....	116
Figure 4.56 : $^1\text{H}$ NMR spectrum of $[\text{Dmae}]^{2+} \cdot 2[\text{Br}]^-$ .....	119
Figure 4.57 : $^1\text{H}$ NMR spectrum of $[\text{Dmae}]^{2+} \cdot 2[\text{NTf}_2]^-$ .....	119
Figure 4.58 : $^1\text{H}$ NMR spectrum of $[\text{Dmae}]^{2+} \cdot 2[\text{PF}_6]^-$ .....	120
Figure 4.59 : $^{13}\text{C}$ NMR spectrum of $[\text{Dmae}]^{2+} \cdot 2[\text{Br}]^-$ .....	122
Figure 4.60 : $^{13}\text{C}$ NMR spectrum of $[\text{Dmae}]^{2+} \cdot 2[\text{NTf}_2]^-$ .....	122
Figure 4.61 : $^{13}\text{C}$ NMR spectrum of $[\text{Dmae}]^{2+} \cdot 2[\text{PF}_6]^-$ .....	123
Figure 4.62 : $^1\text{H}$ NMR spectrum of $[\text{Deae}]^{2+} \cdot 2[\text{Br}]^-$ .....	125
Figure 4.63 : $^1\text{H}$ NMR spectrum of $[\text{Deae}]^{2+} \cdot 2[\text{NTf}_2]^-$ .....	125
Figure 4.64 : $^1\text{H}$ NMR spectrum $[\text{Deae}]^{2+} \cdot 2[\text{PF}_6]^-$ .....	126
Figure 4.65 : $^{13}\text{C}$ NMR spectrum of $[\text{Deae}]^{2+} \cdot 2[\text{Br}]^-$ .....	128
Figure 4.66 : $^{13}\text{C}$ NMR spectrum of $[\text{Deae}]^{2+} \cdot 2[\text{NTf}_2]^-$ .....	128
Figure 4.67 : $^{13}\text{C}$ NMR spectrum of $[\text{Deae}]^{2+} \cdot 2[\text{PF}_6]^-$ .....	129
Figure 4.68 : TGA curves of $N,N'$ -[(1,4-diphenylenebis(methylene)]dipyridinium series; Br, $\text{NTf}_2$ and $\text{PF}_6$ .....	131
Figure 4.69 : DSC plot of $[\text{Pyr}]^+ \cdot 2[\text{Br}]^-$ .....	132
Figure 4.70 : DSC plot of $[\text{Pyr}]^+ \cdot 2[\text{NTf}_2]^-$ .....	132
Figure 4.71 : DSC plot of $[\text{Pyr}]^+ \cdot 2[\text{PF}_6]^-$ .....	132
Figure 4.72 : TGA curves of $N,N'$ -[1,4-phenylenebis(methylene)]bis( $N,N$ -diethylethanaminium) series; Br, $\text{NTf}_2$ and $\text{PF}_6$ . ....	133
Figure 4.73 : DSC plot of $[\text{Tea}]^+ \cdot 2[\text{Br}]^-$ .....	134
Figure 4.74 : DSC plot of $[\text{Tea}]^+ \cdot 2[\text{NTf}_2]^-$ .....	135
Figure 4.75 : DSC plot of $[\text{Tea}]^+ \cdot 2[\text{PF}_6]^-$ .....	135
Figure 4.76 : TGA curves of $N,N'$ -[1,4-Phenylenebis(methylene)]bis-( $N,N$ -dimethylpyrrolinium) series; Br, $\text{NTf}_2$ and $\text{PF}_6$ .....	136
Figure 4.77 : DSC plot of $[\text{Mpyl}]^+ \cdot 2[\text{Br}]^-$ .....	137
Figure 4.78 : DSC plot of $[\text{Mpyl}]^+ \cdot 2[\text{NTf}_2]^-$ .....	138
Figure 4.79 : DSC plot of $[\text{Mpyl}]^+ \cdot 2[\text{PF}_6]^-$ .....	138

Figure 4.80 : TGA curves of <i>N,N'</i> -[1,4-Phenylenebis(methylene)]bis-( <i>N,N</i> -dibutylpyrrolinium) series; Br, NTf <sub>2</sub> and PF <sub>6</sub> .....	139
Figure 4.81 : DSC plot of [Bpyl] <sup>+</sup> .2[Br] <sup>-</sup> .....	140
Figure 4.82 : DSC plot of [Bpyl] <sup>+</sup> .2[NTf <sub>2</sub> ] <sup>-</sup> .....	141
Figure 4.83 : DSC plot of [Bpyl] <sup>+</sup> .2[PF <sub>6</sub> ] <sup>-</sup> .....	141
Figure 4.84 : TGA curves of <i>N,N'</i> -[1,4-phenylenebis(methylene)]bis-( <i>N,N</i> -dimethylpiperidinium) series; Br, NTf <sub>2</sub> and PF <sub>6</sub> .....	142
Figure 4.85 : DSC plot of [Nmpp] <sup>+</sup> .2[Br] <sup>-</sup> .....	143
Figure 4.86 : DSC plot of [Nmpp] <sup>+</sup> .2[NTf <sub>2</sub> ] <sup>-</sup> .....	144
Figure 4.87 : DSC plot of [Nmpp] <sup>+</sup> .2[PF <sub>6</sub> ] <sup>-</sup> .....	144
Figure 4.88 : TGA curves of <i>N,N'</i> -[1,4-phenylenebis(methylene)]bis-( <i>N,N</i> -dimethylmorpholinium) series; Br, NTf <sub>2</sub> and PF <sub>6</sub> .....	145
Figure 4.89 : DSC plot of [Mmorp] <sup>+</sup> .2[Br] <sup>-</sup> .....	146
Figure 4.90 : DSC plot of [Mmorp] <sup>+</sup> .2[NTf <sub>2</sub> ] <sup>-</sup> .....	147
Figure 4.91 : DSC plot of [Mmorp] <sup>+</sup> .2[PF <sub>6</sub> ] <sup>-</sup> .....	147
Figure 4.92 : TGA curves of <i>N,N'</i> -[1,4-phenylenebis(methylene)]bis-( <i>N,N</i> -dimethyl-(2-hydroxy) ethanaminium) series; Br, NTf <sub>2</sub> and PF <sub>6</sub> .....	148
Figure 4.93 : DSC plot of [Dmae] <sup>+</sup> .2[Br] <sup>-</sup> .....	149
Figure 4.94 : DSC plot of [Dmae] <sup>+</sup> .2[NTf <sub>2</sub> ] <sup>-</sup> .....	150
Figure 4.95 : DSC plot of [Dmae] <sup>+</sup> .2[PF <sub>6</sub> ] <sup>-</sup> .....	150
Figure 4.96 : TGA curves of <i>N,N'</i> -[1,4-phenylenebis(methylene)]bis-( <i>N,N</i> -dibutyl-(2-hydroxy) ethanaminium) series; Br, NTf <sub>2</sub> and PF <sub>6</sub> .....	151
Figure 4.97 : DSC plot of [Deae] <sup>2+</sup> .2[Br] <sup>-</sup> .....	152
Figure 4.98 : DSC plot of [Deae] <sup>2+</sup> .2[NTf <sub>2</sub> ] <sup>-</sup> .....	153
Figure 4.99 : DSC plot of [Deae] <sup>2+</sup> .2[PF <sub>6</sub> ] <sup>-</sup> .....	153
Figure 4.100 : TGA curves of bromide salts moieties. ....	155
Figure 4.101: TGA curves of bis(trifluoromethanesulfonyl)imide salts moieties. ...	156
Figure 4.102 : TGA curves of hexafluorophosphate salts moieties. ....	157
Figure 4.103 : The components and ‘molecular capsule’ arrangement in complex <b>1</b> and complex <b>2</b> .....	169
Figure 4.104 : Front and side view of the 1,4-bis(triethylammoniomethyl)benzene cation (space filling) shrouded at the termini by two <i>p</i> -sulfonatocalix[4]arenes.....	170



Figure 4.105 :  $^1\text{H}$  NMR spectra for (a) bis-triethylammonium, and (b) bis-triethylammonium in *p*-sulfonatocalix[4]arene (1:2), measured in  $\text{D}_2\text{O}$ .....171

## List of Tables:

Table 4.01 : $^1\text{H}$ NMR spectral data of $[\text{Pyr}]^{2+} \cdot 2[\text{A}]^-$ .....	60
Table 4.02 : $^{13}\text{C}$ NMR spectral data of $[\text{Pyr}]^{2+} \cdot 2[\text{A}]^-$ .....	63
Table 4.03 : Crystal data and structure refinements of $[\text{Pyr}]^{2+} \cdot 2[\text{NTf}_2]^-$ and $[\text{Pyr}]^{2+} \cdot 2[\text{PF}_6]^-$ .....	68
Table 4.04 : $^1\text{H}$ NMR spectral data of $[\text{Tea}]^{2+} \cdot 2[\text{A}]^-$ .....	71
Table 4.05 : $^{13}\text{C}$ NMR spectral data of $[\text{Tea}]^{2+} \cdot 2[\text{A}]^-$ .....	74
Table 4.06 : Crystal data and structure refinements of $[\text{Tea}]^{2+} \cdot 2[\text{Br}]^-$ .....	77
Table 4.07 : $^1\text{H}$ NMR spectral data of $[\text{Mpyl}]^{2+} \cdot 2[\text{A}]^-$ .....	80
Table 4.08 : $^{13}\text{C}$ NMR spectral data of $[\text{Mpyl}]^{2+} \cdot 2[\text{A}]^-$ .....	83
Table 4.09 : Crystal data and structure refinements of $[\text{Mpyl}]^{2+} \cdot 2[\text{A}]^-$ series.....	88
Table 4.10 : $^1\text{H}$ NMR spectral data of $[\text{Bpyl}]^{2+} \cdot 2[\text{A}]^-$ .....	91
Table 4.11 : $^{13}\text{C}$ NMR spectral data of $[\text{Bpyl}]^{2+} \cdot 2[\text{A}]^-$ .....	94
Table 4.12 : Crystal data and structural refinements of $[\text{Bpyl}]^{2+} \cdot 2[\text{PF}_6]^-$ .....	97
Table 4.13 : $^1\text{H}$ NMR spectral data of $[\text{Nmpp}]^{2+} \cdot 2[\text{A}]^-$ .....	100
Table 4.14 : $^{13}\text{C}$ NMR spectral data of $[\text{Nmpp}]^{2+} \cdot 2[\text{A}]^-$ .....	103
Table 4.15 : Crystal data and structure refinements of $[\text{Nmpp}]^{2+} \cdot 2[\text{A}]^-$ series .....	108
Table 4.16 : $^1\text{H}$ NMR spectral data of $[\text{Mmorp}]^{2+} \cdot 2[\text{A}]^-$ .....	111
Table 4.17 : $^{13}\text{C}$ NMR spectral data of $[\text{Mmorp}]^{2+} \cdot 2[\text{A}]^-$ .....	114
Table 4.18 : Crystal data and structure refinements of $[\text{Mmorp}]^{2+} \cdot 2[\text{NTf}_2]^-$ .....	117
Table 4.19 : $^1\text{H}$ NMR spectral data of $[\text{Dmae}]^{2+} \cdot 2[\text{A}]^-$ .....	120
Table 4.20 : $^{13}\text{C}$ NMR spectral data of $[\text{Dmae}]^{2+} \cdot 2[\text{A}]^-$ .....	123
Table 4.21 : $^1\text{H}$ NMR spectral data of $[\text{Deae}]^{2+} \cdot 2[\text{A}]^-$ .....	126
Table 4.22 : $^{13}\text{C}$ NMR spectral data of $[\text{Deae}]^{2+} \cdot 2[\text{A}]^-$ .....	129
Table 4.23: Melting temperature ( $T_m$ ) and decomposition temperature ( $T_d$ ) of synthesized dicationic ionic liquids.....	154
Table 4.24 : IR spectral data of synthesized dicationic ionic liquids. ....	159
Table 4.25 : Elemental Analysis.....	162
Table 4.26 : Chromatographic analysis data of $\text{NTf}_2$ and $\text{PF}_6$ moieties. ....	164
Table 4.27 : Solubility behaviour of ionic liquids in water and common organic solvents.....	167

## List of Symbols and Abbreviations

$^1\text{H}$ NMR	Proton Nuclear Magnetic Resonance Spectroscopy
$^{13}\text{C}$ NMR	Carbon-13 Nuclear Magnetic Resonance Spectroscopy
FT-IR	Fourier-Transform Infra-Red Spectroscopy
ATR	Attenuated total reflectance
CHNS	Carbon Hydrogen Nitrogen Sulfur elemental analysis
TGA	Thermogravimetric Analysis
DSC	Differential Scanning Calorimetry
IC	Ion Chromatography
$\text{CD}_3\text{CN-D}_3$	Deuterated acetonitrile
$\text{DMSO-D}_6$	Deuterated dimethylsulfoxide
$\text{D}_2\text{O}$	Deuterium oxide
$\text{CH}_3\text{CN}$	Acetonitrile
MeOH	Methanol
EtOH	Ethanol
EA	Ethyl acetate
$\text{NTf}_2^-$	Bis(trifluoromethanesulfonyl)imide
$\text{PF}_6^-$	Hexafluorophosphate/hexafluoridophosphate
$\text{Br}^-$	Bromide
ILs	Ionic Liquids
TSIL	Task-specific Ionic Liquids
RTIL	Room Temperature Ionic Liquids
ppm	part per million
$^\circ\text{C}$	degree Celsius
$\delta$	chemical shift
$J_{(\text{H,H})}$	J coupling constant
mg	milligram

## List of Synthesized Dicationic Ionic Liquids:

Abbreviation	Dicationic ionic liquids
[Pyr] <sup>2+</sup> .2[Br] <sup>-</sup>	<i>N,N'</i> -[1,4-phenylenebis(methylene)]dipyridinium dibromide
[Tea] <sup>2+</sup> .2[Br] <sup>-</sup>	<i>N,N'</i> -[1,4-phenylenebis(methylene)]bis-( <i>N,N</i> -diethylethanaminium) dibromide
[Mpyl] <sup>2+</sup> .2[Br] <sup>-</sup>	<i>N,N'</i> -[1,4-phenylenebis(methylene)]bis-( <i>N,N</i> -dimethylpyrrolinium) dibromide
[Bpyl] <sup>2+</sup> .2[Br] <sup>-</sup>	<i>N,N'</i> -[1,4-phenylenebis(methylene)]bis-( <i>N,N</i> -dibutylpyrrolinium) dibromide
[Nmpp] <sup>2+</sup> .2[Br] <sup>-</sup>	<i>N,N'</i> -[1,4-phenylenebis(methylene)]bis-( <i>N,N</i> -dimethylpiperidinium) dibromide
[Mmorp] <sup>2+</sup> .2[Br] <sup>-</sup>	<i>N,N'</i> -[1,4-phenylenebis(methylene)]bis-( <i>N,N</i> -dimethylmorpholinium) dibromide
[Dmae] <sup>2+</sup> .2[Br] <sup>-</sup>	<i>N,N'</i> -[1,4-phenylenebis(methylene)]bis-( <i>N,N</i> -dimethyl-2-hydroxyethanaminium) dibromide
[Deae] <sup>2+</sup> .2[Br] <sup>-</sup>	<i>N,N'</i> -[1,4-phenylenebis(methylene)]bis-( <i>N,N</i> -dimethyl-2-hydroxyethanaminium) dibromide
[Pyr] <sup>2+</sup> .2[NTf <sub>2</sub> ] <sup>-</sup>	<i>N,N'</i> -[1,4-phenylenebis(methylene)]dipyridinium bis[bis(trifluoromethanesulfonyl)imide]
[Tea] <sup>2+</sup> .2[NTf <sub>2</sub> ] <sup>-</sup>	<i>N,N'</i> -[1,4-phenylenebis(methylene)]bis-( <i>N,N</i> -diethylethanaminium) bis[bis(trifluoromethanesulfonyl)imide]
[Mpyl] <sup>2+</sup> .2[NTf <sub>2</sub> ] <sup>-</sup>	<i>N,N'</i> -[1,4-phenylenebis(methylene)]bis-( <i>N,N</i> -dimethylpyrrolinium) bis[bis(trifluoromethanesulfonyl)imide]
[Bpyl] <sup>2+</sup> .2[NTf <sub>2</sub> ] <sup>-</sup>	<i>N,N'</i> -[1,4-phenylenebis(methylene)]bis-( <i>N,N</i> -dibutylpyrrolinium) bis[bis(trifluoromethanesulfonyl)imide]
[Nmpp] <sup>2+</sup> .2[NTf <sub>2</sub> ] <sup>-</sup>	<i>N,N'</i> -[1,4-phenylenebis(methylene)]bis-( <i>N,N</i> -dimethylpiperidinium) bis[bis(trifluoromethanesulfonyl)imide]

[Mmorp] <sup>2+</sup> .2[NTf <sub>2</sub> ] <sup>-</sup>	<i>N,N'</i> -[1,4-phenylenebis(methylene)]bis-( <i>N,N</i> -dimethylmorpholinium) bis[bis(trifluoromethanesulfonyl)imide]
[Dmae] <sup>2+</sup> .2[NTf <sub>2</sub> ] <sup>-</sup>	<i>N,N'</i> -[1,4-phenylenebis(methylene)]bis-( <i>N,N</i> -diethyl-2-hydroxyethanaminium) bis[bis(trifluoromethanesulfonyl)imide]
[Deae] <sup>2+</sup> .2[NTf <sub>2</sub> ] <sup>-</sup>	<i>N,N'</i> -[1,4-phenylenebis(methylene)]bis-( <i>N,N</i> -dimethyl-2-hydroxyethanaminium) bis[bis(trifluoromethanesulfonyl)imide]
[Pyr] <sup>2+</sup> .2[PF <sub>6</sub> ] <sup>-</sup>	<i>N,N'</i> -[1,4-phenylenebis(methylene)]dipyridinium bis(hexafluoridophosphate)
[Tea] <sup>2+</sup> .2[PF <sub>6</sub> ] <sup>-</sup>	<i>N,N'</i> -[1,4-phenylenebis(methylene)]bis-( <i>N,N</i> -diethylethanaminium) bis(hexafluoridophosphate)
[Mpyl] <sup>2+</sup> .2[PF <sub>6</sub> ] <sup>-</sup>	<i>N,N'</i> -[1,4-phenylenebis(methylene)]bis-( <i>N,N</i> -dimethylpyrrolinium) bis(hexafluoridophosphate)
[Bpyl] <sup>2+</sup> .2[PF <sub>6</sub> ] <sup>-</sup>	<i>N,N'</i> -[1,4-phenylenebis(methylene)]bis-( <i>N,N</i> -dibutylpyrrolinium) bis(hexafluoridophosphate)
[Nmpp] <sup>2+</sup> .2[PF <sub>6</sub> ] <sup>-</sup>	<i>N,N'</i> -[1,4-phenylenebis(methylene)]bis-( <i>N,N</i> -dimethylpiperidinium) bis(hexafluoridophosphate)
[Mmorp] <sup>2+</sup> .2[PF <sub>6</sub> ] <sup>-</sup>	<i>N,N'</i> -[1,4-phenylenebis(methylene)]bis-( <i>N,N</i> -dimethylmorpholinium) bis(hexafluoridophosphate)
[Dmae] <sup>2+</sup> .2[PF <sub>6</sub> ] <sup>-</sup>	<i>N,N'</i> -[1,4-phenylenebis(methylene)]bis-( <i>N,N</i> -dimethyl-2-hydroxyethanaminium) bis(hexafluoridophosphate)
[Deae] <sup>2+</sup> .2[PF <sub>6</sub> ] <sup>-</sup>	<i>N,N'</i> -[1,4-phenylenebis(methylene)]bis-( <i>N,N</i> -diethyl-2-hydroxyethanaminium) bis(hexafluoridophosphate)

---



## **CHAPTER 1**

### **Introduction**

#### **1.1 Introduction to Ionic Liquids**

Ionic liquids have created a huge interest among scientists from all over the world. Since the 19<sup>th</sup> century, the number of publications related to ionic liquids has increased tremendously, with numbers of significant development and improvement in the synthesis or applications of ionic liquids. The rapid growth of interest is clearly due to the realization that these materials, commonly used for specialized electrochemical application may have greater utility in various industrial applications as well as in academic research area.<sup>1</sup>

Ionic liquids are known for their distinctive chemical and physical properties such as negligible vapour pressure, nonflammability, reasonable stability over high temperature, chemically stability, excellent dissolving capacity, wide liquidus range, wide electrochemical window and have low melting point, thus appear as liquids at ambient temperature.<sup>2</sup> Furthermore, ionic liquids exhibit remarkable solvating properties which permit the stabilization of rare species.<sup>3</sup>

Compared to molecular organic solvent, ionic liquids are non-volatile and have extremely low vapour pressure. Owing to these special features, ionic liquids are regarded as being environmentally friendly. Therefore chemists as well as processes engineers have proposed them as a suitable candidate to supersede flammable and toxic volatile organic solvents (VOCs) in the quest for a safer and cleaner technology.

Liquidus range refers to the span of temperature between freezing point and boiling point of a liquid. Previous reports show that the ionic liquids have wide liquidus range, which is another advantage of ionic liquids over molecular organic solvents because reaction can be done at low or high temperature (thermally stable).<sup>4-5</sup>



## 1.2 The Importance of Study

The field of research in ionic liquids has expanded drastically year by year with ionic liquids designed and tailored in order to fulfill the requirement of specific applications. This has resulted in a large number of reported synthetic approach.<sup>1</sup> Consequently, there are a number of new ionic liquids synthesized with unknown degree of purity. Apart from having a wide variety of ionic liquids, the problem on the purity of synthesized ionic liquids cannot be taken lightly. The quality and purity of synthesized ionic liquids cannot be compromise as these will affect the physicochemical properties of ionic liquids. Thus, thorough investigations on the purification methods must be done while the existing purification techniques must be improved.

In recent years, the synthesis of a new class of dicationic ionic liquids has captured the attention of a lot of researchers. Dicationic ionic liquids are a group of compounds having two *N*-containing head group linked together by a flexible spacer group, either short to long alkyl chains or rigid aromatic group to form a dication moiety with the charge balanced by two separate anionic moiety.<sup>6-9</sup> Reports have proven that this new class of ionic liquids possesses superior physical properties in terms of dissolving capacity, thermal stability and volatility<sup>10</sup> as well as wider electrochemical window<sup>11</sup> compared to conventional monocationic ionic liquids. Due to the fact that they have excellent solvation properties rather than common singly charged ionic liquids, they might be capable of dissolving all kinds of polar and non-polar molecules such as cellulose, polymers and simple organic molecules.

Compared to traditional singly charged ionic liquids, dicationic ionic liquids has greater combinations of various cationic and anionic moieties thus producing a wide variety of physicochemical properties in terms of viscosity, melting temperature, miscibility in solvents, thermal and chemical stability, hydrophobicity as well as the ability to dissolve things. Therefore, dicationic ionic liquids are used in various applications apart from electrochemical purposes,<sup>12</sup> for example as dye sensitized solar cell, lubricant,<sup>13</sup> gas liquid chromatography column,<sup>14</sup> solvent in high temperature reaction<sup>8</sup> and surfactant,<sup>15</sup> as well as multi-site phase transfer catalyst.<sup>16</sup>

To date, there are very few reports on the physical and chemical behaviors of dicationic ionic liquids. Due to their versatility and usefulness, further investigations are needed on the characterization to predict its suitable applications.

### 1.3 The Scope of Research

This research will focus on the synthesis, purification and characterization of dicationic ionic liquids. The ionic liquids synthesized are composed of various tertiary amines linked with a phenylene group to form cation moiety with bromide, hexafluorophosphate or bis(trifluoromethanesulfonyl)imide as the anion. This type of ionic liquids is easily synthesized using typical methods of alkylation followed by anion exchange reaction (metathesis) with lithium, sodium or ammonium salts of the desired anions in water.

Furthermore, purification of the synthesized ionic liquids is crucial since the quality and performance of ionic liquids depends on the purity of product. Several purification techniques for dicationic ionic liquids such as liquid-liquid extraction method, anion exchange column, electrodialysis through membrane and recrystallization were considered. Since most of the synthesized ionic liquids were obtained as solid organic salts in room temperature, recrystallization in an appropriate solvent was proposed to be the best solution. As a result of recrystallization, some ionic liquids produced single crystals suitable for single crystal x-ray diffraction determination.

The synthesized ionic liquids were characterized using Nuclear Magnetic Resonance (NMR) spectroscopy, carbon, hydrogen, nitrogen and sulfur (CHNS) elemental analyses and ion chromatography (IC) while thermal studies were accomplished using thermogravimetric analysis (TGA) and differential scanning calorimetry (DSC). Single crystal X-ray diffraction technique is a powerful tool in the prediction of molecular structure as well as providing useful information on

the arrangement of atom in a crystal lattice, bond length, bond angle as well as the interaction between atoms and molecules.

#### 1.4 The Objectives of The Research

The first objective is to synthesize six series of dicationic ionic liquids namely pyridinium, methylpyrrolidinium, butylpyrrolidinium, methylmorpholinium, methylpiperidinium, triethylammonium and two series of functionalized dicationic ionic liquids; *N,N*-dimethyl-2-hydroxyethanaminium and *N,N*-diethyl-2-hydroxyethanaminium with three types of anions; bromide, bis(trifluoromethanesulfonyl)imide and hexafluorophosphate.

The second objective is to carry out a suitable method of purification for the synthesized dicationic ionic liquids.

The third aim of this research is to characterize the physical properties such as melting and decomposition temperature as well as the purity level of synthesized dicationic ionic liquids using NMR spectroscopy, Infra Red (IR) spectroscopy and elemental analysis.

The forth objective of the research is to structurally characterize the synthesized dicationic ionic liquids using a single-crystal X-ray diffraction technique.

Final objective is to implement the synthesized dicationic ionic liquids in the self-assembly chemistry as a building component in forming multi-component materials with water soluble *p*-sulfonatocalix[4]arene and mono-phosphonium cation.

## **The Outline of Thesis.**

### **Chapter 1 : Introduction**

This chapter describes the background of this project including the importance and the purposed of the proposed research on the synthesis, purification and characterization of dicationic type ionic liquids.

### **Chapter 2 : Literature Review**

This chapter introduces the brief history and background of ionic liquids such as the first material considered as an ionic liquid which is the starting era of ever growing research of ionic liquids as well as their distinguish characteristics which make these materials a popular topic in scientific research. Because of the ionic liquids' uniqueness, scientists had implemented these molten salts in variety of experiments, thus their possible applications also been stated in this chapter.

### **Chapter 3 : Experimental Procedures**

This chapter explains the preparation methods of synthesis and purification technique as well as the analyses performed on the characterization part. The characterization techniques used in this research were  $^1\text{H}$  NMR,  $^{13}\text{C}$  NMR, CHNS elemental analysis, ion chromatography, TGA, DSC and single crystal x-ray diffraction.

## Chapter 4 : Results and Discussions

This chapter discusses on the results obtained from the experiments in details, namely  $^1\text{H}$  NMR,  $^{13}\text{C}$  NMR, FT-IR spectra of all compounds. Thermal studies performed on the TGA and DSC techniques revealed the temperature profiles and phase transitions of those dicationic ionic liquids upon temperature changes. The solubility behavior of organic salt towards organic solvent explains the polarity of salts based on 'like dissolves like' principle. The purity of dicationic salts was determined using ion chromatography method while the results on the composition of elements (*e.g* carbon, hydrogen, nitrogen and sulfur) were tabulated and compared with the theoretical values. On the other hands, the single-crystal X-ray crystallography data of compounds provides the arrangement of atoms in a crystal lattice as well as the molecular interaction involved between anions and cations in a crystal packing. Finally, the synthesized dicationic ionic liquids were found to be useful as a versatile building component in forming multi-component materials with water soluble *p*-sulfonatocalix[4]arene and mono-phosphonium cation. The details on how the molecules arrange themselves to form a multi-component material were discussed.

## Chapter 5 : Conclusion

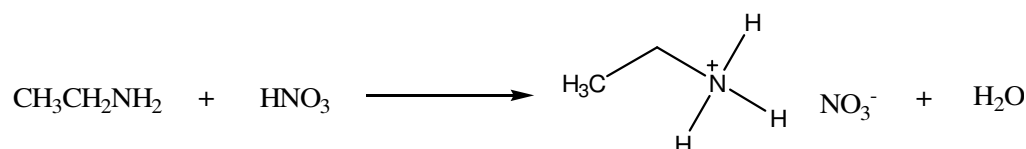
This chapter emphasizes and summarizes all the significant findings of this research.

## CHAPTER 2

### Literature Review

#### 2.1 Introduction of Ionic Liquids

The history of ionic liquids started with the interest in low melting temperature organic salts as new electrolytes. One of the earliest widely reported synthesis of room temperature ionic liquids was the preparation of ethylammonium nitrate by Paul Walden in 1914.<sup>1</sup> This salt was synthesized by addition of concentrated nitric acid into ethylamine and the equivalent amount of water was produced and then removed by distillation to give a pure salt (m.p. 12°C) that remained as a fluid at room temperature.



**Scheme 2.01** : Synthesis route of ethylammonium nitrate.

In 1963, a research project under U.S Air Force Academy lead by Major (Dr.) Lowell A. King aimed to find a replacement for the LiCl/KCl molten salt electrolyte used in thermal batteries. Even though LiCl/KCl eutectic mixture has a low melting temperature (355°C) for an inorganic salt, the relatively high temperature causes materials problems inside the battery and incompatibilities with nearby devices.<sup>17</sup>

The Air Force Academy continued to produce various salts based on the dialkylimidazolium and pyridinium cations while introducing new tetrafluoroborate, hexafluorophosphate, nitrate, sulfate and acetate anions that



were stable towards hydrolysis at room temperature. Fortunately, these salts are not only proved to be useful as a battery electrolyte but worked better for other applications too.<sup>17</sup> To date, research on ionic liquids is still progressing and developing with the production of various kinds of ionic liquids including functionalized ionic liquids as well as geminal dicationic ionic liquids and their seemingly limitless applications.

Ionic liquids are materials comprised entirely of ions which have melting point below the boiling point of water and commonly appear as viscous liquid around room temperature. The distinctive feature of ionic liquids which differentiates them from common inorganic salt, besides having low melting temperature, is that most of them have bulky and unsymmetrical organic cations and inorganic anions.

Initially, ionic liquids were characterized as ‘molten salt’ which is often mistaken with common inorganic salt such as NaCl (m.p 801°C). Since then, the term room temperature ionic liquids (RTIL) were slowly used to define and to differentiate between ionic liquids and the molten salt of inorganic salt. A room temperature ionic liquid is commonly defined as an ionic compound that is liquid below 100°C, has immeasurable vapour pressure and thus non-volatile in nature. Ionic liquids are also known as fused salts, liquid salts, organic salt, liquids electrolytes or ionic glasses.

A couple of decades ago, ionic liquids’ methodologies were still young and developing. This opened huge opportunities for scientists to explore different approaches and techniques of synthesizing ionic liquids. Nowadays, there are various kinds of ionic liquids being synthesized either for industrial applications

or in-house uses. The area of ionic liquids synthesis is indeed interesting. One type of cation can be paired with different kind of anions to produce great variety of ionic liquids having totally different physical properties each.

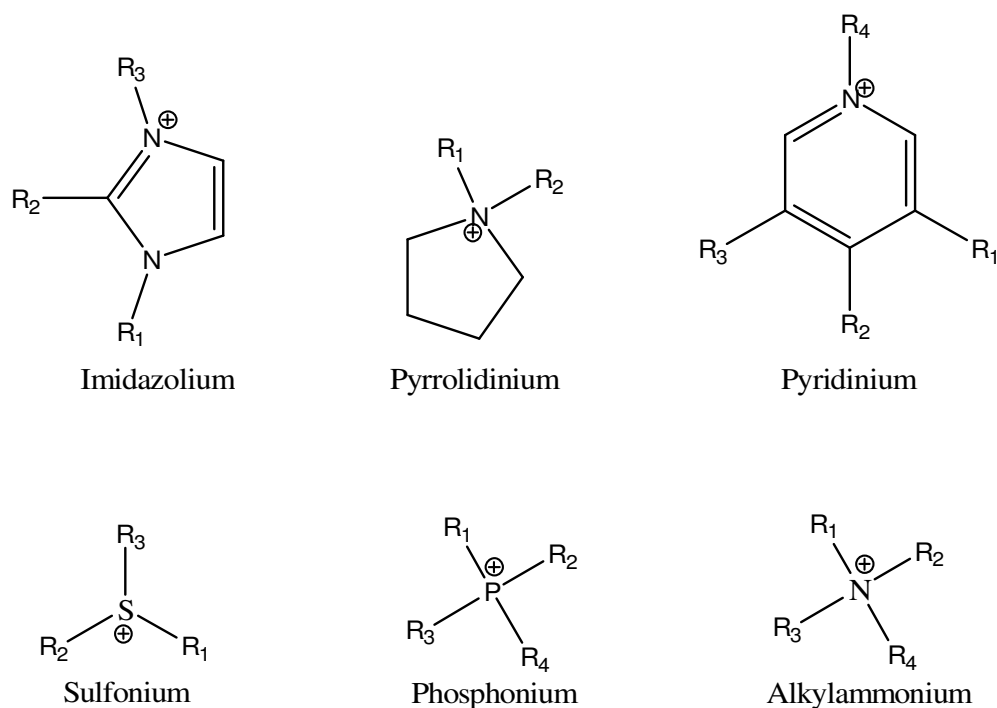
Ionic liquids are known to have special characteristics such as negligible vapour pressure, high thermal, chemical and electrochemical stability. With that, ionic liquids are the best candidate to play the role as solvent to replace the conventional volatile organic solvents which are known to be very toxic and highly flammable. In addition, ionic liquids are well known as the ‘designer solvent’ which explains the versatility and the uniqueness of this material since one can ‘tailor’ an ionic liquid to possess the criteria needed for any specific application. These kind of ionic liquids are commonly known as task-specific ionic liquids (TSIL).

The physical and chemical properties of several ionic liquids are extensively and thoroughly investigated due to their expanding scope of applications. These versatile materials are used in various applications such as electrical conducting fluids (or electrolyte) in batteries,<sup>18</sup> a powerful solvent<sup>19</sup> and catalyst<sup>20-23</sup> in organic synthesis, dye sensitized solar cell,<sup>24</sup> cellulose dissolution,<sup>25</sup> phase transfer catalyst,<sup>26</sup> separation<sup>27</sup> and extraction.<sup>28-30</sup>

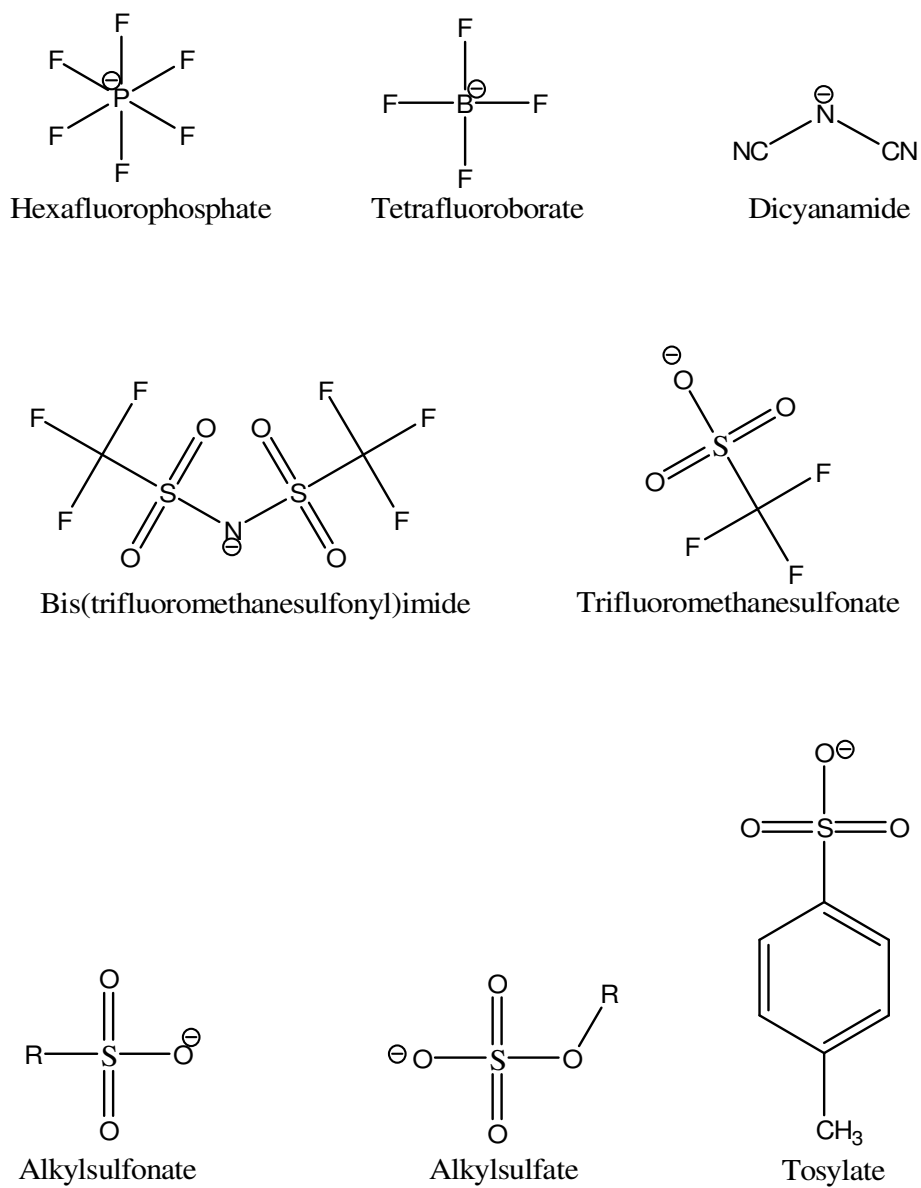
In spite of the versatility of ionic liquids, there are limitations and disadvantages associated with these unique materials. The term ‘ionic liquids’ are strictly applied for highly pure ionic liquids because the purity of these organic salts affects the physicochemical properties as well as their performance. Therefore, purification methods are indeed critical in the synthesis of ionic liquids especially when they are produced in a bulk quantity. On the other hands, most of

ionic liquids cannot be purified directly by distillation or recrystallisation as they have very low vapour pressure and relatively low melting point.<sup>31</sup>

The most widely studied ionic liquids are 1-alkylimidazolium based salts with various kind of anions such as chloride, bromide, tetrafluoroborate ( $\text{BF}_4^-$ ), hexafluorophosphate ( $\text{PF}_6^-$ ) trifluomethanesulfonate ( $\text{OTf}$ ), bis(trifluoromethanesulfonyl)imide ( $\text{NTf}_2^-$ ) and *etc.* These salts are used in many research areas, for example electrochemistry, organic synthesis, separation, extraction, cellulose dissolution and biotechnology.<sup>32-33</sup>



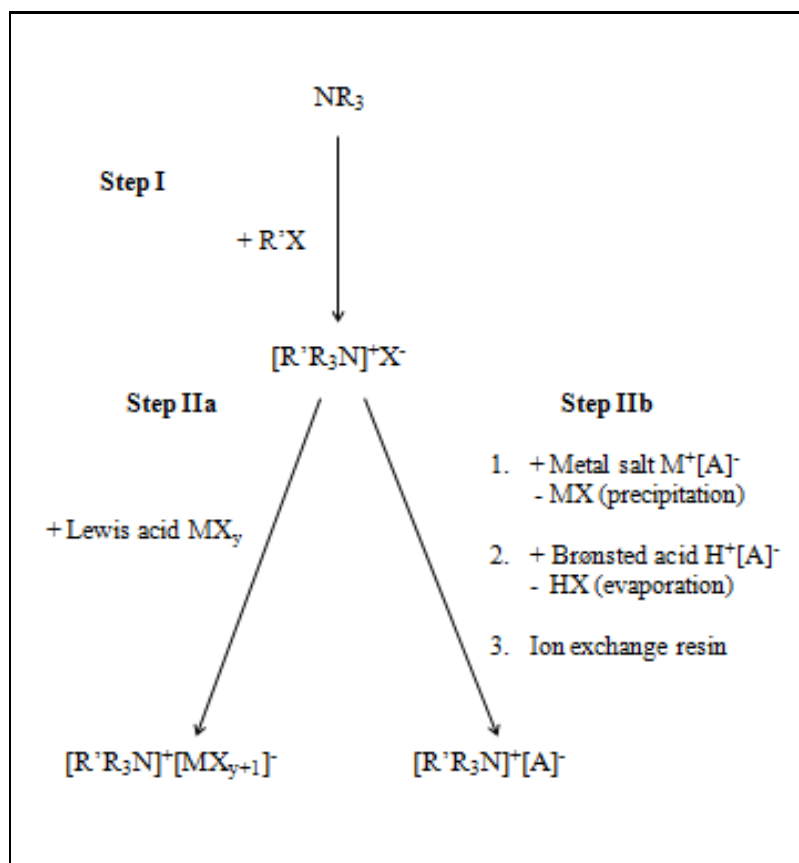
**Scheme 2.02** : Example of common cations used for the formation of ionic liquids.



**Scheme 2.03** : Examples of common anions used for the formation of ionic liquids.

## 2.2 Synthesis of Ionic Liquids

The most common synthesis of ionic liquids can be divided into two major steps; alkylation and anion exchange (most commonly known as metathesis). The typical synthesis routes of ionic liquids are shown in the **Figure 2.2**.



**Figure 2.01** : Common synthesis pathway for the preparation of ionic liquids exemplified for an ammonium salt (adaptation from reference <sup>23</sup>).

Alkylation step is a straight forward reaction. There is various kind of amine compound available commercially. The most widely synthesized ionic liquids are the dialkyl substituted imidazolium based ionic liquids. In this reaction, dialkylimidazolium was reacted with an excess molar ratio of alkyl halides (*e.g* chloroethane, bromoethane, bromobutane *etc.*) without or with a suitable organic solvent. The product was then used as a precursor either in a metathesis reaction

(anion exchange reaction), where the organic salt is reacted with a group 1 metal salt, in particular sodium salt (*e.g.* sodium tetrafluoroborate, sodium hexafluorophosphate *etc.*) or a silver salt of the desired anion (for example silver nitrate), or in an acid-base neutralization reaction. The reaction produces an equimolar amount of side product, MX or HX. The metathesis reaction and acid-base reaction are carried out in aqueous solution at room temperature. Depending on the anions chosen, the products formed are either a biphasic system with water or a homogeneous solution.

If the resulting ionic liquids forms a biphasic mixture with water (for PF<sub>6</sub> and NTf<sub>2</sub> anions), halide removal with aqueous extraction results in halide-free ionic liquids. However, for water-miscible ionic liquids, the work-up of the metathetic reaction involves removal of water under reduced pressure, followed by repeated dissolution with suitable organic solvent and cooling to 5°C to precipitate the group 1 metal halide and finally followed by several filtration steps. However, this method is very tedious while the effectiveness of halides removal is only mediocre.<sup>34</sup>

Product separation and purification are the most tedious parts in the alkylation step, while the presence of traces of starting materials (*e.g.* 1-methylimidazole) and the discoloration of product are the problems frequently encountered in the synthesis of ionic liquids.<sup>17</sup> Even though the excess solvent and starting materials can be simply removed by decantation as ionic liquid is denser than solvent used, this is not a proper method to remove these impurities completely. Therefore, the solvent extraction method is often used to separate and purify the ionic liquids which are in liquid form while recrystallisation method is applied to ionic liquids which are in solid form. The discoloration of products

usually caused during refluxing at high temperature for a long period of time and not distilling starting materials prior to use. These traces of impurities cannot be detected by Nuclear Magnetic Resonance (NMR) spectroscopy or Fourier-Transform Infra Red (FT-IR) spectroscopy either.<sup>31</sup>

## 2.3 Purification of Ionic Liquids

Conventionally, ionic liquids were synthesized by alkylating 1-methylimidazole with alkyl halide (chloride or bromide) producing organic salts (example dialkylimidazolium salt) and inorganic salts. Then, the resulting 1,3-dialkylimidazolium salts was used for subsequent metathesis. However, the resulting ionic liquid may contain a significant level of halide that is very difficult to be removed especially in hydrophilic ionic liquids consisting of anions such as  $\text{BF}_4^-$ ,  $\text{OTf}^-$ , nitrate ( $\text{NO}_3^-$ ) and acetate ( $\text{CH}_3\text{COO}^-$ ).

From the previous works reported, the most common impurities in conventional ionic liquids were the unreacted starting materials, water and halides. Halides are known to coordinate to the transition metal centers of catalyst and thus affect the rate of reaction. The presence of chloride ( $\text{Cl}^-$ ) may affect some physicochemical properties of ionic liquids. In ionic liquids, the presence of chloride impurities have been reported to have a detrimental effect on transition metal catalyzed reaction such as hydrogenations whereas in Heck-type reactions, bromide has a stabilizing effect on palladium. On the other hand, to the process engineers' point of view, chloride ion in ionic liquids might cause corrosion to the plant which leads to a huge loss to an industrial company.<sup>34</sup>

Ionic liquids can be divided into two major classes; water soluble (hydrophilic) and water insoluble (hydrophobic) ionic liquids. The most common examples for the water soluble organic salts are  $\text{Cl}^-$ ,  $\text{Br}^-$ ,  $\text{NO}_3^-$ ,  $\text{BF}_4^-$ ,  $\text{OTf}^-$ ,  $\text{CH}_3\text{COO}^-$ , alkylsulfate and sulfate while bis(trifluoromethanesulfonyl)imide ( $\text{NTf}_2^-$ ) and hexafluorophosphate ( $\text{PF}_6^-$ ) are the common anions for water insoluble ionic liquids. Indeed, purification following metathesis is the most challenging

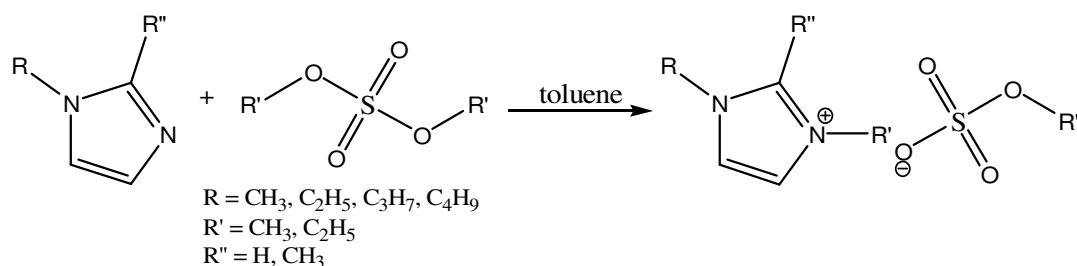


part especially in the synthesis of water miscible ionic liquids. This is due to both the product and inorganic salt (by-product) are soluble in water. In addition to the hygroscopic nature of the makes the removal of inorganic salt difficult as it has high tendency to absorb moisture and will easily dissolve back into the ionic liquid layer. Therefore, halide content will be higher in these hydrophilic ionic liquids originating either from inorganic salt or incomplete metathesis. Precipitations of chloride as silver chloride (AgCl) does not lead to entirely halides free ILs associated with. In addition, there are limited variety of commercially available silver salts which are often high cost.<sup>19</sup> The usual method used is to filter out the inorganic salt after evaporating the solvent and water out of the ionic liquid mixture.

Therefore, we would like to highlight some of works done by researchers related to synthesis of halides free ionic liquids as well as the purification of ionic liquids to get highly pure ionic liquids with halides and water content as low as possible. However, those works have limitation and disadvantages.

Holbrey *et. al.* had proposed the method to synthesize halide-free ILs by reacting 1-alkylimidazolium with dimethyl sulfate and diethyl sulfate to produce 1-alkyl-3-methylimidazolium methyl sulfate and 1-alkyl-3-ethylimidazolium ethyl sulfate which are stable, water soluble, inherently halide-free, display an electrochemical window of greater than 4V and can be used as alternatives in metathesis reaction to prepare other ionic liquids.<sup>33</sup> There are a few advantages regarding to this method such as faster reaction time as alkylation rate of dimethyl sulfate is 60 times faster than of methyl iodide,<sup>17</sup> requires less expensive processing equipment and the resulting salts can be considered as less toxic.

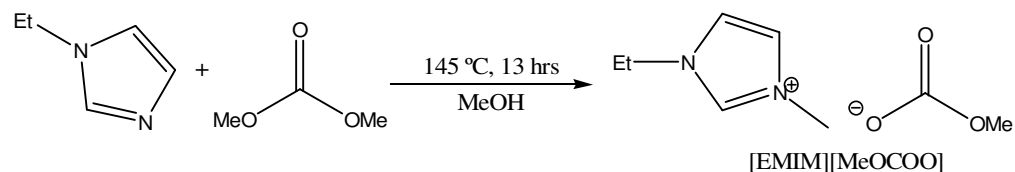
Furthermore, alkyl sulfate salts causes less corrosion to the processing equipment compare with halides salts.



**Scheme 2.04** : Synthesis route of 1-alkyl-3-methylimidazolium alkyl sulfate ionic liquids.

Bonhote *et al.* have described the synthesis of triflate and trifluoroacetate containing ILs by alkylation of 1-methylimidazole with ethyl triflate and ethyl trifluoroacetate respectively as the alternative synthetic strategies. Even though this synthesis route might take a longer reaction time, the ionic liquids can be prepared on a large scale with high yields and highly purity. These ILs have also been used as intermediate to prepare other ionic liquids.<sup>32</sup>

On the other hands, Ue *et. al.*, developed a method of halide free ionic liquids synthesis. 1-Ethyl-3-methylimidazolium methyl carbonate salts was prepared in solution by direct alkylation of 1-ethylimidazole with dimethyl carbonate at 145 °C where methanol and carbon dioxide are the only by product. The product 1-ethyl-3-methylimidazolium methyl carbonate can be used as a precursor to synthesize the desired ionic liquids by neutralization with acids containing the corresponding fluoroanions. The new synthesis route was proved effective in producing pure ionic liquids with good yields.<sup>33</sup>



**Scheme 2.05** : Synthesis pathway to synthesize halides-free ionic liquid precursor.

Z. Li *et. al.* described an interesting work on environmental friendly halides removal. This is done by applying constant electrolysis to oxidize  $\text{Br}^-$  and  $\text{Cl}^-$  to their corresponding  $\text{Br}_2$  and  $\text{Cl}_2$  through anion exchange membrane. The resulting  $\text{Br}_2$  and  $\text{Cl}_2$  in electrolyzed ionic liquid were treated with ethylene to form the corresponding 1,2-dibromo (or dichloro) ethane which can be easily removed by volatilization in vacuo.<sup>36</sup>

Yeon *et. al.* conducted low temperature filtration method using celite to remove halides from ionic liquids. This method proved to be effective in removing residual chloride ion in water soluble ionic liquids but causes some loss of ionic liquids.<sup>37</sup>

Ohno's group introduced a new method of synthesis of halides-free room temperature ionic liquids involving the preparation of imidazolium hydroxide intermediate to neutralize a series of amino acids. The common method of anion exchange with metal salts seems to be unsuitable for preparing highly pure and various RTILs due to contamination of halides salts and limited variety of commercially available metals salts. Furthermore, because amino acids coordinate transition metal salts, pure amino acid RTILs cannot be obtained using conventional method with metal salts. The general procedure to prepare the imidazolium hydroxide ILs involved the use of anion exchange resin such as

AMBERLITE IRA400CL or AMBERLITE IRA400OH followed by the addition of amino acids.<sup>38</sup>

Inspired by the impressive work done by Ohno's group in synthesizing RTILs through hydroxide-based precursor, for the first time P. Wasserscheid *et. al.* implemented the electrodialysis with bipolar membrane (EDBM) method to produce this precursor in 5% concentration in water from the non-toxic bulk ionic liquids [Emim][EtOSO<sub>3</sub>]. However, this method is limited to ILs with small cation because it involves the movement of anion and cation through an ion permeable membrane.<sup>39</sup>

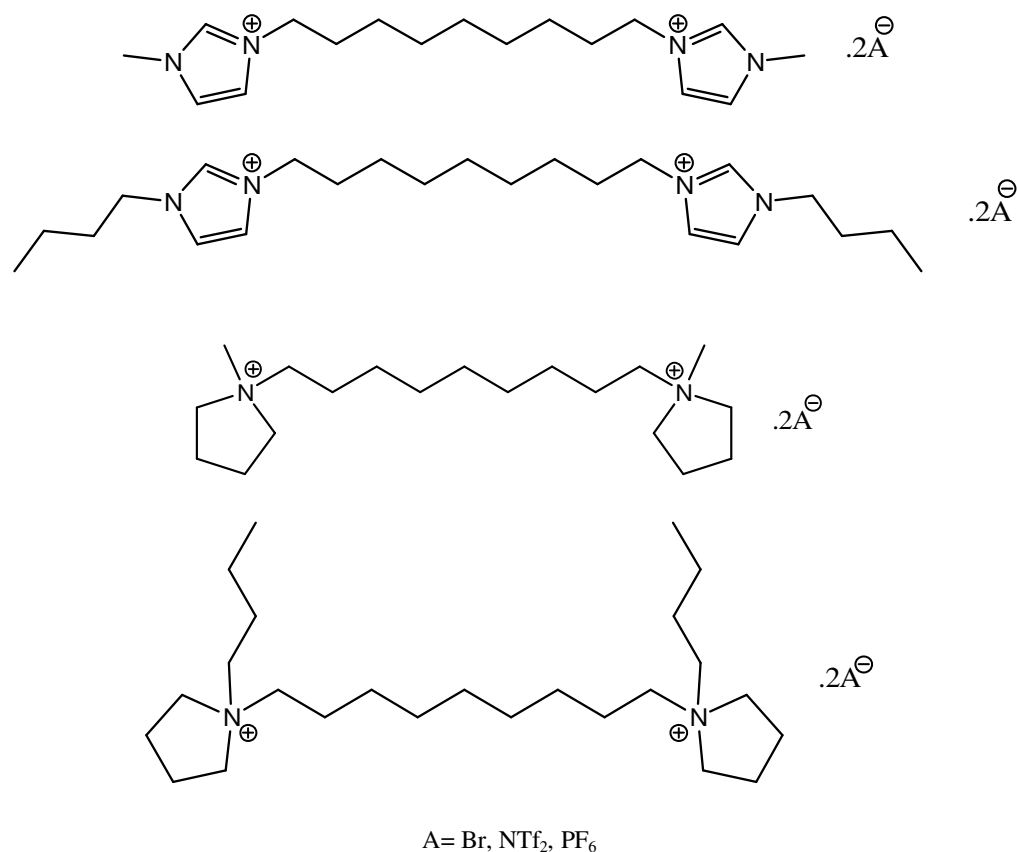
## 2.4 Functionalized Ionic Liquids

The structure and properties of ionic liquids can be custom-tailored to fit each specific purpose, through incorporating anions or cations with functionalized groups, such as  $\text{-NH}_2$ ,<sup>40</sup>  $\text{-COOH}$ ,<sup>41-42</sup>  $\text{-SO}_3\text{H}$ ,<sup>43</sup>  $\text{-OH}$ ,<sup>44-45</sup>  $\text{-CN}$ <sup>46</sup> and  $\text{-SH}$ ,<sup>47</sup> *etc.*, which provides more promising perspectives in both fundamental and practical aspects. Functionalized ionic liquids are usually much more viscous than their non-functionalized analogues, since the incorporation of any functional group will inevitably lead to an increase in both polarity and molecular size. In many fields, the required viscosity should be as low as possible, including heterogeneous catalysis and supporting electrolytes, except viscous lubricant.

Among various types of functional groups, alkoxy groups are exceptional due to their ability to form low-viscosity ionic liquids, since the highly flexible alkoxy chains do not pack as efficiently as alkyl chains. Deng *et al.* prepared a series of new ionic liquids based on dialkoxy-functionalized quaternary ammonium cations with  $\text{BF}_4$ ,  $\text{NTf}_2$  and  $\text{CH}_3\text{COO}^-$  as counteranions. The incorporation of two flexible alkoxy chains makes the quaternary ammonium salts highly qualified to be low-viscous and high-conductive room temperature ionic liquids. In addition, the dialkoxy  $\text{CH}_3\text{COO}^-$  ionic liquids were found to have excellent solvent power for cellulose dissolution with the help of the hydrogen accepting ether bonds.<sup>25</sup>

## 2.5 Introduction to Dicationic Ionic Liquids

The investigation on the physical properties of monocationic ionic liquids were done extensively while there are not much work done on the dicationic ionic liquids since they were just developed couple of years ago. Dicationic ionic liquids are a new class of ionic liquids with two *N*-containing compounds (e.g 1-alkylimidazole, pyridine, 1-alkylpyrrolidine, triethylamine etc.) linked together with rigid or flexible bridging group such as a polyalkylether, polyfluoroalkyl, 1,4-bismethylenebenzene or 1,4-bismethylene-2,3,5,6-tetrafluorobenzene.<sup>48-50</sup>



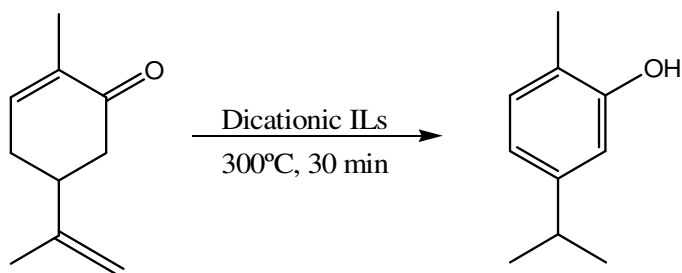
**Scheme 2.06** : Examples of geminal dicationic ionic liquids;  $C_9(mim)_2$ ,  $C_9(bim)_2$ ,  $C_9(mpy)_2$  and  $C_9(bpy)_2$  respectively.

## 2.6 Applications of Dicationic Ionic Liquids:

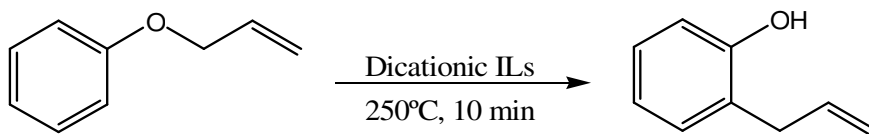
### 2.6.1 Dicationic ionic liquids as a solvent

It is well known that the advantages of ionic liquids over conventional organic solvents are their extremely low vapour pressure and high thermal stability. Meanwhile, dicationic ionic liquids proved to have a better thermal stability and wider liquidus range compared to single charged ionic liquids. Such features allow these materials to be used as solvent for high temperature organic synthesis.

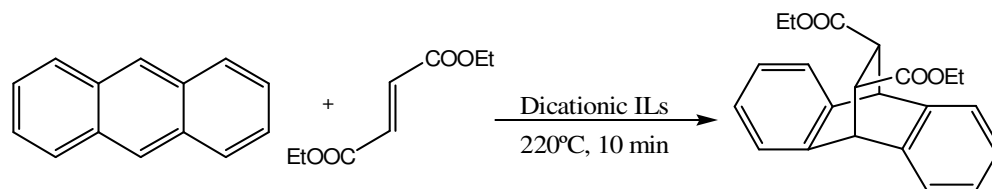
Recently, Armstrong and his group developed a series of geminal dicationic ionic liquids which is able to withstand high temperature organic synthesis up to 300°C. They applied the three highly stable geminal dicationic ionic liquids abbreviated  $C_9(mim)_2-NTf_2$ ,  $C_9(bim)_2-NTf_2$ , and  $C_9(mpy)_2-NTf_2$ <sup>51</sup> (Scheme 2.6) for high-temperature organic reaction including isomerization reaction, Claisen rearrangement and thermo-induced Diels-Alder reaction.<sup>19</sup>



**Scheme 2.07** : Isomerization of carvone in dicationic ionic liquids.



**Scheme 2.08** : Claisen rearrangement of allyl phenyl ether in dicationic ionic liquids.



**Scheme 2.09** : Diels-Alder reaction of anthracene and diethyl fumarate in dicationic ionic liquids.

Previous work on the isomerization of carvone was reported where the reaction was done in the aqueous media at temperature 250°C. The advantages of using geminal dicationic ionic liquids as a replacement of water for this high temperature organic reaction is the reaction can be done at atmospheric pressure without more complex high pressure reactor, while the time taken for the reaction to complete is shorten.<sup>52</sup>

The investigations of these three germinal dicationic ionic liquids showed that these materials have potential as a solvent for high temperature organic synthesis even though they darken upon exposure to high temperature. Although the colour of dicationic ionic liquids changes after heating at high temperature, they still can be reused or recycled several times without lost of efficiency.<sup>19</sup>





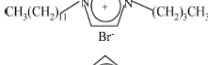

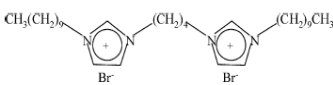
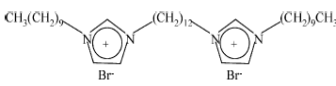
### 2.6.2 Dicationic ionic liquids as a surfactant

Surfactants are organic compounds that lower the surface tension of a liquid. They exhibit amphiphilic behaviour where both hydrophilic heads and hydrophobic tails are at the same molecules. Therefore, surfactants have the ability to mix organic phase with aqueous phase where their molecules will diffuse in water and adsorb at interfaces between air and water or at the interface between oil and water, in cases where water is mixed with oil.<sup>53</sup>

Gemini surfactants are relatively new class of amphiphilic molecules containing two head group and two aliphatic chains, linked by a rigid or flexible spacer. Ding *et. al.* had synthesized a novel geminal imidazolium ionic liquid with long hydrocarbon group, 1,4-bis(3-tetradecylimidazolium-1-yl) butane bromide. Compared with conventional mono-chain surfactants, gemini surfactants demonstrate unique features in critical micelle concentration, interface property and solubility in water. These surfactants are about three orders of magnitude more efficient at reducing surface tension and more than two orders of magnitude more efficient at forming micelles than conventional surfactants. Furthermore, they have high density and unusual rheological properties.<sup>54-55</sup>

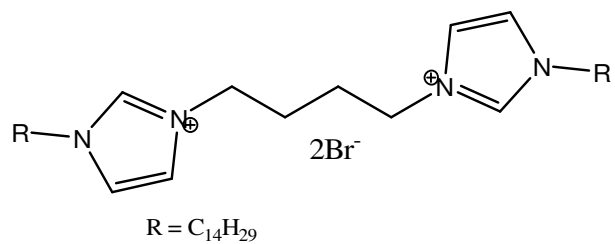
On the other hand, Anderson and coworkers studied how the ionic liquids aggregates behave in aqueous system in order to understand the correlation between the structure of ionic liquids and their possible toxicity information. Due to the extensive use of ionic liquids in a vast area of research, it is expected that ionic liquids will eventually reach living organism through our water system such as wastewaters, lakes, rivers, aquifers etc in the not too distant future. While there are some researchers studying the toxicity and biodegradability of ionic liquids,

the available information are insufficient due to the huge number of ionic liquids synthesized and produced year by year. They also studied the partitioning behavior of 14 different analytes such as aliphatic hydrocarbons, polycyclic aromatic hydrocarbon, phenols and esters to several monocationic ionic liquids and two dicationic ionic liquids in solid phase microextraction coupled to gas chromatography.<sup>56</sup>

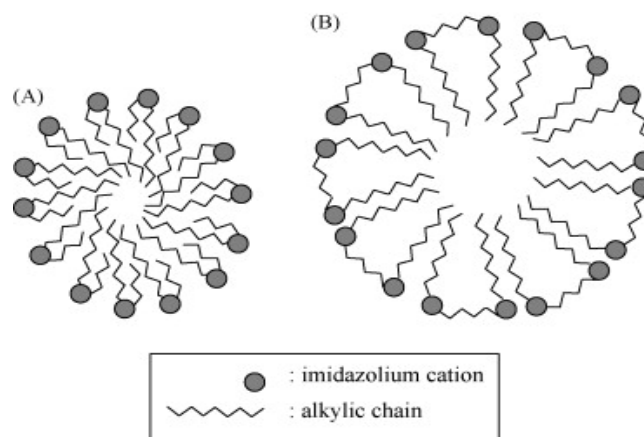
IL	Structure	CMC (mM)
Monocationics		
HDMIIm-Br		0.76
HDBIm-Br		0.08
DDBIm-Br		2.37
DDDIIm-Br		0.10
Dicationics		
C <sub>4</sub> (DIM) <sub>2</sub> -2Br		2.02
C <sub>12</sub> (DIM) <sub>2</sub> -2Br		0.60

**Figure 2.02 :** The type of monocationic ionic liquids and analogous dicationic ionic liquids studied for analytes partitioning behavior and their critical micelle concentrations (CMC) values.

Based on the surfactant principle, ionic liquids which have the ability to form micelle were used to extract and separate the analytes of different polarity by forming aggregates system with ionic liquids. The results show the monocationic ionic liquids-aggregates generally exhibit higher partitioning coefficients compared to analogous dicationic ionic liquids. The micellar shape of the ionic liquids-aggregates also influence the extent of the analyte partitioning.<sup>56-57</sup>



**Scheme 2.10** : Example of long side chain geminal dicationic ionic liquids surfactant.



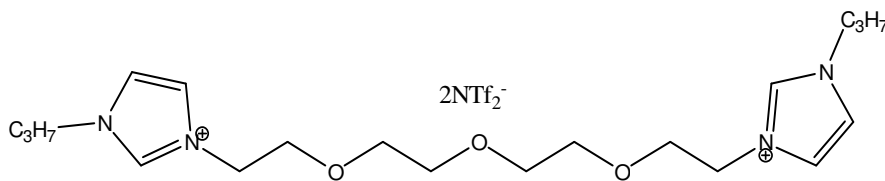
**Scheme 2.11** : Tentative scheme with the micellar shape for (A) monocationic ionic liquids and (B) dicationic ionic liquids.<sup>56</sup>

### 2.6.3 Dicationic ionic liquids as a lubricant

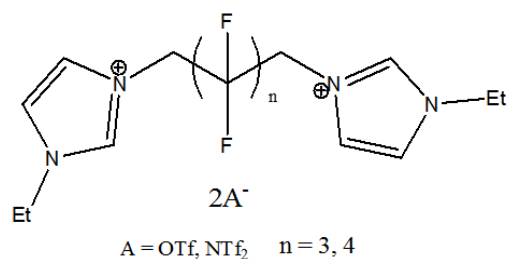
Current high temperature aircrafts lubricant can operate only up to a temperature of 150°C. New aerospace technologies demand lubricants that can perform well at temperature between -40°C and 330°C. So far, most of geminal dicationic ionic liquids reported have higher (thermal stability with a liquid/stability range of over 300°C) than traditional monocationic ionic liquids. Due to the excellent thermal property, dicationic ionic liquids might have potential as a new generation of synthetic lubricants.

Currently, geminal dicationic liquids received attention because they were highly stable in terms of thermal properties. Zhuo Zeng and coworkers synthesized new series of geminal dicationic ionic liquids by employing polyalkylether, polyfluoroalkyl, 1,4-bismethylenebenzene and 1,4-bismethylene-2,3,5,6-tetrafluorobenzene as bridging moieties on different alkyl substituent of imidazolium rings.<sup>50</sup>

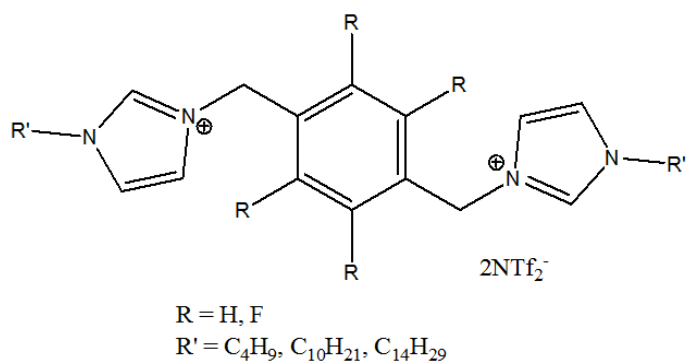
By varying the linker chains and/or alkyl substituent on the imidazolium ring, the properties such as thermal stability, melting temperature and viscosity of the dicationic ionic liquids change accordingly.<sup>58</sup>



**Scheme 2.12** : Structure of polyethylene-glycol functionalized dicationic ionic liquids.



**Scheme 2.13** : Structure of polyfluoroalkyl functionalized dicationic ionic liquids.



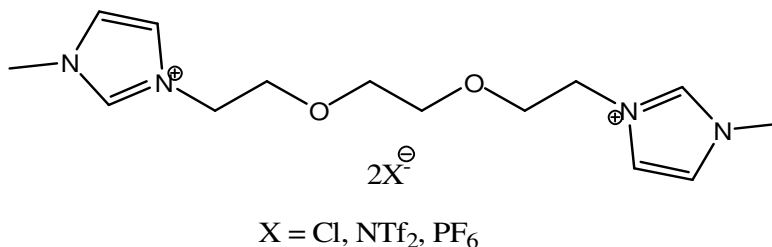
**Scheme 2.14** : Structure of benzene and tetrafluorobenzene functionalized dicationic ionic liquids.

According to their report, the geminal dicationic ionic liquids exhibit very good tribological characteristics. In addition, the ability to withstand high temperature up to 300°C is one of the required criteria for high-temperature lubricant, thus these materials could be used as a high temperature lubricant, besides having very low volatility.<sup>50,59</sup> Even so, careful search for a suitable candidate to be used in tribological study is extremely crucial especially when dealing with fluorine containing ionic liquids.<sup>60</sup>

#### 2.6.4 Dicationic ionic liquids in chemical separation and extraction

1,1'-[1,2-Ethanediybis(oxy-1,2-ethanediyl)] bis[3-methyl-1*H*-imidazolium-1-yl] bis(trifluoromethanesulfonyl)imide is a room temperature ionic liquid containing a bis-imidazolium cation incorporating a short ethylene-glycol spacer was prepared from corresponding chloride salt for extracting metal by forming metal-ether complex,<sup>28,61</sup> in this case mercury (II) from two phase systems.

In comparison to bis-imidazolium salts containing alkane spacer groups, the ether linkage possessed higher degree of flexibility (resulting in lower melting points) and greater tendency towards water compared to conventional imidazolium-based ionic liquids.

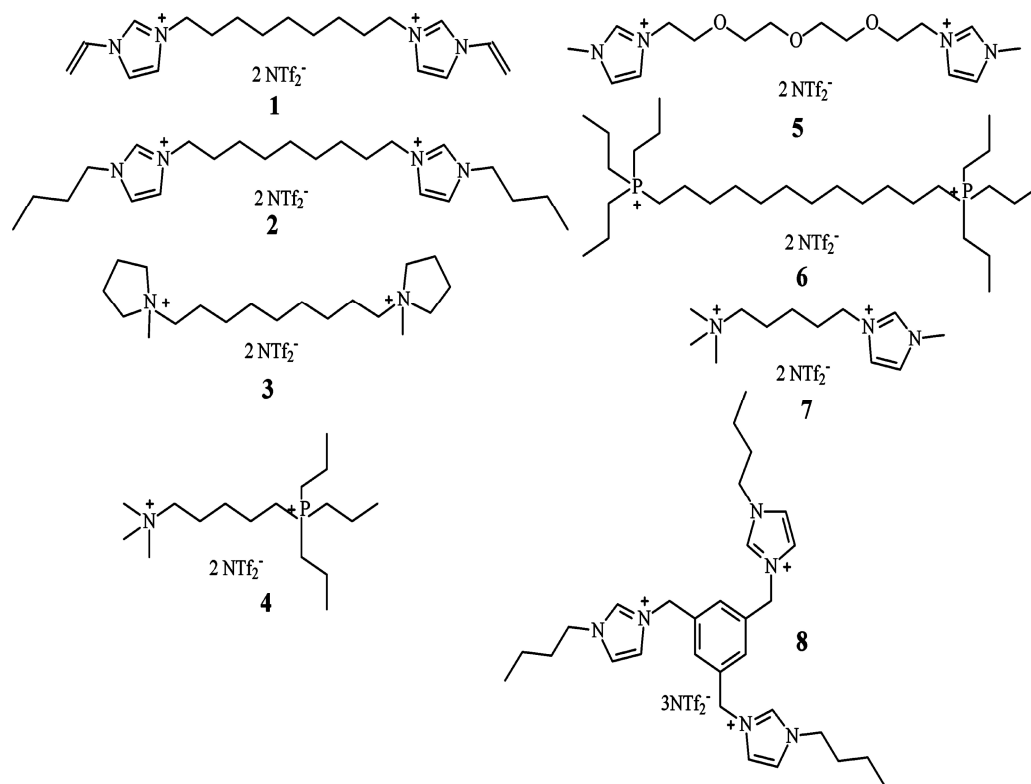


**Scheme 2.15** : Structure of the ionic liquids containing the 1,1'-[1,2-ethanediybis(oxy-1,2-ethanediyl)] bis[3-methyl-1*H*-imidazolium-1-yl] cation with [Cl], [NTf<sub>2</sub>] and [PF<sub>6</sub>] as the counteranions.

It has been proved that by introducing the ethylene-glycol functionality the distribution ratio of mercury ion from aqueous solution to the hydrophobic ionic liquids increases dramatically compared to normal alkyl-substitute/imidazolium ionic liquids although it is not optimal compared to polydentate ethers. On the other hand, the crystal structure of the related mercury (II) carbene complex, obtained from the reaction of mercury (II) acetate with 1,1'-[oxybis(2,1-ethanediyl)oxy-2,1-ethanediyl]]bis[3-methyl-1*H*-imidazolium-1-yl] tosylate,

containing a three ether-spacer revealed the possibility of a carbene extraction mechanism.<sup>28</sup>

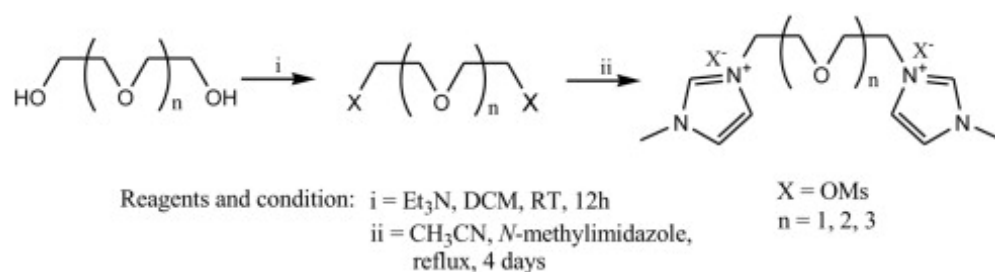
Armstrong and coworkers were actively doing research in analytical chemistry and separation of organic mixtures, recently implemented what they called multifunctional ionic liquids such as geminal dicationic ionic liquids,<sup>62</sup> unsymmetrical dicationic ionic liquids<sup>63</sup> and tricationic ionic liquids<sup>64</sup> as the stationary phase for gas liquid chromatography column. Many of them had stable liquid range from at least -8°C to greater than 410°C. This column proved to have better separation without losing its efficiency upon longer uses compared with other common stationary phase.<sup>65</sup>



**Scheme 2.16** : Examples of symmetric and unsymmetric dicationic ionic liquids and a tricationic ionic liquids developed by D. W. Anderson *et. al.*<sup>65</sup>

### 2.6.5 Dicationic ionic liquids as a catalyst

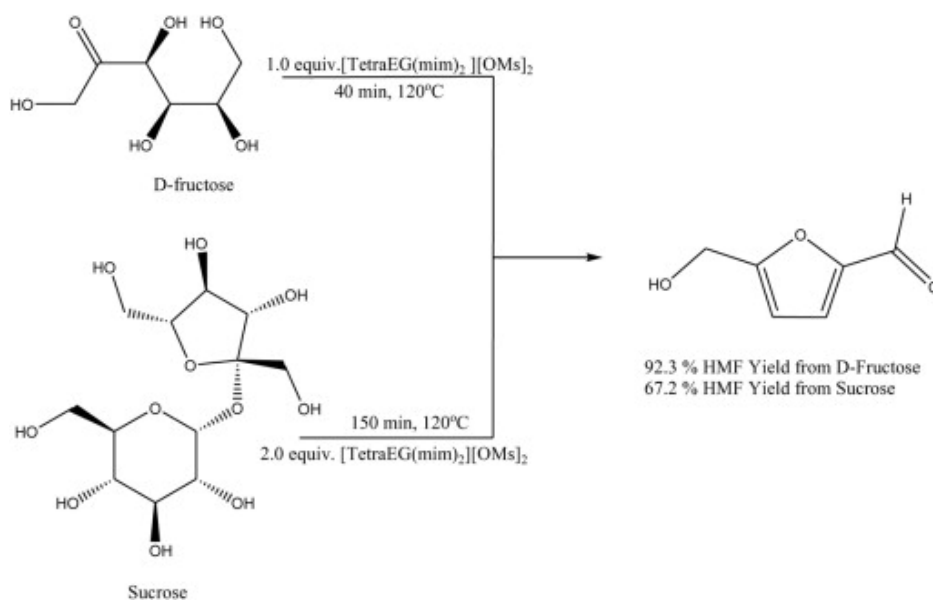
Three different kind of dicationic room temperature ionic liquids, [DiEG(mim)<sub>2</sub>][OMs]<sub>2</sub>, [TriEG(mim)<sub>2</sub>][OMs]<sub>2</sub> and [TetraEG(mim)<sub>2</sub>][OMs]<sub>2</sub> were synthesized using appropriate precursors and *N*-methylimidazole with a good yield. These three dicationic room temperature ionic liquids have different linker chain length of oligo ethylene glycol and they were investigated for the dehydration of fructose and sucrose.



**Scheme 2.17** : The reaction pathway for the synthesis of imidazolium dicationic room temperature ionic liquids (abbreviates [TetraEG(mim)<sub>2</sub>][OMs]<sub>2</sub>).

The oligo ethylene glycol chains makes the ionic liquids more hydrophilic in nature where the oxygen atoms in the oligo ethylene glycol chains of cation could acts as hydrogen bond acceptor and form hydrogen bond with sugar, thus promoting the sugar dissolution. The capability of these ionic liquids to form hydrogen bonds was believed to be the main mechanism of sugar dissolution and formation of 5-hydroxymethylfurfural (HMF). In this study, the synthesized ionic liquids possessed Lewis acid characters<sup>66</sup> because according to the previous works, Lewis acidic ionic liquids were more effective in converting sugar and gave higher yield of HMF than Brønsted acidic ionic liquids.<sup>67</sup>





**Scheme 2.18** : The dehydration reaction of D-fructose and sucrose with dicationic room temperature ionic liquids.

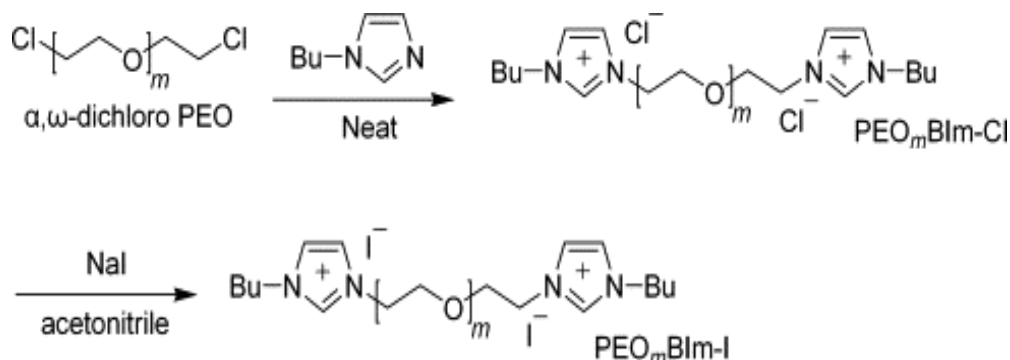
Based on the result of the experiment conducted by Kim and his coworkers, the dicationic [TetraEG(mim)<sub>2</sub>][OMs]<sub>2</sub> ionic liquids was the most effective catalyst for the achievement of the highest HMF yield with 100% conversion of sugar. Hence they concluded that as the length of the oligo ethylene glycol chains between the two imidazolium rings increases, the catalytic activity and hydrophobicity is correspondingly higher. Therefore, the activity order between those ionic liquids and their HMF yield can be summarized as followed:

$$[\text{TetraEG(mim)}_2][\text{OMs}]_2 > [\text{TriEG(mim)}_2][\text{OMs}]_2 > [\text{DiEG(mim)}_2][\text{OMs}]_2.^{66}$$

## 2.6.6 Dicationic ionic liquids in dye sensitized solar cell

Dye-sensitized solar cell (DSSC) is a type of solar cell formed between a photo-sensitized anode and an electrolyte. A new generation of DSSC called the Grätzel cell was invented by Michael Grätzel and Brian O'Regan at the École Polytechnique Fédérale de Lausanne in 1991.<sup>68</sup> Grätzel cell mimic the process of plant photosynthesis where the combination of porphyrin and cobalt allows the DSSC to enhance the efficiency of electron exchange by optimizing the absorption of sunlight. The process of electron exchange from dye to the substrate produces electricity.<sup>69</sup>

Novel thixotropic gel electrolytes have been successfully prepared by utilizing oligomeric poly(ethylene oxide) (PEO)-based bis-imidazolium diiodide salts and hydrophilic silica nanoparticles for application in quasi-solid-state dye-sensitized solar cell (DSSCs).<sup>24</sup>



**Scheme 2.19** : Synthesis of oligomeric poly(ethylene oxide) (PEO)-based bis imidazolium diiodide (PEO<sub>m</sub>BIm-I).

The TiO<sub>2</sub> based dye sensitized solar cell which had been developed by Grätzel has several advantages such as better conversion efficiency and material that made of the cell is cheaper than conventional inorganic photovoltaic devices even though the instability of the dye solar cell was identified as a main challenge. Therefore, there is a need to optimize these properties since solar energy has a great potential to fulfill an important part of the sustainable energy demand for future generation.<sup>70</sup>

Since ionic liquids are known for their chemical and thermal stability, extremely low vapour pressure, nonflammable, high ionic conductivity and wide electrochemical window, this new class of solvent might be a good replacement to the previous organic solvent-based electrolytes. The most frequent ionic liquids used as an electrolyte in DSSCs is iodide-based ionic liquids because of their light sensitivity behavior.

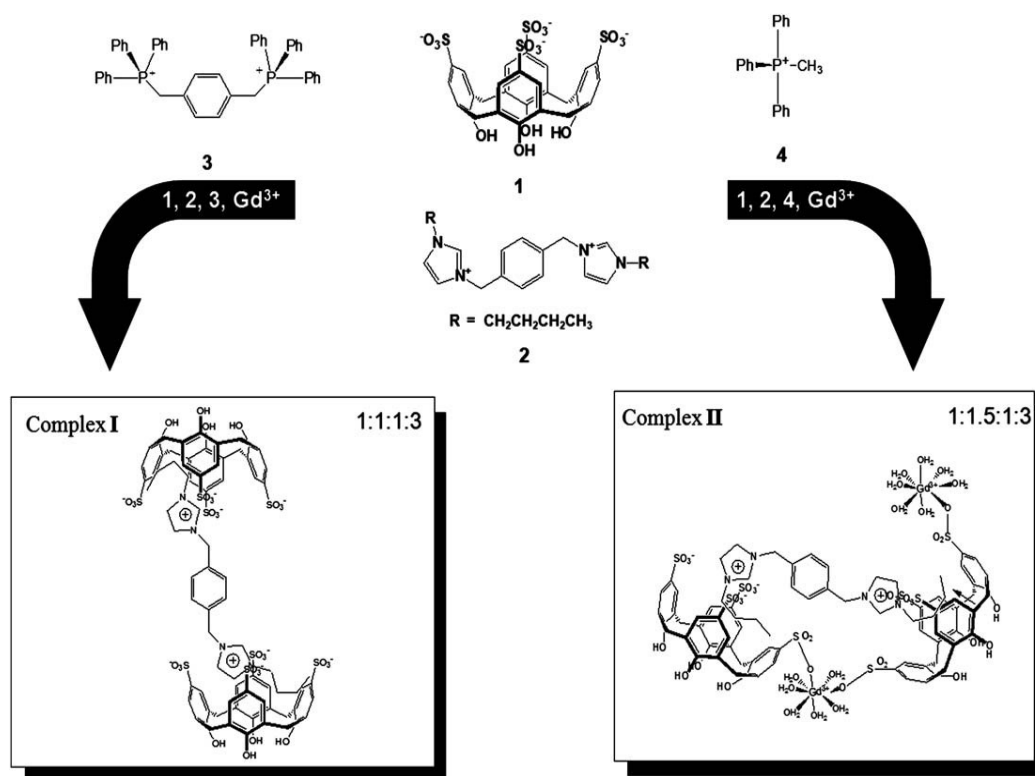
### 2.6.7 Dicationic ionic liquids in self-assembly chemistry

Self-assembly is regarded as a part of supramolecular synthesis since it involves generation of supramolecular entities from molecular components involving inherently weak interactions. Self-assembly is a very powerful strategy for the formation of structural and functional complexes.<sup>71</sup> The design and characterization of self-assembled molecular capsules is gaining prominence, mainly because of their potential application in biological system.

*p*-Sulfonatocalix[4]arene is a bucket-shaped macromolecule with the smallest ring size among the cavities of calixarenes. Its cavity is known to selectively entrap a wide range of guest molecules with various size, shape and chemical functionality through intermolecular forces. The lower rim is functionalized by phenolic –OH groups while the upper rim is functionalized with sulfonate groups creating an amphiphilic behavior and has been extensively investigated in self-assembly chemistry.<sup>72</sup>

Ling, I., *et. al.* had done few experiments on multi-component self assembled systems involving monocationic ionic liquids and dicationic ionic liquids with *p*-sulfonatocalix[4]arene.<sup>73-78</sup> One of the experiments reported the self-assembly of *N,N'*-[1,4-phenylenebis(methylene)]bis(*N,N*-dibutylimidazolium) ([Bim]<sup>2+</sup>) cation, bis-phosphonium cations or methyl triphenyl phosphonium cation and *p*-sulfonatocalix[4]arene. The [Bim] cations are selectively filled into the cavities of the calixarene, constructing diverse structural configuration of host-guest complexes. The synthesis of complexes **I** and **II** were done by varying the molar ratio of the [Bim] cation, with the formation of complex **II** involving an excess of the cation. The [Bim] moiety in both complexes is effectively end-capped by two calixarenes with the [Bim] cation selectively drawn into the

cavities of calixarene in a slight pinched cone configuration with the two calixarene phenyl rings pinching the imidazolium molecule while the other two phenyl rings splayed apart. Complex **I** forms a ‘molecular capsule’, shrouded by scaffold networks of the bis-phosphonium cations, whereas complex **II** has calixarenes arranged at 90° with respect to each other, forming a continuous polymeric material.<sup>76</sup>



Scheme 2.20 : Schematic representation of the formation of complex **I** and **II**.<sup>76</sup>

From the result, it can be concluded that the imidazolium cation is selectively taken up into the cavities of *p*-sulfonatocalix[4]arene rather than phosphonium cation and the length of the alkyl side chain attached to the imidazolium cation affect the nature of the structure formation.

## CHAPTER 3 :

### Experimental Procedures

#### 3.1 Chemicals :

Pyridine, triethylamine, 1-methylpiperidine, 1-methylmorpholine, 1-methylpyrrolidine, 1-butylpyrrolidine, 2-(dimethylamino)ethanol and 2-(diethylamino)ethanol were purchased from Merck Chemicals and used as received.  $\alpha,\alpha$ -Dibromo-*p*-xylene (98%) was purchased from Sigma-Aldrich<sup>®</sup> and recrystallized from acetonitrile prior to use. Dry acetonitrile (0.005% water) was purchased from Sigma-Aldrich<sup>®</sup>. Lithium bis(trifluoromethanesulfonyl)imide and ammonium hexafluorophosphate were purchased from Across Organics. All solvents used were analytical grade and used as received. Deuterated solvents were purchased from Merck Chemicals and Sigma-Aldrich<sup>®</sup>.

#### 3.2 Instrumentations :

##### 3.2.1 <sup>1</sup>H NMR and <sup>13</sup>C NMR spectra:

<sup>1</sup>H NMR (400 MHz) and <sup>13</sup>C NMR (100 MHz) spectra were recorded on Lambda JEOL 400 FT-NMR spectrometer. Acetonitrile (CD<sub>3</sub>CN-D<sub>3</sub>), deuterium oxide (D<sub>2</sub>O), and dimethylsulfoxide (DMSO-D<sub>6</sub>) were used as solvents.

##### 3.2.2 Infra red spectra:

Infra-red spectra were recorded on a Perkin Elmer RX-1 FT-IR Spectrometer for moisture-stable dicationic ionic liquids (PF<sub>6</sub><sup>-</sup> and NTf<sub>2</sub><sup>-</sup>) as KBr discs. An ATR-FTIR Perkin Elmer Spectrum 400 FT-IR/FT-FIR Spectrometer was used for moisture sensitive ionic liquids (Br<sup>-</sup>).

### 3.2.3 Elemental analysis:

Carbon, hydrogen, nitrogen and sulfur analyses were performed on the Perkin Elmer Series II 2400 CHNS/O Analyzer. Sample was weighted between 1.5-2.0 mg weight averages for carbon, hydrogen and nitrogen analyses while 2.0-2.5 mg weight average for carbon, hydrogen, nitrogen and sulfur analyses.

### 3.2.4 Differential scanning calorimetry (DSC) experiment:

The phase transitions such as melting temperature of ionic liquids were measured in Perkin Elmer<sup>®</sup> Pyris 6 DSC. The samples were weight between 1-1.5 mg and then heated at the rate of 10°Cmin<sup>-1</sup> from 40°C to 400°C.

### 3.2.5 Thermo gravimetric analysis (TGA):

The decomposition temperature was carried out on a Perkin Elmer<sup>®</sup> Pyris Diamond TG/DTA. Samples of average weight of ca. 5 mg were placed in a ceramic pan and heated at scan rate of 10°Cmin<sup>-1</sup> from 40°C to 900°C.

### 3.2.6 Halides analysis:

The analysis of bromide levels in bistriflamide (NTf<sub>2</sub><sup>-</sup>) and hexafluorophosphate (PF<sub>6</sub><sup>-</sup>) ionic liquids was conducted using Metrohm 850 Professional Ion Chromatography with suppressor module, equipped with an Metrosep A supp 4 column (250 x 4.0 mm) in part per million (ppm) levels. The anions were detected using a suppressed conductivity detector. The injection volume was 20 µL for each sample. The flow rate of eluent was maintained at 1.0 cm<sup>3</sup>/min. Data were collected using a Metrohm 850 data acquisition system interfaced to a computer running MagICNet software (Metrohm).

Millipore Milli-Q 18 M $\Omega$  water were used for all eluent, sample and standard preparation. HPLC grade acetonitrile were used as solvents to dilute the ionic liquids. Analytical sodium carbonate (Merck) and sodium hydrogen carbonate (Merck) used to prepare the eluent.

IC samples were prepared by dissolving 0.010 g of organic salt in acetonitrile before being diluted with deionized water to give 25% CH<sub>3</sub>CN/H<sub>2</sub>O solution.

### 3.2.7 X-Ray crystallography studies:

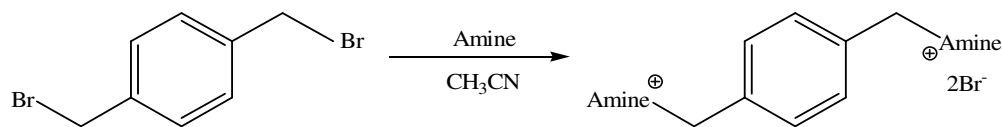
The crystal data collected from a Bruker SMART APEX2 diffractometer Bruker (2009); cell refinement: SAINT Bruker (2009); data reduction: SAINT; program(s) used to solve crystal structure: SHELXS97 Sheldrick (2008); program(s) used to refine structure: SHELXL97 Sheldrick (2008) ; molecular graphics : XSEED (L. J. Barbour *et. al.*, 2001) software used to prepare material for publication : publCIF (S. P. Westrip, 2010). All the non-hydrogen atoms were refined anisotropically and all the hydrogen atoms were placed at calculated positions and refined isotropically.



### 3.3 Synthesis Section:

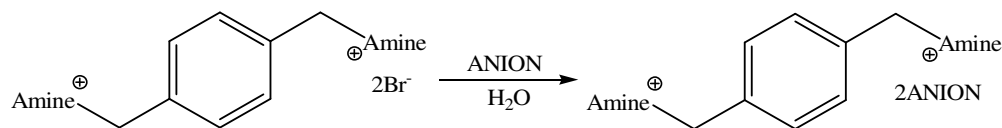
The schematic diagram of reactions can be simplified as follows:

1. Alkylation reaction :



Amine = pyridine (pyr), triethylamine (tea), 1-methylpyrrolidine (mpyl), 1-butylpyrrolidine (bpyl), 1-methylpiperidine (nmpp), 1-methylmorpholine (mmorp), 2-(dimethylamino)ethanol (dmae), 2-(diethylamino)ethanol (deae).

2. Anion exchange reaction (metathesis) :



ANIONS =  $\text{PF}_6^-$  and  $\text{NTf}_2^-$

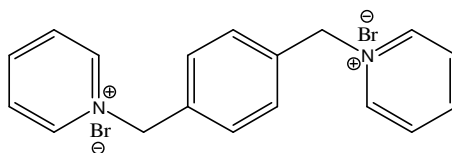
**Scheme 3.01:** Synthesis routes of dicationic ionic liquids.

#### 3.3.1 Preparation and characterization of **bromide** salts

In a round bottom flask, 2.6397 g (0.010 mol) of  $\alpha,\alpha$ -dibromo-*p*-xylene was dissolved in dried acetonitrile (50 mL) and stirred to accelerate the dissolution. An excess amount of tertiary amine (0.011 mol) was added dropwise to the stirred solution. The mixture was stirred for 24 hour in room temperature to ensure the completeness of the reaction. The product was immiscible in acetonitrile and precipitated out as a white solid. The solid was filtered quickly and washed with hot acetonitrile (2 x 20mL) to dissolve the unreacted reagent and then dried under vacuum for at least 24 hours to remove traces of solvents and moisture. The product was recrystallized in an appropriate solvent. Traces of solvent was again removed under vacuum for several hours and then stored in a desiccator for future use. The chemical structure was confirmed by  $^1\text{H}$  NMR and  $^{13}\text{C}$  NMR spectroscopy.

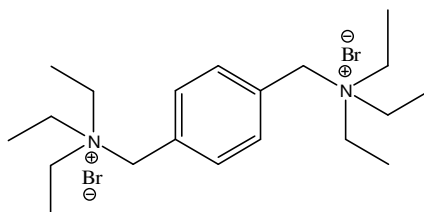
### 3.3.1.1 [Pyr]<sup>2+</sup>.2[Br]<sup>-</sup>

The product was a colourless needle-shaped crystal and further recrystallized from ethanol/methanol mixture (yield 88%). <sup>1</sup>H NMR result for the solid is as follows (400 MHz, D<sub>2</sub>O) δ (ppm) : 4.67 (dd, methylene carbon), 7.49 (d, phenylene ring), 8.01 (t, J<sub>(H,H)</sub> = 7.08 Hz, -NCH=CH-), 8.49 (t, J<sub>(H,H)</sub> = 7.70 Hz, HC-CH=C), 9.16 (d, J<sub>(H,H)</sub> = 6.36 Hz, -NCH=). <sup>13</sup>C NMR result is as follows (100 MHz, D<sub>2</sub>O) δ (ppm) : 64.92, 129.95, 131.30, 135.01, 145.56 and 146.98. Anal. Calcd. for C<sub>18</sub>H<sub>18</sub>N<sub>2</sub>Br<sub>2</sub> (%) : C 51.21 H 4.30 N 6.64; Found : C 51.02 H 4.51 N 6.58.



### 3.3.1.2 [Tea]<sup>2+</sup>.2[Br]<sup>-</sup>

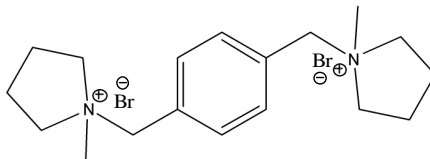
The product was a colourless block-shaped crystal and further recrystallized from methanol (yield 95%). The <sup>1</sup>H NMR spectrum results for the solid are as follows (400MHz, D<sub>2</sub>O) δ (ppm) : 1.31 (t, J<sub>(H,H)</sub> = 7.20 Hz, -CH<sub>3</sub>), 3.17 (q, J<sub>(H,H)</sub> = 7.32 Hz, -NCH<sub>2</sub>-), 4.39 (dd, methylene carbon), 7.52 (d, phenylene ring). <sup>13</sup>C NMR result is as follows (100 MHz, D<sub>2</sub>O) δ (ppm) : 7.99, 53.38, 60.03, 130.41 and 134.05. Anal. Calcd. for C<sub>20</sub>H<sub>38</sub>N<sub>2</sub>Br<sub>2</sub> (%) : C 51.51 H 8.21 N 6.01; Found C 50.97 H 8.74 N 5.97.



### 3.3.1.3 [Mpyl]<sup>2+</sup>.2[Br]<sup>-</sup>

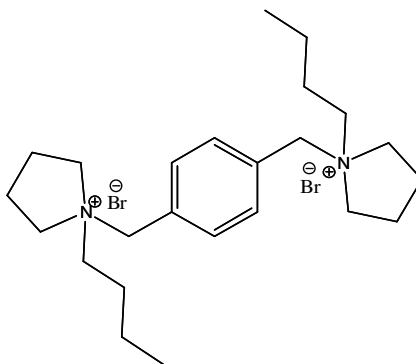
The product was a colourless block-shaped crystal (yield 85%). The single crystal of compound was obtained from cold acetonitrile. The <sup>1</sup>H NMR spectrum results for the solid are as follows (400 MHz, D<sub>2</sub>O) δ (ppm) : 2.16 (m, J<sub>(H,H)</sub> = 4 Hz, -NCH<sub>2</sub>CH<sub>2</sub>-), 2.87 (s, -CH<sub>3</sub>), 3.38 (m, J<sub>(H,H)</sub> = 4.00 Hz, -NCH<sub>2</sub>), 3.52 (m, J<sub>(H,H)</sub> = 4.00 Hz, -NCH<sub>2</sub>), 4.44 (dd, methylene carbon), 7.62 (d, phenylene ring). <sup>13</sup>C NMR result is

as follows (100 MHz, D<sub>2</sub>O)  $\delta$  (ppm) : 22.37, 45.04, 65.02, 67.34, 131.27 and 134.92. Anal. Calcd. for C<sub>18</sub>H<sub>30</sub>N<sub>2</sub>Br<sub>2</sub> (%) : C 49.79 H 6.96 N 6.45; Found C 49.98 H 7.13 N 6.06.



#### 3.3.1.4 [Bpyl]<sup>2+</sup>.2[Br]<sup>-</sup>

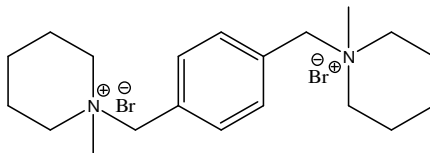
The product was a white precipitate. The solid was further recrystallized from methanol (yield 85%). The <sup>1</sup>H NMR spectrum results for the solid are as follows (400 MHz, D<sub>2</sub>O)  $\delta$  (ppm) : 0.82 (t, J<sub>(H,H)</sub> = 7.32 Hz, -CH<sub>3</sub>), 1.24 (sextet, J<sub>(H,H)</sub> = 7.32 Hz, -CH<sub>2</sub>CH<sub>3</sub>), 1.77 (m, J<sub>(H,H)</sub> = 4.00 Hz, -CH<sub>2</sub>CH<sub>2</sub>CH<sub>3</sub>), 2.12 (m, -NCH<sub>2</sub>CH<sub>2</sub>-), 3.02 (q, J<sub>(H,H)</sub> = 4.28 Hz, -NCH<sub>2</sub>CH<sub>2</sub>CH<sub>2</sub>CH<sub>3</sub>), 3.48 (m, J<sub>(H,H)</sub> = 4.00 Hz, -NCH<sub>2</sub>-), 4.45 (dd, methylene carbon), 7.57 (d, phenylene ring). <sup>13</sup>C NMR result is as follows (100 MHz, D<sub>2</sub>O)  $\delta$  (ppm) : 13.75, 20.63, 22.47, 26.25, 60.04, 62.68, 131.25 and 133.75. Anal. Calcd. for C<sub>24</sub>H<sub>42</sub>N<sub>2</sub>Br<sub>2</sub> (%) : C 55.60 H 8.17 N 5.40; Found C 55.83 H 9.73 N 5.39.



#### 3.3.1.5 [Nmpp]<sup>2+</sup>.2[Br]<sup>-</sup>

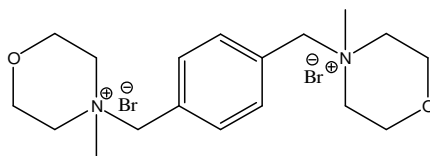
The product was a white precipitate. The solid was further recrystallized from methanol (yield 85%). The <sup>1</sup>H NMR spectrum results for the solid are as follows (400 MHz, D<sub>2</sub>O)  $\delta$  (ppm) : 1.56 (m, J<sub>(H,H)</sub> = 4.00 Hz, -CH<sub>2</sub>CH<sub>2</sub>CH<sub>2</sub>-), 1.66 (m, J<sub>(H,H)</sub> = 4.00 Hz, -NCH<sub>2</sub>-), 1.88 (m, J<sub>(H,H)</sub> = 4.00 Hz, -CH<sub>2</sub>N-), 2.94 (s, -CH<sub>3</sub>), 3.34 (m, J<sub>(H,H)</sub> = 4.00 Hz, -NCH<sub>2</sub>CH<sub>2</sub>-), 4.57 (dd, methylene carbon), 7.62 (d, phenylene ring). <sup>13</sup>C NMR result is as follows (100 MHz, D<sub>2</sub>O)  $\delta$  (ppm) : 20.47,

21.38, 47.42, 61.75, 67.88, 130.05 and 134.46. Anal. Calcd. for  $C_{20}H_{34}N_2Br_2$  (%) :  
 C 51.96 H 7.41 N 6.06 ; Found  
 C 51.29 H 8.61 N 5.98.



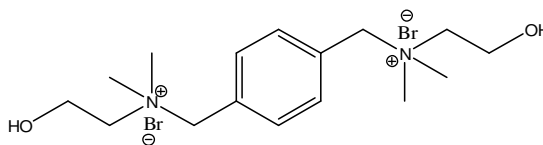
### 3.3.1.6 [Mmorp]<sup>2+</sup>.2[Br]<sup>-</sup>

The product was a white precipitate (yield 90%). The <sup>1</sup>H NMR spectrum results for the solid are as follows (400 MHz, D<sub>2</sub>O) δ (ppm) : 3.07 (s, -CH<sub>3</sub>), 3.34 (d, J<sub>(H,H)</sub> = 12.72 Hz, -NCH<sub>2</sub>-), 3.57 (m, J<sub>(H,H)</sub> = 4.40 Hz, -CH<sub>2</sub>N-), 3.97 (m, J<sub>(H,H)</sub> = 12.00 Hz, -CH<sub>2</sub>O-), 4.68 (dd, methylene carbon), 7.65 (d, phenylene ring). <sup>13</sup>C NMR result is as follows (100 MHz, D<sub>2</sub>O) δ (ppm) : 46.65, 60.11, 61.27, 69.52, 129.60 and 134.76. Anal. Calcd. for  $C_{18}H_{30}N_2O_2Br_2$  (%) : C 46.37 H 6.49 N 6.01; Found C 45.77 H 7.68 N 5.93.



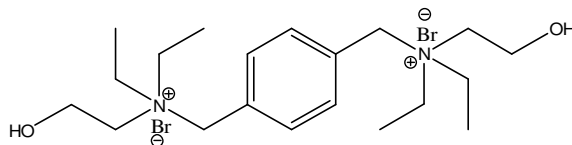
### 3.3.1.7 [Dmae]<sup>2+</sup>.2[Br]<sup>-</sup>

The product was a white precipitate (yield 90%). The <sup>1</sup>H NMR spectrum results for the solid are as follows (400 MHz, D<sub>2</sub>O) δ (ppm) : 3.07 (s, -CH<sub>3</sub>), 3.43 (t, -NCH<sub>2</sub>-), 4.04 (s, -CH<sub>2</sub>OH), 4.55 (dd, methylene carbon), 7.67 (d, phenylene ring). <sup>13</sup>C NMR result is as follows (100 MHz, D<sub>2</sub>O) δ (ppm) : 51.50, 56.35, 66.45, 69.29, 130.53 and 134.70. Anal. Calcd. for  $C_{16}H_{30}N_2O_2Br_2$  (%) : C 43.46 H 6.84 N 6.33; Found : C 43.45 H 7.30 N 6.26.



### 3.3.1.8 [Deae]<sup>2+</sup>.2[Br]<sup>-</sup>

The product was a white precipitate (yield 90%). The solid was further recrystallized from methanol (yield 85%). The <sup>1</sup>H NMR spectrum results for the solid are as follows (400 MHz, D<sub>2</sub>O) δ (ppm) : 1.32 (t, J<sub>(H,H)</sub> = 7.07 Hz, -CH<sub>3</sub>), 3.27 (q, J<sub>(H,H)</sub> = 7.08 Hz, -NCH<sub>2</sub>-), 3.99 (s, -CH<sub>2</sub>OH), 4.48 (dd, methylene carbon), 7.53 (d, phenylene ring). <sup>13</sup>C NMR result is as follows (100 MHz, D<sub>2</sub>O) δ (ppm) : 8.81, 55.10, 56.30, 58.75, 61.88, 131.20 and 134.34. Anal. Calcd. for C<sub>20</sub>H<sub>38</sub>N<sub>2</sub>O<sub>2</sub>Br<sub>2</sub> (%): C 48.20 H 7.69 N 5.62; Found : C 47.87 H 8.59 N 5.54.

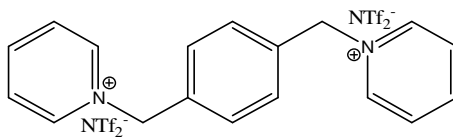


### 3.3.2 Preparation and characterization of bis(trifluoromethanesulfonyl)imide salts (NTf<sub>2</sub><sup>-</sup>)

The series of quarternized salt from section 3.3.1 (0.010 mol) was dissolve in water (20 mL), lithium bis(trifluoromethanesulfonyl)imide (0.022 mol, g) was added to the solution and was stirred overnight. The resulting product precipitated out from the aqueous solution as a white solid. The insoluble product was separated from water solution by filtration and was washed with distilled water (3 x 50 mL) to remove excess starting materials. The product was recrystallized in an appropriate solvent before drying under vacuum at 60-70°C for several hours. The chemical structure was confirmed by <sup>1</sup>H NMR and <sup>13</sup>C NMR spectroscopy to ensure if there are any changes to the chemical structure of cation after metathesis takes place.

#### 3.3.2.1 [Pyr]<sup>2+</sup>.2[NTf<sub>2</sub>]<sup>-</sup>

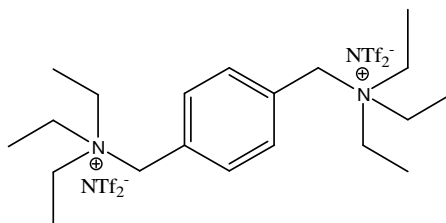
The product was a white precipitate. This solid was recrystallized from ethyl acetate (yield 93%). The <sup>1</sup>H NMR spectrum results for the solid are as follows (400 MHz, CD<sub>3</sub>CN) δ (ppm) : 5.73 (dd, methylene carbon), 7.50 (d, phenylene ring), 8.04 (t, J<sub>(H,H)</sub> = 7.08 Hz, -NCH=CH-), 8.53 (t, J<sub>(H,H)</sub> = 7.70 Hz, HC-CH=C), 8.73 (d, J<sub>(H,H)</sub> = 6.36 Hz, -NCH=). <sup>13</sup>C NMR result is as follows: (100 MHz, CD<sub>3</sub>CN) δ (ppm) : 63.86, 115.13, 118.35, 121.57, 124.78, 128.79, 130.18, 134.58, 144.65 and 146.52. IR results: 1056.72 cm<sup>-1</sup> (ν S=O), 1140.05, 1186.86 cm<sup>-1</sup> (ν C-N), 1358.92 cm<sup>-1</sup> (ν -CF<sub>3</sub>). Anal. Calcd. for C<sub>22</sub>H<sub>18</sub>N<sub>4</sub>F<sub>12</sub>O<sub>8</sub>S<sub>4</sub> (%) : C 32.12 H 2.21 N 6.81 S 15.59; Found C 32.37 H 2.12 N 7.24 S 16.23.



#### 3.3.2.2 [Tea]<sup>2+</sup>.2[NTf<sub>2</sub>]<sup>-</sup>

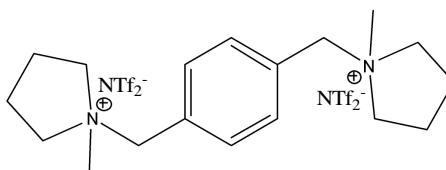
The product was a white precipitate and was further recrystallized from ethanol/methanol mixture (yield 97%). The <sup>1</sup>H NMR spectrum results for the solid are as follows (400 MHz, DMSO) δ (ppm) : 1.31 (t, J<sub>(H,H)</sub> = 7.20 Hz, -CH<sub>3</sub>), 3.16 (q, J<sub>(H,H)</sub> = 7.32 Hz, -NCH<sub>2</sub>-), 4.47 (dd, methylene carbon), 7.58 (d,

phenylene ring).  $^{13}\text{C}$  NMR result is as follows (100 MHz,  $\text{CD}_3\text{CN}$ )  $\delta$  (ppm) : 7.15, 52.67, 59.37, 115.15, 118.37, 121.59, 124.81, 129.63 and 133.33. IR results:  $1049.01\text{ cm}^{-1}$  ( $\nu\text{ S=O}$ ),  $1138.23$ ,  $1180.90\text{ cm}^{-1}$  ( $\nu\text{ C-N}$ ),  $1354.12\text{ cm}^{-1}$  ( $\nu\text{ -CF}_3$ ). Anal. Calcd. for  $\text{C}_{24}\text{H}_{38}\text{N}_4\text{F}_{12}\text{O}_8\text{S}_4$  (%) : C 33.25 H 4.42 N 6.46 S 14.48; Found C 33.51 H 4.29 N 6.58 S 14.89.



### 3.3.2.3 [Mpyl] $^{2+}$ .2[NTf $_2$ ] $^-$

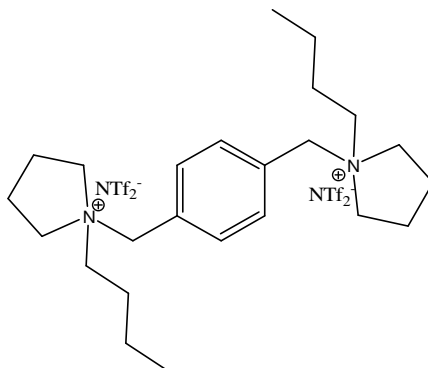
The product was a colourless block-shaped crystal and it was recrystallized from acetonitrile (yield 90%). The  $^1\text{H}$  NMR spectrum results for the solid are as follows (400 MHz,  $\text{CD}_3\text{CN}$ )  $\delta$  (ppm) : 1.81 (m,  $J_{(\text{H,H})} = 4\text{ Hz}$ ,  $-\text{NCH}_2\text{CH}_2-$ ), 2.51 (s,  $-\text{CH}_3$ ), 3.00 (m,  $J_{(\text{H,H})} = 4.00\text{ Hz}$ ,  $-\text{NCH}_2-$ ), 3.17 (m,  $J_{(\text{H,H})} = 4.00\text{ Hz}$ ,  $-\text{NCH}_2-$ ), 4.12 (dd, methylene carbon), 7.28 (d, phenylene ring).  $^{13}\text{C}$  NMR result is as follows (100 MHz,  $\text{CD}_3\text{CN}$ )  $\delta$  (ppm) : 20.87, 47.73, 63.64, 65.76, 115.13, 118.35, 121.57, 124.78, 130.70 and 133.22. IR results:  $1054.17\text{ cm}^{-1}$  ( $\nu\text{ S=O}$ ),  $1140.10$ ,  $1201.50\text{ cm}^{-1}$  ( $\nu\text{ C-N}$ ),  $1354.27\text{ cm}^{-1}$  ( $\nu\text{ -CF}_3$ ). Anal. Calcd. for  $\text{C}_{22}\text{H}_{30}\text{N}_4\text{F}_{12}\text{O}_8\text{S}_4$  (%) : C 31.65 H 3.62 N 6.71 S 15.37; Found C 31.81 H 3.18 N 6.90 S 14.97.



### 3.3.2.4 [Bpyl] $^{2+}$ .2[NTf $_2$ ] $^-$

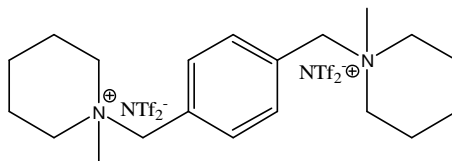
The product was a colourless block-shaped crystal and it was recrystallized from acetonitrile (yield 95%). The  $^1\text{H}$  NMR spectrum results for the solid are as follows ( $\text{CD}_3\text{CN}$ )  $\delta$  (ppm) : 1.07 (t,  $J_{(\text{H,H})} = 7.32\text{ Hz}$ ,  $-\text{CH}_3$ ), 1.46 (sextet,  $J_{(\text{H,H})} = 7.32\text{ Hz}$ ,  $-\text{CH}_2\text{CH}_3$ ), 1.97 (m,  $J_{(\text{H,H})} = 4.00\text{ Hz}$ ,  $-\text{CH}_2\text{CH}_2\text{CH}_3$ ), 2.23 (m,  $-\text{NCH}_2\text{CH}_2-$ ), 3.15 (q,  $J_{(\text{H,H})} = 4.28\text{ Hz}$ ,  $-\text{NCH}_2\text{CH}_2\text{CH}_2\text{CH}_3$ ), 3.49 (m,  $J_{(\text{H,H})} = 4.00\text{ Hz}$ ,  $-\text{NCH}_2-$ ), 4.52 (dd, methylene carbon), 7.70 (d, phenylene ring).  $^{13}\text{C}$  NMR result is as follows (100 MHz,  $\text{CD}_3\text{CN}$ )  $\delta$  (ppm) : 13.79, 20.31, 21.95, 25.73,

60.23, 62.44, 116.56, 119.37, 122.55, 125.98, 131.53 and 134.21. **IR** results: 1054.72  $\text{cm}^{-1}$  ( $\nu$  S=O), 1142.74, 1197.11  $\text{cm}^{-1}$  ( $\nu$  C-N), 1351.49  $\text{cm}^{-1}$  ( $\nu$  -CF<sub>3</sub>). Anal. Calcd. for C<sub>28</sub>H<sub>42</sub>N<sub>4</sub>F<sub>12</sub>O<sub>8</sub>S<sub>4</sub> (%) : C 36.60 H 4.61 N 6.10 S 13.96; Found C 36.99 H 4.30 N 6.40 S 14.37.



### 3.3.2.5 [Nmpp]<sup>2+</sup>.2[NTf<sub>2</sub>]<sup>-</sup>

The product was a colourless block-shaped crystal and it was recrystallized from acetonitrile (yield 95%). The <sup>1</sup>H NMR spectrum results for the solid are as follows (400 MHz, CD<sub>3</sub>CN)  $\delta$  (ppm) : 1.57 (m,  $J_{\text{(H,H)}} = 4.00$  Hz, -CH<sub>2</sub>CH<sub>2</sub>CH<sub>2</sub>-), 1.73 (m,  $J_{\text{(H,H)}} = 4.00$  Hz, -NCH<sub>2</sub>-), 1.90 (m,  $J_{\text{(H,H)}} = 4.00$  Hz, -CH<sub>2</sub>N-), 2.97 (s, -CH<sub>3</sub>), 3.31 (m,  $J_{\text{(H,H)}} = 4.00$  Hz, -NCH<sub>2</sub>CH<sub>2</sub>-), 4.50 (dd, methylene carbon), 7.65 (d, phenylene ring). <sup>13</sup>C NMR result is as follows (100 MHz, CD<sub>3</sub>CN)  $\delta$  (ppm) : 19.63, 20.66, 46.38, 60.90, 67.17, 115.14, 118.36, 121.58, 124.80, 129.45 and 133.71. **IR** results: 1055.21  $\text{cm}^{-1}$  ( $\nu$  S=O), 1143.36, 1194.17  $\text{cm}^{-1}$  ( $\nu$  C-N), 1351.51  $\text{cm}^{-1}$  ( $\nu$  -CF<sub>3</sub>). Anal. Calcd. for C<sub>24</sub>H<sub>34</sub>N<sub>4</sub>F<sub>12</sub>O<sub>8</sub>S<sub>4</sub> (%) : C 33.41 H 3.97 N 6.49 S 14.87; Found C 33.71 H 3.92 N 6.61 S 14.34.

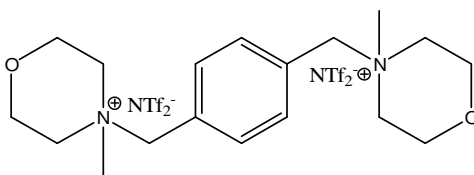


### 3.3.2.6 [Mmorp]<sup>2+</sup>.2[NTf<sub>2</sub>]<sup>-</sup>

The product was a colourless block-shaped crystal and it was recrystallized from acetonitrile (yield 95%). The <sup>1</sup>H NMR spectrum results for the solid are as follows (400 MHz, CD<sub>3</sub>CN)  $\delta$  (ppm) : 3.03 (s, -CH<sub>3</sub>), 3.23 (d,  $J_{\text{(H,H)}} = 12.72$  Hz, -NCH<sub>2</sub>-), 3.50 (m,  $J_{\text{(H,H)}} = 4.40$  Hz, -CH<sub>2</sub>N-), 3.95 (m,  $J_{\text{(H,H)}} = 12.00$  Hz, -CH<sub>2</sub>O-),

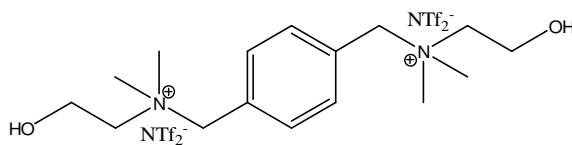


4.48 (dd, methylene carbon), 7.61 (d, phenylene ring).  $^{13}\text{C}$  NMR result is as follows (100 MHz,  $\text{CD}_3\text{CN}$ )  $\delta$  (ppm) : 45.40, 59.40, 60.19, 68.40, 115.11, 118.33, 121.55, 124.77, 128.99, and 133.93. **IR** results:  $1057.19\text{ cm}^{-1}$  ( $\nu\text{ S=O}$ ),  $1128.29$ ,  $1209.67\text{ cm}^{-1}$  ( $\nu\text{ C-N}$ ),  $1356.63\text{ cm}^{-1}$  ( $\nu\text{ -CF}_3$ ). Anal. Calcd. for  $\text{C}_{22}\text{H}_{30}\text{N}_4\text{F}_{12}\text{O}_{10}\text{S}_4$  (%): C 30.49 H 3.49 N 6.46 S 14.80; Found C 30.30 H 3.13 N 6.25 S 15.88.



### 3.3.2.7 [Dmae] $^{2+}$ .2[NTf $_2$ ] $^-$

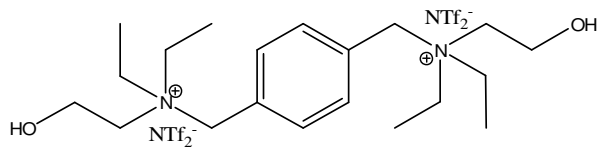
The product was a white precipitate and it was recrystallized from acetonitrile (yield 95%). The  $^1\text{H}$  NMR spectrum results for the solid are as follows (400 MHz,  $\text{CD}_3\text{CN}$ )  $\delta$  (ppm) : 3.05 (s,  $-\text{CH}_3$ ), 3.43 (t,  $-\text{NCH}_2-$ ), 3.64 (t,  $J_{(\text{H,H})} = 4.76\text{ Hz}$ ,  $-\text{OH}$ ), 4.04 (s,  $-\text{CH}_2\text{OH}$ ), 4.55 (dd, methylene carbon), 7.67 (d, phenylene ring).  $^{13}\text{C}$  NMR result is as follows (100 MHz,  $\text{CD}_3\text{CN}$ )  $\delta$  (ppm) : 51.87, 56.90, 66.88, 69.38, 116.25, 118.13 (slvt), 118.75, 122.50, 125.63, 130.71 and 134.94. **IR** results:  $1046.31\text{ cm}^{-1}$  ( $\nu\text{ S=O}$ ),  $1135.37$ ,  $1186.71\text{ cm}^{-1}$  ( $\nu\text{ C-N}$ ),  $1344.11\text{ cm}^{-1}$  ( $\nu\text{ -CF}_3$ ). Anal. Calcd. for  $\text{C}_{20}\text{H}_{30}\text{N}_4\text{F}_{12}\text{O}_{10}\text{S}_4$  (%): C 28.50 H 3.59 N 6.65 S 15.22; Found C 28.89 H 3.51 N 6.89 S 15.41.



### 3.3.2.8 [Deae] $^{2+}$ .2[NTf $_2$ ] $^-$

The product was a white precipitate and it was recrystallized from acetonitrile (yield 95%). The  $^1\text{H}$  NMR spectrum results for the solid are as follows (400 MHz,  $\text{CD}_3\text{CN}$ )  $\delta$  (ppm) : 0.87 (t,  $J_{(\text{H,H})} = 7.08\text{ Hz}$ ,  $-\text{CH}_3$ ), 2.77 (q,  $J_{(\text{H,H})} = 7.08\text{ Hz}$ ,  $-\text{NCH}_2-$ ), 3.51 (s,  $-\text{CH}_2\text{OH}$ ), 3.49 (dd, methylene carbon), 7.10 (d, phenylene ring).  $^{13}\text{C}$  NMR result is as follows (100 MHz,  $\text{CD}_3\text{CN}$ )  $\delta$  (ppm) : 8.41, 55.01, 56.19, 59.35, 116.22, 118.45 (slvt), 119.38, 122.67, 125.83, 130.96 and 134.78. **IR**

results: 1049.66  $\text{cm}^{-1}$  ( $\nu$  S=O), 1136.92, 1187.70  $\text{cm}^{-1}$  ( $\nu$  C-N), 1344.18  $\text{cm}^{-1}$  ( $\nu$  – CF<sub>3</sub>). Anal. Calcd. for C<sub>24</sub>H<sub>38</sub>N<sub>4</sub>F<sub>12</sub>O<sub>10</sub>S<sub>4</sub> (%) : C 32.07 H 4.26 N 6.23 S 14.27; Found C 31.96 H 4.38 N 6.44 S 14.71.

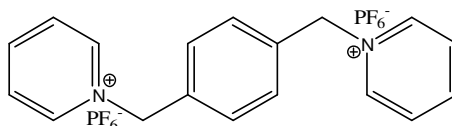


### 3.3.3 Preparation and characterization of hexafluorophosphate salts ( $\text{PF}_6^-$ )

The series of quarternized salt from section 3.3.1 (0.010 mol) was dissolve in water (20 mL), the ammonium hexafluorophosphate (0.022 mol, g) was added to the solution and was stirred overnight. The resulting product was precipitate out from the aqueous solution as a white solid. The insoluble product was separated from water solution by filtration and was washed with water (3 x 50 mL) to remove excess starting materials. The product was recrystallized in an appropriate solvent before drying under vacuum at 60-70°C for several hours. The chemical structure was confirmed by  $^1\text{H}$  NMR and  $^{13}\text{C}$  NMR spectroscopy to ensure if there are any changes to the chemical structure of cation after metathesis takes place.

#### 3.3.3.1 $[\text{Pyr}]^{2+} \cdot 2[\text{PF}_6]^-$

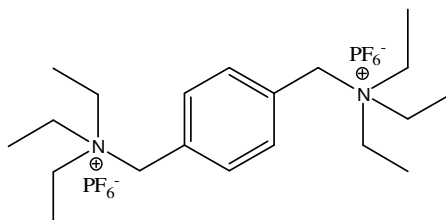
The product was a colourless block-shaped crystal and it was recrystallized from acetonitrile (yield 92%). The  $^1\text{H}$  NMR spectrum results for the solid are as follows (400 MHz, DMSO)  $\delta$  (ppm) : 5.83 (dd, methylene carbon), 7.60 (d, phenylene ring), 8.16 (t,  $J_{(\text{H,H})} = 7.08$  Hz,  $-\text{NCH}=\text{CH}-$ ), 8.60 (t,  $J_{(\text{H,H})} = 7.70$  Hz,  $\text{HC}-\text{CH}=\text{C}$ ), 9.15 (d,  $J_{(\text{H,H})} = 6.36$  Hz,  $-\text{NCH}=\text{C}$ ).  $^{13}\text{C}$  NMR result is as follows (100 MHz, DMSO)  $\delta$  (ppm) : 62.55, 128.13, 128.78, 135.05, 144.95 and 146.25. IR results:  $556.99\text{ cm}^{-1}$  and  $835.16\text{ cm}^{-1}$  ( $\nu$   $\text{PF}_6$ ). Anal. Calcd. for  $\text{C}_{18}\text{H}_{18}\text{N}_2\text{F}_{12}\text{P}_2$  (%): C 39.15, H 3.28, N 5.07; Found : C 38.71, H 2.89, N 5.06.



#### 3.3.3.2 $[\text{Tea}]^{2+} \cdot 2[\text{PF}_6]^-$

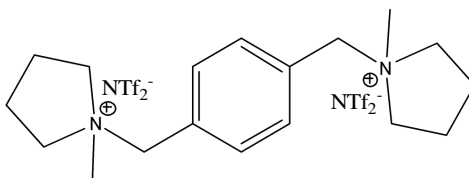
The product was a colourless prism-shaped crystal and it was recrystallized from acetonitrile (yield 92%). The  $^1\text{H}$  NMR spectrum results for the solid are as follows (400 MHz,  $\text{CD}_3\text{CN}$ )  $\delta$  (ppm) = 1.33 (t,  $J_{(\text{H,H})} = 7.20$  Hz,  $-\text{CH}_3$ ), 3.16 (q,  $J_{(\text{H,H})} = 7.32$  Hz,  $-\text{NCH}_2-$ ), 4.37 (dd, methylene carbon), 7.57 (d, phenylene ring).  $^{13}\text{C}$  NMR result is as follows (100 MHz,  $\text{CD}_3\text{CN}$ )  $\delta$  (ppm) : 8.14, 53.71, 60.46,

130.68 and 134.34. **IR** results: 558.18  $\text{cm}^{-1}$  and 838.63  $\text{cm}^{-1}$  ( $\nu$   $\text{PF}_6$ ). Anal. Calcd. for  $\text{C}_{20}\text{H}_{38}\text{N}_2\text{F}_{12}\text{P}_2$  (%) : C 40.27, H 6.42, N 4.70; Found : C 39.65, H 6.23, N 4.50.



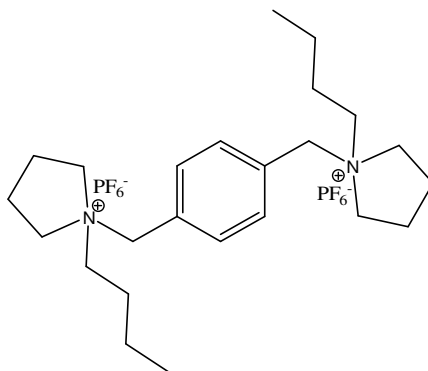
### 3.3.3.3 [Mpyl]<sup>2+</sup>.2[PF<sub>6</sub>]<sup>-</sup>

The product was a white precipitate and it was recrystallized from acetonitrile (yield 88%). The <sup>1</sup>H NMR spectrum results for the solid are as follows (400 MHz, CD<sub>3</sub>CN)  $\delta$  (ppm) : 2.19 (m,  $J_{(\text{H,H})} = 4$  Hz,  $-\text{NCH}_2\text{CH}_2-$ ), 2.88 (s,  $-\text{CH}_3$ ), 3.38 (m,  $J_{(\text{H,H})} = 4.00$  Hz,  $-\text{NCH}_2-$ ), 3.52 (m,  $J_{(\text{H,H})} = 4.00$  Hz,  $-\text{NCH}_2-$ ), 4.46 (dd, methylene carbon), 7.62 (d, phenylene ring). <sup>13</sup>C NMR result is as follows (100 MHz, DMSO)  $\delta$  (ppm) : 21.89, 48.77, 64.64, 66.77, 131.72, and 134.20. **IR** results: 556.16  $\text{cm}^{-1}$  and 827.78  $\text{cm}^{-1}$  ( $\nu$   $\text{PF}_6$ ). Anal. Calcd. for  $\text{C}_{18}\text{H}_{30}\text{N}_2\text{F}_{12}\text{P}_2$  (%) : C 38.31, H 5.36, N 4.96; Found : C 38.27, H 5.14, N 5.02.



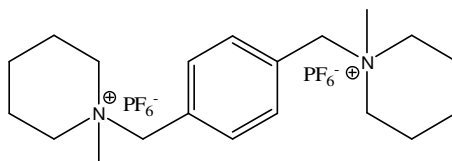
### 3.3.3.4 [Bpyl]<sup>2+</sup>.2[PF<sub>6</sub>]<sup>-</sup>

The product was a colourless block-shaped crystal and it was recrystallized from acetonitrile (yield 96%). The <sup>1</sup>H NMR spectrum results for the solid are as follows (CD<sub>3</sub>CN)  $\delta$  (ppm) : 1.03 (t,  $J_{(\text{H,H})} = 7.32$  Hz,  $-\text{CH}_3$ ), 1.44 (sextet,  $J_{(\text{H,H})} = 7.32$  Hz,  $-\text{CH}_2\text{CH}_3$ ), 1.91 (m,  $J_{(\text{H,H})} = 4.00$  Hz,  $-\text{CH}_2\text{CH}_2\text{CH}_3$ ), 2.23 (m,  $-\text{NCH}_2\text{CH}_2-$ ), 3.15 (q,  $J_{(\text{H,H})} = 4.28$  Hz,  $-\text{NCH}_2\text{CH}_2\text{CH}_2\text{CH}_3$ ), 3.57 (m,  $J_{(\text{H,H})} = 4.00$  Hz,  $-\text{NCH}_2-$ ), 4.50 (dd, methylene carbon), 7.68 (d, phenylene ring). <sup>13</sup>C NMR result is as follows (100 MHz, CD<sub>3</sub>CN)  $\delta$  (ppm) : 12.88, 19.35, 20.93, 24.71, 59.04, 61.36, 130.56 and 133.22. **IR** results: 554.84  $\text{cm}^{-1}$  and 824.60  $\text{cm}^{-1}$  ( $\nu$   $\text{PF}_6$ ). Anal. Calcd. for  $\text{C}_{24}\text{H}_{42}\text{N}_2\text{F}_{12}\text{P}_2$  (%) : C 44.45, H 6.53, N 4.32; Found : C 43.96, H 6.29, N 4.51.



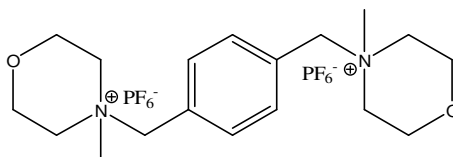
### 3.3.3.5 [Nmpp]<sup>2+</sup>.2[PF<sub>6</sub>]<sup>-</sup>

The product was a white precipitate and it was recrystallized from acetonitrile (yield 96%). The <sup>1</sup>H NMR spectrum results for the solid are as follows (400 MHz, CD<sub>3</sub>CN) δ (ppm) : 1.60 (m, J<sub>(H,H)</sub> = 4.00 Hz, -CH<sub>2</sub>CH<sub>2</sub>CH<sub>2</sub>-), 1.73 (m, J<sub>(H,H)</sub> = 4.00 Hz, -NCH<sub>2</sub>-), 1.92 (m, J<sub>(H,H)</sub> = 4.00 Hz, -CH<sub>2</sub>N-), 2.90 (s, -CH<sub>3</sub>), 3.31 (m, J<sub>(H,H)</sub> = 4.00 Hz, -NCH<sub>2</sub>CH<sub>2</sub>-), 4.46 (dd, methylene carbon), 7.63 (d, phenylene ring). <sup>13</sup>C NMR result is as follows (100 MHz, CD<sub>3</sub>CN) δ (ppm) : 19.90, 20.12, 45.82, 60.36, 66.65, 116.83 (slvt), 128.93 and 133.16. IR results: 553.30 cm<sup>-1</sup> and 827.18 cm<sup>-1</sup> (ν PF<sub>6</sub>). Anal. Calcd. for C<sub>20</sub>H<sub>34</sub>N<sub>2</sub>F<sub>12</sub>P<sub>2</sub> (%) : C 40.55, H 5.78, N 4.73; Found : C 40.80, H 5.35, N 4.79.



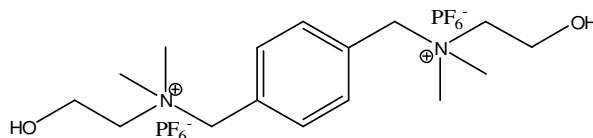
### 3.3.3.6 [Mmorp]<sup>2+</sup>.2[PF<sub>6</sub>]<sup>-</sup>

The product was a white precipitate and it was recrystallized from acetonitrile (yield 96%). The <sup>1</sup>H NMR spectrum results for the solid are as follows (400 MHz, CD<sub>3</sub>CN) δ (ppm) : 3.02 (s, -CH<sub>3</sub>), 3.22 (d, J<sub>(H,H)</sub> = 12.72 Hz, -NCH<sub>2</sub>-), 3.47 (m, J<sub>(H,H)</sub> = 4.40 Hz, -CH<sub>2</sub>N-), 3.94 (m, J<sub>(H,H)</sub> = 12.00 Hz, -CH<sub>2</sub>O-), 4.55 (dd, methylene carbon), 7.58 (d, phenylene ring). <sup>13</sup>C NMR result is as follows: (100 MHz, DMSO) δ (ppm) : 45.03, 58.90, 59.68, 68.08, 116.87 (slvt), 128.49 and 133.40. IR results: 554.55 cm<sup>-1</sup> and 816.91 cm<sup>-1</sup> (ν PF<sub>6</sub>). Anal. Calcd. for C<sub>18</sub>H<sub>30</sub>N<sub>2</sub>O<sub>2</sub>F<sub>12</sub>P<sub>2</sub> (%) : C 36.25, H 5.07, N 4.70; Found : C 36.20, H 4.95, N 4.74.



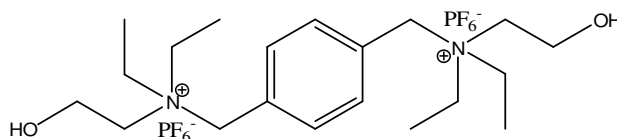
### 3.3.3.7 [Dmae]<sup>2+</sup>.2[PF<sub>6</sub>]<sup>-</sup>

The product was a white precipitate and it was recrystallized from acetonitrile (yield 96%). The <sup>1</sup>H NMR spectrum results for the solid are as follows (400 MHz, CD<sub>3</sub>CN) δ (ppm) : 3.00 (s, -CH<sub>3</sub>), 3.38 (t, -NCH<sub>2</sub>-), 3.65 (t, J<sub>(H,H)</sub> = 4.76 Hz, -OH), 4.01 (s, -CH<sub>2</sub>OH), 4.48 (dd, methylene carbon), 7.62 (d, phenylene ring). <sup>13</sup>C NMR result is as follows (100 MHz, DMSO) δ (ppm) : 52.15, 57.07, 67.05, 69.01, 118.75 (slvt), 131.02, and 134.75. IR results: 555.68 cm<sup>-1</sup> and 824.23 cm<sup>-1</sup> (ν PF<sub>6</sub>). Anal. Calcd. for C<sub>16</sub>H<sub>30</sub>N<sub>2</sub>F<sub>12</sub>O<sub>2</sub>P<sub>2</sub> (%) : C 33.58 H 5.28 N 4.89; Found : C 33.56 H 4.87 N 4.86.



### 3.3.3.8 [Deae]<sup>2+</sup>.2[PF<sub>6</sub>]<sup>-</sup>

The product was a white precipitate and it was recrystallized from acetonitrile (yield 96%). The <sup>1</sup>H NMR spectrum results for the solid are as follows (400 MHz, CD<sub>3</sub>CN) δ (ppm) : 0.85 (t, J<sub>(H,H)</sub> = 7.07 Hz, -CH<sub>3</sub>), 2.77 (q, J<sub>(H,H)</sub> = 7.08 Hz, -NCH<sub>2</sub>-), 3.49 (s, -OH), 3.98 (dd, methylene carbon), 7.09 (d, phenylene ring). <sup>13</sup>C NMR result is as follows (100 MHz, CD<sub>3</sub>CN) δ (ppm) : 8.70, 54.90, 56.25, 59.38, 62.25, 118.75 (slvt), 130.98, and 134.89. IR results: 556.02 cm<sup>-1</sup> and 827.70 cm<sup>-1</sup> (ν PF<sub>6</sub>). Anal. Calcd. for C<sub>20</sub>H<sub>38</sub>N<sub>2</sub>F<sub>12</sub>O<sub>2</sub>P<sub>2</sub> (%) : C 38.22 H 6.09 N 4.46; Found C 38.32 H 6.12 N 4.48.



## Chapter 4:

### Results and Discussions

Eight series of dications including two series of functionalized dications were successfully synthesized namely, pyridinium (Pyr), triethylammonium (Tea), 1-methylpyrrolidinium (Mpyl), 1-butylpyrrolidinium (Bpyl), 1-methylpiperidinium (Nmpp), 1-methylmorpholinium (Mmorp), *N,N*-dimethyl-(2-hydroxy)ethanaminium (Dmae) and *N,N*-diethyl-(2-hydroxy)ethanaminium (Deae) with three types of anion which were bromide ( $\text{Br}^-$ ), hexafluoridophosphate ( $\text{PF}_6^-$ ), bis(trifluoromethanesulfonyl)imide ( $\text{NTf}_2^-$ ), producing 24 kind of ionic liquids. The characterization was done using  $^1\text{H}$  NMR Spectroscopy,  $^{13}\text{C}$  NMR Spectroscopy, FT-IR Spectroscopy, TGA experiment, DSC experiment, CHNS elemental analyses, ion chromatography analysis as well as the solubility test for dicationic ionic liquids in common solvents. The results are presented and discussed as follows.

#### 4.1 : *N,N'*-[1,4-Phenylenebis(methylene)]dipyridinium series

##### 4.1.1 : $^1\text{H}$ NMR and $^{13}\text{C}$ NMR Spectroscopy

Dicationic organic salt  $[\text{Pyr}]^{2+}.2[\text{Br}]^-$  was obtained from the reaction of  $\alpha,\alpha$ -dibromo-*p*-xylene with pyridine producing a white precipitate. The  $^1\text{H}$  NMR spectrum of compound  $[\text{Pyr}]^{2+}.2[\text{Br}]^-$  (Figure 4.01) showed five signals of unsymmetrical hydrogen from a total number of 18 hydrogen atoms. Only one peak was observed at the aliphatic region which belonged to the methylene groups, resonated at  $\delta$  4.67 ppm as a doublet of doublet. The rest of four signals were due to the hydrogen attached to the aromatic group. At  $\delta$  7.49 ppm, a doublet was observed due to the signal from four hydrogen atoms of phenylene ring. The signal at  $\delta$  8.01 ppm was belonged to the H-10, H-12, H-15 and H-17 of pyridine ring which appeared as a triplet. The hydrogen at position H-11 and H-16 of pyridine ring were resonated as a triplet at  $\delta$  8.49 ppm. Lastly, the signal for H-9, H-13, H-14 and H-18 of pyridine ring was observed at the lower field,  $\delta$  9.16 ppm as a doublet.

Noted that the  $^1\text{H}$  NMR spectra of compounds  $[\text{Pyr}]^{2+}.2[\text{NTf}_2]^-$  (Figure 4.02) and  $[\text{Pyr}]^{2+}.2[\text{PF}_6]^-$  (Figure 4.03) also recorded the identical signals and multiplication except the chemical shift has been shifted towards down or up field regions due to the influence of deuterated solvent used.



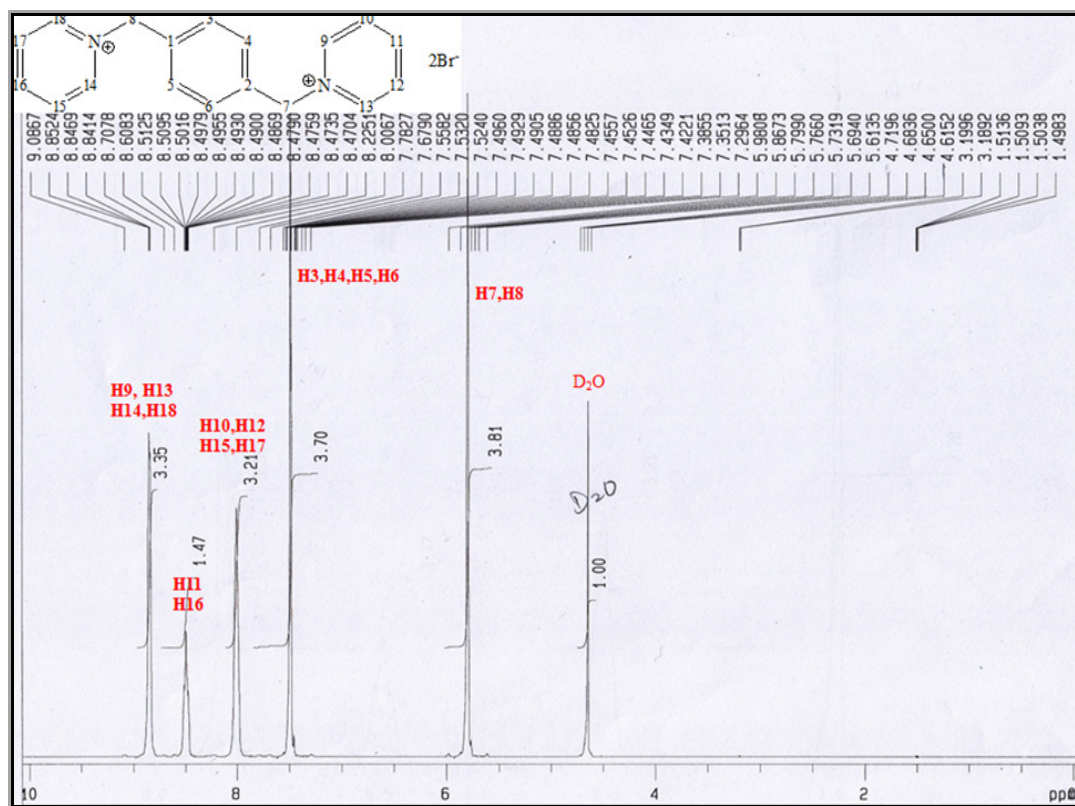


Figure 4.01 :  $^1\text{H}$  NMR spectrum of  $[\text{Pyr}]^{2+} \cdot 2[\text{Br}]^-$

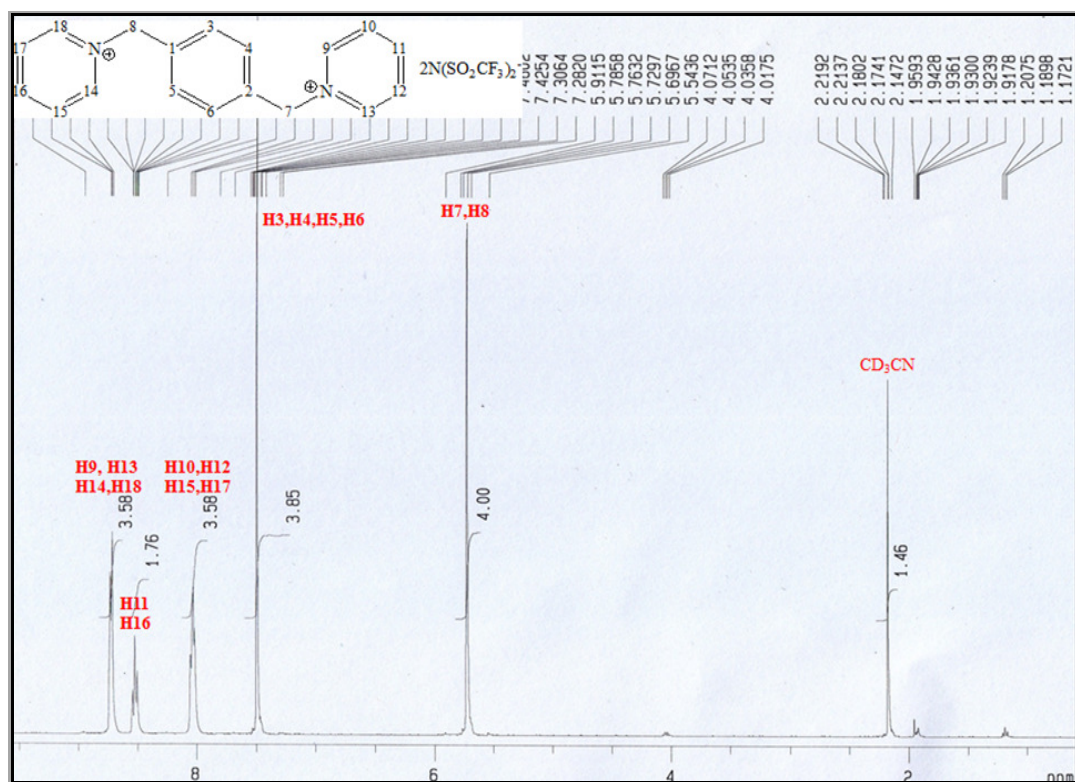
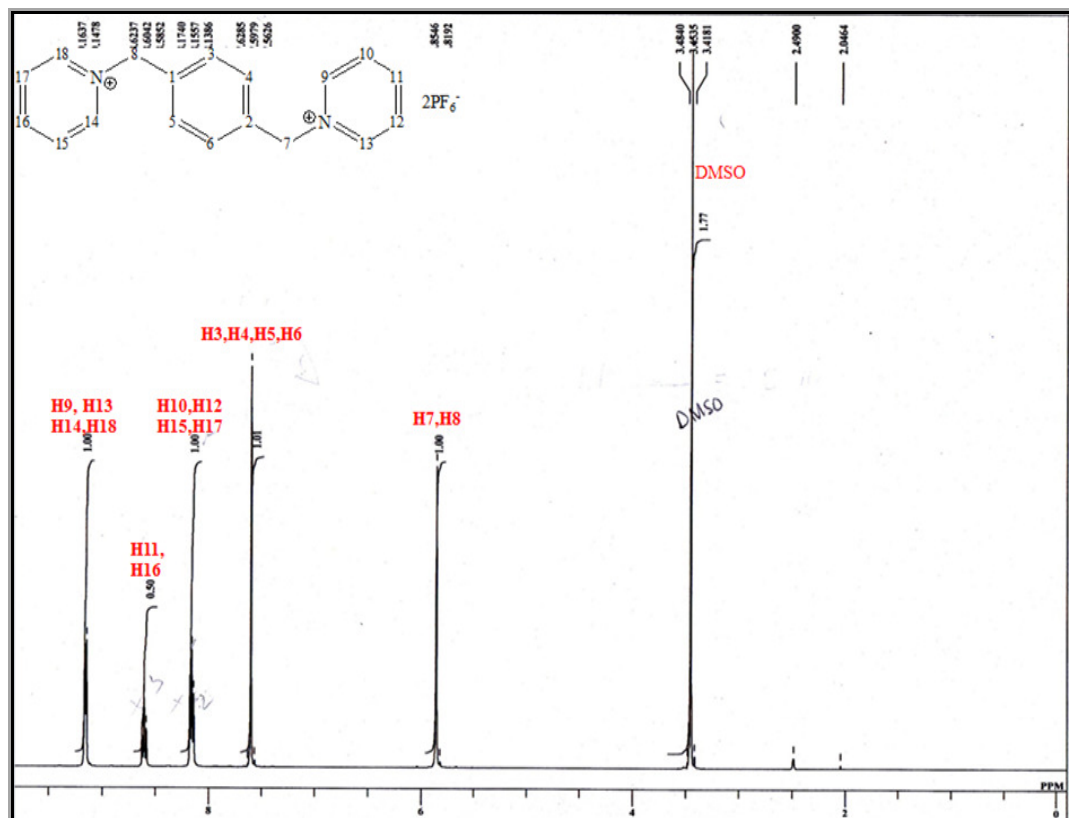


Figure 4.02 :  $^1\text{H}$  NMR spectrum of  $[\text{Pyr}]^{2+} \cdot 2[\text{NTf}_2]^-$



**Figure 4.03 :**  $^1\text{H}$  NMR spectrum of  $[\text{Pyr}]^{2+} \cdot 2[\text{PF}_6]^-$

The complete results of  $[\text{Pyr}]^{2+} \cdot 2[\text{A}]^-$  series were presented in the Table 4.01 below:

**Table 4.01 :**  $^1\text{H}$  NMR spectral data of  $[\text{Pyr}]^{2+} \cdot 2[\text{A}]^-$

Chemical shift (ppm)			Coupling constant (Hz)	Multiplication	Assignment
Br	NTf <sub>2</sub>	PF <sub>6</sub>			
4.67	5.73	5.83	-	dd	Methylene group
7.49	7.50	7.60	-	d	Phenylene ring
8.01	8.04	8.16	7.08	t	H-10, H-12, H-15, H-17
8.49	8.53	8.60	7.70	t	H-11, H-16
9.16	8.73	9.15	6.36	d	H-9, H-13, H-14, H-18

The  $^{13}\text{C}$  NMR spectrum of  $[\text{Pyr}]^{2+} \cdot 2[\text{Br}]^{-}$  (Figure 4.04) displayed a total of six unequivalent carbon atoms. The identical carbons appeared at the same chemical shift. The peak at  $\delta$  64.92 ppm was assigned to the two  $\text{sp}^3$  methylene carbons. The signal of two quaternary carbons of phenylene ring appeared at  $\delta$  145.56 ppm. The carbon atoms of aromatic phenylene ring were observed at  $\delta$  129.95 ppm which was assigned to the C-3, C-4, C-5 and C-6 carbons. The signals at  $\delta$  131.30,  $\delta$  135.01 and  $\delta$  146.98 ppm were belonged to the pyridine ring. The  $\delta$  131.30 ppm signal was attributed to the four equivalent carbons at position C-10, C-12, C-15 and C-17. The two carbons signal at position C-11 and C-16 were shown at  $\delta$  135.01 ppm while at  $\delta$  146.98 ppm, the signal were assigned to another four equivalent carbons at position C-9, C-13, C-14 and C-18. The  $^{13}\text{C}$  NMR spectra of  $[\text{Pyr}]^{2+} \cdot 2[\text{PF}_6]^{-}$  (Figure 4.06) displayed an identical signals and multiplication with compound  $[\text{Pyr}]^{2+} \cdot 2[\text{Br}]^{-}$  but differ in the chemical shift which has been shifted towards upper or lower field regions depending on the deuterated solvent used. On the other hand, the  $^{13}\text{C}$  NMR spectrum of  $[\text{Pyr}]^{2+} \cdot 2[\text{NTf}_2]^{-}$  (Figure 4.05) recorded four additional weak peaks at  $\delta$  115.13,  $\delta$  118.35,  $\delta$  121.57 and  $\delta$  124.57 ppm which were assigned to the carbon  $-\text{CF}_3$  of  $\text{NTf}_2$  anions.

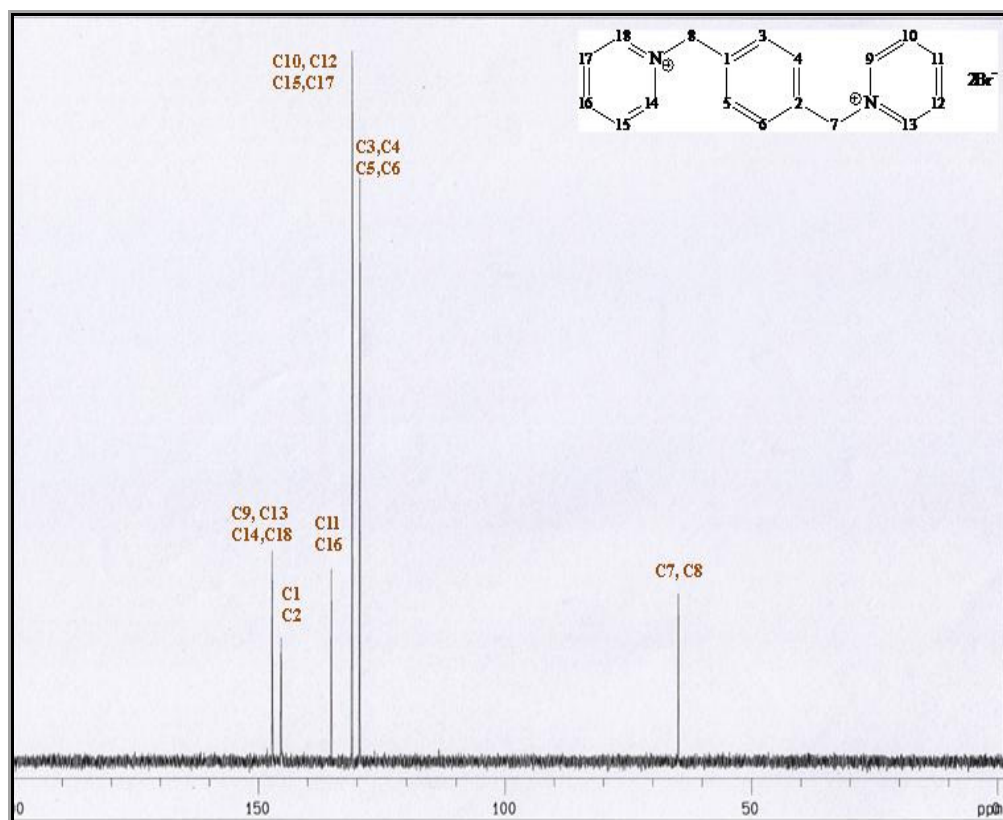


Figure 4.04 :  $^{13}\text{C}$  NMR spectrum of  $[\text{Pyr}]^{2+} \cdot 2[\text{Br}]^{-}$

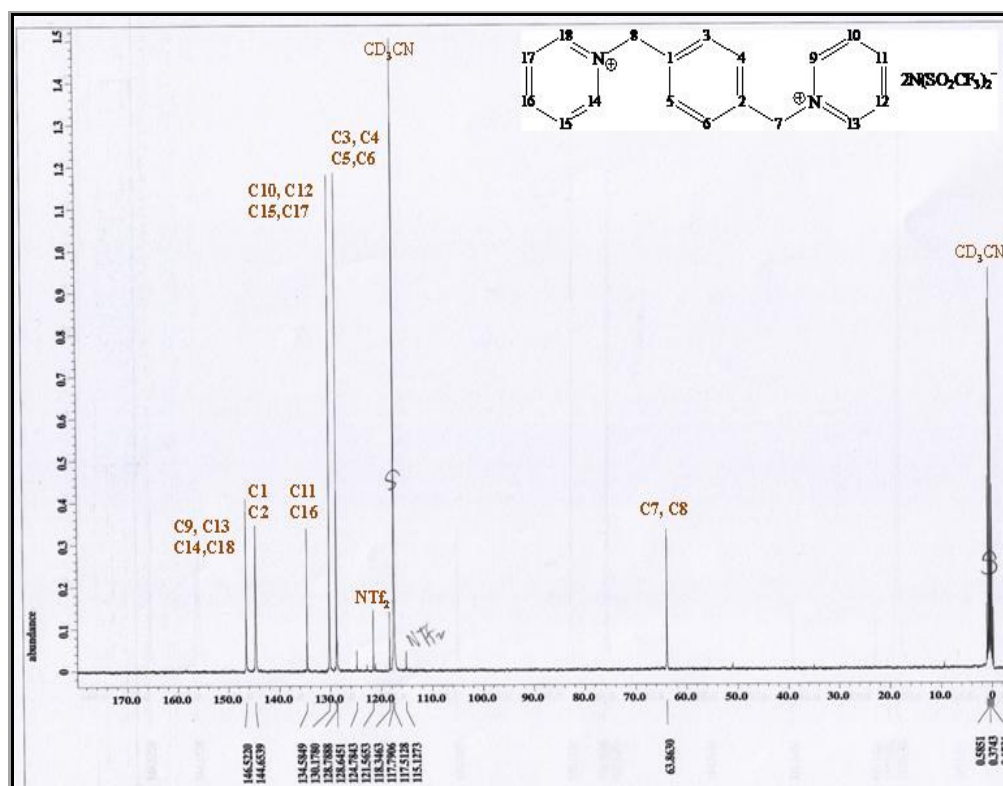


Figure 4.05 :  $^{13}\text{C}$  NMR spectrum of  $[\text{Pyr}]^{2+} \cdot 2[\text{NTf}_2]^{-}$

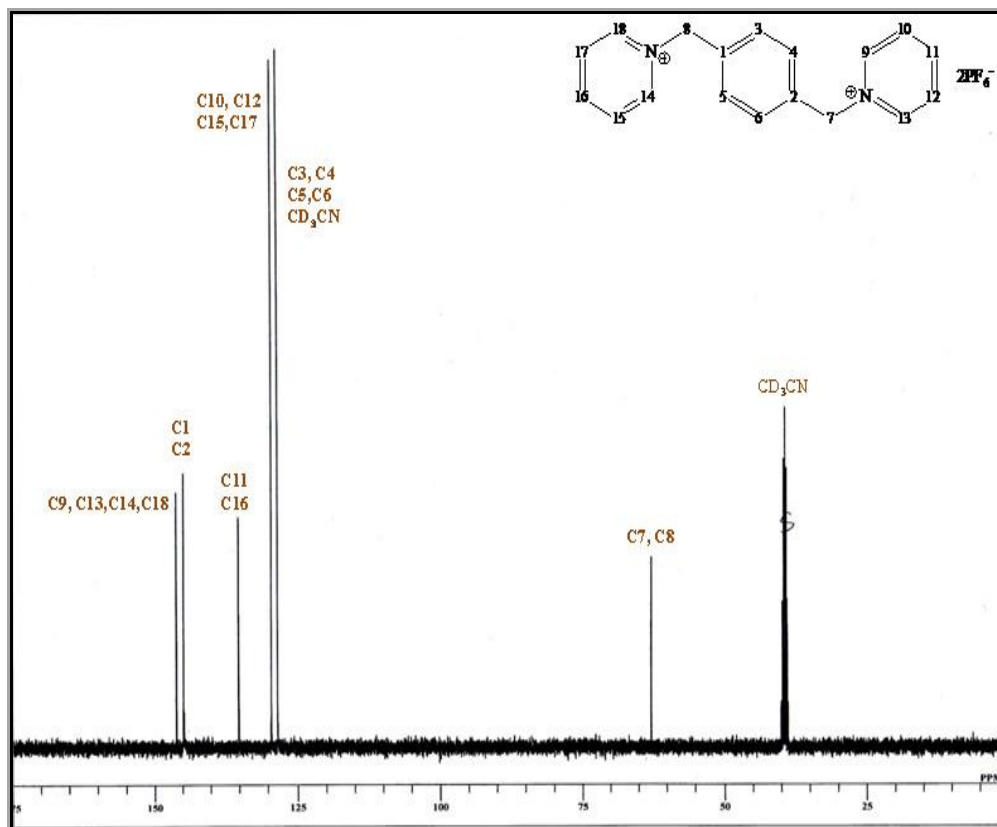


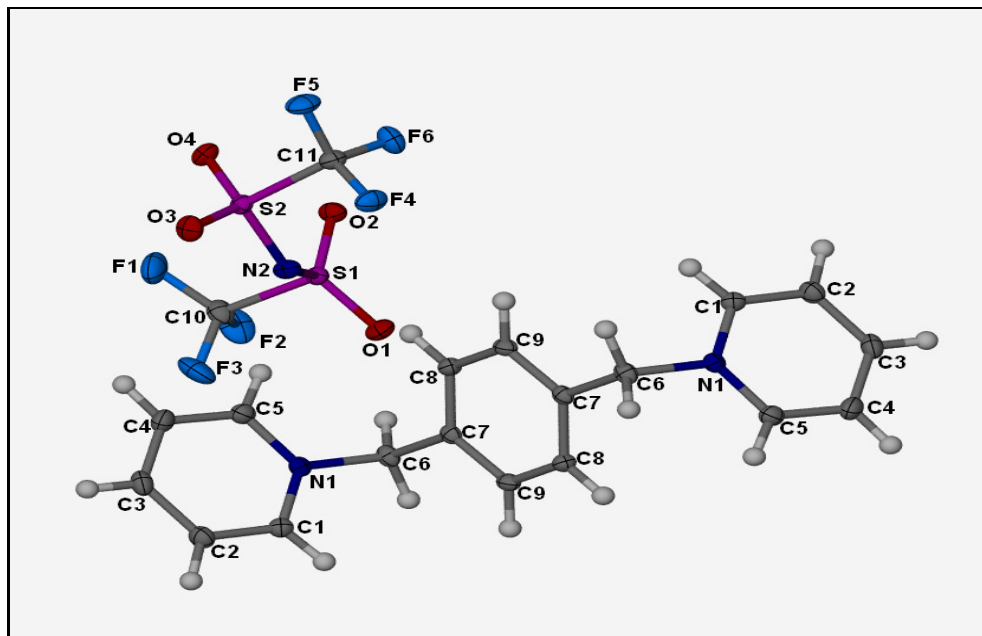
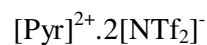
Figure 4.06 :  $^{13}\text{C}$  NMR spectrum of  $[\text{Pyr}]^{2+} \cdot 2[\text{PF}_6]^-$

The complete results of  $[\text{Pyr}]^{2+} \cdot 2[\text{A}]^-$  series were presented in the Table 4.02:

Table 4.02 :  $^{13}\text{C}$  NMR spectral data of  $[\text{Pyr}]^{2+} \cdot 2[\text{A}]^-$

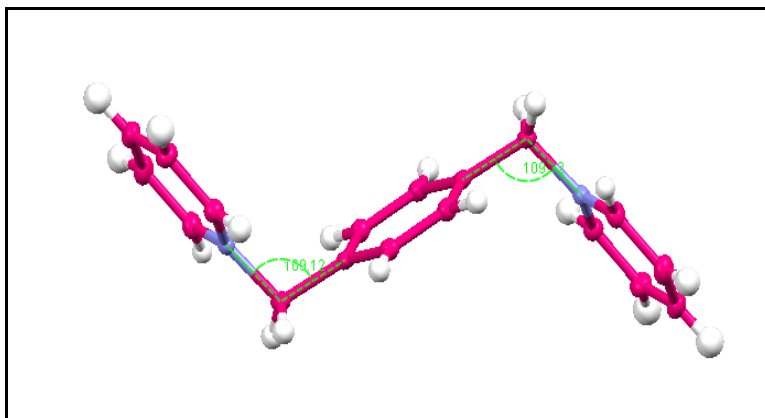
Chemical shift (ppm)			Assignment
Br	NTf <sub>2</sub>	PF <sub>6</sub>	
64.92	63.86	62.55	Methylene group
-	115.13	-	-CF <sub>3</sub> (NTf <sub>2</sub> )
-	118.35	-	
-	121.57	-	
-	124.57	-	
129.95	128.79	128.13	C-3, C-4, C-5, C-6
131.30	130.18	128.78	C-10, C-12, C-15, C-17
135.01	134.58	135.05	C-11, C16
145.56	144.65	144.95	Quaternary carbon
146.98	146.52	146.25	C-9, C-13, C-14, C-18

#### 4.1.4 : X-ray Crystallography



**Figure 4.07** : Thermal ellipsoid plot of compound  $[\text{Pyr}]^{2+} \cdot 2[\text{NTf}_2]^-$  at the 70% probability level; hydrogen atoms are drawn as spheres of arbitrary radius. Symmetry-related atoms are not labeled.

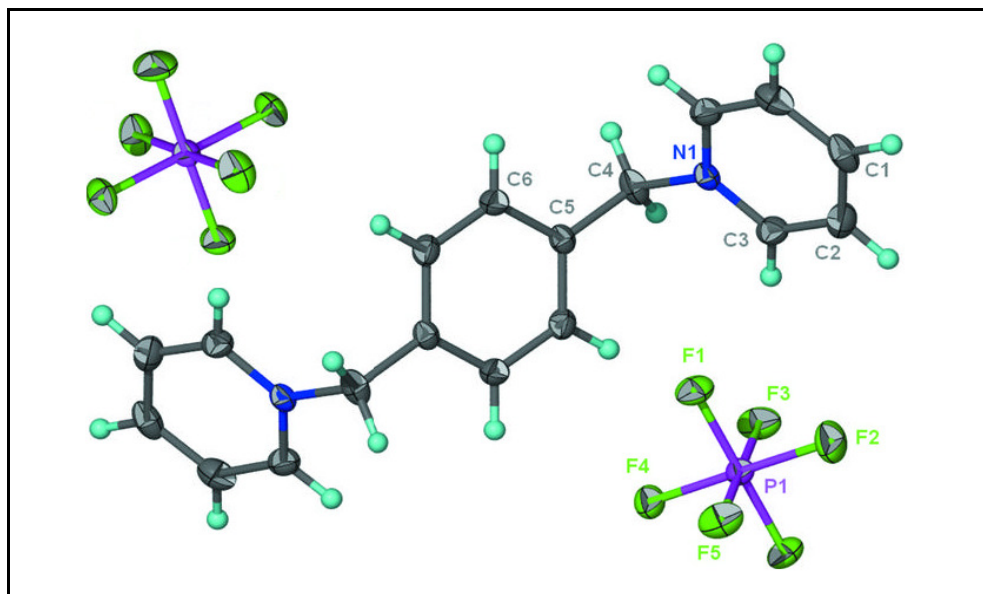
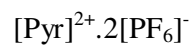
The dicationic organic salt,  $[\text{Pyr}]^{2+} \cdot 2[\text{NTf}_2]^-$  was crystallized in a monoclinic  $C_2/c$  space group. The crystal formed a plate-shaped colourless crystal. The cation of this organic salt was generated from a crystallographic inversion centre whereby the asymmetric unit consists of one-half molecule of the dication and one bis(trifluoromethanesulfonyl)imide anion.



**Figure 4.08** : [Pyr] cation moiety in compound  $[\text{Pyr}]^{2+} \cdot 2[\text{NTf}_2]^-$ .

A six-membered phenylene ring as linker and six-membered pyridine ring at both ends construct the cation. The pyridine rings are aligned at  $109.12(1)^\circ$  at both ends with respect to phenylene ring where five carbon atoms and nitrogen atom are lying on the same plane. Both pyridine rings are parallel to each other but lie on the same plane as phenylene group.

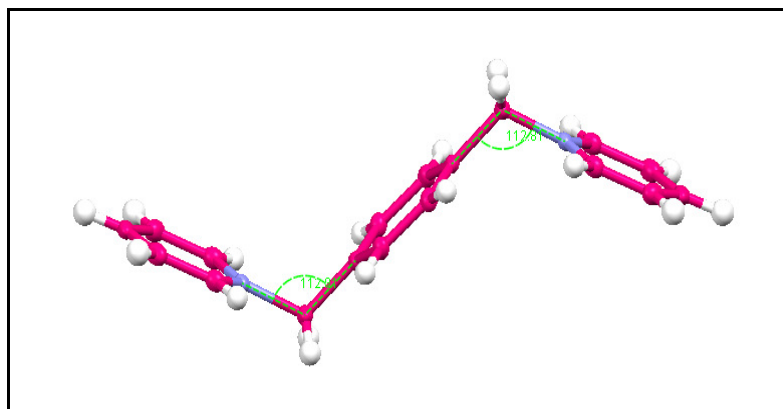




**Figure 4.10** : Thermal ellipsoid plot of compound  $[\text{Pyr}]^{2+}.2[\text{PF}_6]^-$  at the 70% probability level, hydrogen atoms are drawn as spheres of arbitrary radius.

Compound  $[\text{Pyr}]^{2+}.2[\text{PF}_6]^-$  was crystallized in a orthorhombic Pbam space group. The crystal formed a colourless block-shaped colourless crystal. The cation of this organic salt was generated from a crystallographic inversion centre whereby the asymmetric unit consists of one-half molecule of the dication and one hexafluoridophosphate anion.





**Figure 4. 11** : [Pyr] cation moiety in compound  $[\text{Pyr}]^{2+} \cdot 2[\text{PF}_6]^-$ .

In the cation part, pyridine and phenylene rings are aligned at  $62.9 (1)^\circ$ . The pyridine ring lies on a special position of m site symmetry and the phenylene ring on a special position of 2/m site symmetry. The angle at the methylene C atom is  $112.8 (1)^\circ$ . The anion lies on a special position of m site symmetry whereby four F atoms lie on this mirror plane.

**Table 4.03** : Crystal data and structure refinements of [Pyr]<sup>2+</sup>.2[NTf<sub>2</sub>]<sup>-</sup> and [Pyr]<sup>2+</sup>.2[PF<sub>6</sub>]<sup>-</sup>

Ionic Liquids	[Pyr] <sup>2+</sup> .2[NTf <sub>2</sub> ] <sup>-</sup>	[Pyr] <sup>2+</sup> .2[PF <sub>6</sub> ] <sup>-</sup>
Empirical Formula	[C <sub>18</sub> H <sub>18</sub> N <sub>2</sub> ] <sup>2+</sup> . 2[C <sub>4</sub> N <sub>2</sub> F <sub>12</sub> O <sub>8</sub> S <sub>4</sub> ] <sup>-</sup>	[C <sub>18</sub> H <sub>18</sub> N <sub>2</sub> ] <sup>2+</sup> . 2[PF <sub>6</sub> ] <sup>-</sup>
Molecular weight /g mol <sup>-1</sup>	822.64	552.28
Colour	Colourless	Colourless
Size/mm <sup>3</sup>	0.30 x 0.17 x 0.05	0.30 x 0.20 x 0.10
Crystal system	Monoclinic	Orthorhombic
Space group	C2/c	Pbam
a/Å	27.071(3)	11.1013 (11)
b/Å	8.3090(8)	12.6742 (12)
c/Å	15.4115(16)	7.3483 (7)
α (°)	90.00	90.00
β (°)	114.1500 (10)	90.00
γ (°)	90.00	90.00
Vol Å <sup>3</sup>	3163.1 (5)	1033.91 (17)
Z, Dc/g cm <sup>-3</sup>	4	2
F(000)	1656	556
μ/mm <sup>-1</sup>	0.423	0.423
θ range (°)	2.59-30.59	2.44-27.50
Reflections collected	23355	6200
Data/restraints/parameter	4255/0/246	1121/0/91
R <sub>int</sub>	0.0236	0.0276
Ref <sub>Ins</sub> (total)	4811	1280
Ref <sub>Ins</sub> (unique)	4255	1121
Final R indices [I>2σ(I)]	R <sub>1</sub> = 0.0286 wR <sub>2</sub> = 0.0774	R <sub>1</sub> = 0.0290 wR <sub>2</sub> = 0.0840
R indices (all data)	R <sub>1</sub> = 0.0332 wR <sub>2</sub> = 0.0813	R <sub>1</sub> = 0.0337 wR <sub>2</sub> = 0.0881
ρ <sub>max</sub>  /e/Å <sup>3</sup>	0.452 and -0.398	0.332 and -0.440

## 4.2: *N,N'*-[1,4-Phenylenebis(methylene)]bis(*N,N*-diethylethanaminium) series

### 4.2.1 : $^1\text{H}$ NMR and $^{13}\text{C}$ NMR Spectroscopy

Dicationic organic salt  $[\text{Tea}]^{2+}.2[\text{Br}]^-$  was synthesized from the reaction of  $\alpha,\alpha$ -dibromo-*p*-xylene with triethylamine and the product is a white solid. The  $^1\text{H}$  NMR spectrum of this compound (Figure 4.12) recorded four signals from four unsymmetrical protons; three signals at upfield region correspond to the proton attached to the aliphatic carbon while the only peaks at the aromatic region was assigned to the hydrogen of phenylene ring. A triplet was observed at  $\delta$  1.31 ppm belonged to the hydrogen from six methyl groups of triethylamine. The signal of proton from six methylene groups was recorded at  $\delta$  3.17 ppm as a quartet. While the peak appeared as a doublet of doublet at  $\delta$  4.39 ppm was attributed to the hydrogen of methylene carbon attached between phenylene ring and triethylemine groups. The hydrogen of aromatic phenylene ring resonated at  $\delta$  7.52 as a doublet.

On the other hand, the spectra recorded for the same cation of different anions;  $[\text{Tea}]^{2+}.2[\text{NTf}_2]^-$  (Figure 4.13) and  $[\text{Tea}]^{2+}.2[\text{PF}_6]^-$  (Figure 4.14) showed no different in the total number of hydrogen, signals and multiplication except a slight shifting to the chemical shift towards lower or upper regions probably because of the influence of deuterated solvent.

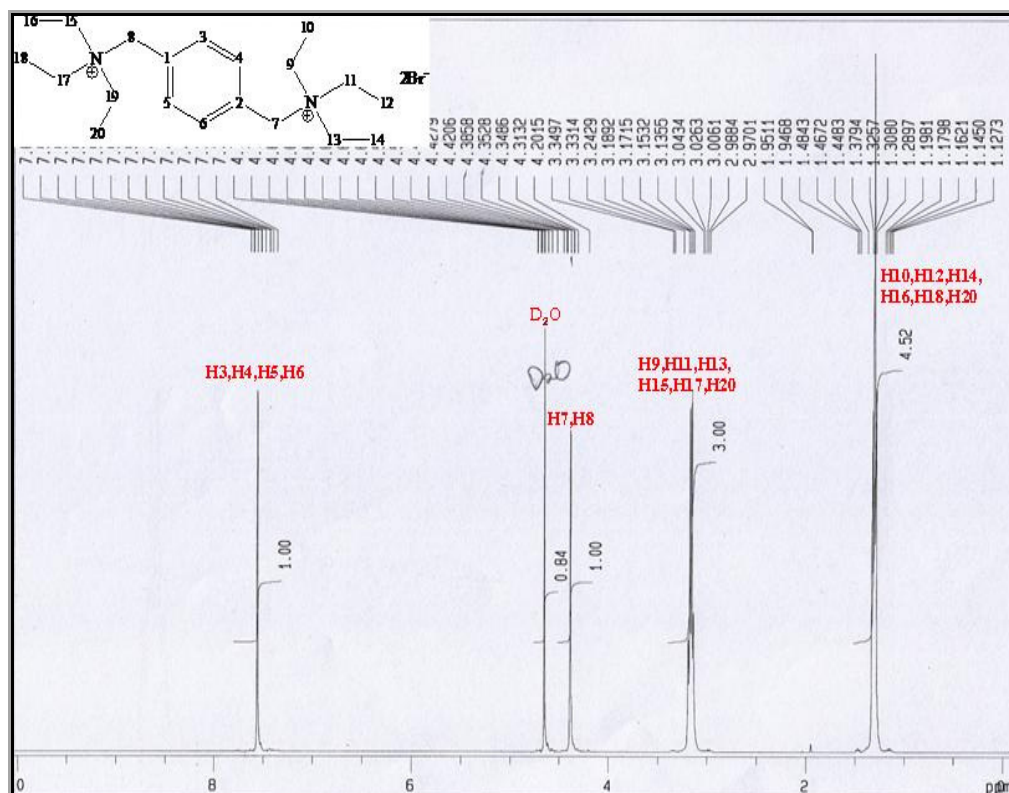


Figure 4.12 :  $^1H$  NMR spectrum of  $[Tea]^{2+}.2[Br]^-$

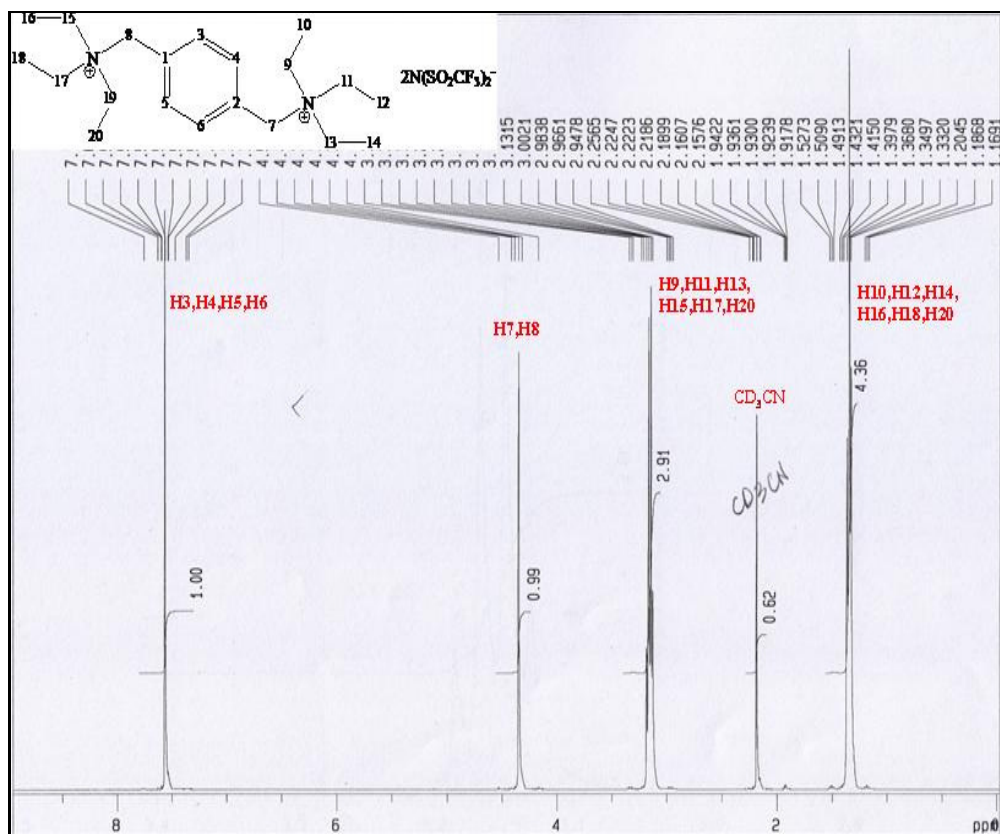


Figure 4.13 :  $^1H$  NMR spectrum of  $[Tea]^{2+}.2[NTf_2]^-$

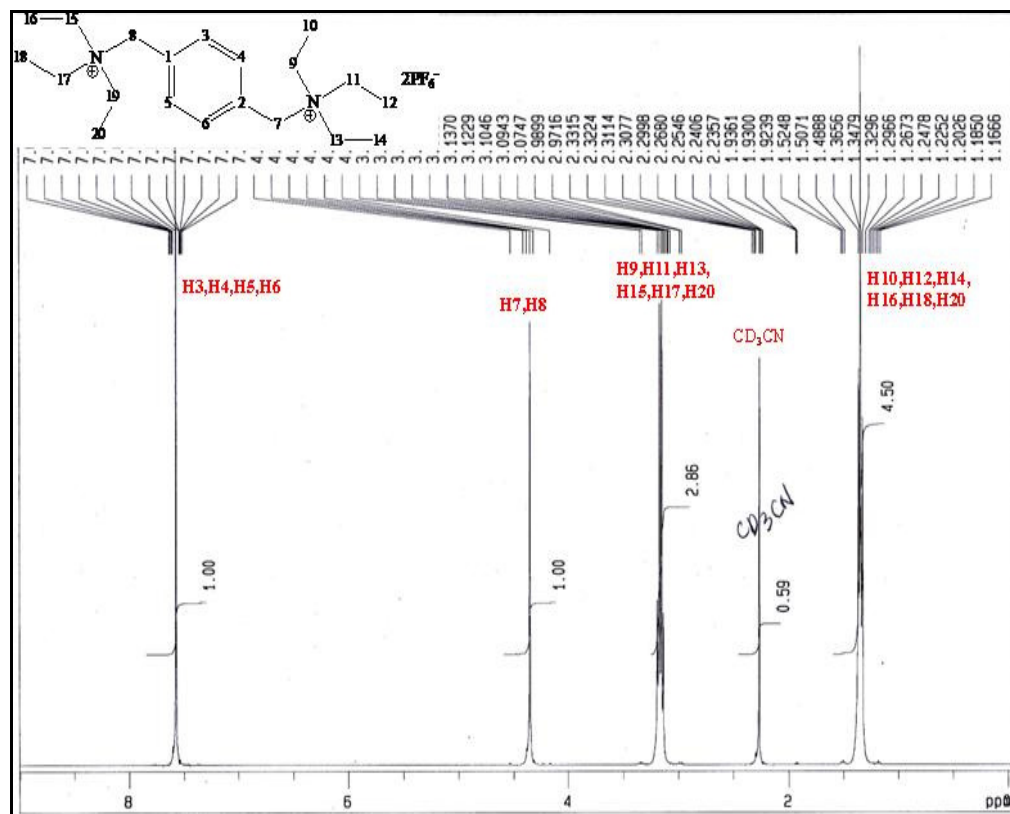


Figure 4.14 :  $^1\text{H}$  NMR spectrum of  $[\text{Tea}]^{2+} \cdot 2[\text{PF}_6]^-$

The complete chemical shift for  $[\text{Tea}]^{2+} \cdot 2[\text{A}]^-$  series were tabulated in the Table 4.04 as follow.

Table 4.04 :  $^1\text{H}$  NMR spectral data of  $[\text{Tea}]^{2+} \cdot 2[\text{A}]^-$

Chemical shift (ppm)			Coupling constant (Hz)	Multiplication	Assignment
Br	NTf <sub>2</sub>	PF <sub>6</sub>			
1.31	1.31	1.33	7.20	t	H-10, H-12, H-14, H-16, H-18, H-20
3.17	3.16	3.16	7.32	quartet	H-9, H-11, H-13, H-15, H-17, H-20
4.39	4.47	4.37	-	dd	Methylene group
7.52	7.58	7.57	-	d	Phenylene ring

The  $^{13}\text{C}$  NMR spectrum of  $[\text{Tea}]^{2+} \cdot 2[\text{Br}]^{-}$  (Figure 4.15) displayed a total of five non-equivalent carbons. The first chemical shift recorded at  $\delta$  7.99 ppm was assigned to the carbon of six methyl groups from triethylamine. The signal from methylene carbon of triethylamine was resonated at  $\delta$  53.38 ppm while another methylene carbon connecting phenylene ring and triethylamine group was appeared at  $\delta$  60.03 ppm. The signal for the quaternary carbon was observed at  $\delta$  130.41 ppm. The last peak at lower field region was attributed to the aromatic carbons of phenylene ring which appeared at  $\delta$  134.05 ppm.

The  $^{13}\text{C}$  NMR spectrum of  $[\text{Tea}]^{2+} \cdot 2[\text{PF}_6]^{-}$  (Figure 4.17) showed similar number of signal except the slight shifting at the individual signal due to the effect of solvent. However, there were additional peaks recorded in the  $^{13}\text{C}$  NMR of  $[\text{Tea}]^{2+} \cdot 2[\text{NTf}_2]^{-}$  spectrum (Figure 4.16);  $\delta$  115.15,  $\delta$  118.39,  $\delta$  121.59 and  $\delta$  124.81 ppm which were corresponded to the carbon of  $-\text{CF}_3$  group of  $\text{NTf}_2$  anions.

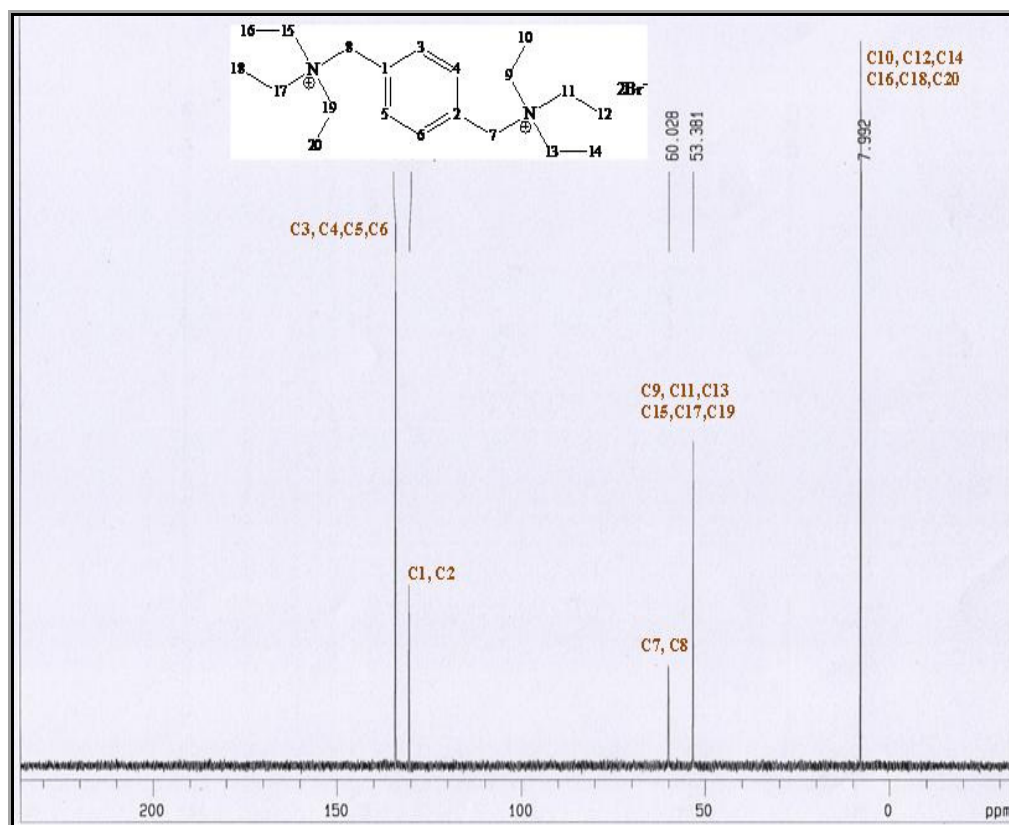


Figure 4.15 :  $^{13}\text{C}$  NMR spectrum of  $[Tea]^{2+} \cdot 2[\text{Br}]^{-}$

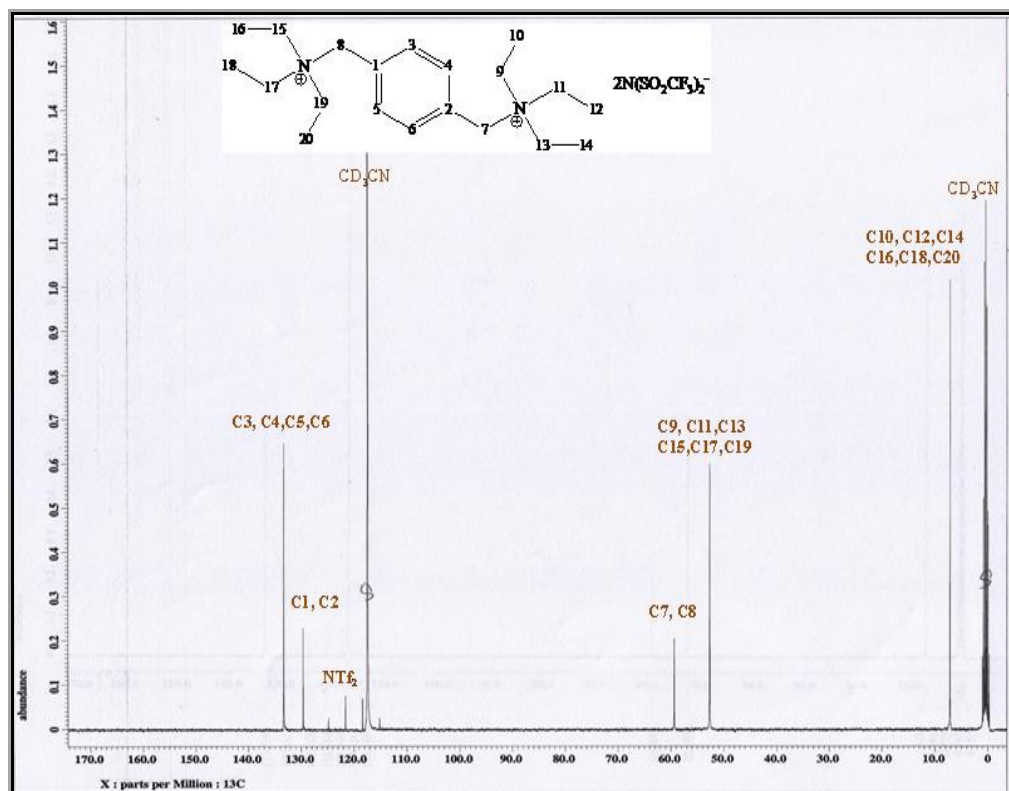


Figure 4.16 :  $^{13}\text{C}$  NMR spectrum of  $[Tea]^{2+} \cdot 2[\text{NTf}_2]^{-}$

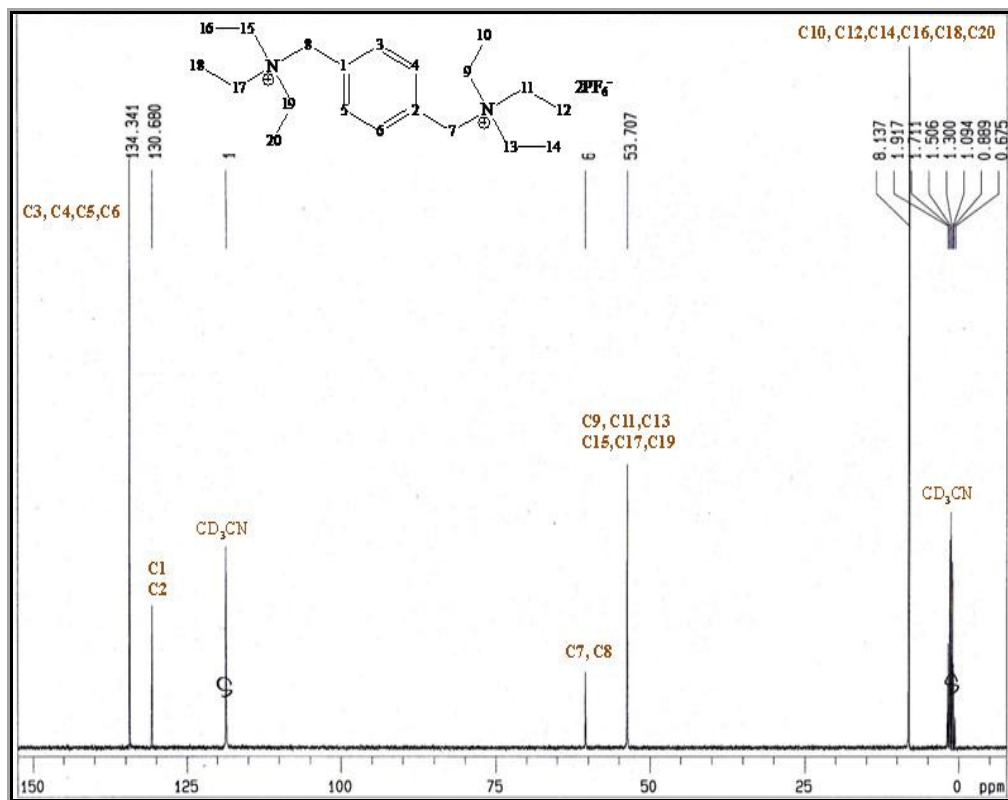


Figure 4.17 :  $^{13}\text{C}$  NMR spectrum of  $[\text{Tea}]^{2+} \cdot 2[\text{PF}_6]^-$

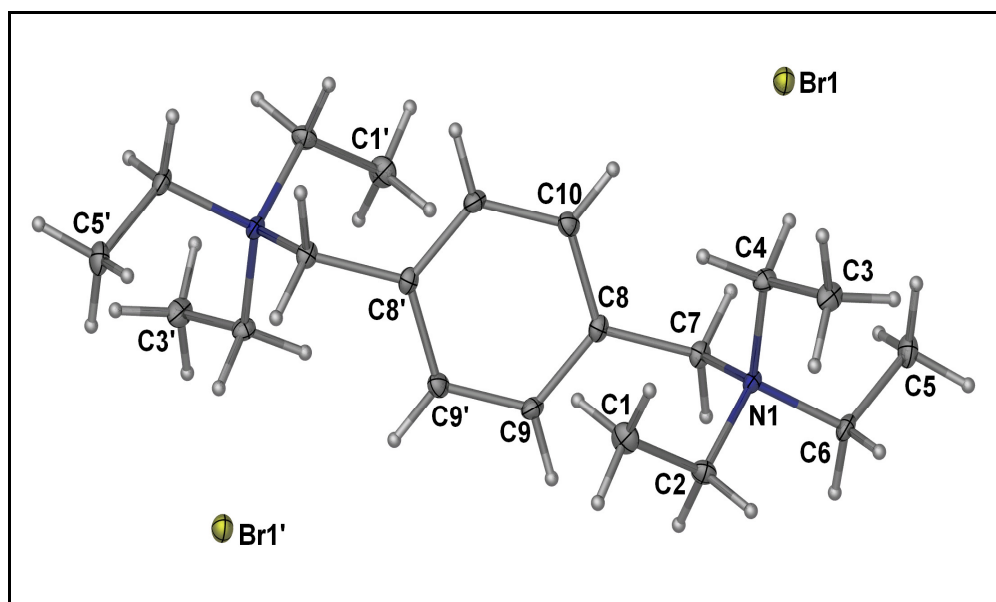
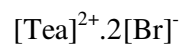
The chemical shift for [Tea] cation series were tabulated in the Table 4.05:

Table 4.05 :  $^{13}\text{C}$  NMR spectral data of  $[\text{Tea}]^{2+} \cdot 2[\text{A}]^-$

Chemical shift (ppm)			Assignment
Br	NTf <sub>2</sub>	PF <sub>6</sub>	
7.99	7.15	8.14	C-10, C-12, C-14, C-16, C-18, C-20
53.38	52.67	53.71	C-9, C-11, C-13, C-15, C-17, C-19
60.03	59.37	60.46	Methylene carbon
-	115.15	-	-CF <sub>3</sub> (NTf <sub>2</sub> )
-	118.37	-	
-	121.59	-	
-	124.81	-	
130.41	129.63	130.68	Quaternary carbon
134.05	133.33	134.34	C-3, C-4, C-5, C-6

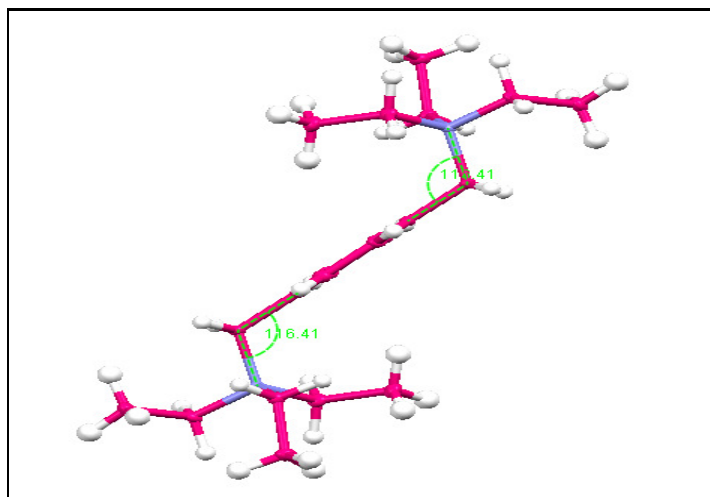


#### 4.2.4 : X-ray Crystallography



**Figure 4.18** : Molecular structure of the compound  $[\text{Tea}]^{2+} \cdot 2[\text{Br}]^{-}$  with displacement ellipsoids drawn at 50% probability level. Hydrogen atoms are drawn as spheres at arbitrary radius.

The dicationic organic salt was crystallized in a monoclinic  $P2_1/n$  space group. The crystal formed a plate-shaped colourless crystal. In the crystal structure of the above compound, the centroid of the aromatic ring was located on an inversion centre, so that the asymmetric unit consists of one-half molecule of the dication and one bromide anion.  $\text{C-H} \cdots \text{Br}$  interactions connect the two components into a three dimensional network.



**Figure 4. 19 :** [Tea] cation moiety in compound  $[\text{Tea}]^{2+} \cdot 2[\text{Br}]^{-}$ .

Triethylamine groups attached to the methylene carbon of phenylene group via nitrogen atom. Both of them were aligned parallel to each other but situated at the trans-position forming Z-shaped conformation with respect to the phenylene group. The angle between the phenylene group to the carbon connecting the nitrogen atom of triethylamine group is  $116.41^\circ$ .

**Table 4.06** : Crystal data and structure refinements of [Tea]<sup>2+</sup>.2[Br]<sup>-</sup>

Ionic Liquids	[Tea] <sup>2+</sup> .2[Br] <sup>-</sup>
Empirical Formula	[C <sub>20</sub> H <sub>38</sub> N <sub>2</sub> ] <sup>2+</sup> .2[Br] <sup>-</sup>
Molecular weight/ g mol <sup>-1</sup>	466.34
Colour	Colourless
Size/mm <sup>3</sup>	0.50 x 0.40 x 0.40
Crystal system	Monoclinic
Space group	P 2 <sub>1</sub> /n
a/Å	8.2713 (5)
b/Å	14.1440 (9)
c/Å	9.0762 (6)
α (°)	90.00
β (°)	97.634 (10)
γ (°)	90.00
Volume/ Å <sup>3</sup>	1052.41 (12)
Z, Dc/g cm <sup>-3</sup>	2
F(000)	484
μ/mm <sup>-1</sup>	3.856
θ range (°)	2.68-27.00
Reflections collected	10066
Data/restraints/parameter	2093/0/112
R <sub>int</sub>	0.0214
Ref <sub>ins</sub> (total)	2304
Ref <sub>ins</sub> (unique)	2093
Final R indices [I>2σ(I)]	R <sub>1</sub> = 0.0174 wR <sub>2</sub> = 0.0423
R indices (all data)	R <sub>1</sub> = 0.0204 wR <sub>2</sub> = 0.0433
ρ <sub>max</sub> /e/Å <sup>3</sup>	0.430 and -0.232

### 4.3: *N,N'*-[1,4-Phenylenebis(methylene)]bis-(*N,N*-dimethylpyrrolinium) series

#### 4.3.1 : $^1\text{H}$ NMR and $^{13}\text{C}$ NMR Spectroscopy

Dicationic organic salt  $[\text{Mpyl}]^{2+} \cdot 2[\text{Br}]^-$  was obtained from the reaction of  $\alpha, \alpha$ -dibromo-*p*-xylene with 1-methylpyrrolidine as a white solid. The  $^1\text{H}$  NMR spectra of  $[\text{Mpyl}]^{2+} \cdot 2[\text{Br}]^-$  (Figure 4.20) displayed six signals of non-equivalent proton. At the down field region, the doublet at  $\delta$  7.62 ppm was assigned to the proton of aromatic phenylene ring. The proton of methylene group at position H-7 and H-8 were observed at  $\delta$  4.44 ppm as a doublet of doublet. Meanwhile, there were two multiplets at  $\delta$  3.38 and  $\delta$  3.52 ppm attributed to the protons at position H-9, H-11, H-13 and H-15 of the 1-methylpyrrolidine ring. A singlet was detected at  $\delta$  2.87 ppm clearly belonged to the proton of methyl group of pyrrolidine ring. At the upper field region, a broad peak at  $\delta$  2.16 ppm was assigned to the proton situated at position H-10, H-12, H-14 and H-16 of 1-methylpyrrolidine ring.

The  $^1\text{H}$  NMR spectra of the other two compound namely  $[\text{Mpyl}]^{2+} \cdot 2[\text{NTf}_2]^-$  (Figure 4.21) and  $[\text{Mpyl}]^{2+} \cdot 2[\text{PF}_6]^-$  (Figure 4.22) are similar to the previous compound with slightly shifting in chemical shift towards the upper or lower field due to the effect of solvent and anions.

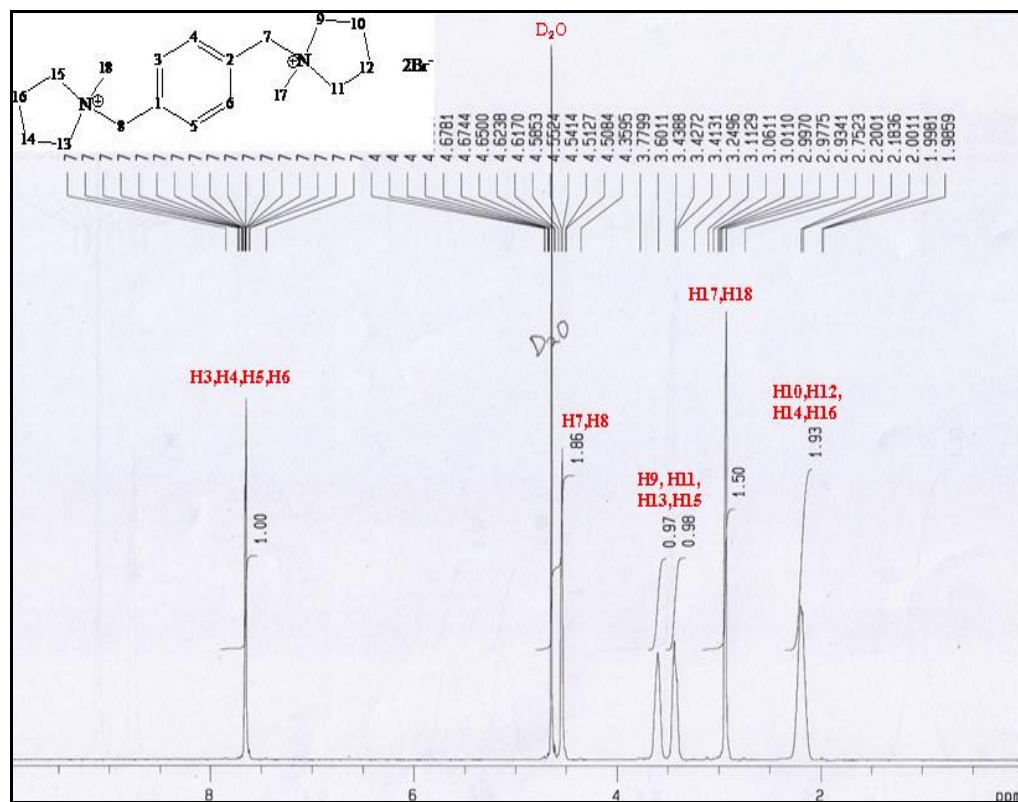


Figure 4.20 : <sup>1</sup>H NMR spectrum of [Mpyl]<sup>2+</sup>.2[Br]<sup>-</sup>

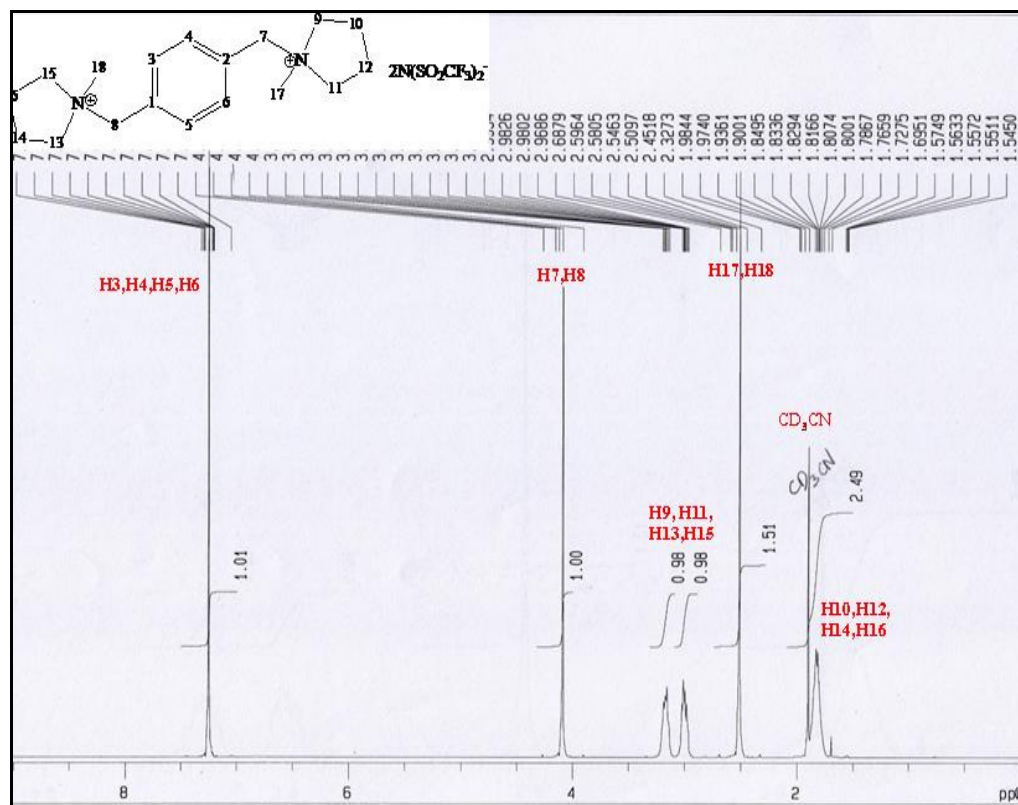


Figure 4.21 : <sup>1</sup>H NMR spectrum of [Mpyl]<sup>2+</sup>.2[NTf<sub>2</sub>]<sup>-</sup>

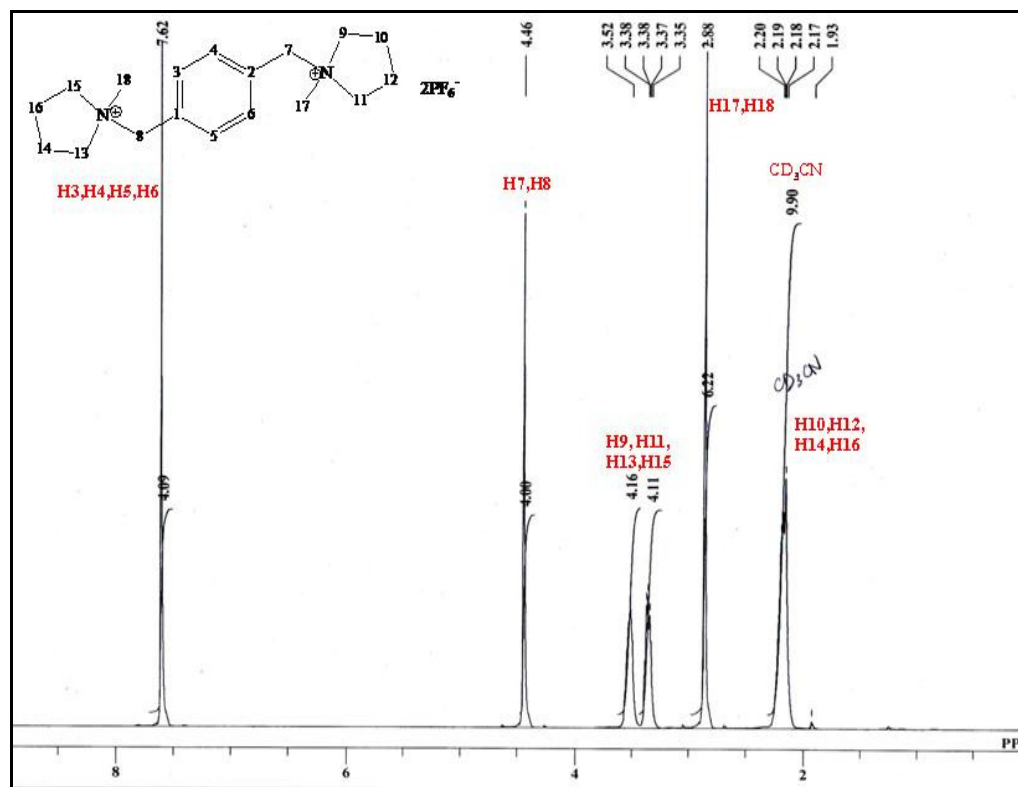


Figure 4.22 :  $^1\text{H}$  NMR spectrum of  $[\text{Mpyl}]^{2+} \cdot 2[\text{PF}_6]^-$

The chemical shift data of this series were compiled in the Table 4.07 as follows:

Table 4.07 :  $^1\text{H}$  NMR spectral data of  $[\text{Mpyl}]^{2+} \cdot 2[\text{A}]^-$

Chemical shift (ppm)			Coupling constant (Hz)	Multiplication	Assignment
Br	NTf <sub>2</sub>	PF <sub>6</sub>			
2.16	1.82	2.19	4.00	m	H-10, H-12, H-14, H-16
2.87	2.51	2.88	-	s	H-17, H-18
3.38	3.00	3.38	4.00	m	H-9, H-13
3.52	3.17	3.52	4.00	m	H-11, H-15
4.44	4.12	4.46	-	dd	Methylene group
7.62	7.28	7.62	-	d	Phenylene ring

Compound  $[\text{Mpyl}]^{2+} \cdot 2[\text{Br}]^-$  (Figure 4.23) has six unsymmetrical carbon signals from a total number of eighteen carbons. Signal at  $\delta$  22.37 ppm was assigned for four carbons at position C-10, C-12, C-14 and C-16 of 1-methylpyrrolidine ring. The methyl group of 1-methylpyrrolidine was observed at  $\delta$  45.04 ppm while the C-9, C-11, C-13 and C-15 carbon of 1-methylpyrrolidine signals were detected at  $\delta$  65.02 ppm. The last signal at the upper region,  $\delta$  67.34 ppm was correspond to the methylene carbon. The quaternary carbon of phenylene ring signal was observed at  $\delta$  131.27 ppm and the remaining four carbon atoms of the aromatic phenylene ring were resonated at  $\delta$  134.92 ppm.

The  $^{13}\text{C}$  NMR spectrum of compound  $[\text{Mpyl}]^{2+} \cdot 2[\text{PF}_6]^-$  (Figure 4.25) was similar with the previous compound except the chemical shift has moved slightly to the upper or lower fields. On the other hands, the  $^{13}\text{C}$  NMR spectrum of  $[\text{Mpyl}]^{2+} \cdot 2[\text{NTf}_2]^-$  (Figure 4.24) showed four additional peaks at  $\delta$  115.13,  $\delta$  118.35,  $\delta$  121.57 and  $\delta$  124.78 ppm due to the carbon signals from  $-\text{CF}_3$  of  $\text{NTf}_2$  anion.

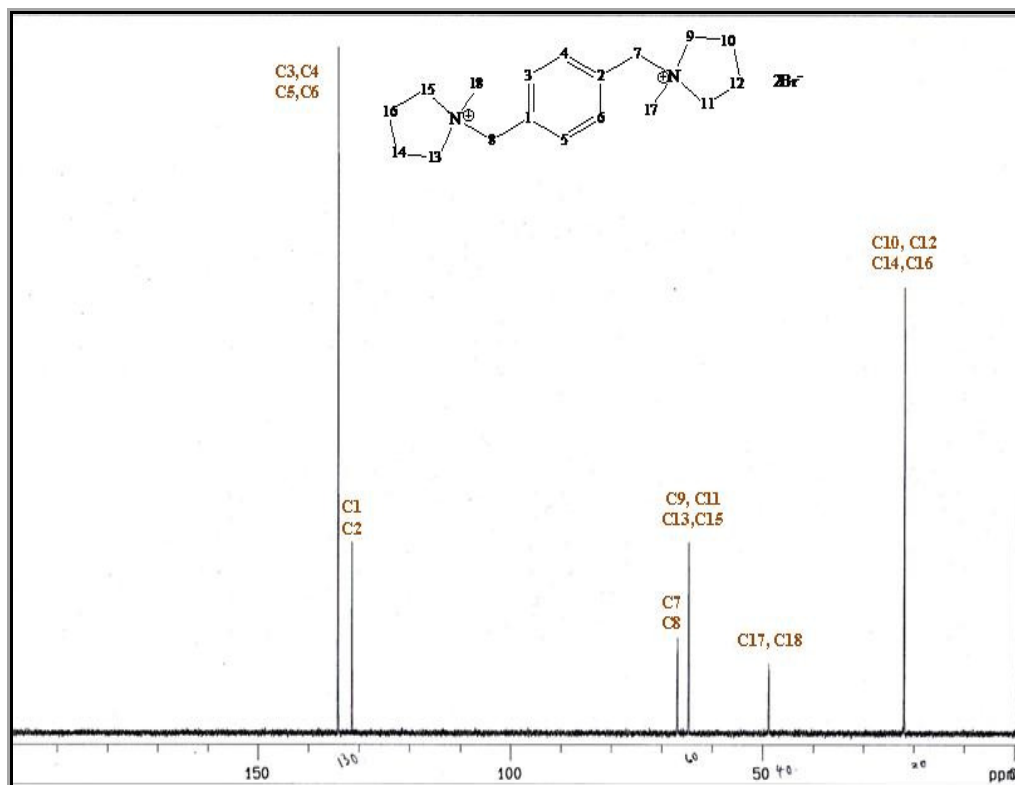


Figure 4.23 :  $^{13}\text{C}$  NMR spectrum of  $[\text{Mpyl}]^{2+} \cdot 2[\text{Br}]^{-}$

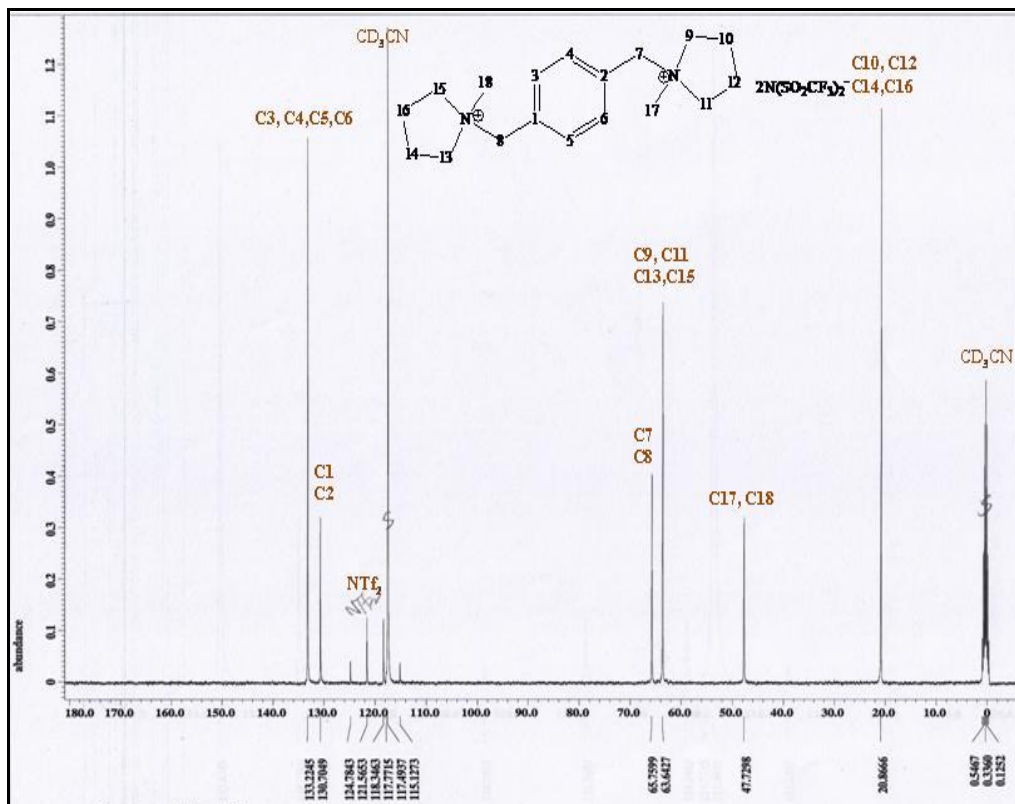


Figure 4.24 :  $^{13}\text{C}$  NMR spectrum of  $[\text{Mpyl}]^{2+} \cdot 2[\text{NTf}_2]^{-}$



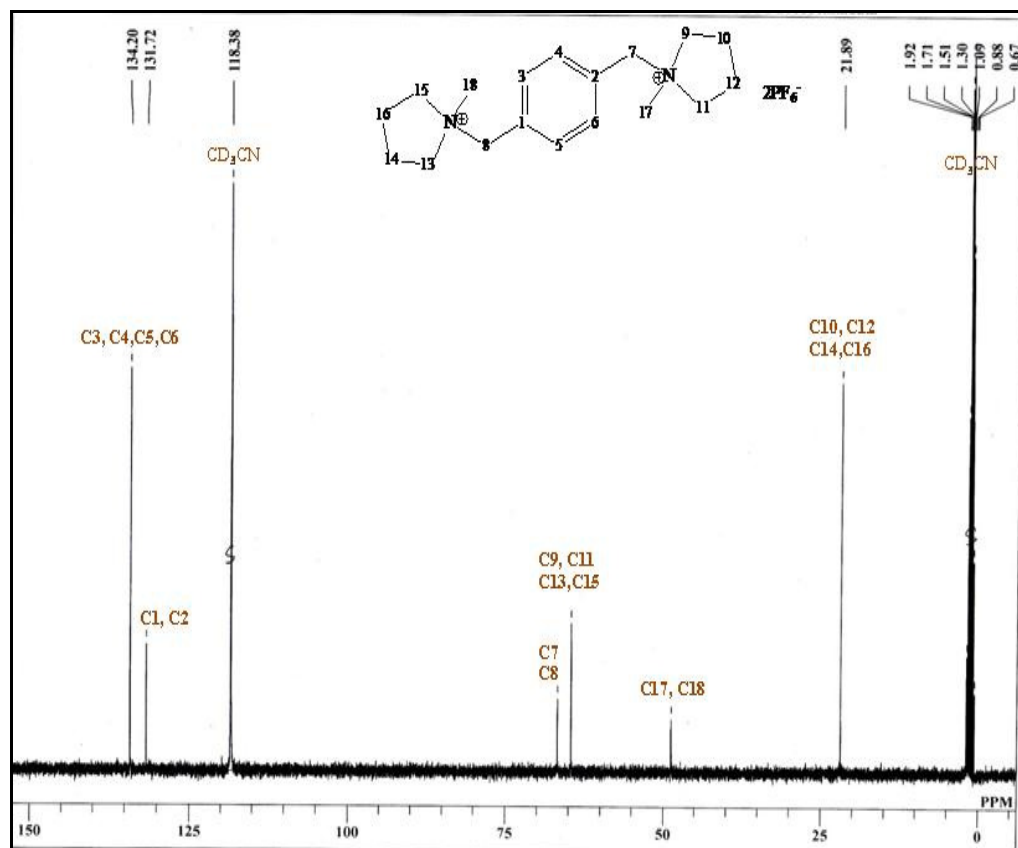


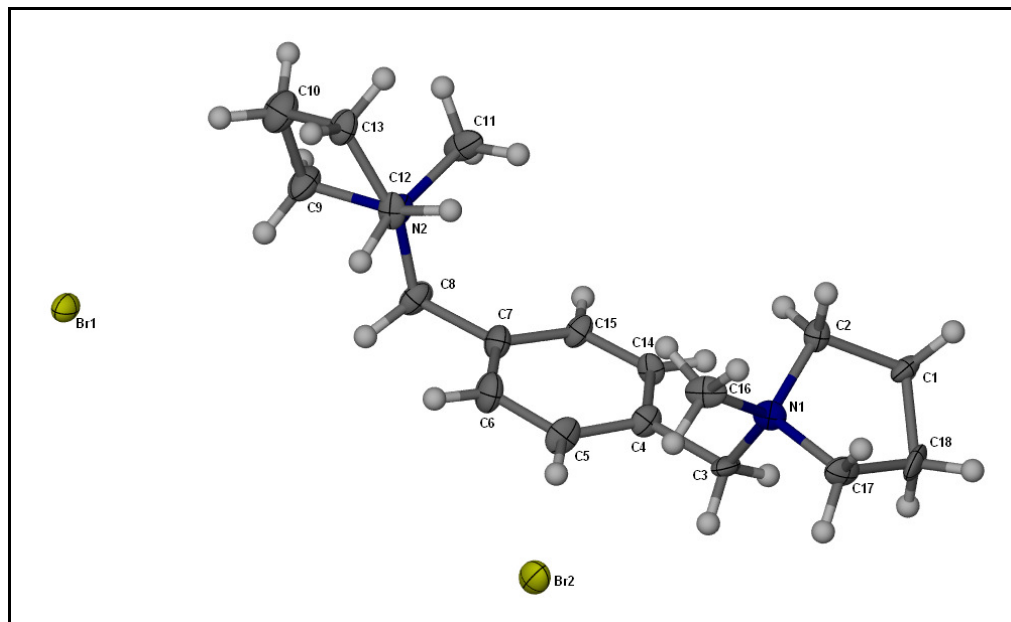
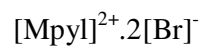
Figure 4.25 :  $^{13}\text{C}$  NMR spectrum of  $[\text{Mpyl}]^{2+} \cdot 2[\text{PF}_6]^-$

The chemical shift data of this series were compiled in the Table 4.08.

Table 4.08 :  $^{13}\text{C}$  NMR spectral data of  $[\text{Mpyl}]^{2+} \cdot 2[\text{A}]^-$

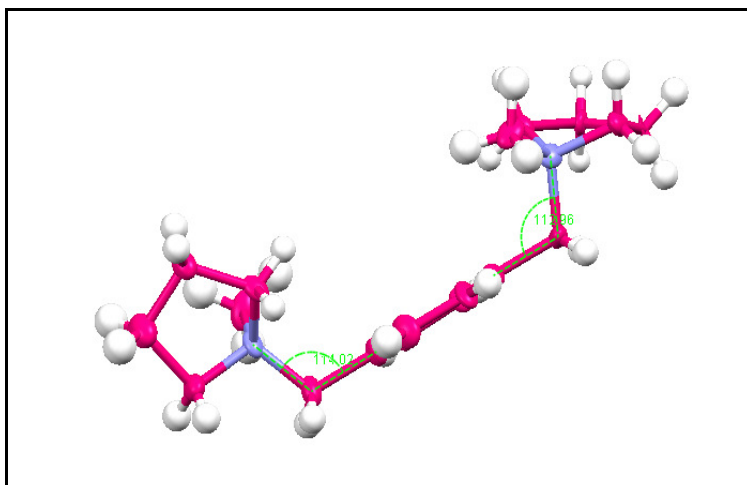
Chemical shift (ppm)			Assignment
Br	NTf <sub>2</sub>	PF <sub>6</sub>	
22.37	20.87	21.89	C-10, C-12, C-14, C-16
45.04	47.73	48.77	C-17, C-18
65.02	63.64	64.64	C-9, C-11, C-13, C-15
67.34	65.76	66.77	Methylene carbon
-	115.13	-	-CF <sub>3</sub> (NTf <sub>2</sub> )
-	118.35	-	
-	121.57	-	
-	124.78	-	
131.27	130.70	131.72	Quaternary carbon
134.92	133.22	134.20	C-3, C-4, C-5, C-6

#### 4.3.4 : X-ray Crystallography



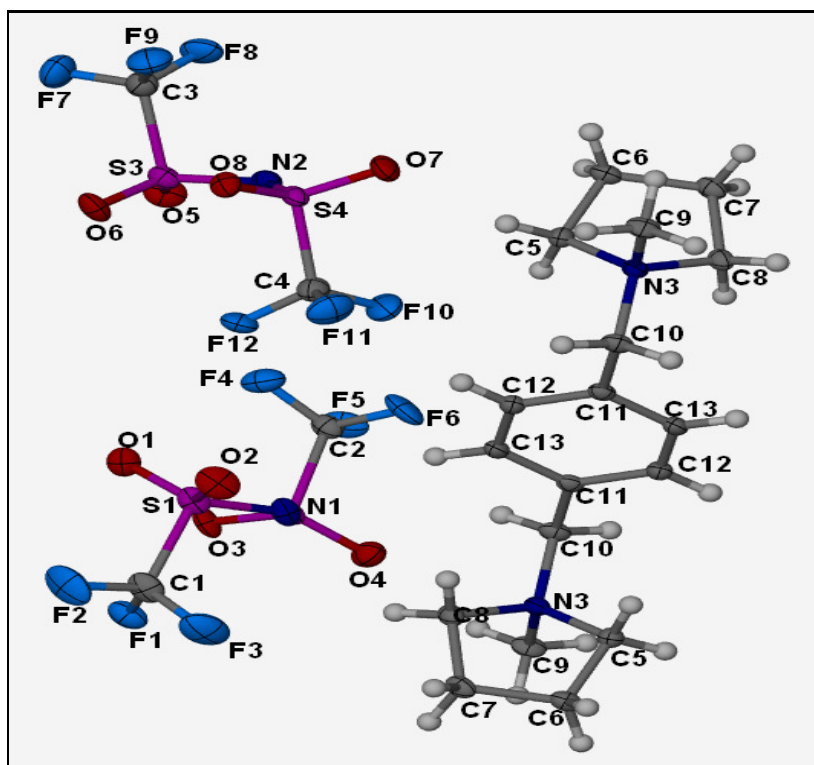
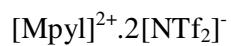
**Figure 4.26** : Molecular structure of the compound  $[\text{Mpyl}]^{2+} \cdot 2[\text{Br}]^{-}$  with displacement ellipsoids drawn at 50% probability level. Hydrogen atoms are drawn as spheres at arbitrary radius.

Compound was crystallized in an orthorhombic  $\text{Pca}2_1$  space group which was appeared as a colourless block-shaped crystal. The  $[\text{Mpyl}]^{2+} \cdot 2[\text{Br}]^{-}$  salt existed as a non-interacting cation and anions molecular organic salt.. The organic salt comprised of an organic dication and two bromide counter anions.



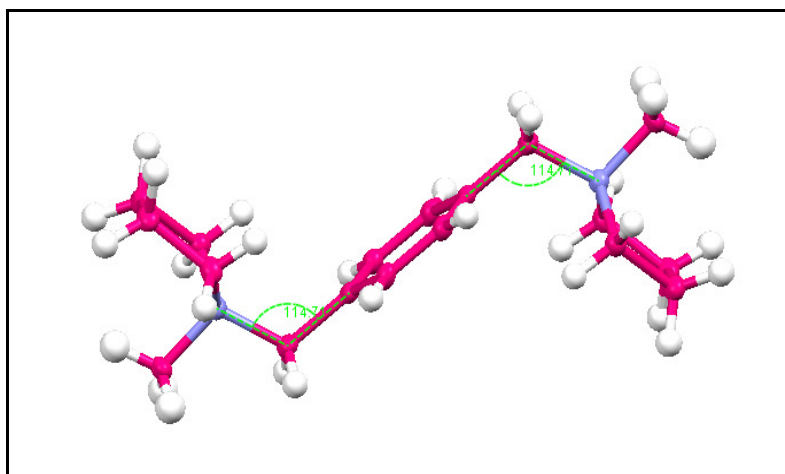
**Figure 4. 27 :** [Mpyl] cation moiety in compound [Mpyl]<sup>2+</sup>·2[Br]<sup>-</sup>.

The cation of this organic salt was built of a phenylene bridge which connected the 1-methylpyrrolidine ring at both ends via methylene carbon at para position. The 1-methylpyrrolidine-phenylene ring-1-methylpyrrolidine portion formed a U-shaped conformation whereby both 1-methylpyrrolidine groups attached on the same side with respect to the phenylene ring. However, some of the cation's structure exhibited a major disorder component.



**Figure 4.28** : Molecular structure of the compound  $[\text{Mpyl}]^{2+} \cdot 2[\text{NTf}_2]^-$  with displacement ellipsoids drawn at 50% probability level. Hydrogen atoms are drawn as spheres at arbitrary radius.

The  $[\text{Mpyl}]^{2+} \cdot 2[\text{NTf}_2]^-$  salt was crystallized in a triclinic, P-1 space group. The crystal had formed a colourless block-shaped crystal. The organic salt has crystallizes in a triclinic P-1 space group where the cation part is built of a 6-membered phenylene ring as the linker with the five-membered *N*-methylpyrrolidine ring at both ends. The cation of the organic salt was lying about a centre of inversion.



**Figure 4.29** : [Mpyl] cation moiety in compound  $[\text{Mpyl}]^{2+} \cdot 2[\text{NTf}_2]^-$ .

The pyrrolidine-phenylene-pyrrolidine portion has a Z-shaped with methyl group is bound at nitrogen of the pyrrolidine ring at both sides. The pyrrolidine ring was approximately perpendicular to the phenylene ring and aligned at  $100.59 (1)^\circ$  with respect to the phenylene ring. The pyrrolidine ring adopts a half-chair conformation which was almost similar to the cyclohexane half-chair conformation. In the half-chair conformation, four adjacent carbon atoms were almost coplanar and the nitrogen atom attaches to the carbon of methylene group were out of the plane. The methyl group of the pyrrolidine ring was aligned at  $107.14 (1)^\circ$  with respect to the methylene carbon at both sides and they were opposite to each other. The angle of methylene carbon atom connecting both pyrrolidine and phenylene rings was  $114.72 (1)^\circ$ .

**Table 4.09** : Crystal data and structure refinements of [Mpyl]<sup>2+</sup>.2[Br]<sup>-</sup> and [Mpyl]<sup>2+</sup>.2[NTf<sub>2</sub>]<sup>-</sup>

Ionic Liquids	[Mpyl] <sup>2+</sup> .2[Br] <sup>-</sup>	[Mpyl] <sup>2+</sup> .2[NTf <sub>2</sub> ] <sup>-</sup>
Empirical Formula	[C <sub>18</sub> H <sub>30</sub> N <sub>2</sub> ] <sup>2+</sup> .2[Br] <sup>-</sup>	[C <sub>18</sub> H <sub>30</sub> N <sub>2</sub> ] <sup>2+</sup> . 2[C <sub>4</sub> N <sub>2</sub> F <sub>12</sub> O <sub>8</sub> S <sub>4</sub> ] <sup>-</sup>
Molecular weight/ g mol <sup>-1</sup>	442.26	834.78
Colour	Colourless	Colourless
Size/mm <sup>3</sup>	0.50 x 0.50 x 0.50	0.30 x 0.22 x 0.18
Crystal system	Orthorhombic	Triclinic
Space group	Pca2 <sub>1</sub>	P -1
a/Å	12.9598 (18)	8.7678 (7)
b/Å	14.2813 (19)	12.9432 (10)
c/Å	21.532 (3)	15.3839 (12)
α (°)	90.00	76.877 (1)
β (°)	90.00	84.828 (1)
γ (°)	90.00	77.834 (1)
Volume/ Å <sup>3</sup>	3985.2 (9)	1660.4 (2)
Z, Dc/g cm <sup>-3</sup>	8	2
F(000)	1808	852
μ/mm <sup>-1</sup>	4.071	0.404
θ range (°)	1.43-28.47	1.36-29.90
Reflections collected	50905	24930
Data/restraints/parameter	7676/1/410	6475/0/451
R <sub>int</sub>	0.0708	0.0483
Ref <sub>ins</sub> (total)	9985	9489
Ref <sub>ins</sub> (unique)	7676	6475
Final R indices [I>2σ(I)]	R <sub>1</sub> = 0.0733	R <sub>1</sub> = 0.0464
	wR <sub>2</sub> = 0.1855	wR <sub>2</sub> = 0.1100
R indices (all data)	R <sub>1</sub> = 0.0991	R <sub>1</sub> = 0.0802
	wR <sub>2</sub> = 0.2031	wR <sub>2</sub> = 0.1317
ρ <sub>max</sub> /e/Å <sup>3</sup>	1.814 and -2.787	0.492 and -0.535

#### 4.4 : *N,N'*-[1,4-Phenylenebis(methylene)]bis-(*N,N*-dibutylpyrrolinium) series

##### 4.4.1 : $^1\text{H}$ NMR and $^{13}\text{C}$ NMR Spectroscopy

Dicationic organic salt  $[\text{Bpyl}]^{2+} \cdot 2[\text{Br}]^-$  (Figure 4.30) was produced from the reaction of  $\alpha,\alpha$ -dibromo-*p*-xylene and 1-butylpyrrolidine. The  $^1\text{H}$  NMR spectrum of  $[\text{Bpyl}]^{2+} \cdot 2[\text{Br}]^-$  recorded eight signals correspond to the eight unsymmetrical protons. A triplet peak was observed at  $\delta$  0.82 ppm which belonged to the four protons of methyl group at position H-20 and H-24. Protons of methylene group at position H-19 and H-23 of 1-butylpyrrolidine ring were detected at  $\delta$  1.24 ppm and appeared as a sextet. At  $\delta$  1.77 ppm, a multiplet peak was assigned to the methylene proton situated at position H-18 and H-22 of 1-butylpyrrolidine. Signal of protons H-10, H-12, H-14 and H-16 appeared at  $\delta$  2.12 ppm as a doublet while another four methylene proton H-17 and H-21 were resonated at  $\delta$  3.02 ppm. Protons of pyrrolidine ring at position H-9, H-11, H-13 and H-15 were observed at  $\delta$  3.48 ppm as a multiplet. Chemical shift appeared at 4.45 ppm was attributed to the proton of methylene group connecting phenylene ring and 1-butylpyrrolidine while aromatic proton of phenylene ring were recorded at  $\delta$  7.57 ppm.

For compound  $[\text{Bpyl}]^{2+} \cdot 2[\text{NTf}_2]^-$  (Figure 4.31) and  $[\text{Bpyl}]^{2+} \cdot 2[\text{PF}_6]^-$  (Figure 4.32), a similar number of chemical shift and multiplication were recorded. However, the effect of solvent causes a slight shifting to the chemical shift towards lower or upper regions of spectra.

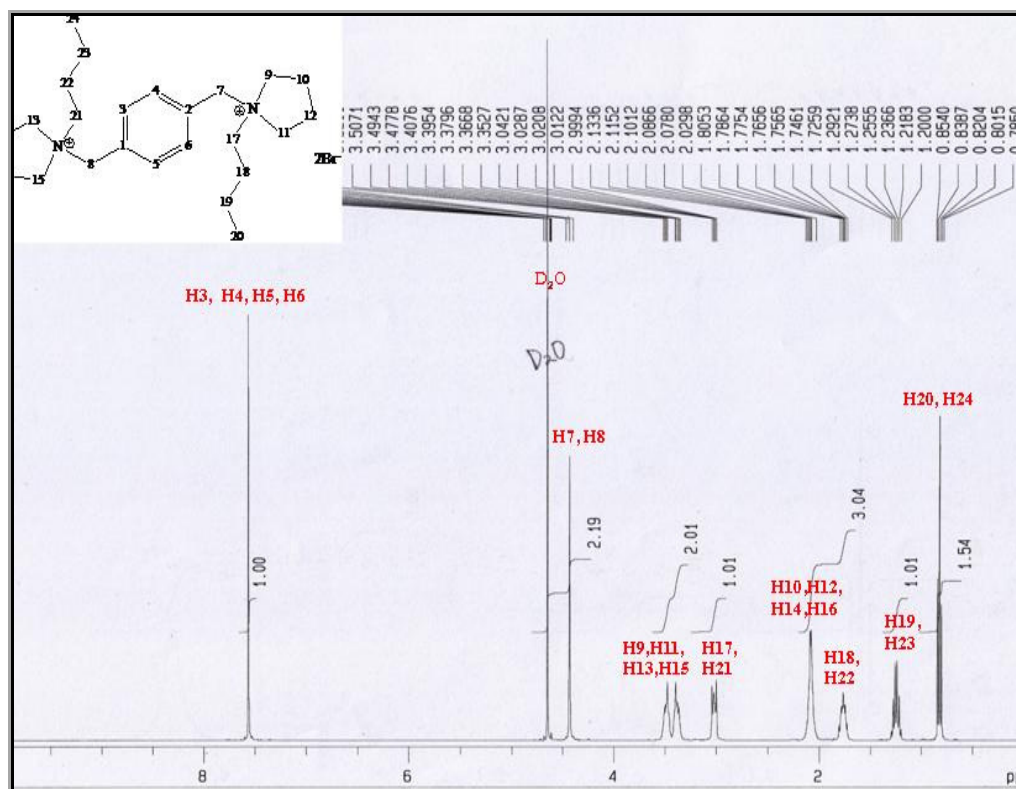


Figure 4.30 : <sup>1</sup>H NMR spectrum of [Bpyl]<sup>2+</sup>.2[Br]<sup>-</sup>

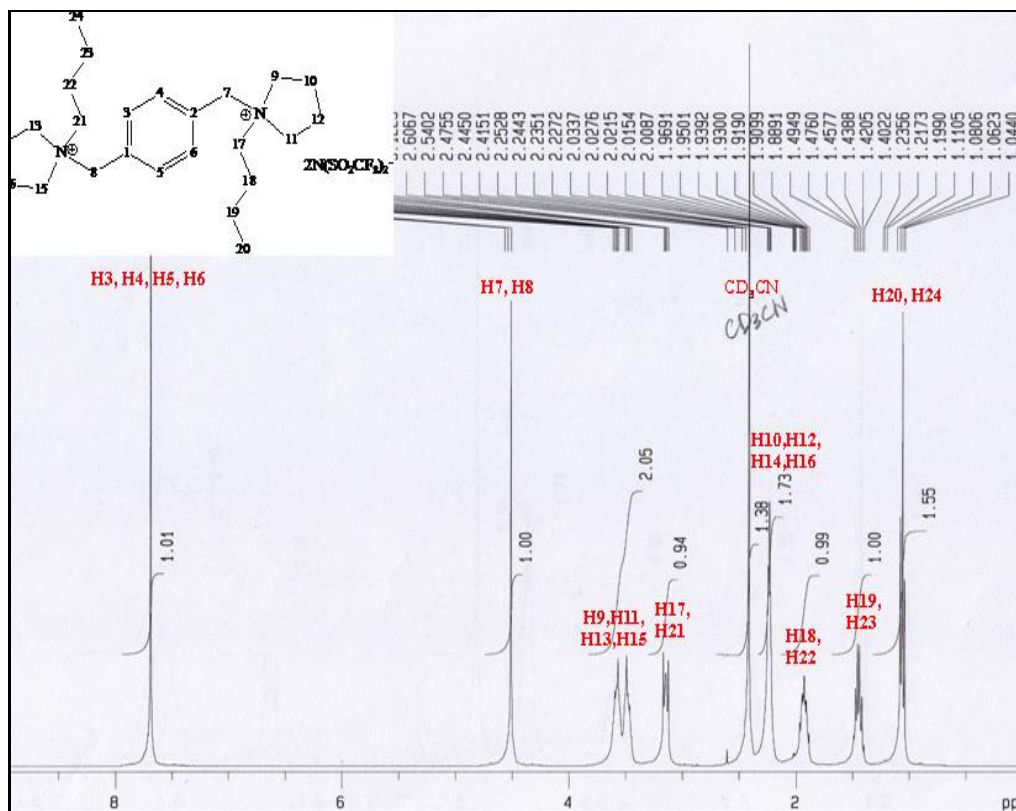
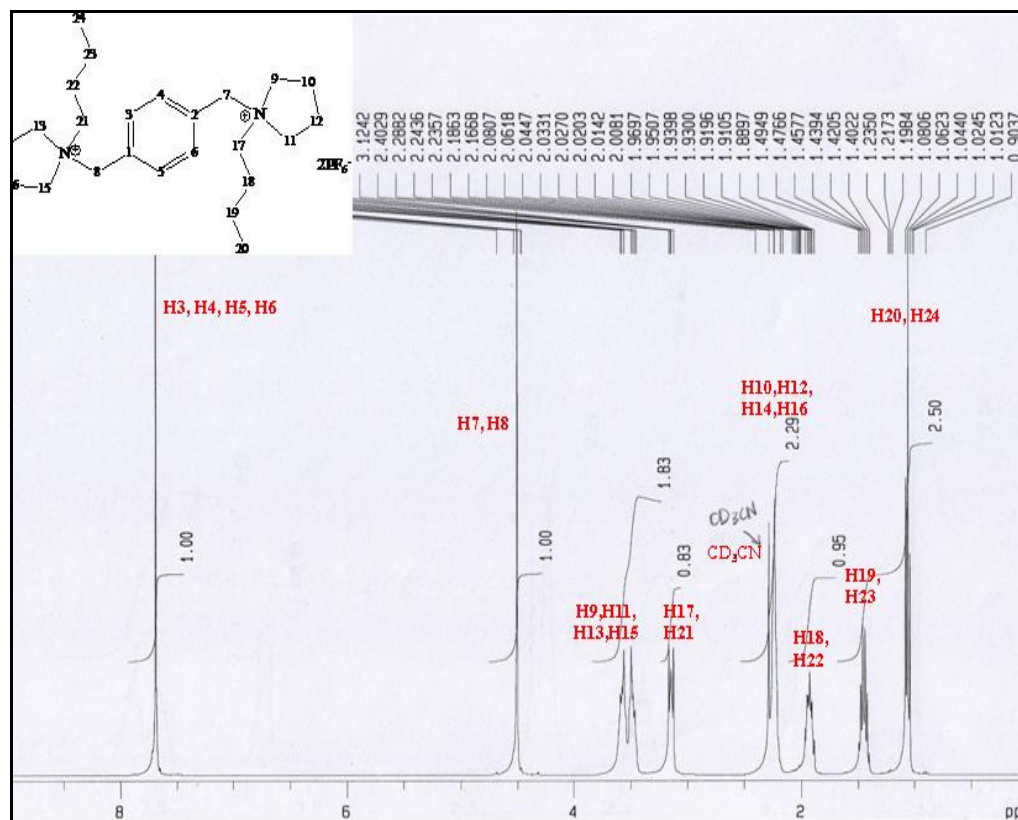


Figure 4.31 : <sup>1</sup>H NMR spectrum of [Bpyl]<sup>2+</sup>.2[NTf<sub>2</sub>]<sup>-</sup>





**Figure 4.32 :**  $^1\text{H}$  NMR spectrum of  $[\text{Bpyl}]^{2+} \cdot 2[\text{PF}_6]^-$

A complete NMR results for the compound in  $[\text{Bpyl}]^{2+} \cdot 2[\text{A}]^-$  series were tabulated in the Table 4.10.

**Table 4.10 :**  $^1\text{H}$  NMR spectral data of  $[\text{Bpyl}]^{2+} \cdot 2[\text{A}]^-$

Chemical shift (ppm)			Coupling constant (Hz)	Multiplication	Assignment
Br	NTf <sub>2</sub>	PF <sub>6</sub>			
0.82	1.07	1.03	7.32	t	H-20, H-24
1.24	1.46	1.44	7.32	sextet	H-19, H-23
1.77	1.97	1.91	4.00	m	H-18, H-22
2.12	2.23	2.23	-	m	H-10, H-12, H-14, H-16
3.02	3.15	3.15	4.28	q	H-17, H-21
3.48	3.49	3.57	4.00	m	H-9, H-11, H-13, H-15
4.45	4.52	4.50	-	dd	Methylene group
7.57	7.70	7.68	-	d	Phenylene ring

The  $^{13}\text{C}$  NMR spectrum of  $[\text{Bpyl}]^{2+} \cdot 2[\text{Br}]^-$  (Figure 4.33) recorded eight non identical resonance signals of carbon. Four  $\text{sp}^3$  carbons of butyl side chain at position C-19, C-20, C-23 and C-24 were resonated at  $\delta$  13.75 ppm carbon signal C-18 and C-22 of the side chain were observed at  $\delta$  20.63 ppm. At  $\delta$  22.47 ppm, the signal was due to the carbons C-10, C-12, C-14 and C-16 of the pyrrolidine ring. The methylene carbons of butyl side chain which was attached to the nitrogen atom were observed at  $\delta$  26.25 ppm. The shortest peak appeared at  $\delta$  60.04 ppm was assigned to the methylene carbon which bridged the phenylene ring and 1-butylpyrrolidine. The signal observed at  $\delta$  62.68 ppm was attributed to the carbons C-9, C-11, C-13 and C-15 of the pyrrolidine ring. Resonance signal of quaternary carbon of phenylene ring were shown at  $\delta$  131.25 ppm while the rest of aromatic  $\text{sp}^2$  carbons of phenylene ring were recorded at  $\delta$  133.75 ppm.

Compound  $[\text{Bpyl}]^{2+} \cdot 2[\text{PF}_6]^-$  (Figure 4.35) recorded a similar results of resonance signals and multiplication with the compound  $[\text{Bpyl}]^{2+} \cdot 2[\text{Br}]^-$  but differ slightly in the chemical shift. In contrary, spectra of compound  $[\text{Bpyl}]^{2+} \cdot 2[\text{NTf}_2]^-$  (Figure 4.34) resulted an additional four signals at  $\delta$  116.56,  $\delta$  119.37,  $\delta$  122.55 and  $\delta$  125.98 ppm which were corresponded to the carbons  $-\text{CF}_3$  of  $\text{NTf}_2$  anion.

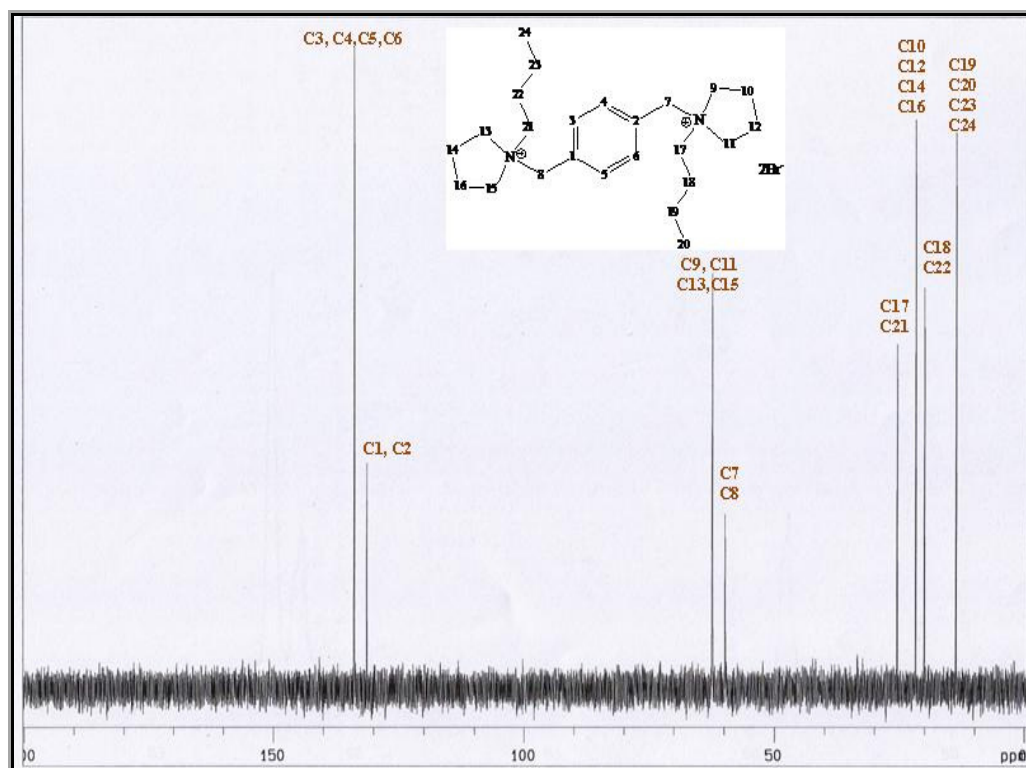


Figure 4.33 :  $^{13}\text{C}$  NMR spectrum of  $[\text{Bpyl}]^{2+} \cdot 2[\text{Br}]^{-}$

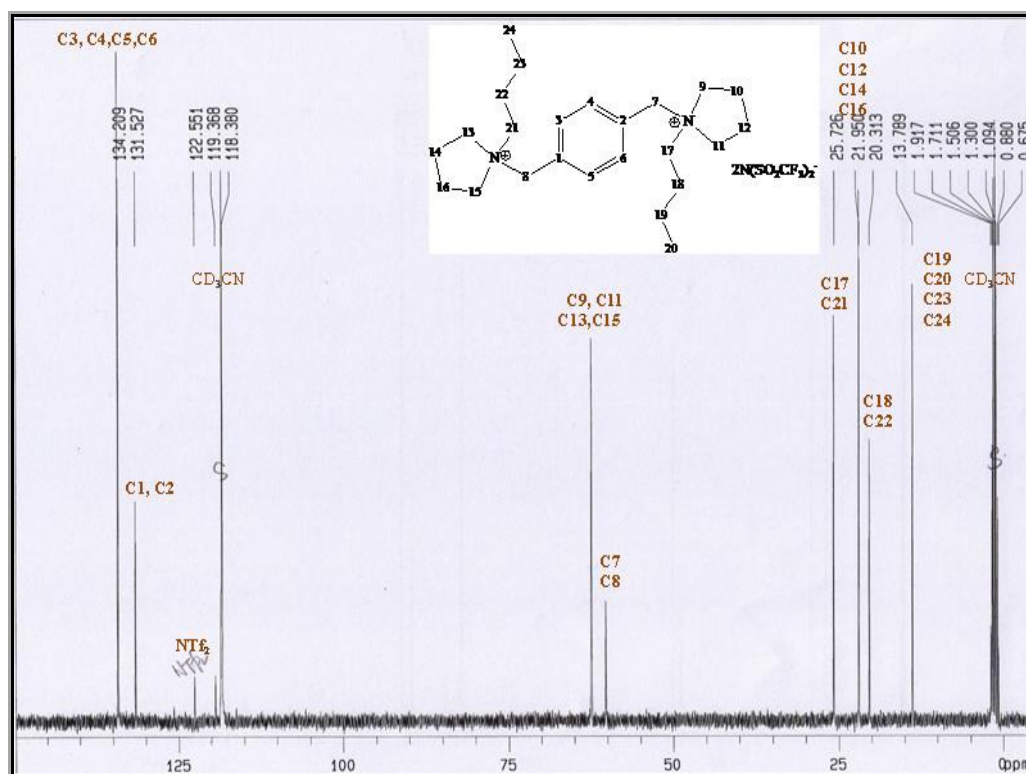


Figure 4.34 :  $^{13}\text{C}$  NMR spectrum of  $[\text{Bpyl}]^{2+} \cdot 2[\text{NTf}_2]^{-}$

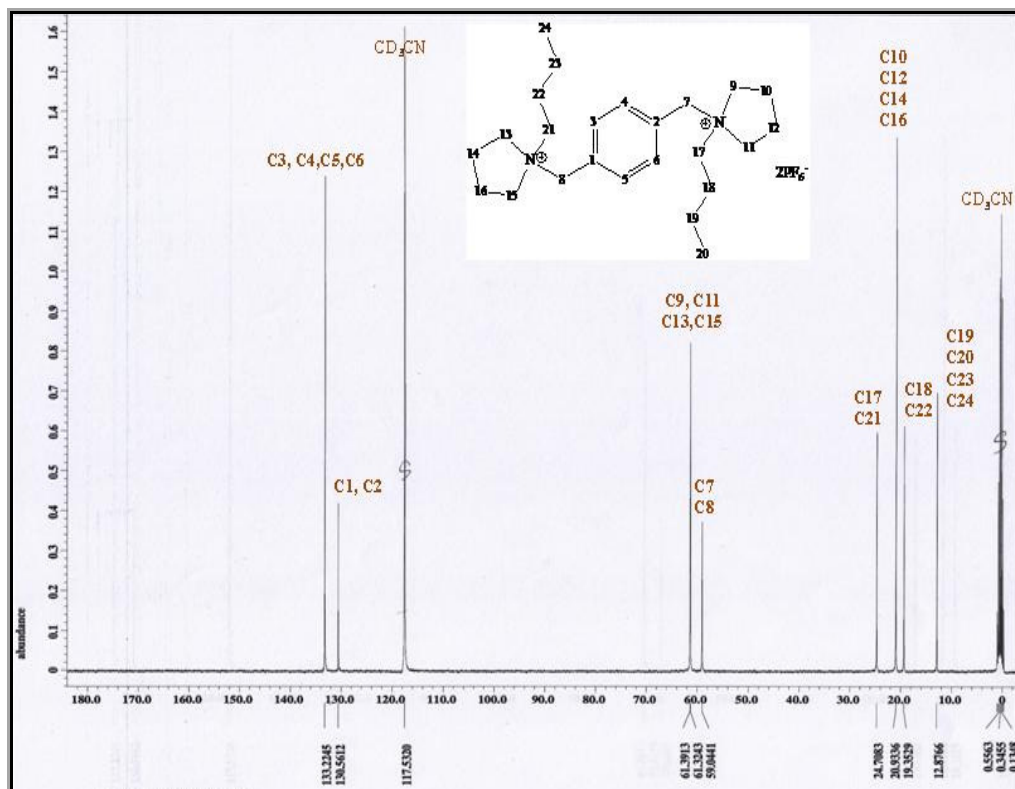


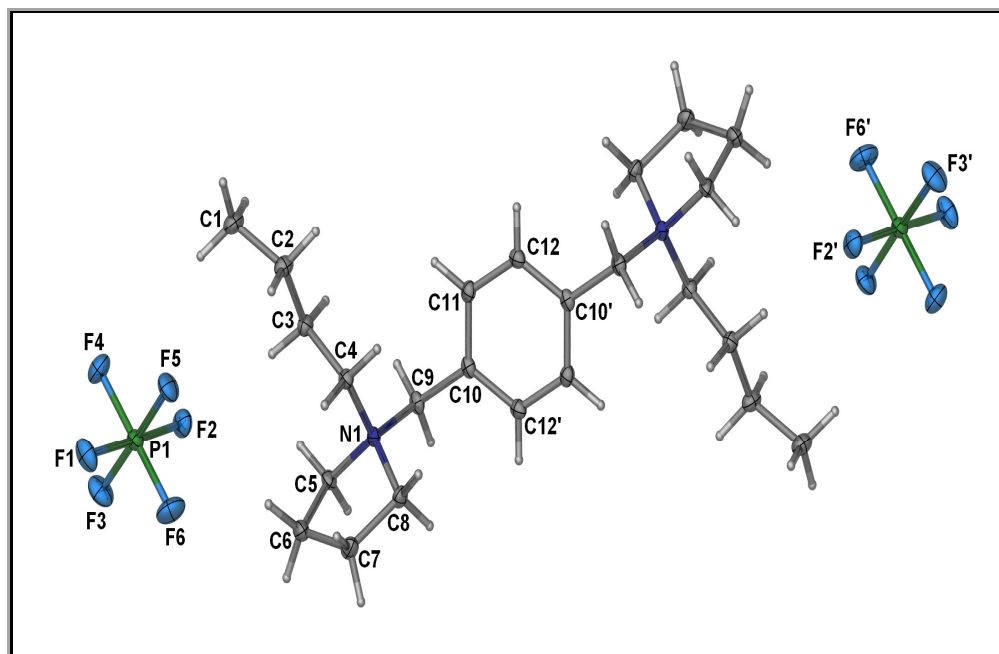
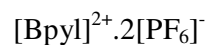
Figure 4.35 :  $^{13}\text{C}$  NMR spectrum of  $[\text{Bpyl}]^{2+} \cdot 2[\text{PF}_6]^-$

A complete NMR results for  $[\text{Bpyl}]^{2+} \cdot 2[\text{A}]^-$  series were tabulated in the Table 4.11.

Table 4.11 :  $^{13}\text{C}$  NMR spectral data of  $[\text{Bpyl}]^{2+} \cdot 2[\text{A}]^-$

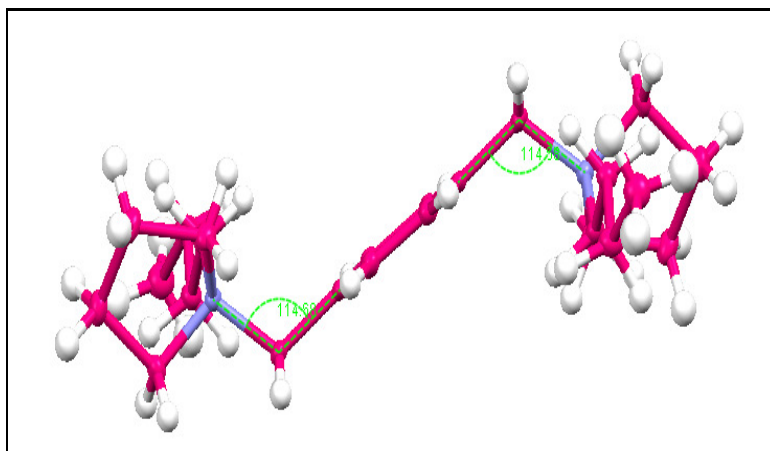
Chemical shift (ppm)			Assignment
Br	NTf <sub>2</sub>	PF <sub>6</sub>	
13.75	13.79	12.88	C-19, C-20, C-23, C-24
20.63	20.31	19.35	C-18, C-22
22.47	21.95	20.93	C-10, C-12, C-14, C-16
26.25	25.73	24.71	C-17, C-21
60.04	60.23	59.04	Methylene carbon
62.68	62.44	61.36	C-9, C-11, C-13, C-15
-	116.56	-	-CF <sub>3</sub> (NTf <sub>2</sub> )
-	119.37	-	
-	122.55	-	
-	125.98	-	
131.25	131.53	130.56	Quaternary carbon
133.75	134.21	133.22	C-3, C-4, C-5, C-6

#### 4.4.4 : X-ray Crystallography



**Figure 4.36 :** Molecular structure of the compound  $[\text{Bpyl}]^{2+} \cdot 2[\text{PF}_6]^-$  with displacement ellipsoids drawn at 50% probability level. Hydrogen atoms are drawn as spheres at arbitrary radius.

The organic salt  $[\text{Bpyl}]^{2+} \cdot 2[\text{PF}_6]^-$  was crystallized in a monoclinic,  $P2_1/c$  space group. The crystal was appeared as a colourless prism-shaped crystal. This organic salt exists as a non-interacting cation and anions compound. The cation of the organic salt was a symmetrical molecule which was lying about the centre of inversion.



**Figure 4.37** : [Bpyl] cation moiety in compound [Bpyl]<sup>2+</sup>·2[PF<sub>6</sub>]<sup>-</sup>.

The cation was built from a phenylene ring as a linker and 1-butylpyrrolidine ring at both ends which were connected via methylene carbon at para position forming a Z-shaped conformation. The methylene carbon opened at angle 114.68 (1)°. The 1-butylpyrrolidine rings were aligned at the parallel position but at the opposite direction to each other. On the other hands, the anion lies on a special position of m site symmetry whereby four F atoms lie on this mirror plane.

**Table 4. 12 :** Crystal data and structural refinements of [Bpyl]<sup>2+</sup>.2[PF<sub>6</sub>]<sup>-</sup>

Ionic Liquids	[Bpyl] <sup>2+</sup> .2[PF <sub>6</sub> ] <sup>-</sup>
Empirical Formula	[C <sub>24</sub> H <sub>42</sub> N <sub>2</sub> ] <sup>2+</sup> . 2[PF <sub>6</sub> ] <sup>-</sup>
Molecular weight/ g mol <sup>-1</sup>	648.53
Colour	Colourless
Size/mm <sup>3</sup>	0.21 x 0.11 x 0.05
Crystal system	Triclinic
Space group	P -1
a/Å	9.350
b/Å	10.754
c/Å	15.084
α (°)	90.034
β (°)	108.765
γ (°)	89.969
Volume/ Å <sup>3</sup>	1440.5 (2)
Z, Dc/g cm <sup>-3</sup>	2
F(000)	676
μ/mm <sup>-1</sup>	0.247
θ range (°)	2.28-27.00
Reflections collected	17275
Data/restraints/parameter	2548/0/182
R <sub>int</sub>	0.0366
Ref <sub>Ins</sub> (total)	3142
Ref <sub>Ins</sub> (unique)	2548
Final R indices [I>2σ(I)]	R <sub>1</sub> = 0.0331 wR <sub>2</sub> = 0.0747
R indices (all data)	R <sub>1</sub> = 0.0453 wR <sub>2</sub> = 0.0813
ρ <sub>max</sub> /e/Å <sup>3</sup>	0.315 and -0.341

#### 4.5 : *N,N'*-[1,4-Phenylenebis(methylene)]bis-(*N,N*-dimethylpiperidinium) series

##### 4.5.1 : $^1\text{H}$ NMR and $^{13}\text{C}$ NMR Spectroscopy

Dicationic organic salt  $[\text{Nmpp}]^{2+} \cdot 2[\text{Br}]^-$  is a white solid and was obtained from the reaction between  $\alpha, \alpha$ -dibromo-*p*-xylene and 1-methylpiperidine. The  $^1\text{H}$  NMR spectra of  $[\text{Nmpp}]^{2+} \cdot 2[\text{Br}]^-$  (Figure 4.38) indicated seven unequivalent protons. The protons labelled H-11 and H-16 of piperidine ring were resonated at  $\delta$  1.56 and  $\delta$  1.66 ppm as two broad peaks. Another multiplet broad signal was recorded at  $\delta$  1.88 ppm which was assigned for proton at position H-9, H-13, H-14 and H-18 of piperidine ring. Protons at methyl group of 1-methylpiperidine were resonated at  $\delta$  2.94 ppm as doublet of doublet signal. At  $\delta$  3.34 ppm, the multiplet was belonged to the protons H-10, H-12, H-15 and H-17 of piperidine ring. Proton of methylene carbon was detected at  $\delta$  4.57 ppm as a doublet of doublet while the aromatic protons of phenylene ring were recorded at  $\delta$  7.62 ppm as a doublet.

The  $^1\text{H}$  NMR spectra of compounds  $[\text{Nmpp}]^{2+} \cdot 2[\text{NTf}_2]^-$  (Figure 4.39) and  $[\text{Nmpp}]^{2+} \cdot 2[\text{PF}_6]^-$  (Figure 4.40) recorded a similar number of signals except the chemical shift is shifting slightly towards down or up field regions due to the effect of solvent.



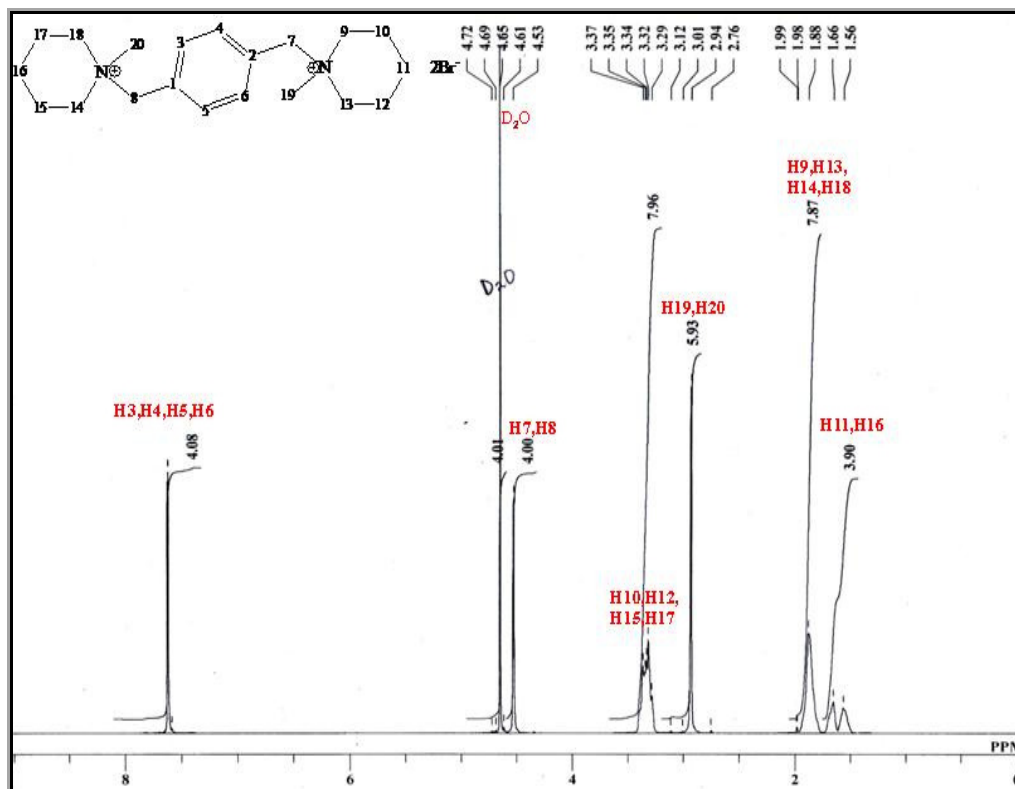


Figure 4.38 :  $^1\text{H}$  NMR spectrum of  $[\text{Nmpp}]^{2+} \cdot 2[\text{Br}]^-$

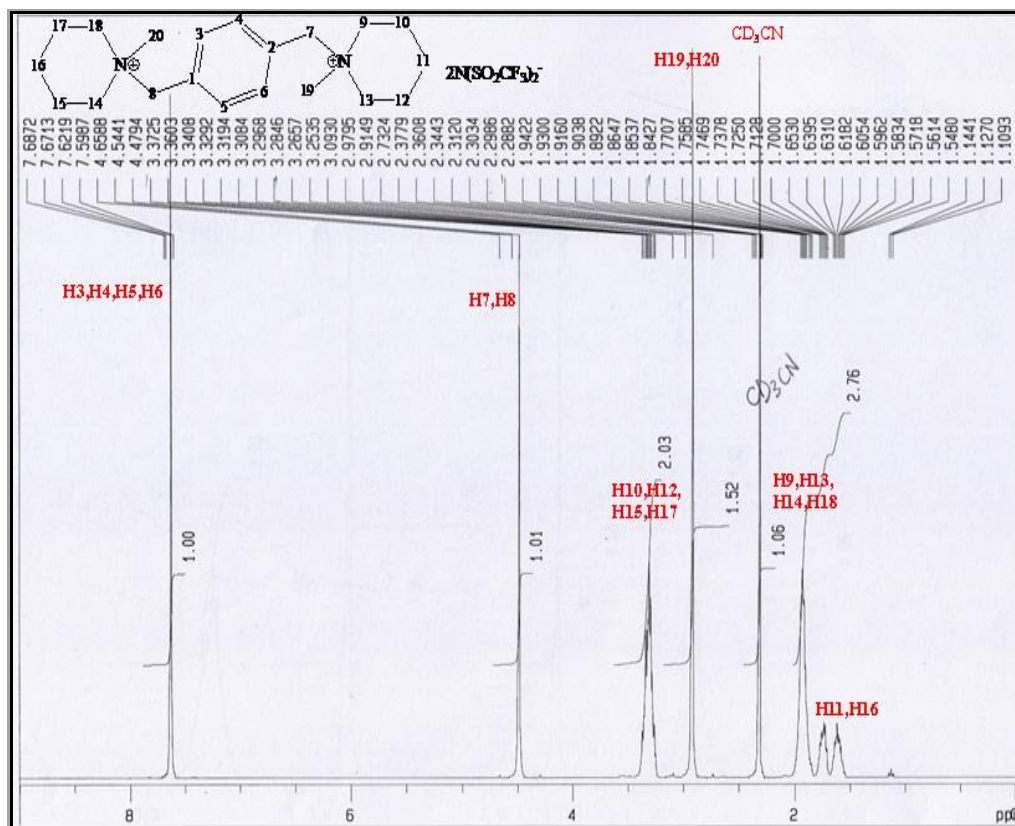


Figure 4.39 :  $^1\text{H}$  NMR spectrum of  $[\text{Nmpp}]^{2+} \cdot 2[\text{NTf}_2]^-$

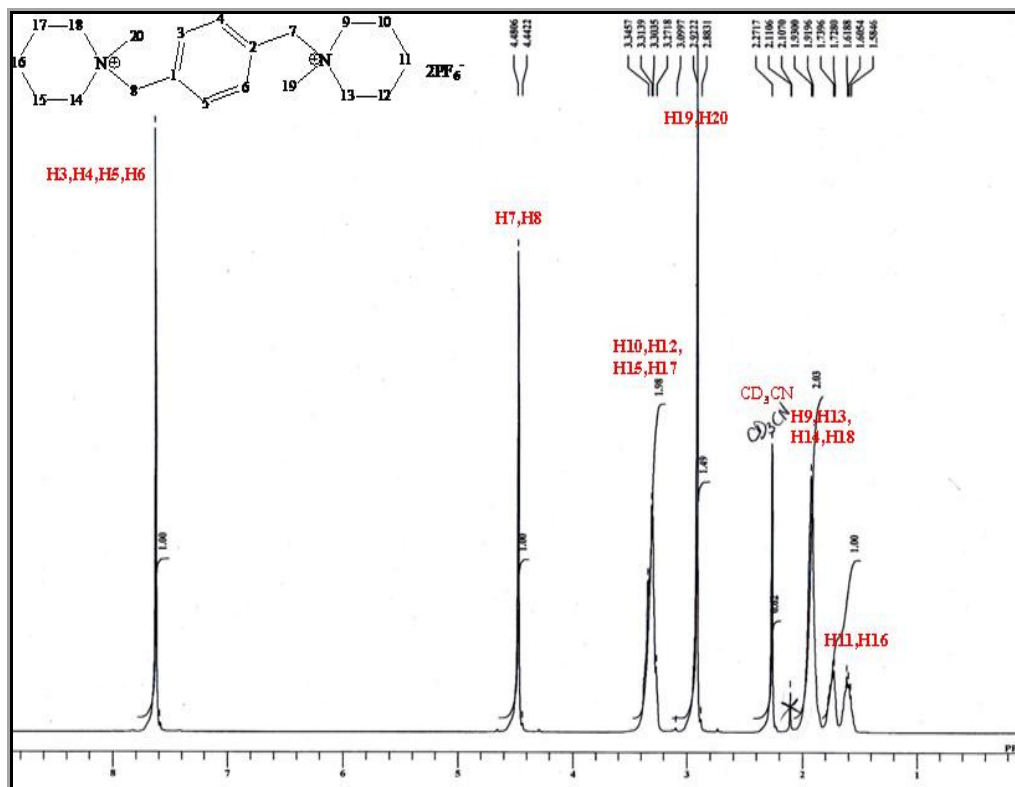


Figure 4.40 :  $^1\text{H}$  NMR spectrum of  $[\text{Nmpp}]^{2+} \cdot 2[\text{PF}_6]^-$

The chemical shifts of these series were simplified in the Table 4.13.

Table 4.13 :  $^1\text{H}$  NMR spectral data of  $[\text{Nmpp}]^{2+} \cdot 2[\text{A}]^-$

Chemical shift (ppm)			Coupling constant (Hz)	Multiplication	Assignment
Br	NTf <sub>2</sub>	PF <sub>6</sub>			
1.56	1.57	1.60	4.00	m	H-11, H-16
1.66	1.73	1.73	4.00	m	H-9, H-14
1.88	1.90	1.92	4.00	m	H-13, H-18
2.94	2.97	2.90	-	s	H-19, H-20
3.34	3.31	3.31	4.00	m	H-10, H-12, H-15, H-17
4.57	4.50	4.46	-	dd	Methylene group
7.62	7.65	7.63	-	d	Phenylene ring

The  $^{13}\text{C}$  NMR spectrum of compound  $[\text{Nmpp}]^{2+} \cdot 2[\text{Br}]^{-}$  (Figure 4.41) indicated seven signals which representing seven non-equivalent carbons. Four  $\text{sp}^3$  carbon labelled C-10, C-12, C-15 and C-17 of piperidine ring were recorded at  $\delta$  20.47 ppm. Signal of carbons C-11 and C-16 of piperidine ring were observed at  $\delta$  21.38 ppm. The signal at  $\delta$  47.42 ppm was assigned to the carbon of two methyl groups. The peak resonance at  $\delta$  61.75 ppm was attributed to the carbons C-9, C-13, C-14 and C-18 of piperidine ring. Methylene carbons at the bridge were appeared at  $\delta$  67.88 ppm. At the down field region, the signal of quaternary carbons was recorded at  $\delta$  130.05 ppm while the aromatic carbons of phenylene ring were observed at  $\delta$  134.46 ppm.

Similar signals were recorded for compound  $[\text{Nmpp}]^{2+} \cdot 2[\text{PF}_6]^{-}$  (Figure 4.43) but the chemical shift differ slightly because the influence of solvent. However, the spectrum of  $[\text{Nmpp}]^{2+} \cdot 2[\text{NTf}_2]^{-}$  (Figure 4.42) showed a distinctive peaks at  $\delta$  115.14,  $\delta$  118.36,  $\delta$  121.58 and  $\delta$  124.80 ppm which were attributed to the  $-\text{CF}_3$  of  $\text{NTf}_2$  groups.

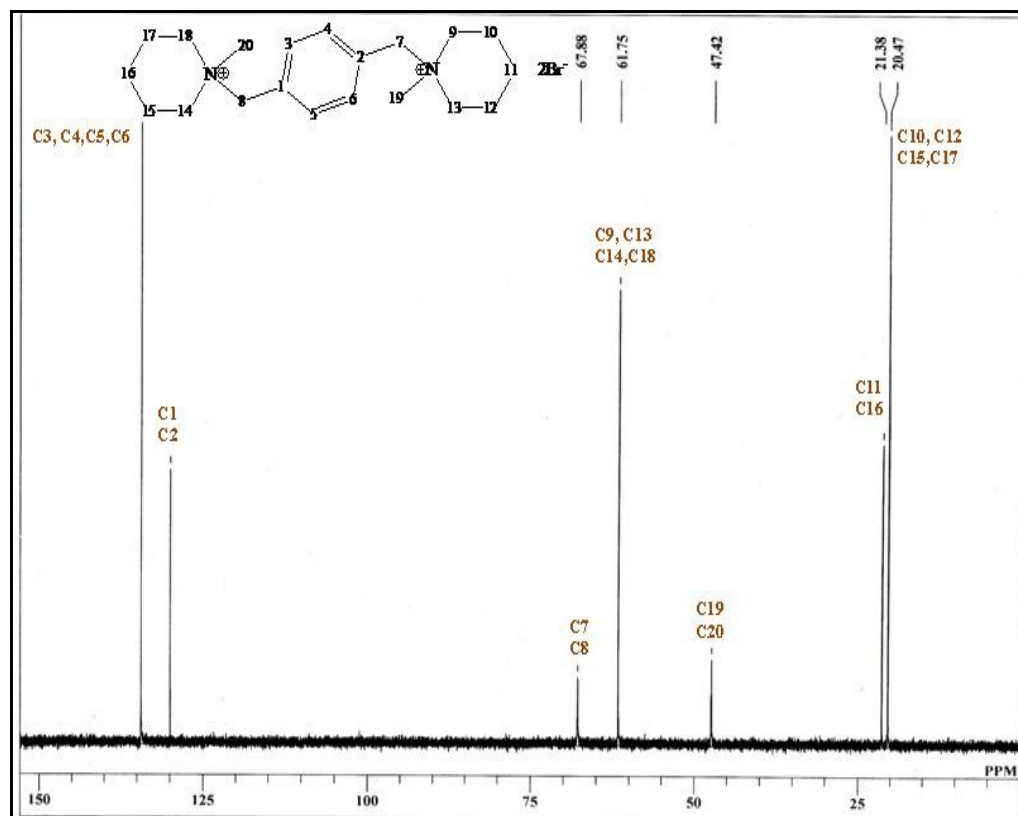


Figure 4.41 :  $^{13}\text{C}$  NMR spectrum of  $[\text{Nmpp}]^{2+} \cdot 2[\text{Br}]^{-}$

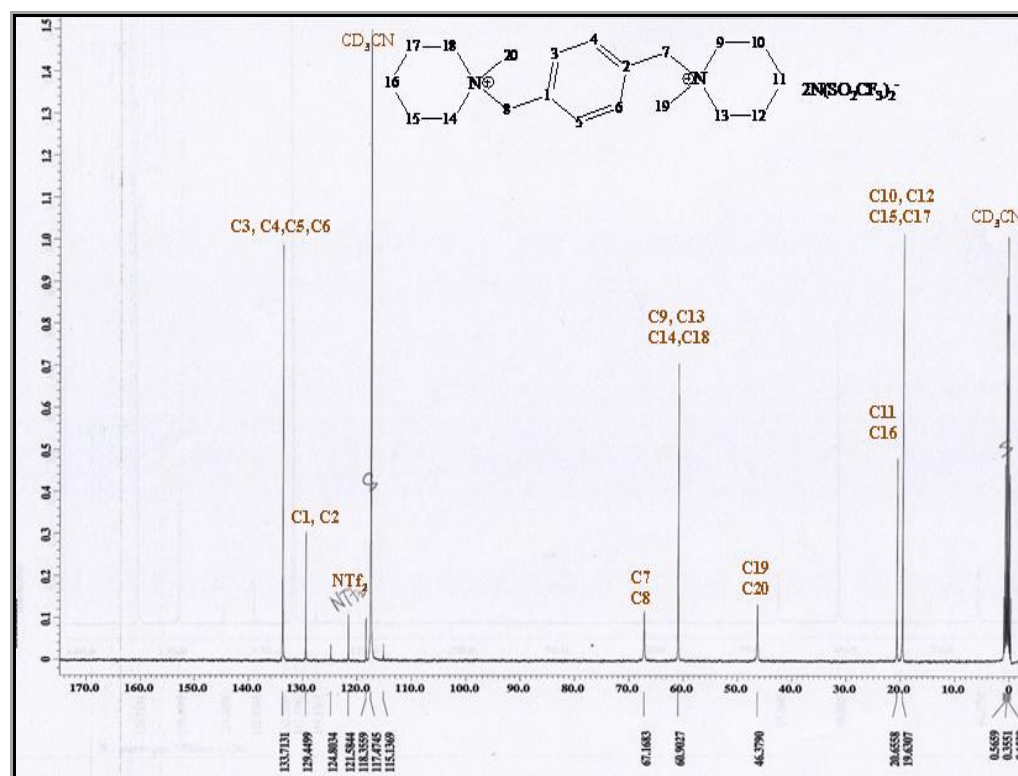
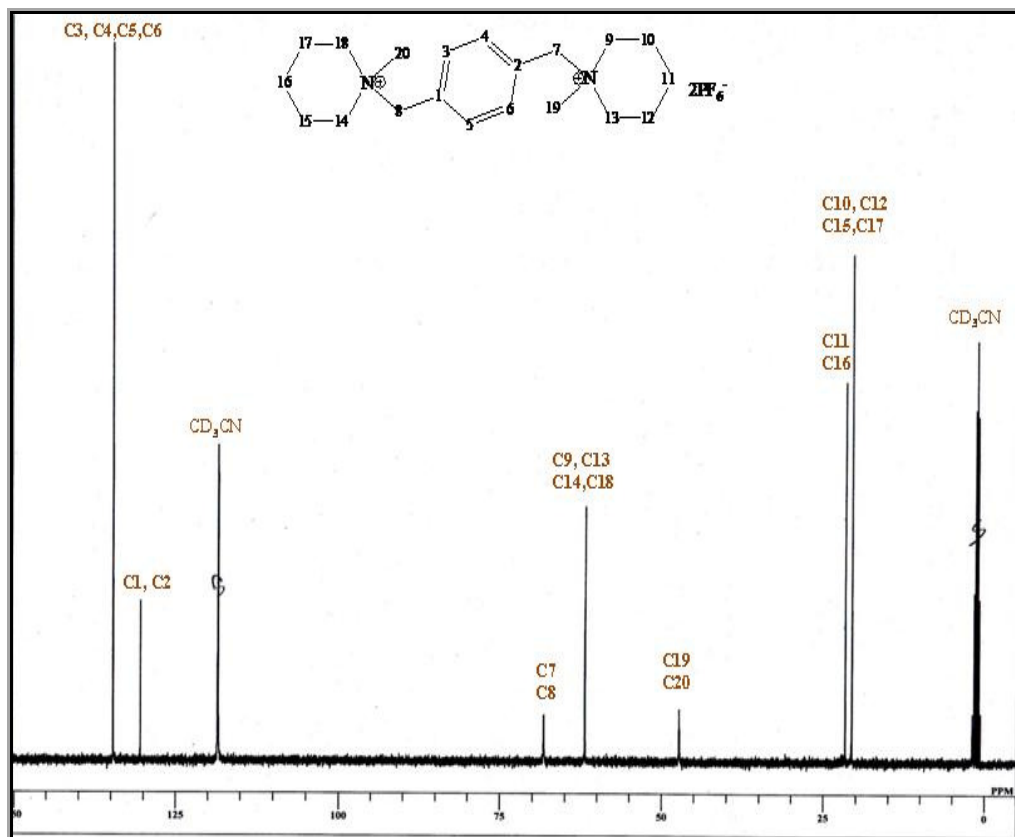


Figure 4.42 :  $^{13}\text{C}$  NMR spectrum of  $[\text{Nmpp}]^{2+} \cdot 2[\text{NTf}_2]^{-}$



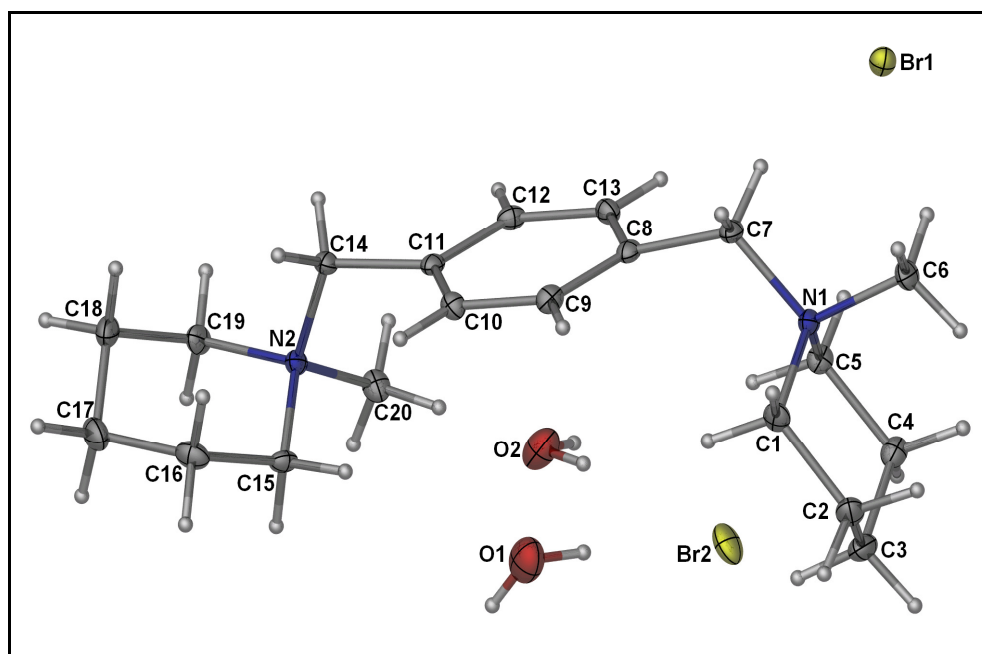
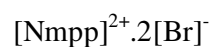
**Figure 4.43 :**  $^{13}\text{C}$  NMR spectrum of  $[\text{Nmpp}]^{2+} \cdot 2[\text{PF}_6]^-$

The chemical shifts of these series were simplified in the Table 4.14.

**Table 4.14 :**  $^{13}\text{C}$  NMR spectral data of  $[\text{Nmpp}]^{2+} \cdot 2[\text{A}]^-$

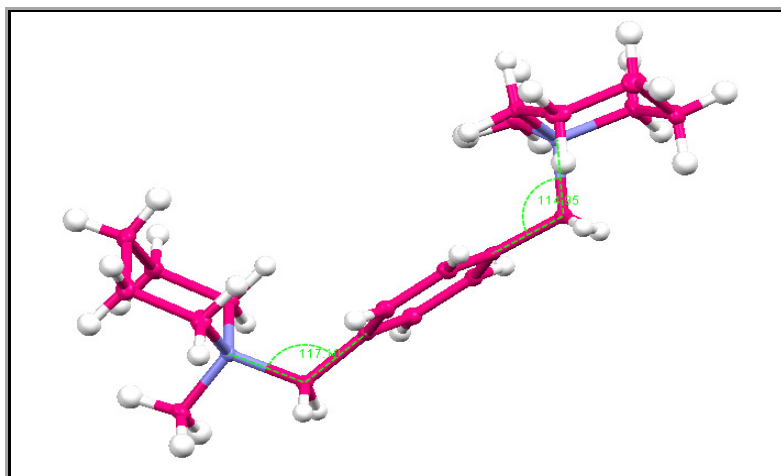
Chemical shift (ppm)			Assignment
Br	NTf <sub>2</sub>	PF <sub>6</sub>	
20.47	19.63	19.90	C-10, C-12, C-15, C-17
21.38	20.66	21.12	C-11, C-16
47.42	46.38	45.82	C-19, C-20
61.75	60.90	60.36	C-9, C-13, C-14, C-18
67.88	67.17	66.65	Methylene carbon
-	115.14	-	-CF <sub>3</sub> (NTf <sub>2</sub> )
-	118.36	-	
-	121.58	-	
-	124.80	-	
130.05	129.45	130.09	Quaternary carbon
134.46	133.71	134.50	C-3, C-4, C-5, C-6

#### 4.5.4 : X-ray Crystallography



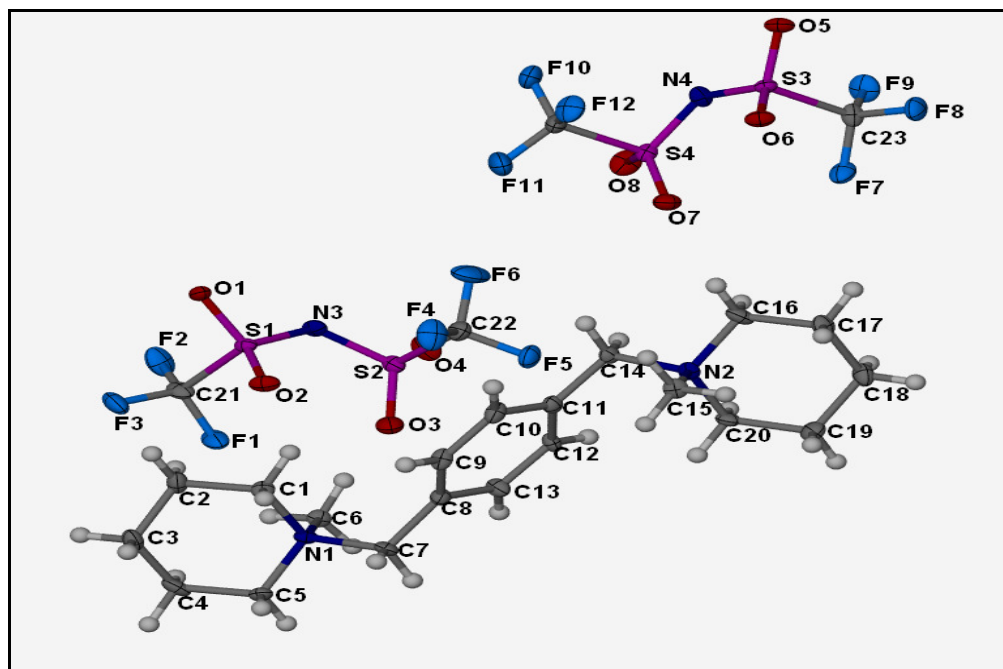
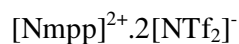
**Figure 4.44** : Molecular structure of the compound  $[\text{Nmpp}]^{2+} \cdot 2[\text{Br}]^{-}$  with displacement ellipsoids drawn at 50% probability level. Hydrogen atoms are drawn as spheres at arbitrary radius.

The compound  $[\text{Nmpp}]^{2+} \cdot 2[\text{Br}]^{-}$  was crystallized in a triclinic, P-1 crystal system which was appeared as a colourless block-shaped crystal. In the crystal packing, this compound existed as a non-interacting cation and anions molecular organic salt. The organic salt comprised of an organic dication and two bromide counter anions.



**Figure 4. 45 :** [Nmpp] cation moiety in compound  $[\text{Nmpp}]^{2+} \cdot 2[\text{Br}]^-$ .

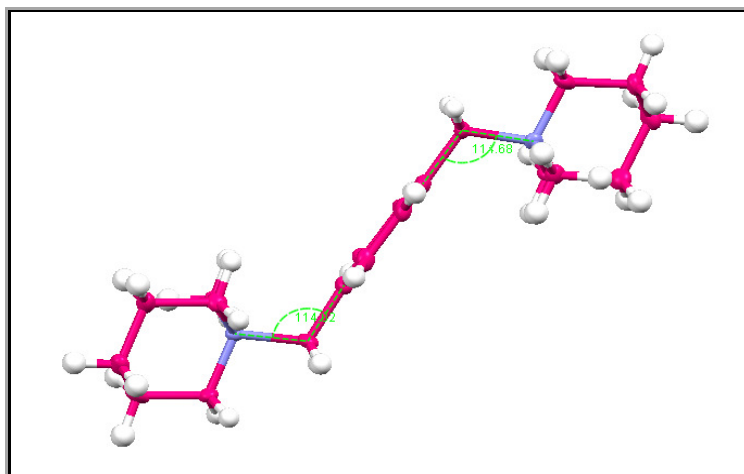
The cation was constructed from a phenylene ring as a bridge which connecting the 1-methylpiperidine ring at para position through methylene carbon of phenylene ring and nitrogen atom of 1-methylpiperidine. This compound was not symmetry since the methylene carbon at both end of phenylene ring opened at different angles; 114.95 and 117.10° depending on how the piperidine ring attached itself to the linker. Therefore, the six-membered phenylene ring was no longer planar. Compared to the compound of the same series  $[\text{Nmpp}]^{2+} \cdot 2[\text{NTf}_2]^-$ , the cation portion in this organic salt possesses a U-shaped conformation whereby the 1-methylpiperidene portion attached themselves at the phenylene ring on the same side. Both piperidine rings adopted a chair conformation which was observed in the cyclohexane chair conformation. In addition, piperidine rings aligned themselves almost perpendicular to each other.



**Figure 4.46** : Molecular structure of the compound  $[\text{Nmpp}]^{2+} \cdot 2[\text{NTf}_2]^-$  with displacement ellipsoids drawn at 50% probability level. Hydrogen atoms are drawn as spheres at arbitrary radius.

Crystals of compound  $[\text{Nmpp}]^{2+} \cdot 2[\text{NTf}_2]^-$  was obtained from slow diffusion of acetonitrile and has been crystallized in the monoclinic,  $P2_1/c$  crystal system. It is appeared as colourless block-shaped crystals. In the crystal packing, the molecule exists as a non-interacting cation and anions. The cation of the organic salt was a symmetrical molecule which was lying about the centre of inversion.





**Figure 4.47 :** [Nmpp] cation moiety in compound  $[\text{Nmpp}]^{2+} \cdot 2[\text{NTf}_2]^-$ .

The cation was built from a phenylene ring as a linker which is connecting the 1-methylpiperidine group at both end of phenylene ring through methylene carbon at para position. The 1-methylpiperidine ring adapted a chair conformation which was similar to the cyclohexane conformation. Besides, the 1-methylpiperidine rings at both ends were aligned parallel to each other and pointing at the opposite direction forming a Z-conformation. The angle of 1-methylpiperidine-phenylene ring-1-methylpiperidine group is  $114.7(1)^\circ$ .

**Table 4.15** : Crystal data and structure refinements of [Nmpp]<sup>2+</sup>.2[Br]<sup>-</sup> and [Nmpp]<sup>2+</sup>.2[NTf<sub>2</sub>]<sup>-</sup>

Ionic Liquids	[Nmpp] <sup>2+</sup> .2[Br] <sup>-</sup>	[Nmpp] <sup>2+</sup> .2[NTf <sub>2</sub> ] <sup>-</sup>
Empirical Formula	[C <sub>20</sub> H <sub>38</sub> N <sub>2</sub> ] <sup>2+</sup> .2[Br] <sup>-</sup>	[C <sub>20</sub> H <sub>34</sub> N <sub>2</sub> ] <sup>2+</sup> . 2[C <sub>4</sub> N <sub>2</sub> F <sub>12</sub> O <sub>8</sub> S <sub>4</sub> ] <sup>-</sup>
Molecular weight/ g mol <sup>-1</sup>	482.34	862.876
Colour	Colourless	Colourless
Size/mm <sup>3</sup>	0.50 x 0.40 x 0.40	0.25 x 0.20 x 0.18
Crystal system	Triclinic	Monoclinic
Space group	P -1	P2 <sub>1</sub> /c
a/Å	6.6166 (5)	17.06 (3)
b/Å	12.7854 (9)	15.38 (3)
c/Å	13.6545 (10)	14.74 (2)
α (°)	93.5290 (10)	90.00
β (°)	96.3290 (10)	115.47 (16)
γ (°)	101.2360 (10)	90.000
Volume/ Å <sup>3</sup>	1121.98 (14)	3492 (10)
Z, Dc/g cm <sup>-3</sup>	2	4
F(000)	500	1768
μ/mm <sup>-1</sup>	3.629	0.387
θ range (°)	1.63-27.00	1.32-30.61
Reflections collected	13811	52707
Data/restraints/parameter	4138/4/249	9095/0/471
R <sub>int</sub>	0.0265	0.0657
Ref <sub>ins</sub> (total)	4896	10627
Ref <sub>ins</sub> (unique)	4138	9095
Final R indices [I>2σ(I)]	R <sub>1</sub> = 0.0242	R <sub>1</sub> = 0.1689
	wR <sub>2</sub> = 0.0551	wR <sub>2</sub> = 0.4148
R indices (all data)	R <sub>1</sub> = 0.0331	R <sub>1</sub> = 0.1791
	wR <sub>2</sub> = 0.0580	wR <sub>2</sub> = 0.4186
lρ <sub>max</sub> /e/Å <sup>3</sup>	0.687 and -0.362	1.802 and -1.122

#### 4.6 : *N,N'*-[1,4-Phenylenebis(methylene)]bis-(*N,N*-dimethylmorpholinium) series

##### 4.6.1 : $^1\text{H}$ NMR and $^{13}\text{C}$ NMR Spectroscopy

Dicationic organic salt  $[\text{Mmorp}]^{2+}.2[\text{Br}]^-$  is a white solid and was synthesized from the reaction of  $\alpha,\alpha$ -dibromo-*p*-xylene with 1-methylmorpholine. The  $^1\text{H}$  NMR spectrum of  $[\text{Mmorp}]^{2+}.2[\text{A}]^-$  (Figure 4.48) recorded six types of proton. The first chemical shift at 3.07 ppm was assigned to the proton of methyl group and appeared as a singlet. Protons labelled H-9, H-13 and H-11 and H-15 of the morpholine ring appeared at  $\delta$  3.34 ppm and  $\delta$  3.57 ppm as multiplets. The signal appeared at  $\delta$  3.97 ppm was a multiplet which was assigned to the protons H-10, H-12, H-14 and H-16 of the morpholine ring. At  $\delta$  4.68 ppm, the resonance signal appeared as a doublet of doublet which was attributed to the methylene protons while aromatic protons were observed at the down field region which resonated at  $\delta$  7.65 as a doublet.

The  $^1\text{H}$  NMR spectra of compounds  $[\text{Mmorp}]^{2+}.2[\text{NTf}_2]^-$  (Figure 4.49) and  $[\text{Mmorp}]^{2+}.2[\text{PF}_6]^-$  (Figure 4.50) recorded similar results with the compound  $[\text{Mmorp}]^{2+}.2[\text{Br}]^-$  with slightly differ in the chemical shift which might be shifted towards down or up field regions.

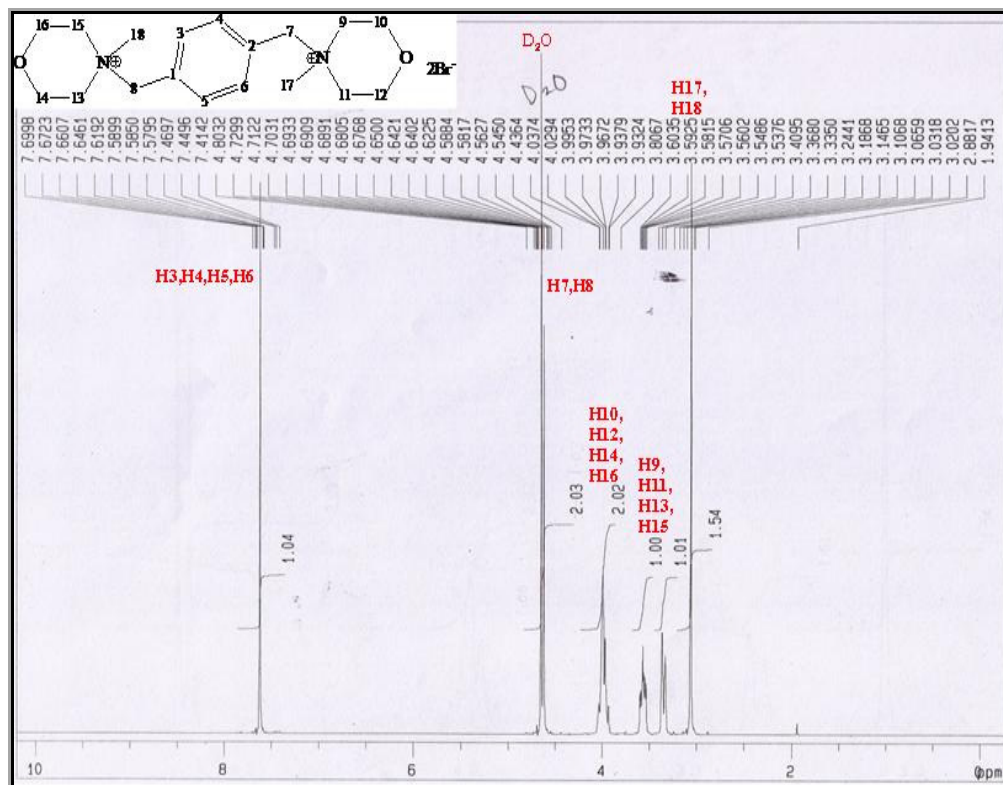


Figure 4.48 : <sup>1</sup>H NMR spectrum of [Mmorp]<sup>2+</sup>.2[Br<sup>-</sup>]

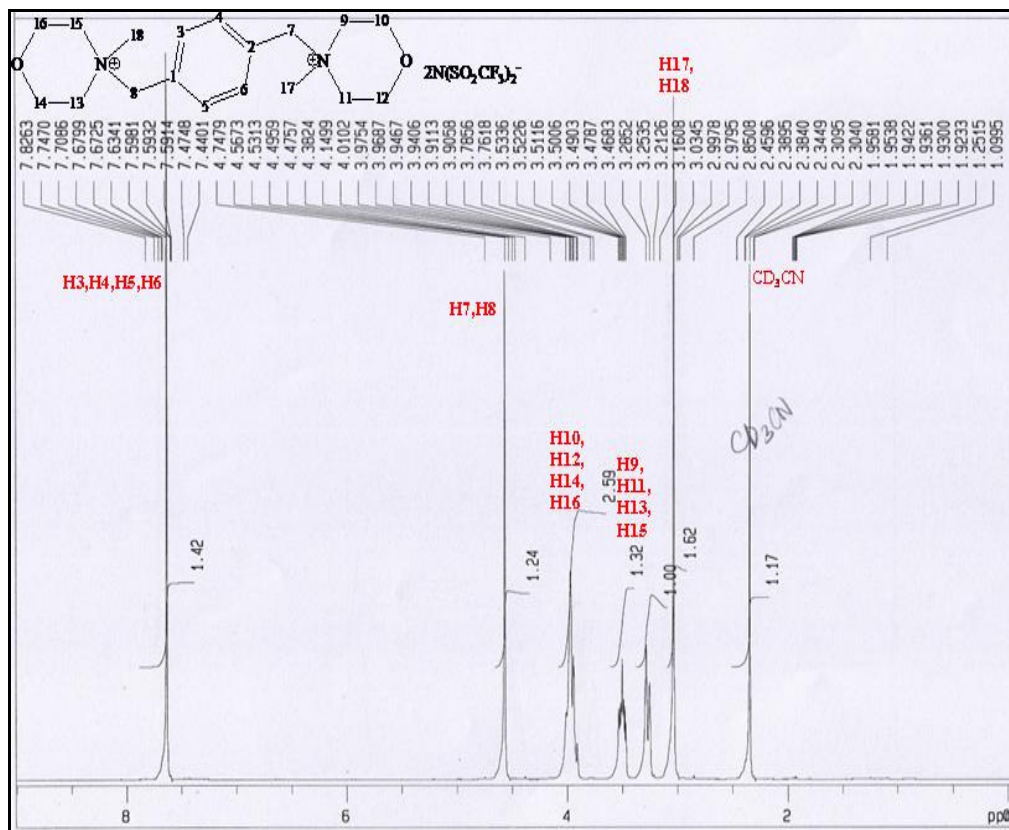


Figure 4.49 : <sup>1</sup>H NMR spectrum of [Mmorp]<sup>2+</sup>.2[NTf<sub>2</sub><sup>-</sup>]

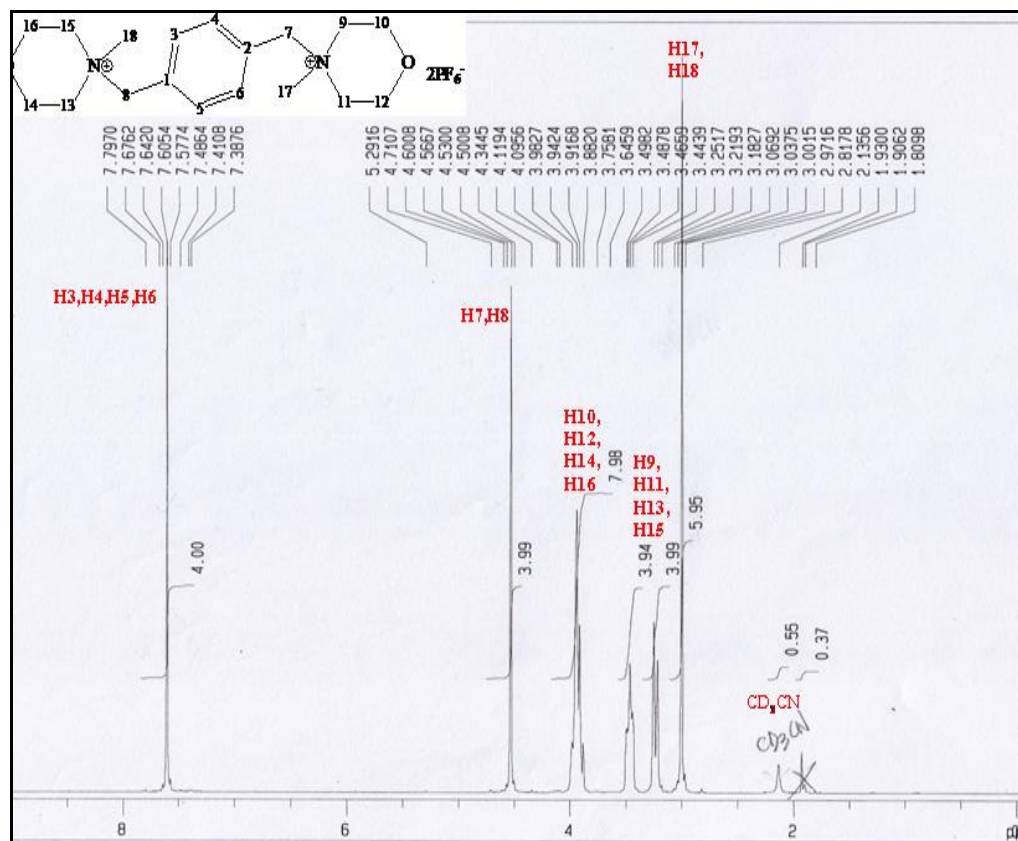


Figure 4.50 :  $^1\text{H}$  NMR spectrum of  $[\text{Mmorp}]^{2+} \cdot 2[\text{PF}_6]^-$

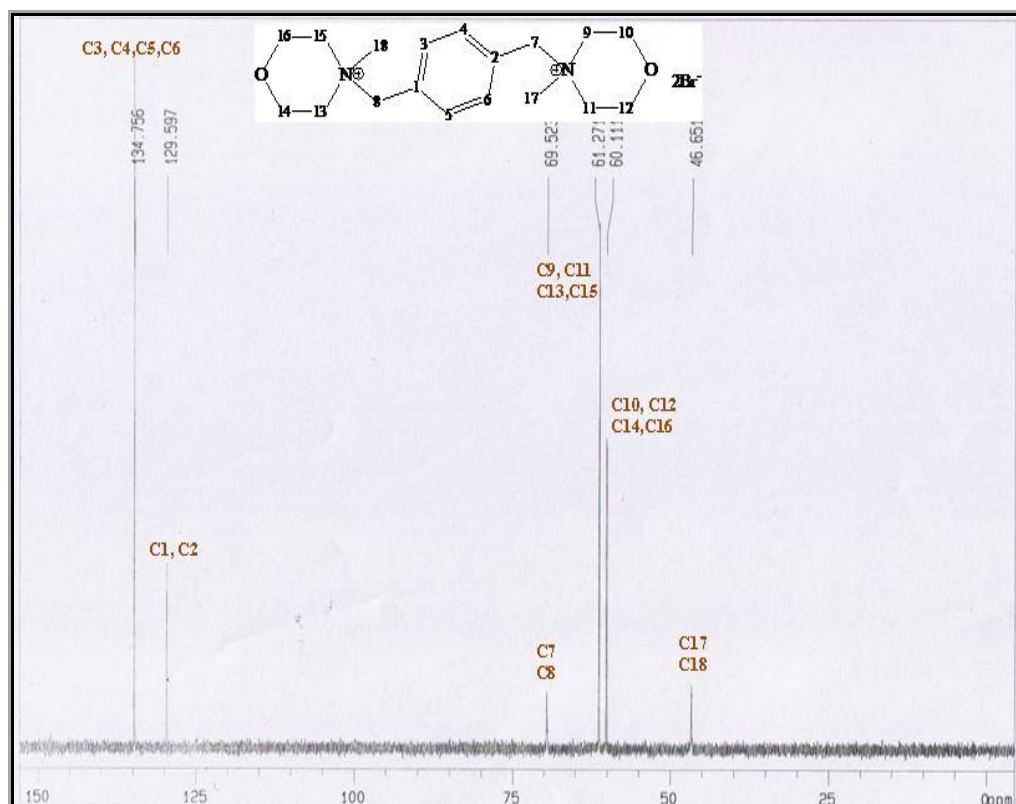
The chemical shift of all  $[\text{Mmorp}]^{2+} \cdot 2[\text{A}]^-$  series were compiled in the Table 4.16.

Table 4.16 :  $^1\text{H}$  NMR spectral data of  $[\text{Mmorp}]^{2+} \cdot 2[\text{A}]^-$

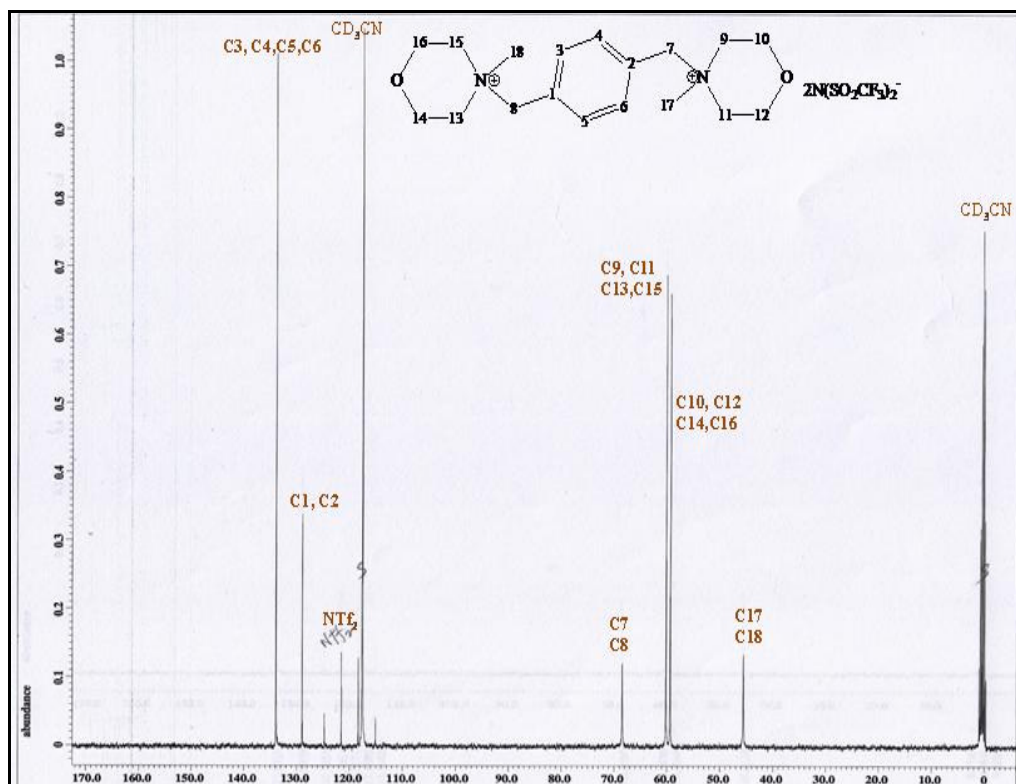
Chemical shift (ppm)			Coupling constant (Hz)	Multiplication	Assignment
Br	NTf <sub>2</sub>	PF <sub>6</sub>			
3.07	3.03	3.02	-	s	H-17, H-18
3.34	3.23	3.22	12.72	d	H-9, H-13
3.57	3.50	3.47	4.40	m	H-11, H-15
3.97	3.95	3.94	12.00	m	H-10, H-12, H-14, H-13
4.68	4.48	4.55	-	dd	Methylene group
7.65	7.61	7.58	-	d	Phenylene ring

On the other hand, the  $^{13}\text{C}$  NMR spectrum clearly indicates the compound,  $[\text{Mmorp}]^{2+} \cdot 2[\text{Br}]^-$  (Figure 4.51) has six non-equivalent carbons resonances. Carbons of methyl groups were observed at the upper field region which resonated at  $\delta$  46.65 ppm. Carbons C-10, C-12, C-14 and C-16 of morpholine ring were detected at  $\delta$  60.11 ppm while the signal at  $\delta$  61.27 ppm was belonged to the carbon C-9, C-11, C-13 and C-15 of morpholine ring. A small signal at  $\delta$  69.52 ppm was assigned to the methylene carbon of the phenylene bridge. Quaternary carbons' signal was appeared at  $\delta$  129.60 ppm while the signal for aromatic  $\text{sp}^2$  carbon of phenylene ring was observed at  $\delta$  134.76 ppm.

The spectra for compound  $[\text{Mmorp}]^{2+} \cdot 2[\text{PF}_6]^-$  (Figure 4.53) was similar in terms of number of signals and multiplication with the previous bromide salts except the chemical shift might be slightly differ. However, spectrum of compound  $[\text{Mmorp}]^{2+} \cdot 2[\text{NTf}_2]^-$  (Figure 4.52) exhibit four extra carbons signal at  $\delta$  115.11,  $\delta$  118.33,  $\delta$  121.55 and  $\delta$  124.77 ppm which were belonged to the carbon  $-\text{CF}_3$  of  $\text{NTf}_2$  anion.



**Figure 4.51** :  $^{13}\text{C}$  NMR spectrum of  $[\text{Mmorp}]^{2+} \cdot 2[\text{Br}]^{-}$



**Figure 4.52** :  $^{13}\text{C}$  NMR spectrum of  $[\text{Mmorp}]^{2+} \cdot 2[\text{NTf}_2]^{-}$

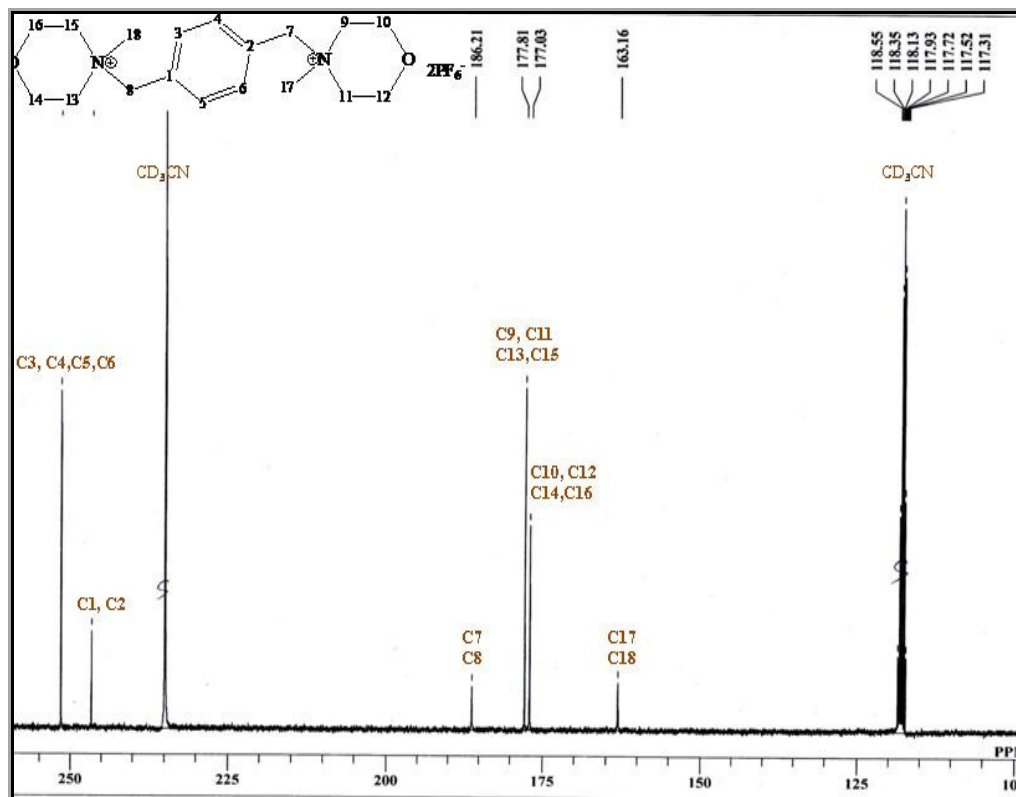


Figure 4.53 :  $^{13}\text{C}$  NMR spectrum of  $[\text{Mmorp}]^{2+} \cdot 2[\text{PF}_6]^-$

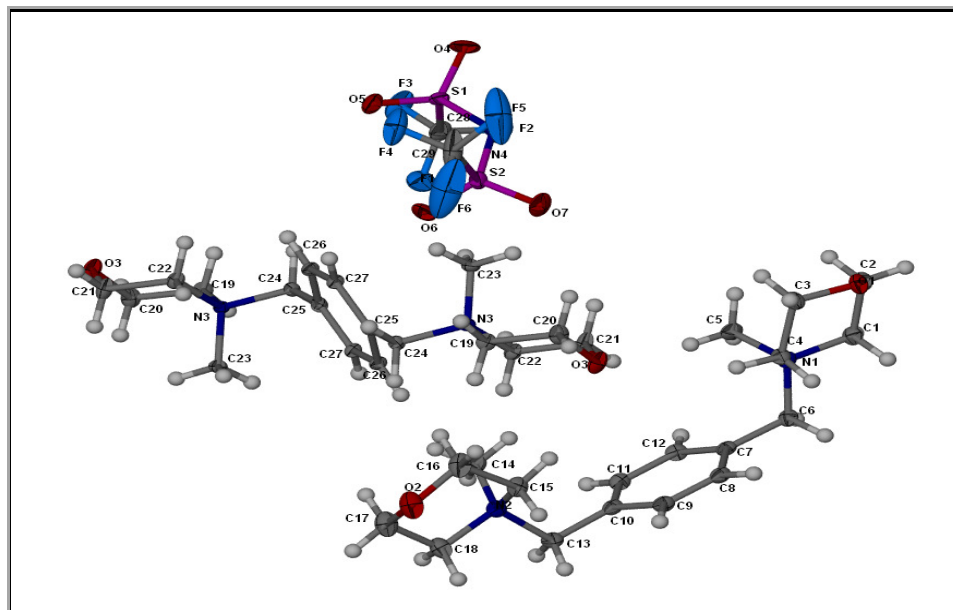
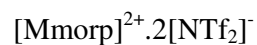
The chemical shift of all  $[\text{Mmorp}]^{2+} \cdot 2[\text{A}]^-$  series were compiled in the table 4.17.

Table 4.17 :  $^{13}\text{C}$  NMR spectral data of  $[\text{Mmorp}]^{2+} \cdot 2[\text{A}]^-$

Chemical shift (ppm)			Assignment
Br	NTf <sub>2</sub>	PF <sub>6</sub>	
46.65	45.40	45.03	C-17, C-18
60.11	59.40	58.90	C-10, C-12, C-14, C-16
61.27	60.19	59.68	C-9, C-11, C-13, C-15
69.52	68.40	68.08	Methylene carbon
-	115.11	-	-CF <sub>3</sub> (NTf <sub>2</sub> )
-	118.33	-	
-	121.55	-	
-	124.77	-	
129.60	128.99	128.49	Quaternary carbon
134.76	133.93	133.40	C-3, C-4, C-5, C-6

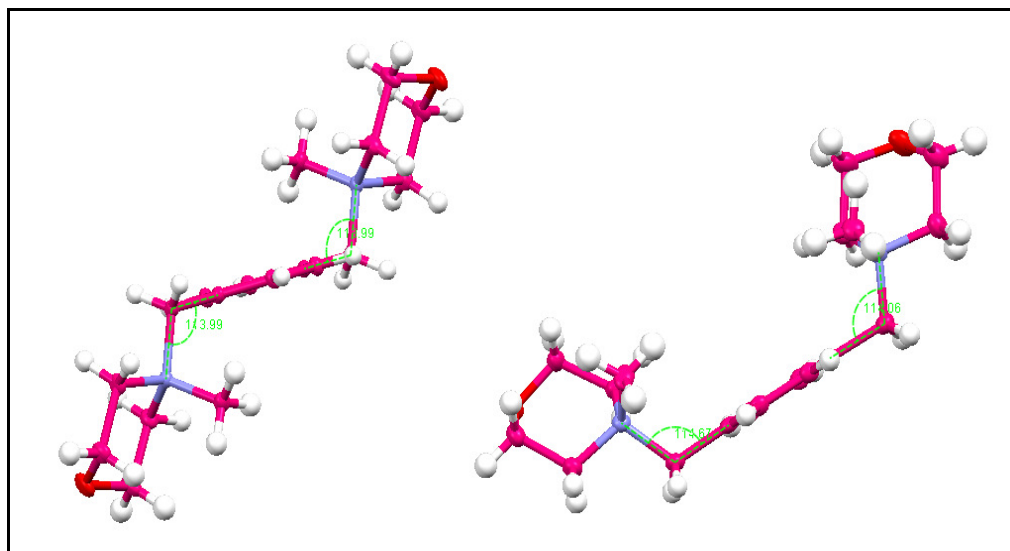


#### 4.6.4: X-ray Crystallography



**Figure 4.54 :** Molecular structure of the compound  $[\text{Mmorp}]^{2+} \cdot 2[\text{NTf}_2]^{-}$  with displacement ellipsoids drawn at 50% probability level. Hydrogen atoms are drawn as spheres at arbitrary radius.

Crystals of compound  $[\text{Mmorp}]^{2+} \cdot 2[\text{NTf}_2]^{-}$  was obtained from slow diffusion of acetonitrile and has been crystallized in the orthorhombic space group  $Pbca$ . It is appeared as colourless block-shaped crystals. In the crystal packing, the molecule exists as a non-interacting cation and anions.



**Figure 4. 55 :** [Mmorp] cation moiety in compound  $[\text{Mmorp}]^{2+} \cdot 2[\text{NTf}_2]$ .

Cation was formed by linking a phenylene ring with two molecules of 1-methylmorpholine via methylene carbon at para position. In a unit cell, the cation had two kind of conformations; cis (U-shaped) and trans (Z-shaped) whereby either 1-methylmorpholine attached themselves at the same side (U-conformation) or at the opposite side (Z-conformation) with respect to the phenylene ring. Z-conformation existed as a symmetrical molecule which was lying about the centre of inversion. However, the U-conformation was a non-symmetrical cation. Because of these two conformations were coexisted, disordered structure was observed to the cation as well as the  $\text{NTf}_2$  anions. Major disorder was detected at the fluorine atoms of the  $\text{NTf}_2$  anions. It was observed that the 1-methylmorpholine rings adopted a chair conformation similar to the chair conformation observed in cyclohexane.

**Table 4.18 :** Crystal data and structure refinements of [Mmorp]<sup>2+</sup>.2[NTf<sub>2</sub>]<sup>-</sup>

Ionic Liquids	[Mmorp] <sup>2+</sup> .2[NTf <sub>2</sub> ] <sup>-</sup>
Empirical Formula	[C <sub>18</sub> H <sub>30</sub> N <sub>2</sub> O <sub>2</sub> ] <sup>2+</sup> . 2[C <sub>4</sub> N <sub>2</sub> F <sub>12</sub> O <sub>8</sub> S <sub>4</sub> ] <sup>-</sup>
Molecular weight/ g mol <sup>-1</sup>	866.78
Colour	Colourless
Size/mm <sup>3</sup>	0.30 x 0.40 x 0.20
Crystal system	Orthorhombic
Space group	Pbca
a/Å	20.2468
b/Å	21.8045
c/Å	23.0916
α (°)	89.9856
β (°)	90.0021
γ (°)	89.9148
Volume/ Å <sup>3</sup>	10197.81 (16)
Z, Dc/g cm <sup>-3</sup>	12
F(000)	5304
μ/mm <sup>-1</sup>	0.403
θ range (°)	1.63-30.53
Reflections collected	152076
Data/restraints/parameter	12399/0/715
R <sub>int</sub>	0.0608
Ref <sub>Ins</sub> (total)	15570
Ref <sub>Ins</sub> (unique)	12399
Final R indices [I>2σ(I)]	R <sub>1</sub> = 0.1048 wR <sub>2</sub> = 0.2605
R indices (all data)	R <sub>1</sub> = 0.1251 wR <sub>2</sub> = 0.2777
ρ <sub>max</sub>  /e/Å <sup>3</sup>	2.830 and -2.301

#### 4.7 : *N,N'*-[1,4-Phenylenebis(methylene)]bis-(*N,N*-dimethyl-(2-hydroxy)ethanaminium) series

##### 4.7.1 : $^1\text{H}$ NMR and $^{13}\text{C}$ NMR Spectroscopy

Functionalized dicationic organic salt  $[\text{Dmae}]^{2+} \cdot 2[\text{Br}]^-$  exist as a white solid. It was obtained by reacting  $\alpha, \alpha$ -dibromo- $p$ -xylene with 2-(dimethylamino)ethanol. The  $^1\text{H}$  NMR spectrum of  $[\text{Dmae}]^{2+} \cdot 2[\text{Br}]^-$  (Figure 4.56) indicated five non-equivalent proton resonance signals with deuterium oxide as the solvent. A singlet was observed at  $\delta$  3.07 ppm correspond to twelve protons of methyl groups. Proton signals from methylene group at position H-11 and H-13 appeared at  $\delta$  3.43 ppm as a triplet. The proton signal of  $-\text{OH}$  disappeared due to the use of deuterium oxide as the solvent since proton is easily exchanged by deuterium. At  $\delta$  4.04 ppm, the broad signal was assigned to methylene protons H-12 and H-14 near the hydroxyl group. The peak at  $\delta$  4.55 ppm was attributed to the proton of methylene bridge which appeared as a doublet of doublet. Protons of the aromatic phenylene ring were observed at  $\delta$  7.67 as a doublet.

For the compound  $[\text{Dmae}]^{2+} \cdot 2[\text{NTf}_2]^-$  (Figure 4.57) and  $[\text{Dmae}]^{2+} \cdot 2[\text{PF}_6]^-$  (Figure 4.58), the proton signal of hydroxyl group can be seen in both spectra which resonated at  $\delta$  3.64 ppm and  $\delta$  3.65 ppm respectively. The rest of proton signals for both compounds were identical but only the chemical shifts vary slightly due to the shifting toward either down or up field regions.

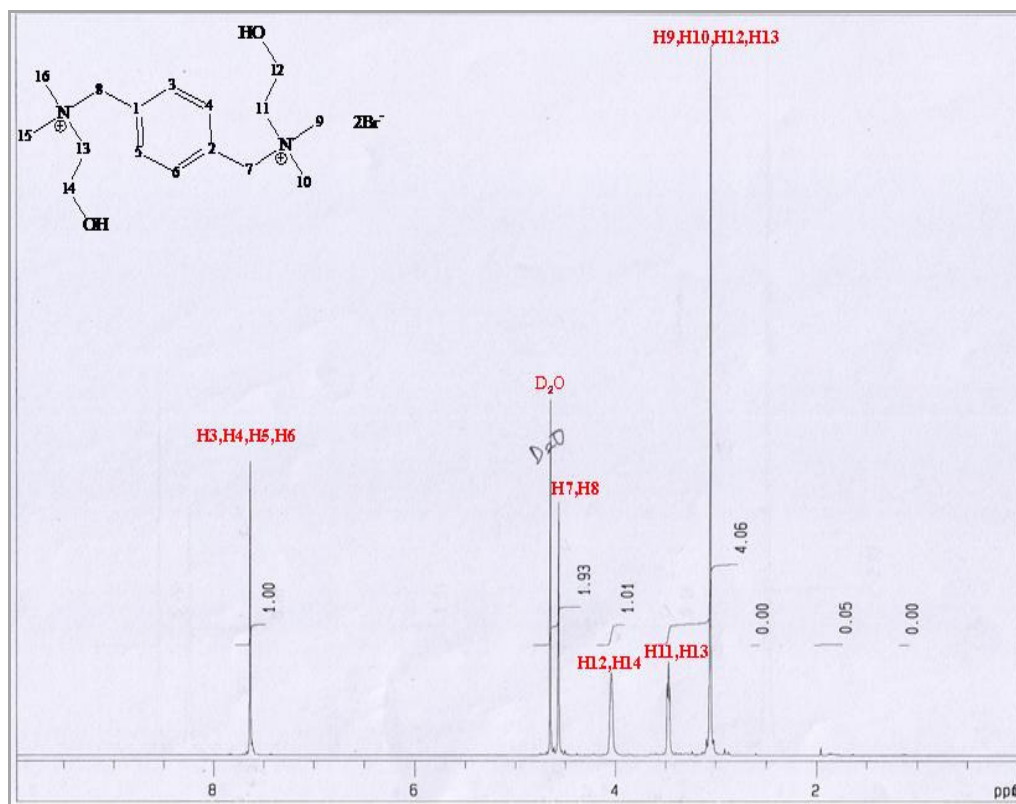


Figure 4.56 : <sup>1</sup>H NMR spectrum of [Dmae]<sup>2+</sup>.2[Br]<sup>-</sup>

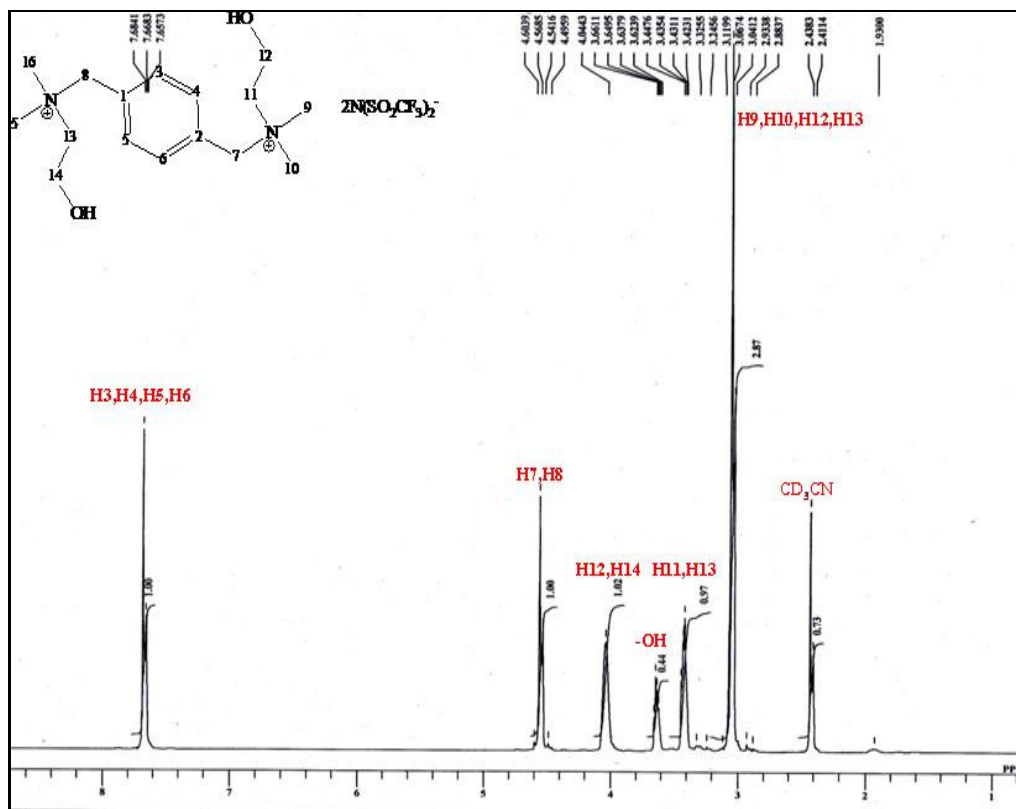


Figure 4.57 : <sup>1</sup>H NMR spectrum of [Dmae]<sup>2+</sup>.2[NTf<sub>2</sub>]<sup>-</sup>

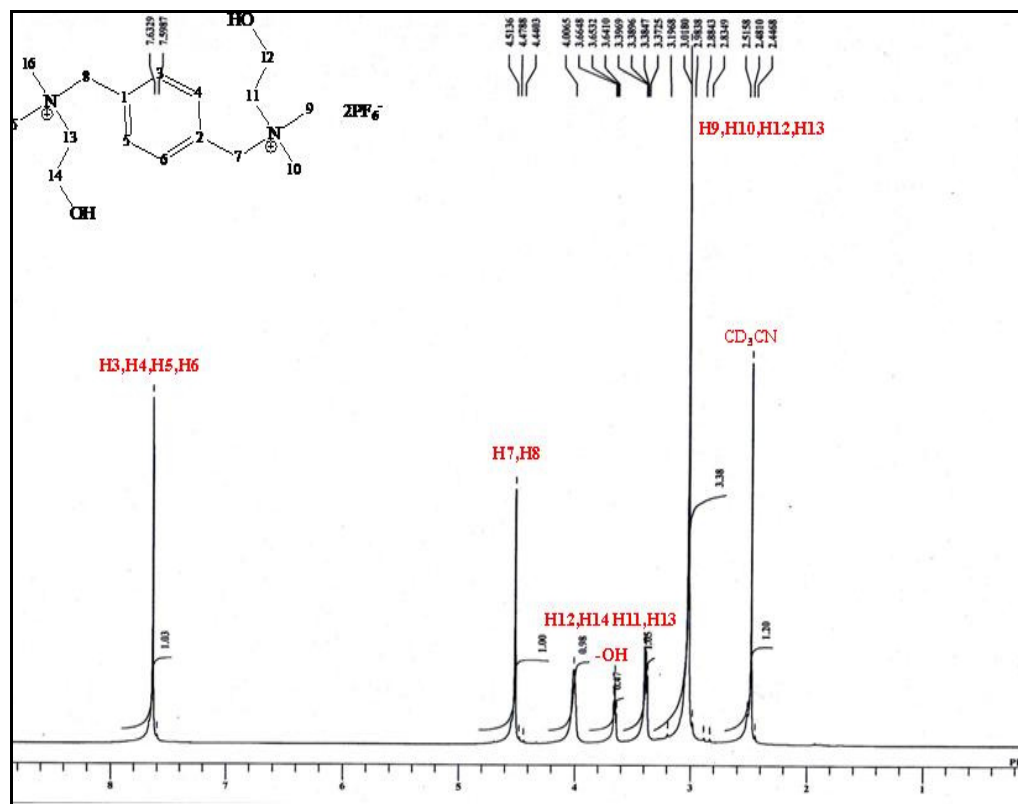


Figure 4.58 :  $^1\text{H}$  NMR spectrum of  $[\text{Dmae}]^{2+} \cdot 2[\text{PF}_6]^-$

The overall NMR data for  $[\text{Dmae}]^{2+} \cdot 2[\text{A}]^-$  series were tabulated in the Table 4.19 as follows:

Table 4.19 :  $^1\text{H}$  NMR spectral data of  $[\text{Dmae}]^{2+} \cdot 2[\text{A}]^-$

Chemical shift (ppm)			Coupling constant (Hz)	Multiplication	Assignment
Br	NTf <sub>2</sub>	PF <sub>6</sub>			
3.07	3.05	3.00	-	s	H-9, H-10, H-12, H-13
3.43	3.43	3.38	-	t	H-11, H-13
-	3.64	3.65	4.76	t	-OH
4.04	4.04	4.01	-	s	H-12, H-14
4.55	4.55	4.48	-	dd	Methylene group
7.67	7.67	7.62	-	d	Phenylene ring

The  $^{13}\text{C}$  NMR spectrum of  $[\text{Dmae}]^{2+}.2[\text{Br}]^{-}$  (Figure 4.59) showed six non-identical carbon signals correspond to the six type of carbon resonances. Carbon of methylene groups attached to the neighbouring hydroxyl group at C-12 and C-14 were recorded at  $\delta$  51.50 ppm. The signal at  $\delta$  56.35 ppm was corresponded to the four carbons of methyl group C-9, C-10, C-15 and C-16. Carbon of methylene groups which were attached to the nitrogen resonated at  $\delta$  66.45 ppm. Besides, the carbon of methylene bridge appeared at  $\delta$  69.29 ppm. At lower field region, the signal at  $\delta$  130.53 ppm was attributed to the quaternary carbon of phenylene ring, C-1 and C-2. Lastly, the signal for carbons of aromatic phenylene ring was observed at  $\delta$  134.34 ppm.

Compound  $[\text{Dmae}]^{2+}.2[\text{PF}_6]^{-}$  (Figure 4.61) exhibited a similar resonance signals with the  $[\text{Dmae}]^{2+}.2[\text{Br}]^{-}$  but differ slightly in chemical shift, while  $[\text{Dmae}]^{2+}.2[\text{NTf}_2]^{-}$  (Figure 4.60) showed an additional four weak signal at  $\delta$  116.25,  $\delta$  118.13,  $\delta$  122.50 and  $\delta$  125.65 ppm correspond to the carbon  $-\text{CF}_3$  of  $\text{NTf}_2$  anion.

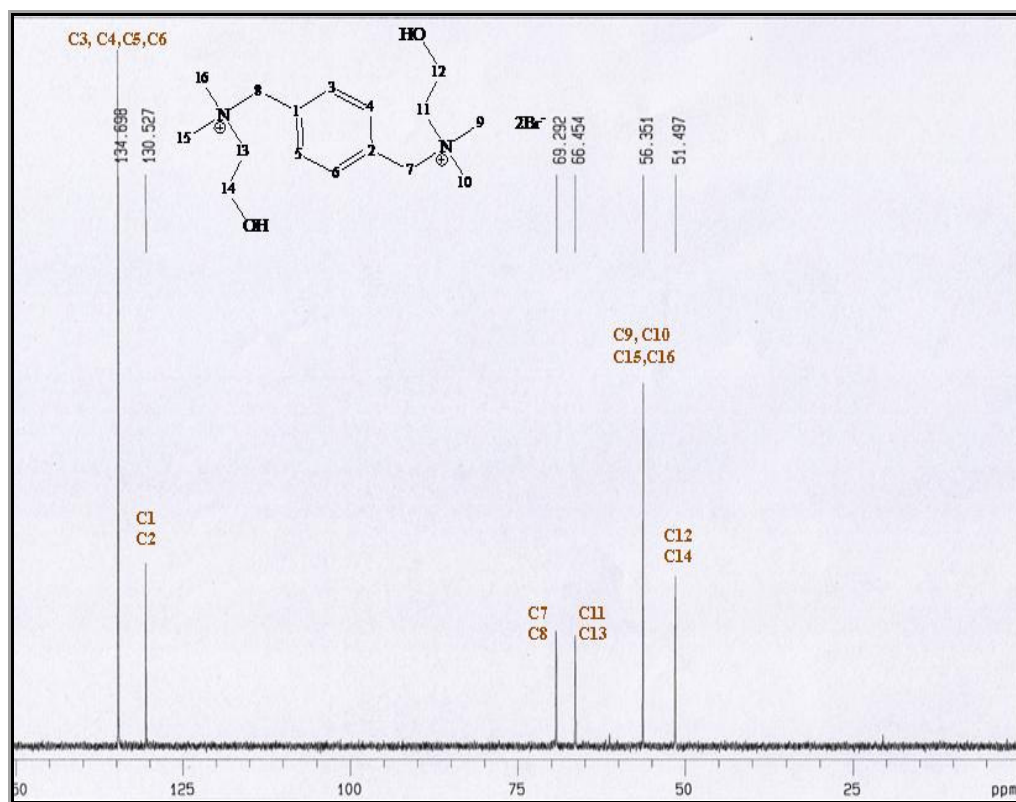


Figure 4.59 :  $^{13}\text{C}$  NMR spectrum of  $[\text{Dmae}]^{2+} \cdot 2[\text{Br}]^{-}$

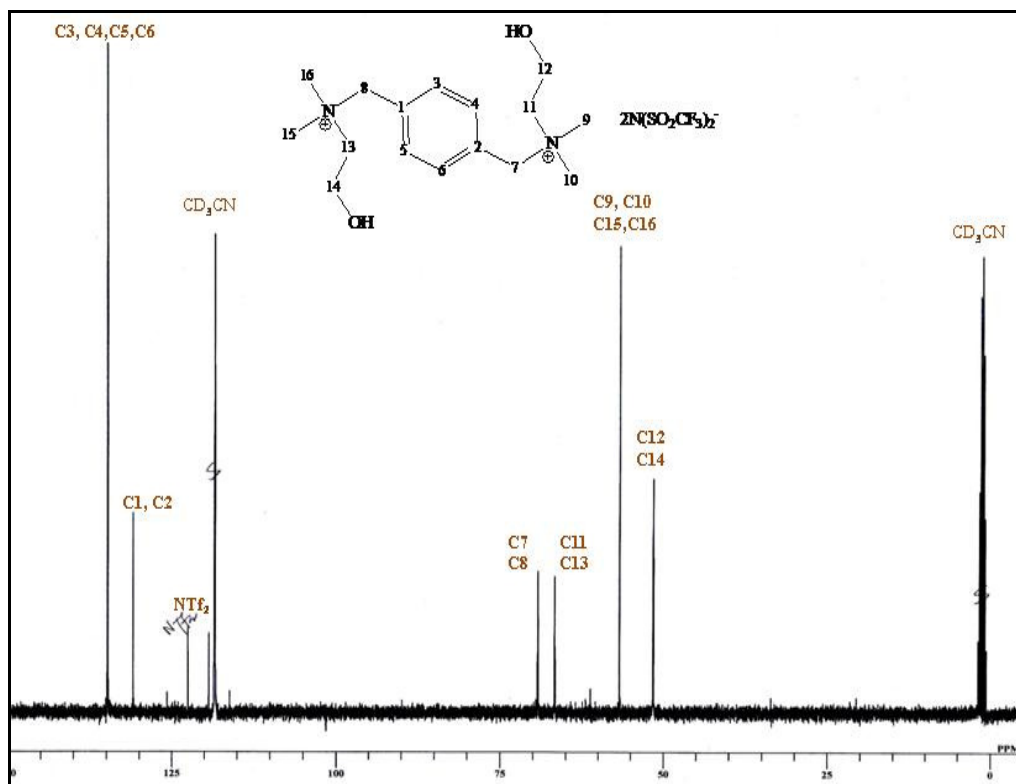
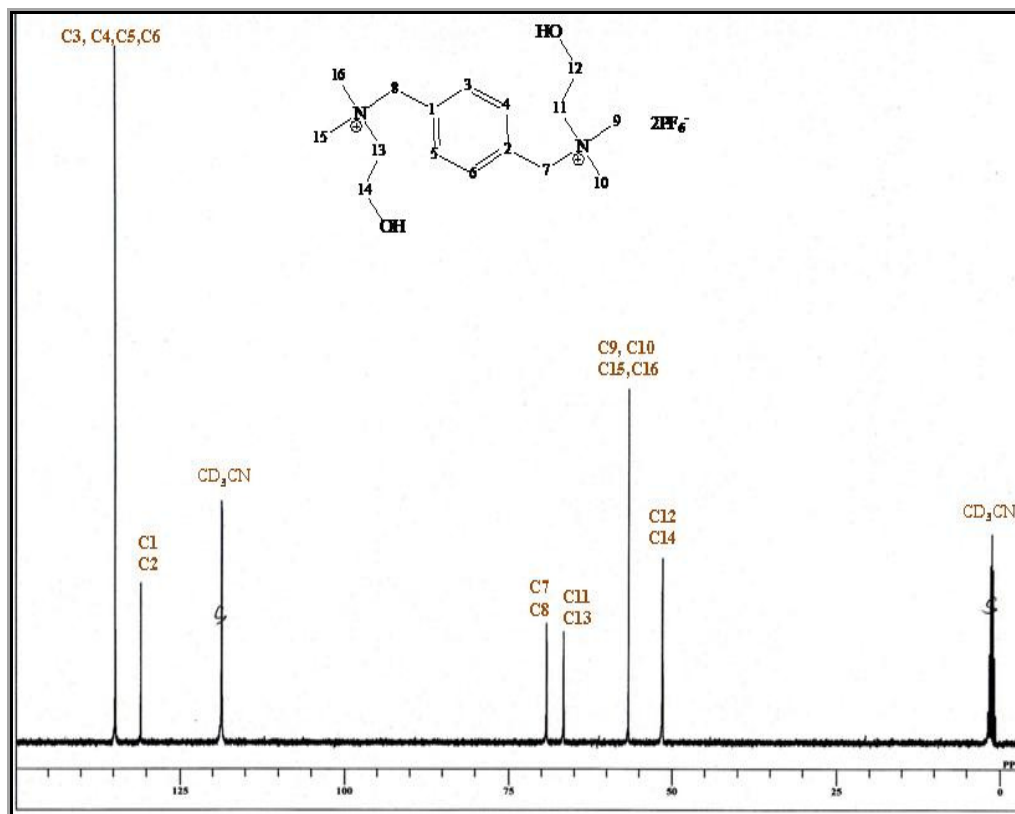


Figure 4.60 :  $^{13}\text{C}$  NMR spectrum of  $[\text{Dmae}]^{2+} \cdot 2[\text{NTf}_2]^{-}$





**Figure 4.61 :**  $^{13}\text{C}$  NMR spectrum of  $[\text{Dmae}]^{2+}.2[\text{PF}_6]^-$

The complete results were shown in the Table 4.20.

**Table 4. 20 :**  $^{13}\text{C}$  NMR spectral data of  $[\text{Dmae}]^{2+}.2[\text{A}]^-$

Chemical shift (ppm)			Assignment
Br	NTf <sub>2</sub>	PF <sub>6</sub>	
51.50	51.87	52.15	C-12, C-14
56.35	56.90	57.07	C-9, C-10, C-15, C-16
66.45	66.88	67.05	C-11, C-13
69.29	69.38	69.01	Methylene carbon
-	116.25	-	-CF <sub>3</sub> (NTf <sub>2</sub> )
-	118.13	-	
-	122.50	-	
-	125.65	-	
130.53	130.71	131.02	Quaternary carbon
134.70	134.94	134.75	C-3, C-4, C-5, C-6

#### **4.8 : *N,N'*-[1,4-Phenylenebis(methylene)]bis-(*N,N*-dibutyl-(2-hydroxy)ethanaminium) series**

##### **4.8.1 : $^1\text{H}$ NMR and $^{13}\text{C}$ NMR Spectroscopy**

Functionalized dicationic organic salt  $[\text{Deae}]^{2+}.2[\text{Br}]^-$  were synthesized by reacting  $\alpha,\alpha$ -dibromo-*p*-xylene with 2-(diethylamino)ethanol to yield white solid. The  $^1\text{H}$  NMR spectrum of  $[\text{Deae}]^{2+}.2[\text{Br}]^-$  (Figure 4.62) exhibit five unsymmetrical proton signals. At  $\delta$  1.32 ppm, a triplet was detected which was attributed to the proton of four methyl groups. A quartet was observed at  $\delta$  3.27 ppm which belonged to the protons of methylene group H-9, H-11, H-15, H-17, H-13 and H-19. The signal of protons H-14 and H-20 appeared as a doublet which was resonated at  $\delta$  3.99 ppm due to the neighbouring hydroxyl group. At  $\delta$  4.48 ppm, the signal of methylene bridge protons was recorded as a doublet of doublet. The peak at  $\delta$  7.53 ppm is a doublet which was assigned to the aromatic proton of the phenylene ring. The signal of hydroxyl proton was disappeared due to the use of deuterium oxide since proton is easily exchanged by deuterium.

Similar results were recorded for another two compounds;  $[\text{Deae}]^{2+}.2[\text{NTf}_2]^-$  (Figure 4.63) and  $[\text{Deae}]^{2+}.2[\text{PF}_6]^-$  (Figure 4.64) since they have the same cation. However, the signals of proton of the hydroxyl group were detected in the spectra of both compounds at  $\delta$  3.02 ppm and  $\delta$  3.49 ppm (buried) respectively.

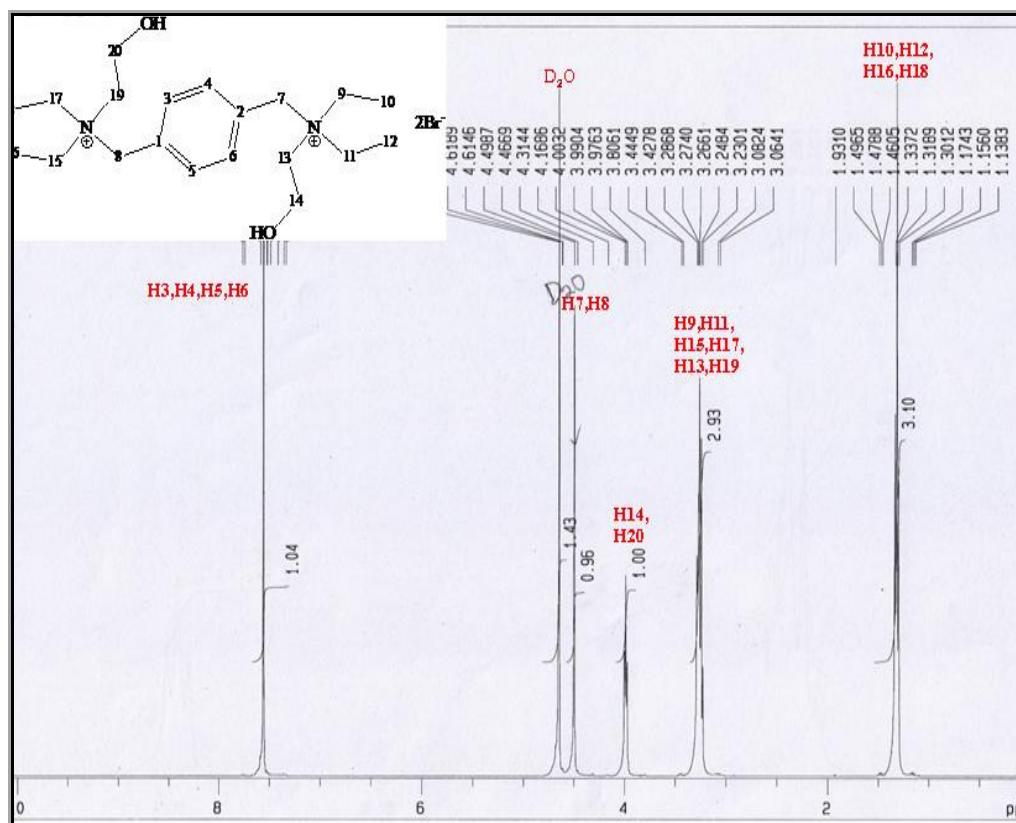


Figure 4.62 :  $^1\text{H}$  NMR spectrum of [Deae] $^{2+}$ .2[Br] $^{-}$

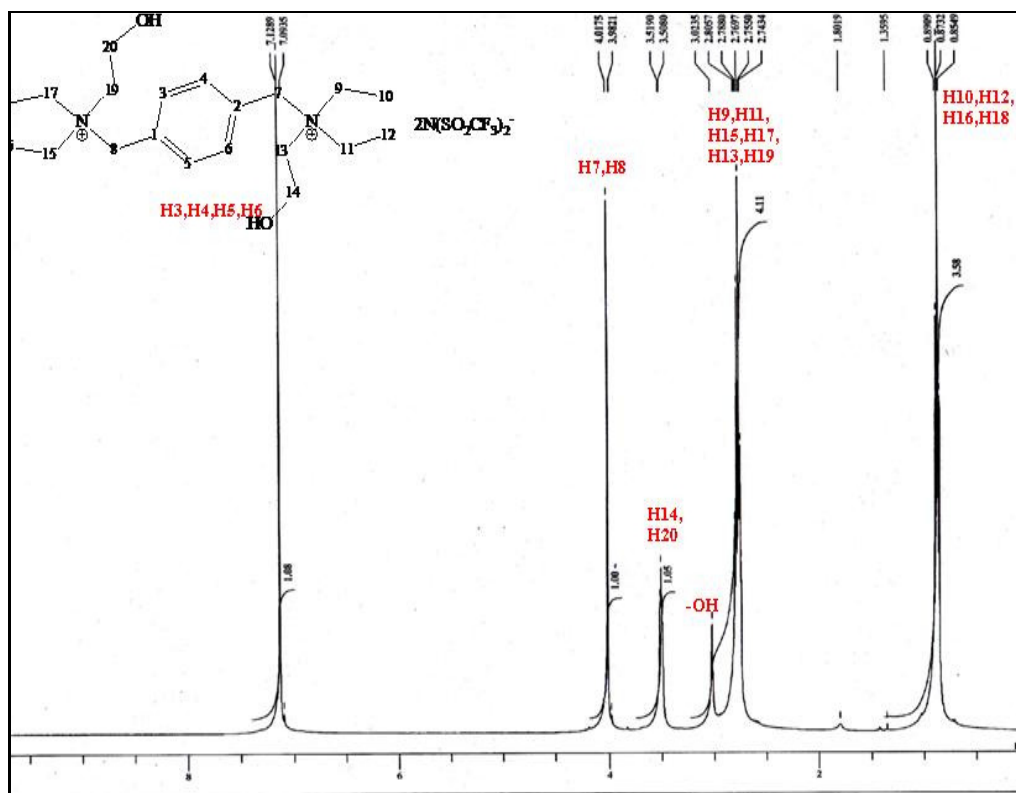


Figure 4.63 :  $^1\text{H}$  NMR spectrum of [Deae] $^{2+}$ .2[NTf $_2$ ] $^{-}$

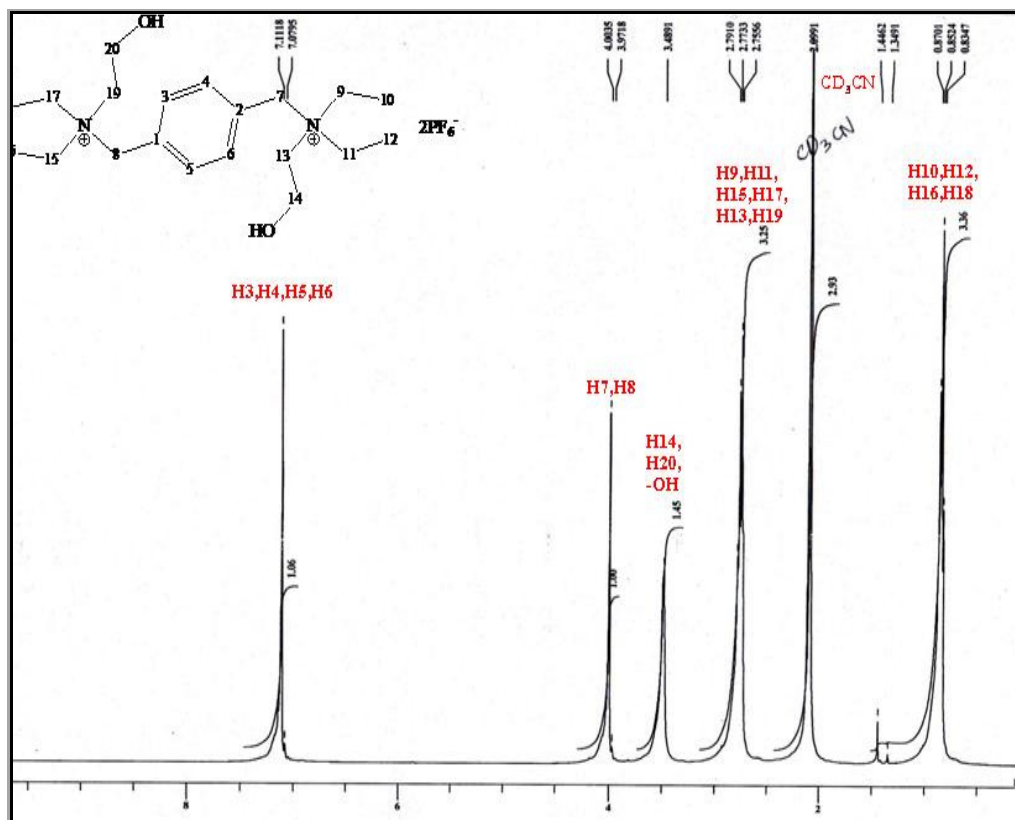


Figure 4.64 :  $^1\text{H}$  NMR spectrum  $[\text{Deae}]^{2+} \cdot 2[\text{PF}_6]^-$

The complete results were shown in the Table 4.21.

Table 4. 21 :  $^1\text{H}$  NMR spectral data of  $[\text{Deae}]^{2+} \cdot 2[\text{A}]^-$

Chemical shift (ppm)			Coupling constant (Hz)	Multiplication	Assignment
Br	NTf <sub>2</sub>	PF <sub>6</sub>			
1.32	0.87	0.85	7.08	t	H-10, H-12, H-16, H-18
3.27	2.77	2.77	7.08	q	H-9, H-11, H-15, H-17 H-13, H19 (overlapped)
-	3.02	3.49 (buried)	-	s	-OH
3.99	3.51	3.49	-	s	H-14, H-20
4.48	3.49	3.98	-	dd	Methylene group
7.53	7.10	7.09	-	d	Phenylene ring

The  $^{13}\text{C}$  NMR spectrum of  $[\text{Deae}]^{2+} \cdot 2[\text{Br}]^-$  (Figure 4.65) showed seven non-identical carbon signals correspond to the seven type of carbon resonances. Carbon of methylene groups C-10, C-12, C-16 and C-18 were recorded at  $\delta$  8.81 ppm. The signal at  $\delta$  55.10 ppm was corresponded to the carbon C-13 and C-19. At  $\delta$  56.30, the signal was assigned to the carbon at position C-9, C-11, C-15 and C-17. Carbon of methylene groups which were attached to the neighbouring hydroxyl group resonated at  $\delta$  58.75 ppm. However, the carbon of methylene bridge appeared at  $\delta$  61.88 ppm. At lower field region, the signal at  $\delta$  131.20 ppm was attributed to the quaternary carbon of phenylene ring. Lastly, the aromatic phenylene ring carbons were observed at  $\delta$  134.34 ppm.

Compound  $[\text{Deae}]^{2+} \cdot 2[\text{PF}_6]^-$  (Figure 4.67) exhibited a similar resonance signals with the  $[\text{Deae}]^{2+} \cdot 2[\text{Br}]^-$  but differ slightly in chemical shift, while  $[\text{Deae}]^{2+} \cdot 2[\text{NTf}_2]^-$  (Figure 4.66) showed an additional four weak signal at  $\delta$  116.22,  $\delta$  118.45,  $\delta$  119.38 and  $\delta$  122.67 ppm correspond to the carbon  $-\text{CF}_3$  of  $\text{NTf}_2$  anion.

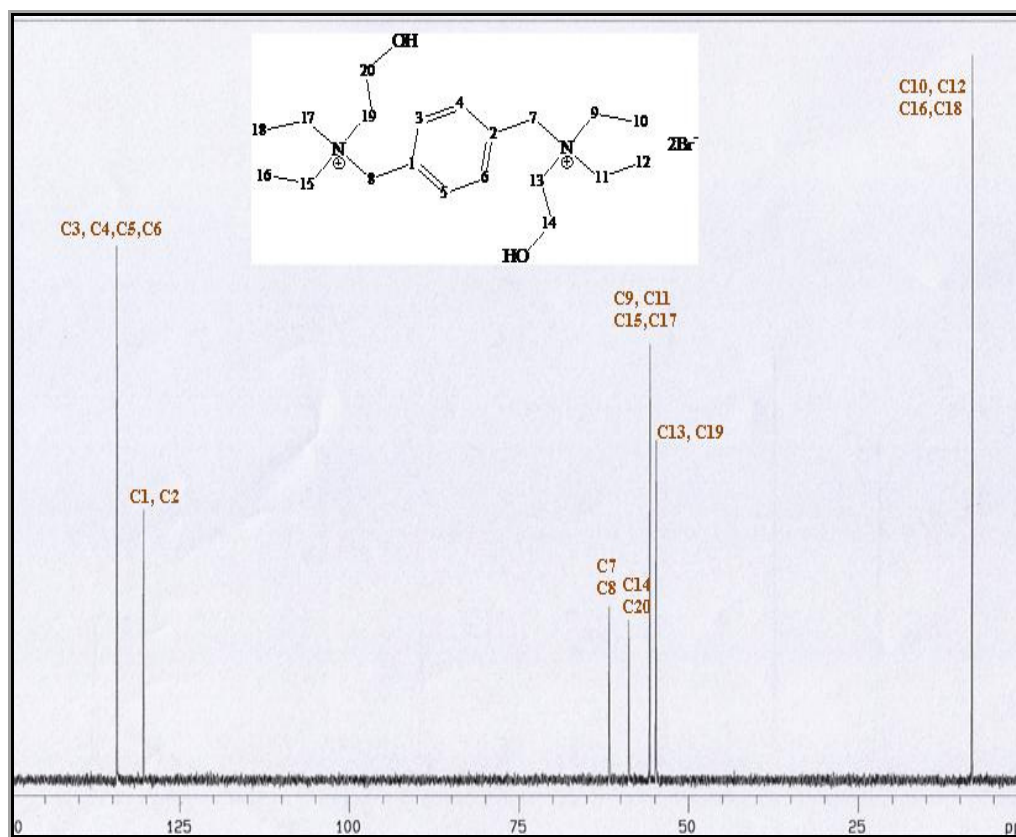


Figure 4.65 :  $^{13}\text{C}$  NMR spectrum of  $[\text{Deae}]^{2+} \cdot 2[\text{Br}]^{-}$

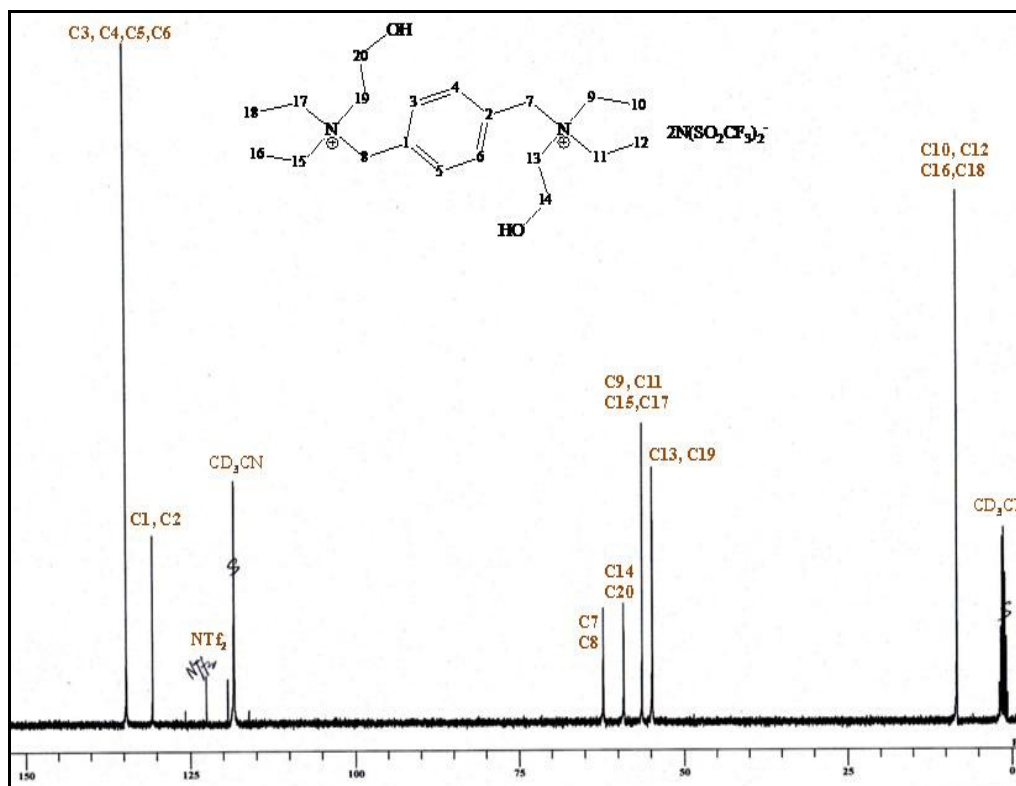


Figure 4.66 :  $^{13}\text{C}$  NMR spectrum of  $[\text{Deae}]^{2+} \cdot 2[\text{NTf}_2]^{-}$

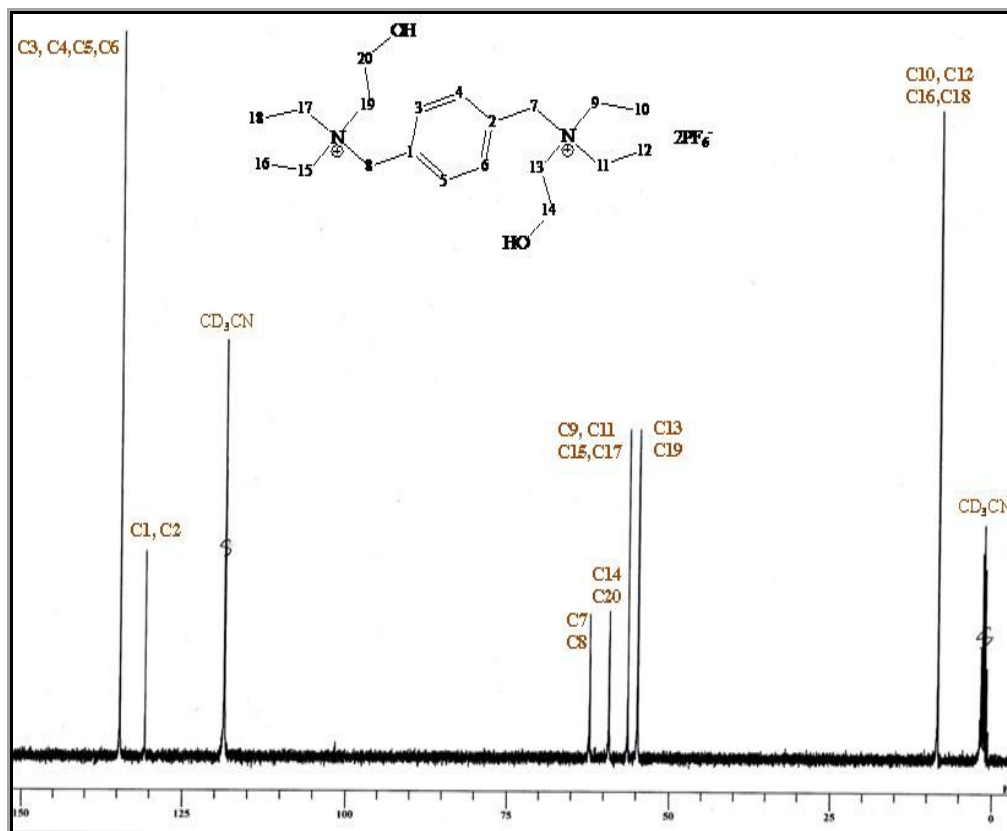


Figure 4.67 :  $^{13}\text{C}$  NMR spectrum of  $[\text{Deae}]^{2+}.2[\text{PF}_6]^-$

The complete results were shown in the Table 4.22.

Table 4.22 :  $^{13}\text{C}$  NMR spectral data of  $[\text{Deae}]^{2+}.2[\text{A}]^-$

Chemical shift (ppm)			Assignment
Br	NTf <sub>2</sub>	PF <sub>6</sub>	
8.81	8.41	8.70	C-10, C-12, C-16, C-18
55.10	55.01	54.90	C-13, C19
56.30	56.19	56.25	C-9, C-11, C-15, C-17
58.75	59.35	59.38	C-14, C-20
61.88	62.32	62.25	Methylene carbon
-	116.22	-	-CF <sub>3</sub> (NTf <sub>2</sub> )
-	118.45	-	
-	119.38	-	
-	122.67	-	
131.20	130.96	130.98	Quaternary carbon
134.34	134.78	134.89	C-3, C-4, C-5, C-6

#### 4.9 : Thermal Properties of Dicationic Ionic Liquids.

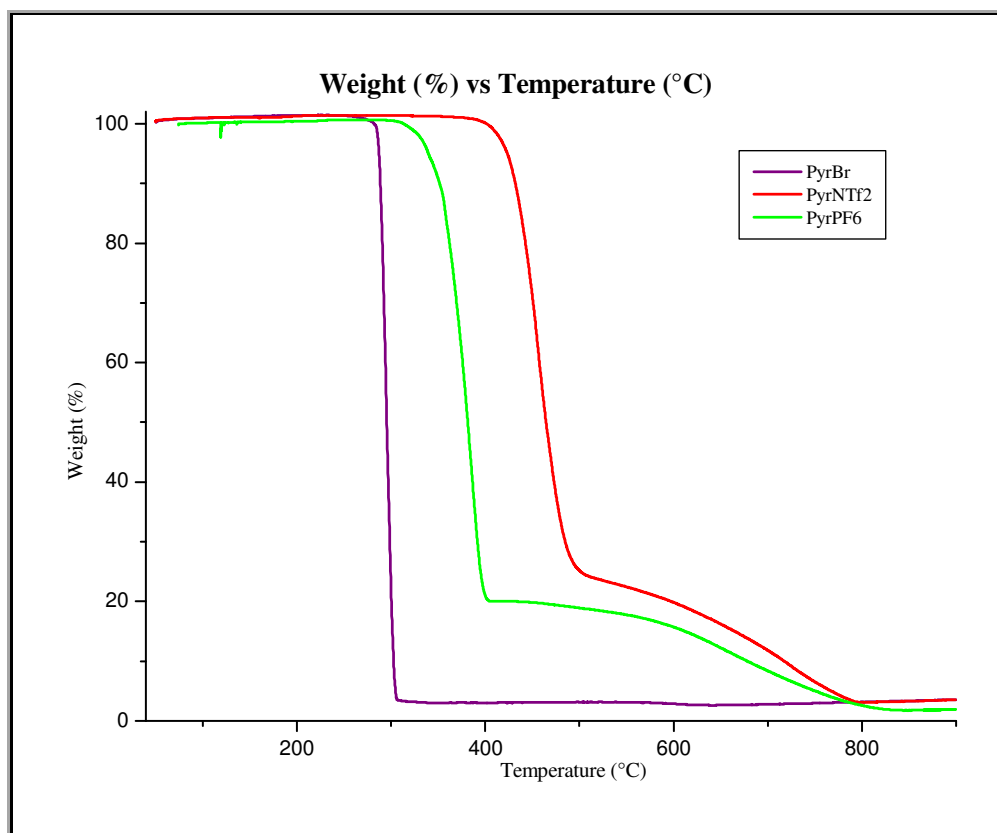
Thermal properties of synthesized dicationic organic salts were determined through thermogravimetric analysis experiments together with differential scanning calorimetry experiments. DSC experiment provides quantitative information about exothermic, endothermic and heat capacity changes as a function of temperature and time (such as melting, crystallization and glass transition temperature). This involves the phase transition of a compound from solid to liquid, liquid to gas or vice versa. In this research, this method was performed to estimate the melting temperature of the synthesized dicationic ionic liquids. Furthermore, TGA provides the information on the thermal stability of the synthesized dicationic ionic liquids. The results of the decomposition temperature,  $T_d$ , glass transition temperature,  $T_g$  and melting temperature,  $T_m$  of synthesized compounds were summarised in the **Table 4.23** (page 154).



#### 4.9.1 : Thermal properties of [Pyr] series

The result (Figure 4.68) clearly showed the NTf<sub>2</sub> salt was the most thermally stable dicationic ionic liquid which was started to decompose at 375 °C. Meanwhile, PF<sub>6</sub> and Br salts were stable up to 291 °C and 253 °C respectively before decomposing.

The plot of weight percent loss versus temperature in the Figure 4.68 represents the thermal decomposition of three dicationic ionic liquids for [Pyr] series. The experiments were run from 40 until 900 °C at heating rate 10 °C/min.



**Figure 4.68** : TGA curves of *N,N'*-[1,4-diphenylenebis(methylene)]dipyridinium series; Br, NTf<sub>2</sub> and PF<sub>6</sub>.

From the DSC plot of NTf<sub>2</sub> salt (Figure 4.70), the only phase transition observed was the melting temperature ( $T_m$ ) which was recorded at 154.75 °C. The cation and anion molecules were large thus affect the arrangement of the molecules in a crystal system. This might explained why the NTf<sub>2</sub> salt melts at lower temperature compared to Br and PF<sub>6</sub> salts which tend to decompose without melting. However, because of the symmetrical structure of the cation the organic salt has high melting point, thus it cannot be classified as ionic liquids since the melting temperature is above 100 °C. However, the phase transition observed for Br (Figure 4.69) and PF<sub>6</sub> (Figure 4.71) salts was the decomposition peaks which were recorded at 291.50 °C and 327.05 °C respectively.

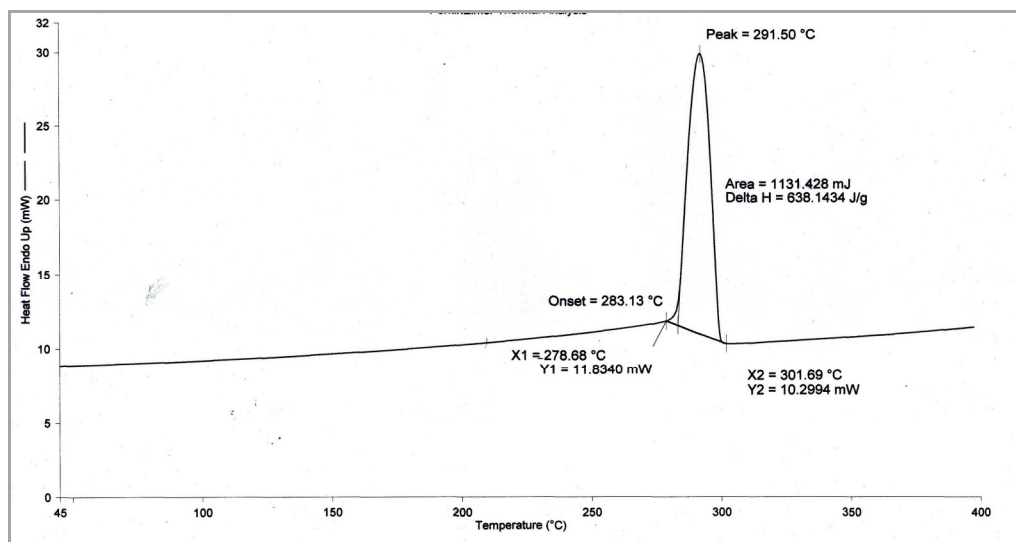


Figure 4.69 : DSC plot of  $[\text{Pyr}]^{2+} \cdot 2[\text{Br}]^-$

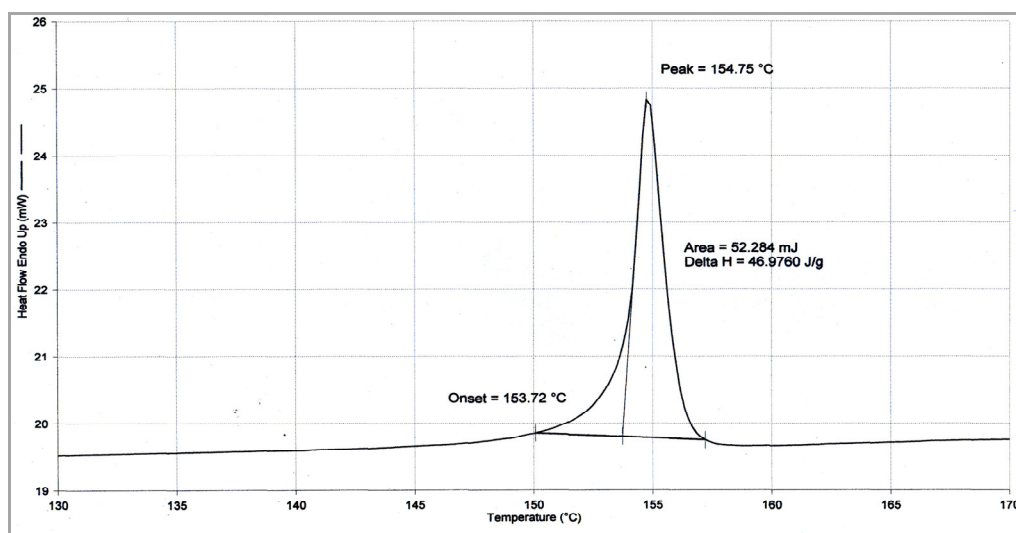


Figure 4.70 : DSC plot of  $[\text{Pyr}]^{2+} \cdot 2[\text{NTf}_2]^-$

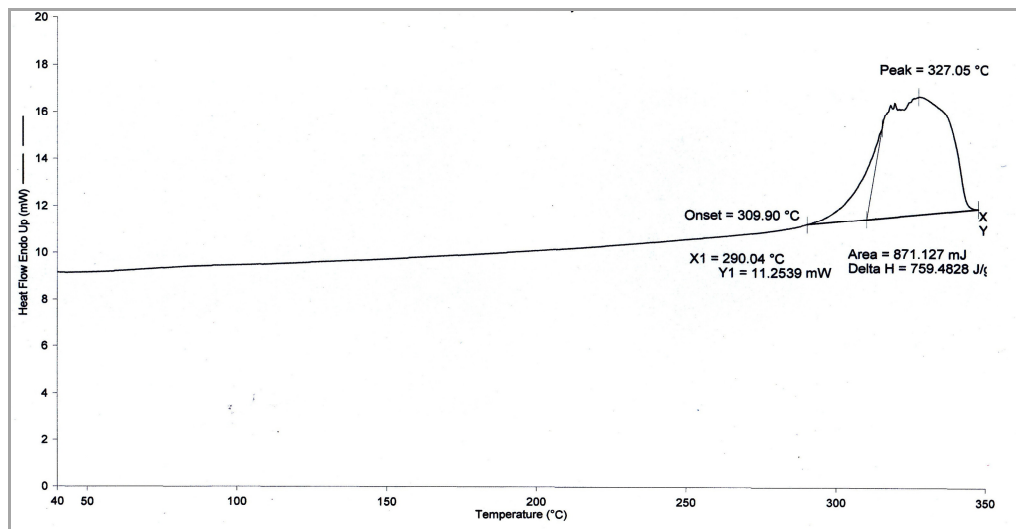
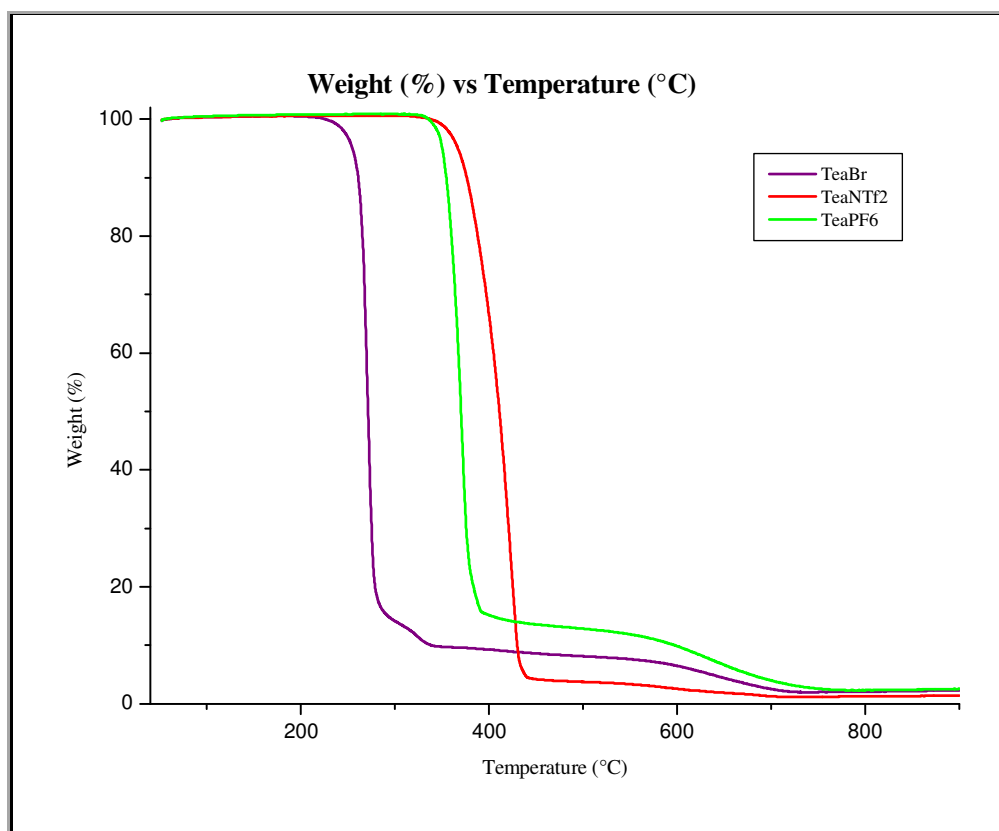


Figure 4.71 : DSC plot of  $[\text{Pyr}]^{2+} \cdot 2[\text{PF}_6]^-$

#### 4.9.2 : Thermal properties of [Tea] series

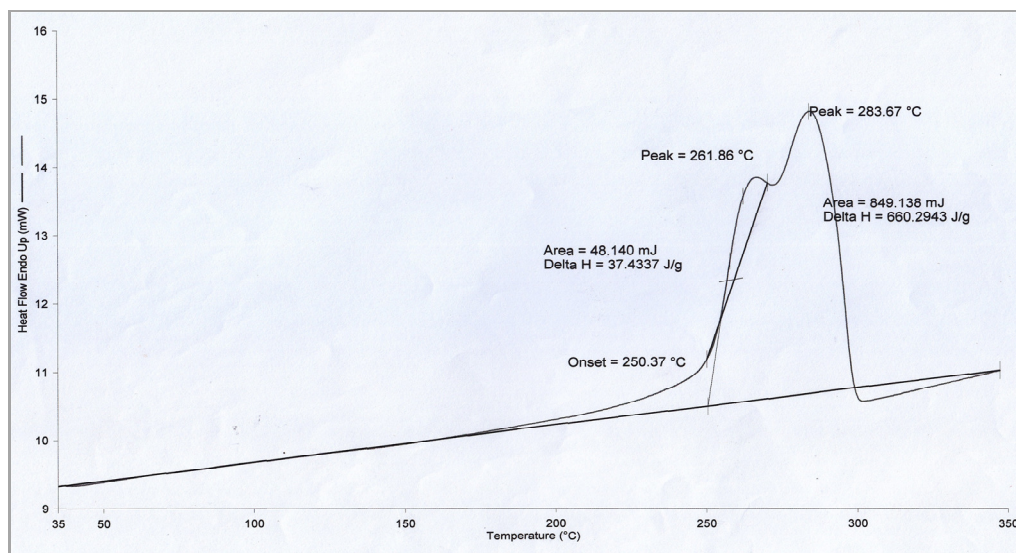
The result (Figure 4.72) clearly showed the NTf<sub>2</sub> salt has a better thermal stability than the other two salts which was decomposing at 321 °C while PF<sub>6</sub> and Br salt was stable up to 319 °C and 226 °C respectively before decomposing.

The plot of weight percent loss versus temperature below represents the thermal decomposition of three dicationic ionic liquids for [Tea] series. The experiments were run from 40 until 900 °C at heating rate 10 °C/min.



**Figure 4.72 :** TGA curves of *N,N'*-[1,4-phenylenebis(methylene)]bis(*N,N*-diethylethanaminium) series; Br, NTf<sub>2</sub> and PF<sub>6</sub>.

DSC experiments illustrate only one significant phase transition for NTf<sub>2</sub> salt (Figure 4.74) that is melting temperature (T<sub>m</sub>) which was recorded at 122.59 °C while the an endothermic peak recorded at 85.86 °C was due to the evaporation of acetonitrile used in recrystallization method. The cation and anion molecules were large therefore affect the arrangement of the molecules in a crystal system. This might explained why the NTf<sub>2</sub> salt melts at lower temperature compared to Br and PF<sub>6</sub> salts which tend to decompose without undergo melting phase. Besides, because of the symmetrical structure of cation the organic salt has high melting point, thus it cannot be classified as ionic liquids too since the melting temperature is above 100 °C. On the other hand, it was suspected that the phase transition observed for Br (Figure 4.73) and PF<sub>6</sub> (Figure 4.75) salts was due to the decomposition peak of the dicationic ionic liquids. Br salt recorded an endothermic peak at 261.86 °C while PF<sub>6</sub> salt does not recorded any phase transition until the temperature above 350 °C.



**Figure 4.73 :** DSC plot of [Tea]<sup>2+</sup>.2[Br]

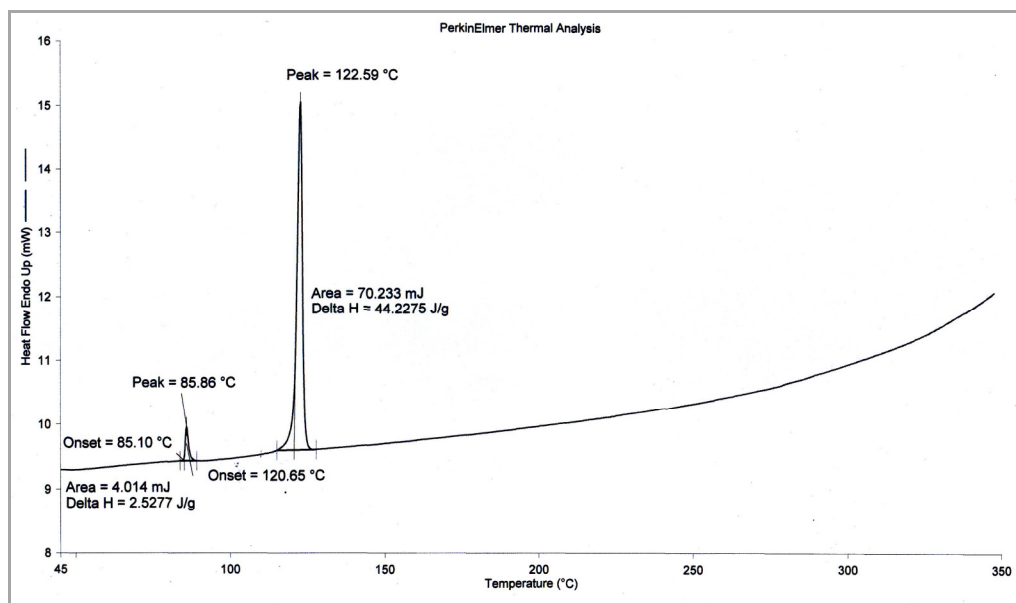


Figure 4.74 : DSC plot of [Tea]<sup>2+</sup>.2[NTf<sub>2</sub>]<sup>-</sup>

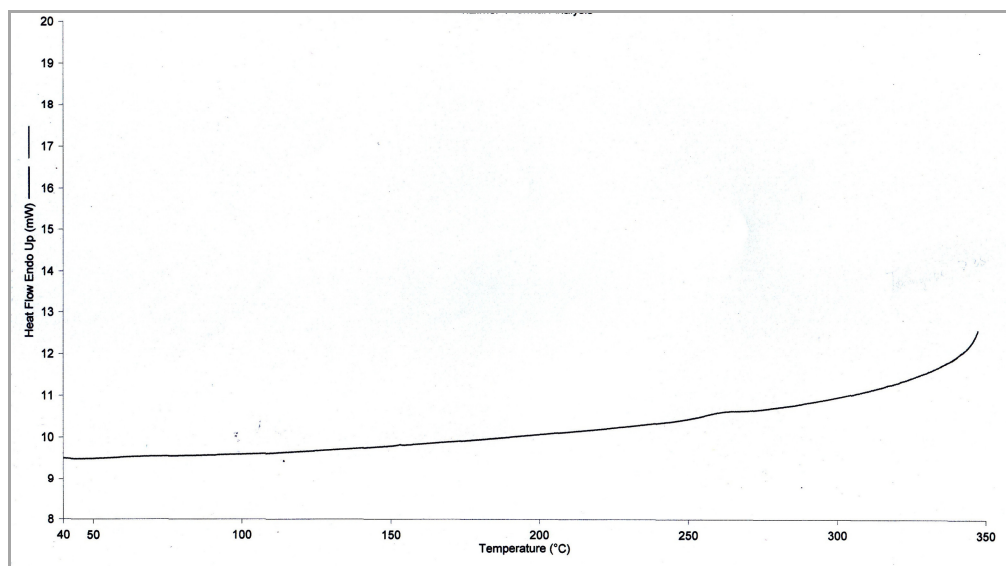
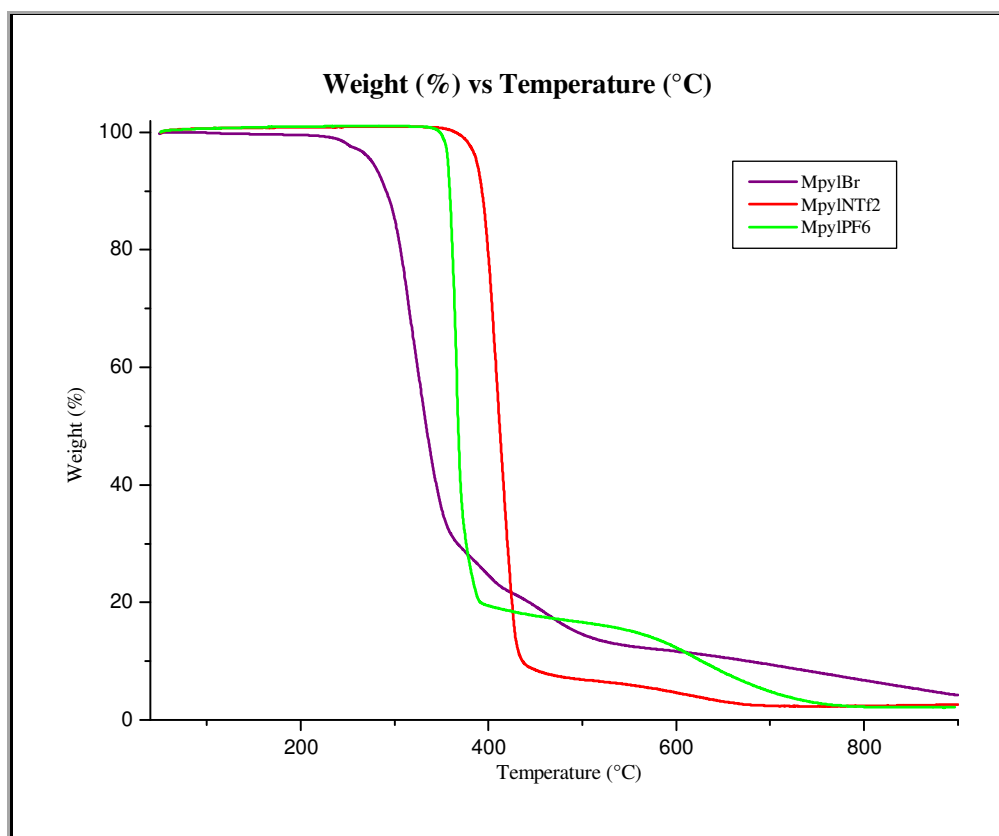


Figure 4.75 : DSC plot of [Tea]<sup>2+</sup>.2[PF<sub>6</sub>]<sup>-</sup>

#### 4.9.3 : Thermal properties of [Mpyl] series

The result (Figure 4.76) clearly showed the NTf<sub>2</sub> salt has better thermal stability than the other two salts which was degrading at 365 °C while PF<sub>6</sub> and Br salts were decomposing at 336 °C and 238 °C respectively.

The plot of weight percent loss versus temperature below represents the thermal decomposition of three dicationic ionic liquids for [Mpyl] series. The experiments were run from 40 until 900 °C at heating rate 10 °C/min.



**Figure 4.76** : TGA curves of *N,N'*-[1,4-Phenylenebis(methylene)]bis-(*N,N*-dimethylpyrrolinium) series; Br, NTf<sub>2</sub> and PF<sub>6</sub>

DSC experiments illustrate only one significant phase transition for NTf<sub>2</sub> salt (Figure 4.78) that is melting temperature (T<sub>m</sub>) which was recorded at 91.56 °C while the peak recorded at 85.86 °C was probably due to the evaporation of acetonitrile used in recrystallization method. The cation and anion molecules were large therefore affect the arrangement of the molecules in a crystal system. This might explained why the NTf<sub>2</sub> salt melts at lower temperature compared to Br and PF<sub>6</sub> salts which tend to decompose without undergo melting phase. It was suspected that the phase transition observed for PF<sub>6</sub> salts (Figure 4.79) was due to the decomposition peak of the dicationic ionic liquids which was recorded at 359.47 °C. The Br salt (Figure 4.77) recorded three endothermic peaks whereas the first broad peak was due to the water evaporation while at 253.48 °C and 297.82 °C probably were the decomposition temperature of dicationic ionic liquids.

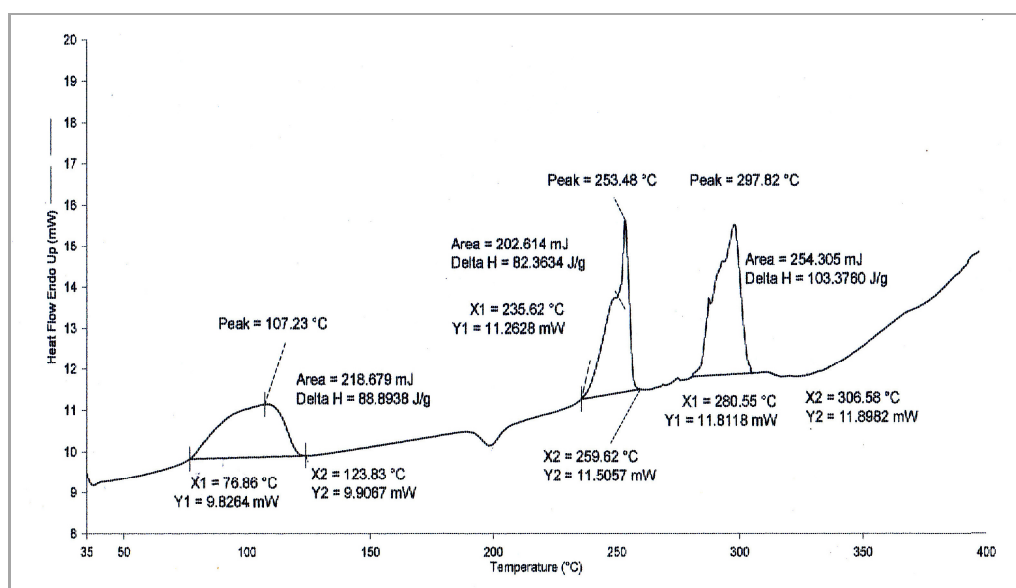
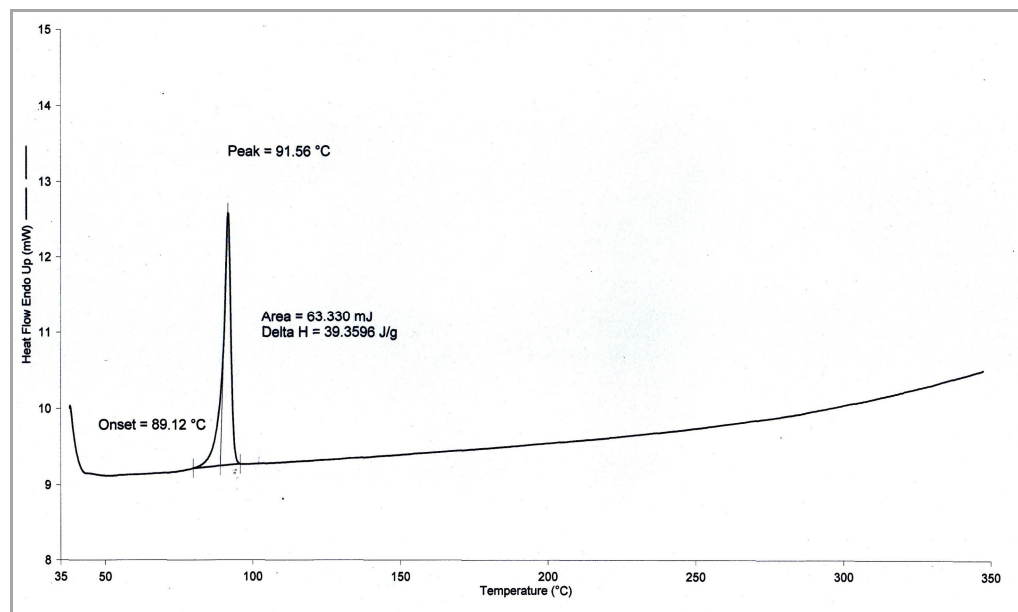
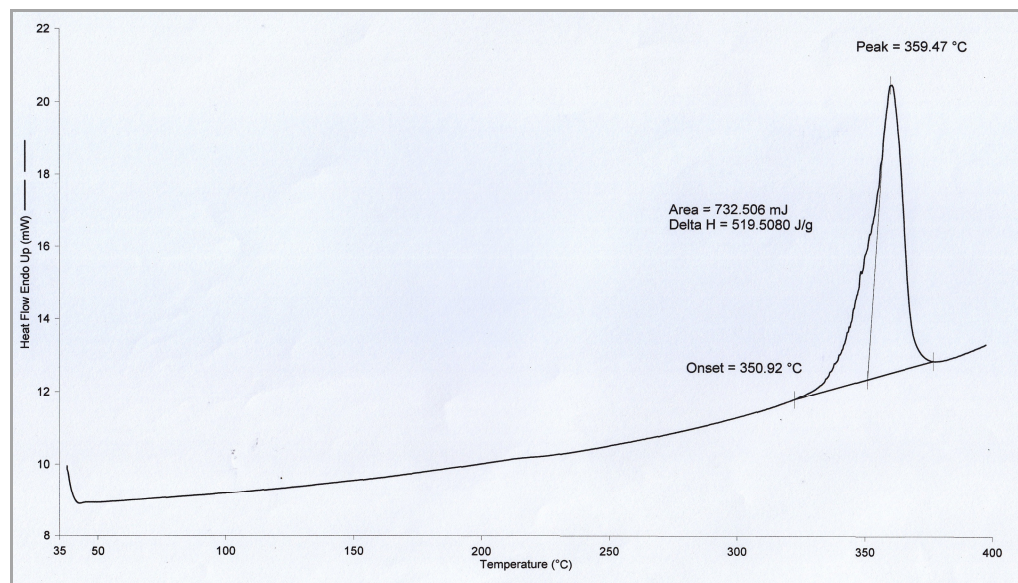


Figure 4.77 : DSC plot of [Mpyl]<sup>2+</sup>.2[Br]<sup>-</sup>





**Figure 4.78** : DSC plot of [Mpyl]<sup>2+</sup>·2[NTf<sub>2</sub>]<sup>-</sup>

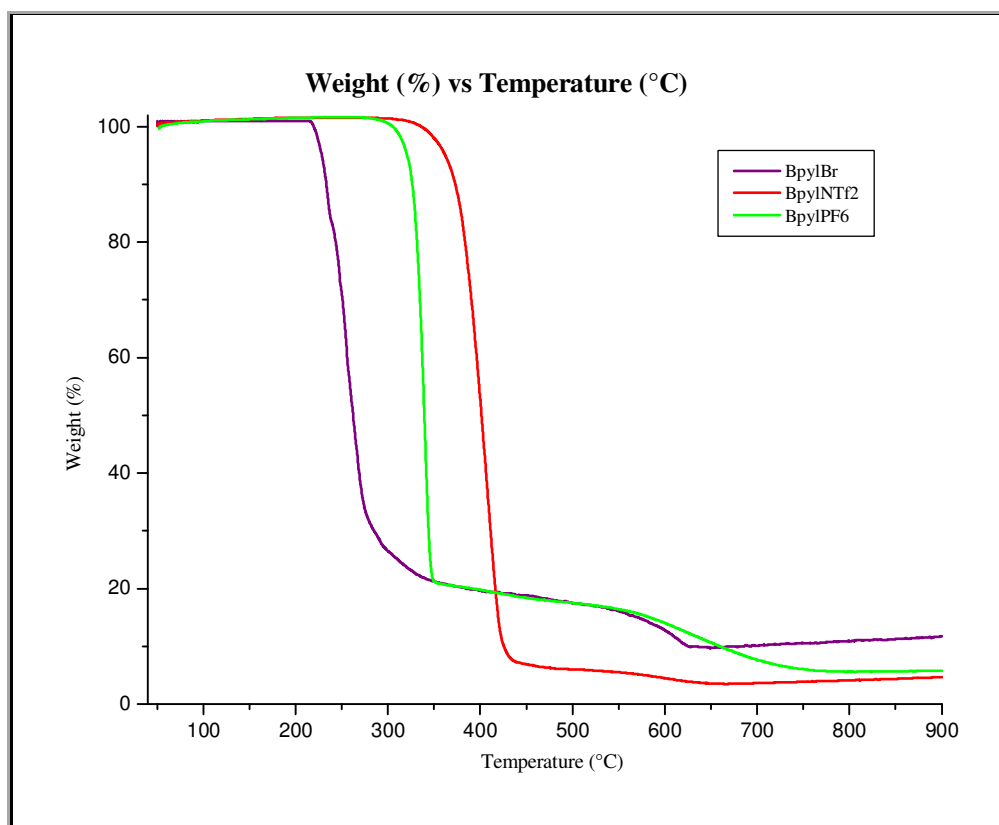


**Figure 4.79** : DSC plot of [Mpyl]<sup>2+</sup>·2[PF<sub>6</sub>]<sup>-</sup>

#### 4.9.4 : Thermal properties of [Bpyl] series

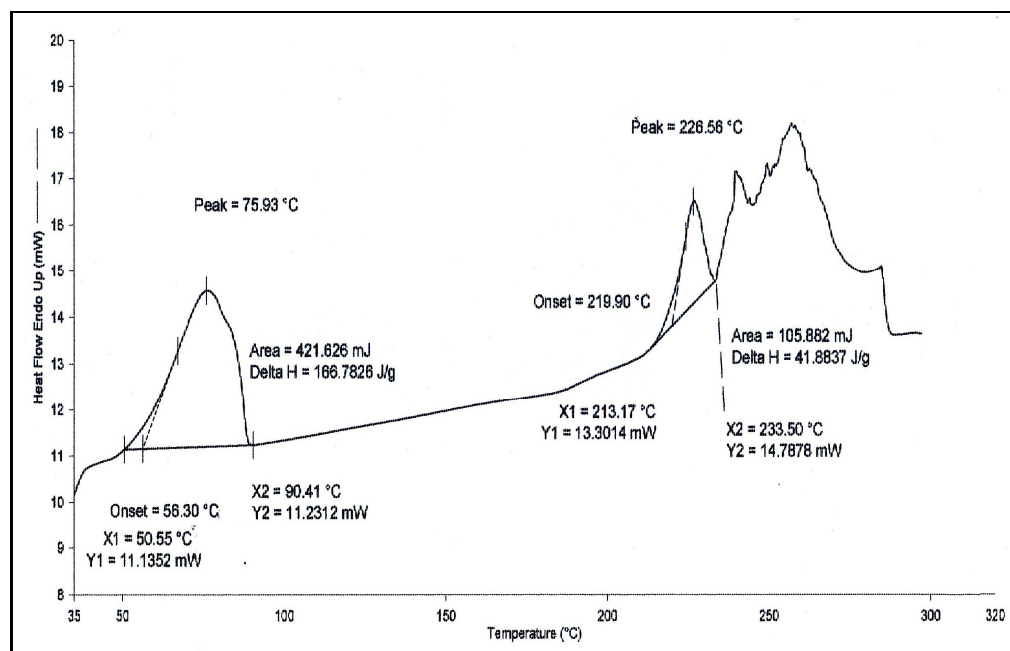
The result (Figure 4.80) clearly showed the Br salt has the lowest degradation temperature which was recorded at 213 °C. The NTf<sub>2</sub> salt was the most stable salt amongst the other two which was started to decompose at 310 °C followed by PF<sub>6</sub> salt which was stable up to 277 °C before degrading.

The plot of weight percent loss versus temperature below represents the thermal decomposition of three dicationic ionic liquids for [Bpyl] series. The experiments were run from 40 °C until 900 °C at heating rate 10 °C/min.

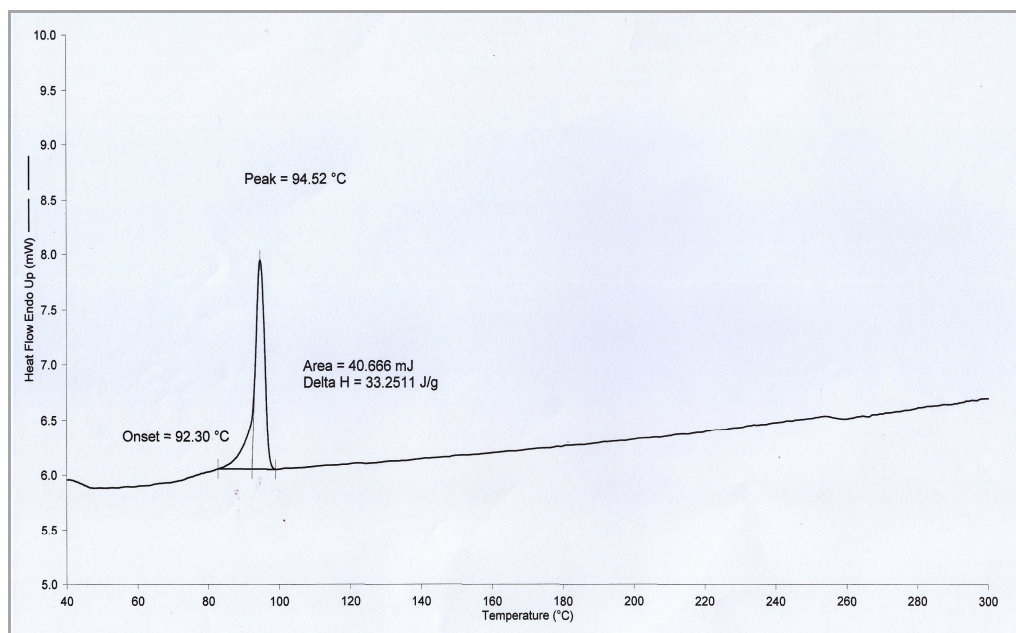


**Figure 4.80 :** TGA curves of *N,N'*-[1,4-Phenylenebis(methylene)]bis-(*N,N*-dibutylpyrrolinium) series; Br, NTf<sub>2</sub> and PF<sub>6</sub>

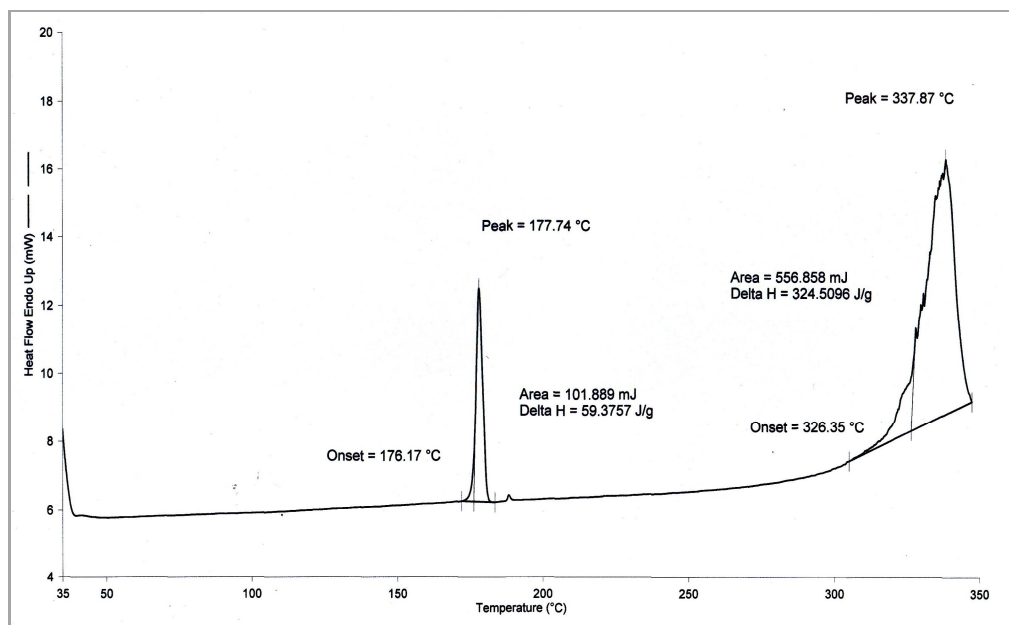
DSC experiments illustrate only one phase transition for NTf<sub>2</sub> salt (Figure 4.82) that is melting temperature (T<sub>m</sub>). The NTf<sub>2</sub> organic salt melts at 94.52 °C. The cation and anion molecules were large thus affect the arrangement of the molecules in a crystal system. This might explained why this salt melts at lower temperature compared to Br and PF<sub>6</sub> salts which tend to decompose without melting. On the other hands, the phase transition observed for Br and PF<sub>6</sub> salts was the decomposition peak of the dicationic ionic liquids. DSC plot of Br salt (Figure 4.81) recorded an endothermic peak at about 76 °C which might due to the evaporation of methanol used in recrystallization process while at temperature above 220 °C the salt is decomposing. Meanwhile, DSC plot of PF<sub>6</sub> salt (Figure 4.83) recorded an endothermic peak which was melting temperature (T<sub>m</sub>) at 177.74 °C while at 337.87 °C the compound was decomposing (T<sub>d</sub>).



**Figure 4.81** : DSC plot of [Bpyl]<sup>2+</sup>.2[Br]<sup>-</sup>



**Figure 4.82** : DSC plot of [Bpyl]<sup>2+</sup>·2[NTf<sub>2</sub>]<sup>-</sup>

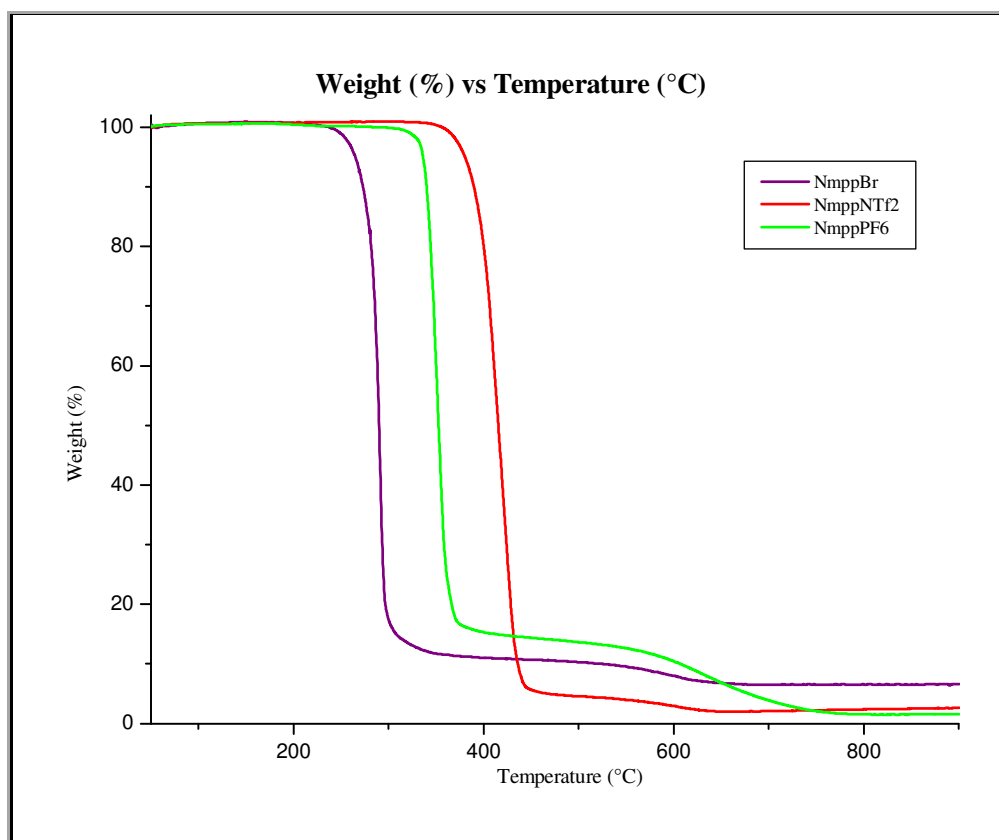


**Figure 4.83** : DSC plot of [Bpyl]<sup>2+</sup>·2[PF<sub>6</sub>]<sup>-</sup>

#### 4.9.5 : Thermal properties of [Nmpp] series

The result (Figure 4.84) clearly showed the NTf<sub>2</sub> salt has better thermal stability than the other two salts which was started to decompose at 334 °C while PF<sub>6</sub> and Br salt were stable up to 278 °C and 237 °C respectively before decomposing.

The plot of weight percent loss versus temperature below represents the thermal decomposition of three dicationic ionic liquids for [Nmpp] series. The experiments were run from 40 °C until 900 °C at heating rate 10 °C/min.



**Figure 4.84** : TGA curves of *N,N'*-[1,4-phenylenebis(methylene)]bis-(*N,N*-dimethylpiperidinium) series; Br, NTf<sub>2</sub> and PF<sub>6</sub>

DSC experiments illustrate only one phase transition for NTf<sub>2</sub> salt (Figure 4.86) that is melting temperature (T<sub>m</sub>). The melting temperature (T<sub>m</sub>) observed in the NTf<sub>2</sub> organic was 129.35 °C. The cation and anion molecules were large thus affect the arrangement of the molecules in a crystal system. This might explained why this salt melts at lower temperature compared to Br and PF<sub>6</sub> salts which were tend to decompose without undergo melting phase. However, because of the symmetrical structure of the cation the organic salt has high melting point, thus it cannot be considered as ionic liquids since the melting temperature is above 100 °C. On the other hands, the phase transition observed for Br and PF<sub>6</sub> salts was the decomposition peak of these dicationic ionic liquids. For Br salt (Figure 4.85), a broad peak recorded at about 60 °C was probably due to the evaporation of methanol used in the recrystallization method while at 298.17 °C, this compound is decomposing. PF<sub>6</sub> salt (Figure 4.87) shows only one phase transition at 356.33 °C which believed to be the decomposition temperature (T<sub>d</sub>) of this dicationic ionic liquid.

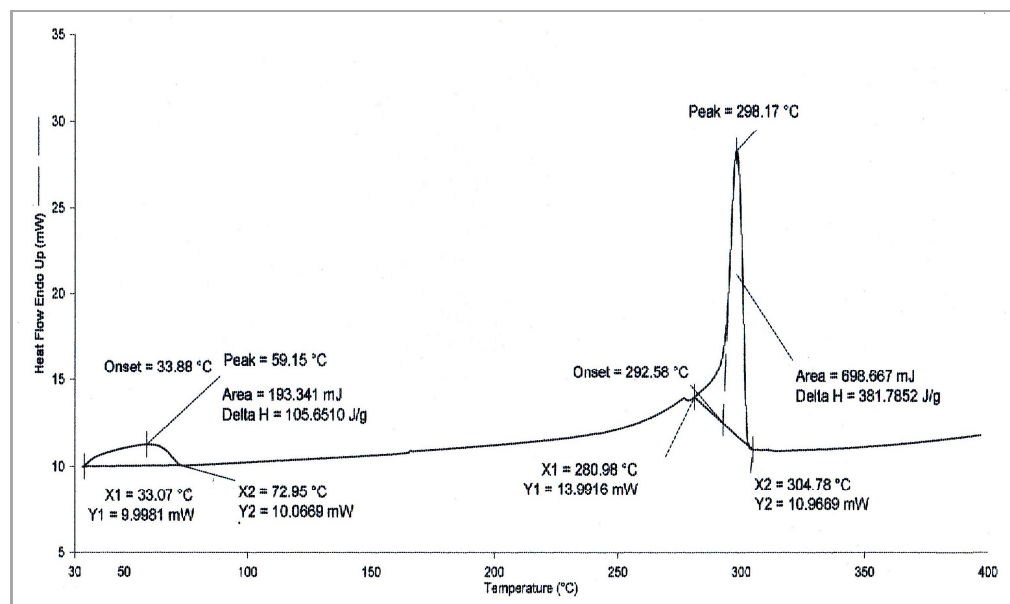


Figure 4.85 : DSC plot of [Nmpp]<sup>2+</sup>.2[Br]<sup>-</sup>

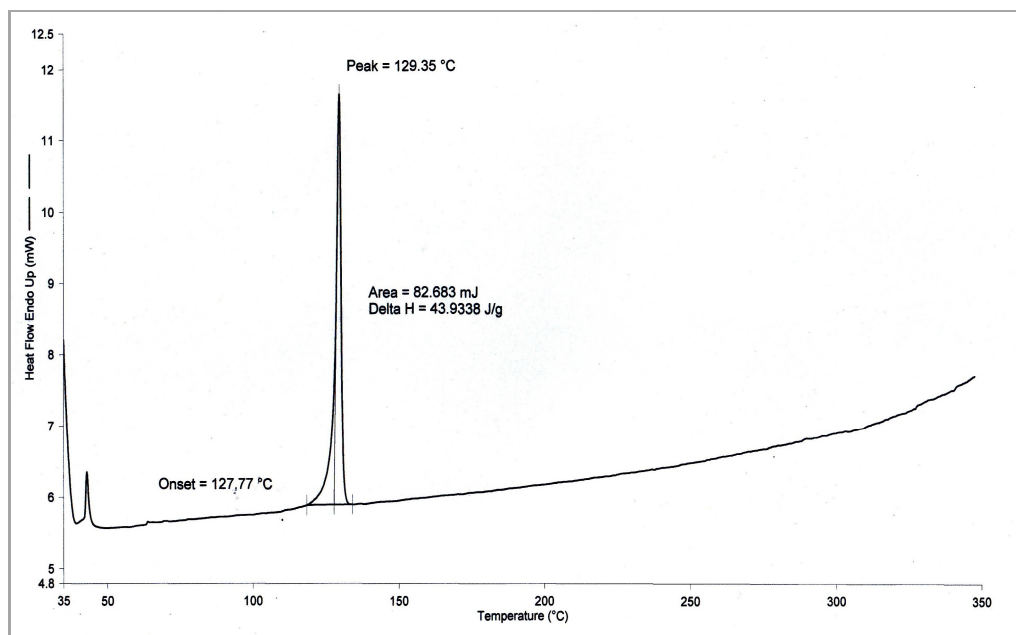


Figure 4.86 : DSC plot of  $[\text{Nmpp}]^{2+} \cdot 2[\text{NTf}_2]^-$

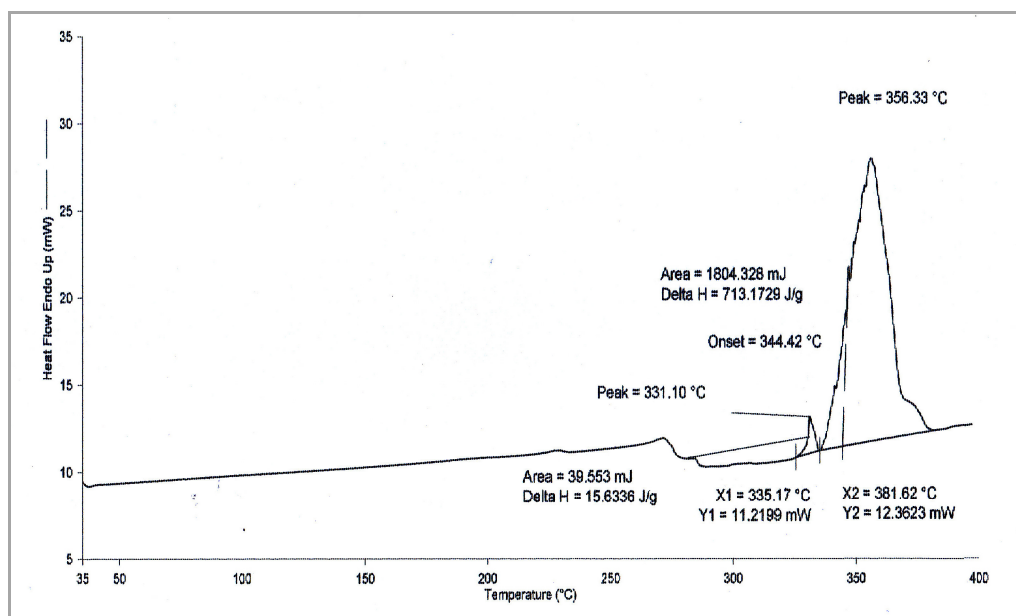
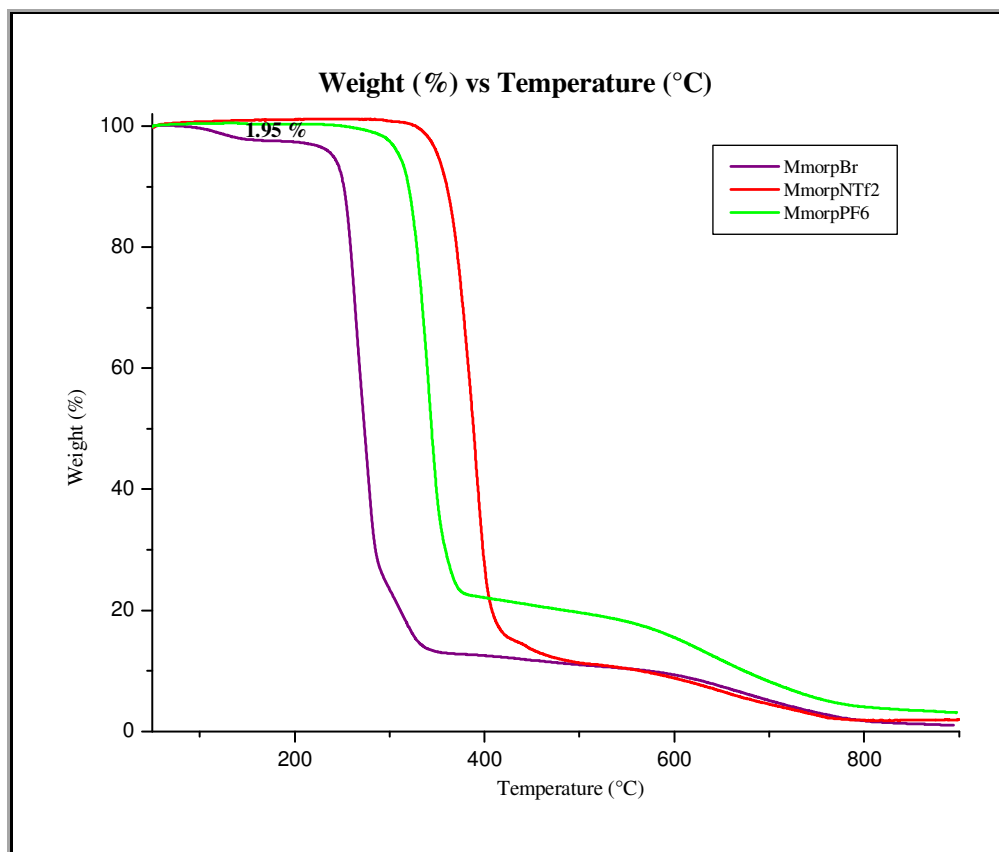


Figure 4.87 : DSC plot of  $[\text{Nmpp}]^{2+} \cdot 2[\text{PF}_6]^-$

#### 4.9.6 : Thermal properties of [Mmorp] series

The result (Figure 4.88) clearly showed the NTf<sub>2</sub> salt has the highest thermal stability than the other two salts which was started to decompose at 293 °C followed by PF<sub>6</sub> salt which was degrading at 271 °C. The Br salt was stable up to 224 °C before deteriorated. However, it was noted that 1.95 % of water was present in Br salt since it absorbs moisture easily once being exposed to the air.

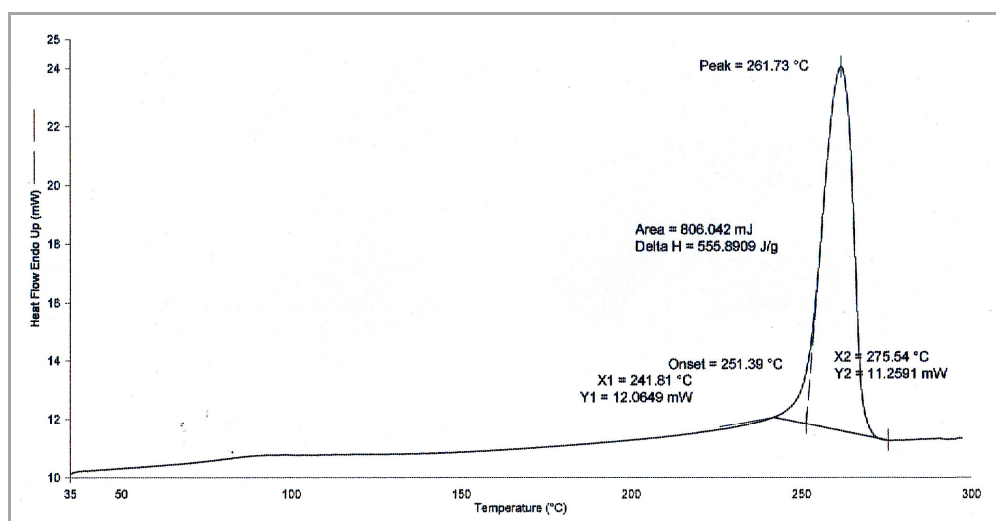
The plot of weight percent loss versus temperature below represents the thermal decomposition of three dicationic ionic liquids for [Mmorp] series. The experiments were run from 40 °C until 900 °C at heating rate 10 °C/min.



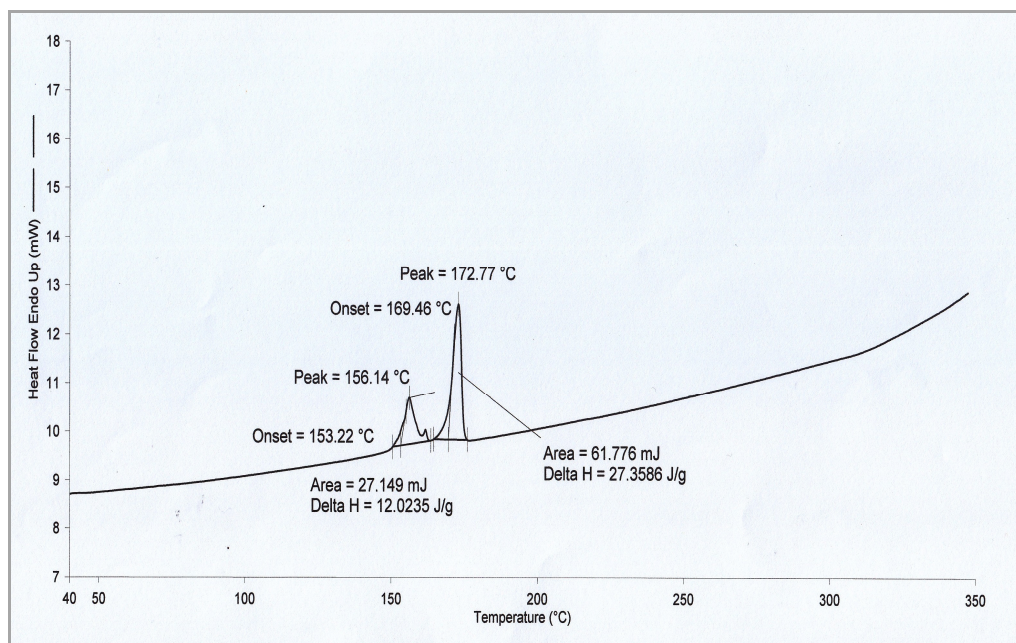
**Figure 4.88** : TGA curves of *N,N'*-[1,4-phenylenebis(methylene)]bis-(*N,N*-dimethylmorpholinium) series; Br, NTf<sub>2</sub> and PF<sub>6</sub>.



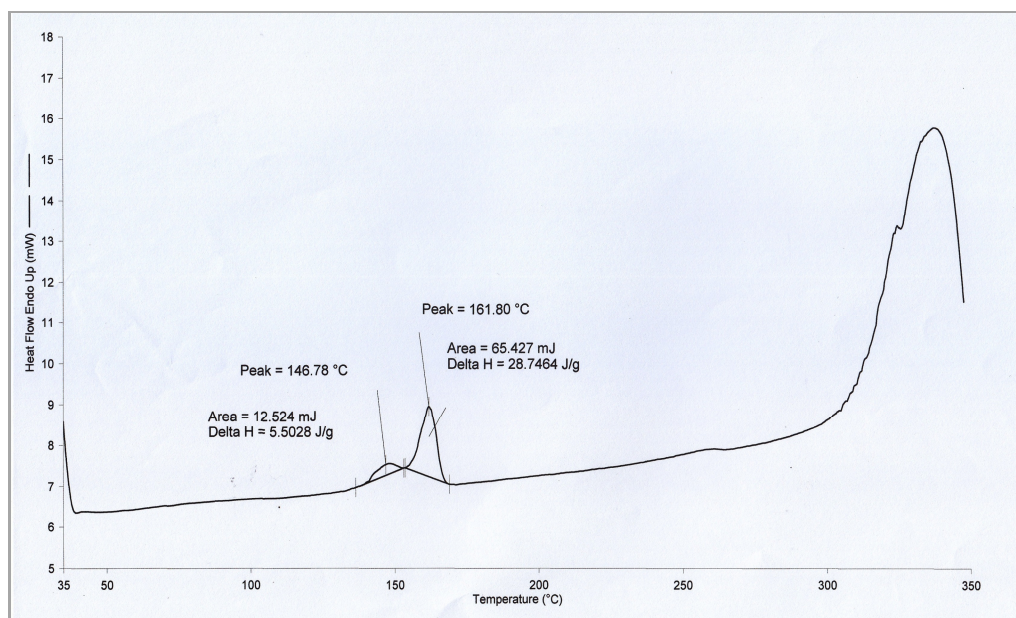
DSC experiments illustrate two phase transition for NTf<sub>2</sub> salt (Figure 4.90) which is melting temperature (T<sub>m</sub>). From the result of single-crystal X-ray diffraction analysis, it was found that the [Mmorp] cation have two type of conformation; cisoid and transoid. Therefore, it was suspected that the peak at 156.14 °C was the melting temperature of cisoid while at 172.77 °C was belonged to the transoid conformation of the NTf<sub>2</sub> organic salt. The cation and anion molecules were large thus affect the arrangement of the molecules in a crystal system. This might explain why the NTf<sub>2</sub> salt melts at lower temperature compared to Br and PF<sub>6</sub> salts which were tend to decompose without undergo melting phase. Besides, because of the symmetrical structure of cation the NTf<sub>2</sub> salt has high melting point. DSC plot of PF<sub>6</sub> salt (Figure 4.91) recorded a similar pattern of phase transition at 146.78 °C and 161.80 °C which are believed to be the melting temperature of cisoid and transoid conformation respectively. In addition, at temperature 336.98 °C the compound was decomposing. On the other hands, the phase transition observed for Br salt (Figure 4.89) was the decomposition temperature which was recorded at 261.73 °C.



**Figure 4.89 :** DSC plot of [Mmorp]<sup>2+</sup>.2[Br]<sup>-</sup>



**Figure 4.90** : DSC plot of  $[\text{Mmorp}]^{2+} \cdot 2[\text{NTf}_2]$

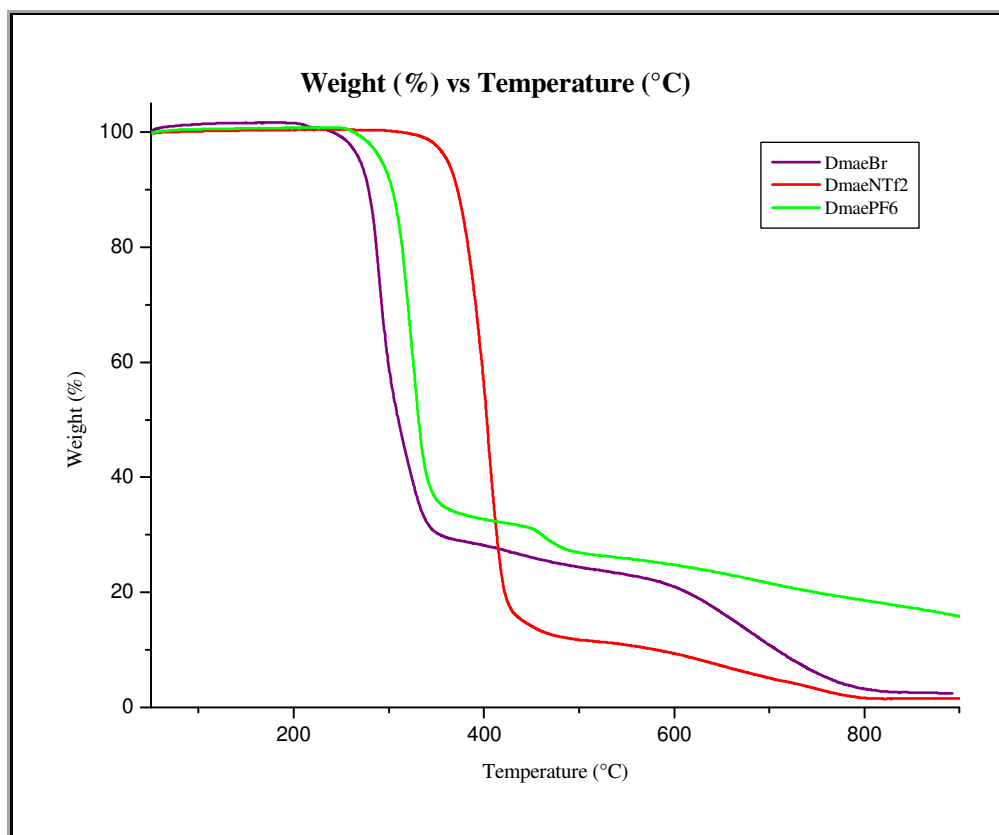


**Figure 4.91** : DSC plot of  $[\text{Mmorp}]^{2+} \cdot 2[\text{PF}_6]$

#### 4.9.7 : Thermal properties of [Dmae] series

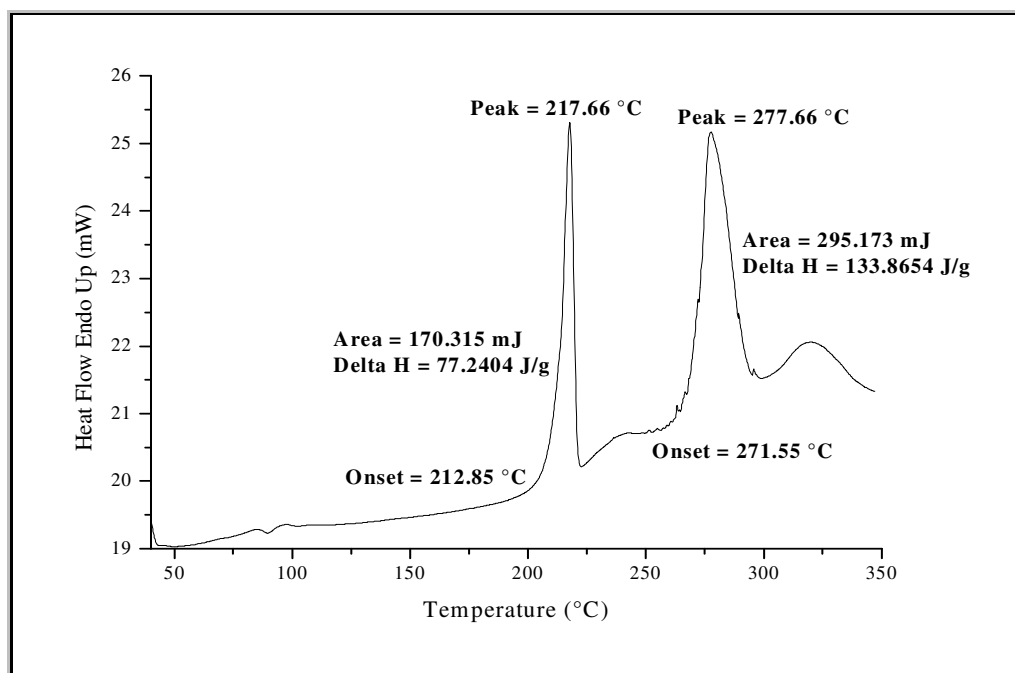
The result (Figure 4.92) clearly showed the NTf<sub>2</sub> salt has better thermal stability than the other two salts which started to decompose at 296 °C while PF<sub>6</sub> and Br salt were stable up to 255 °C and 230 °C respectively before decomposing.

The plot of weight percent loss versus temperature below represents the thermal decomposition of three dicationic ionic liquids for [Dmae] series. The experiments were run from 40 °C until 900 °C at heating rate 10 °C/min.



**Figure 4.92** : TGA curves of *N,N'*-[1,4-phenylenebis(methylene)]bis-(*N,N*-dimethyl-(2-hydroxy) ethanaminium) series; Br, NTf<sub>2</sub> and PF<sub>6</sub>.

DSC experiments illustrate only one phase transition for NTf<sub>2</sub> salt (Figure 4.94) that is melting temperature (T<sub>m</sub>). The melting temperature was observed in the NTf<sub>2</sub> organic salt which melts at 94.59 °C. The cation and anion molecules were large thus affect the arrangement of the molecules in a crystal system. This might explained why this salt melts at lower temperature compared to Br and PF<sub>6</sub> salts which were tend to decompose without undergo melting phase. For PF<sub>6</sub> salt (Figure 4.95), melting transition was observed at 135.25 °C. Besides, it was found that there were two decomposition peaks recorded at 251.97 °C and 311.55 °C for this compound. On the other hand, Br salt (Figure 4.93) showed two decomposition peaks which were recorded at 217.66 °C and 277.66 °C.



**Figure 4.93 :** DSC plot of [Dmae]<sup>2+</sup>.2[Br]<sup>-</sup>

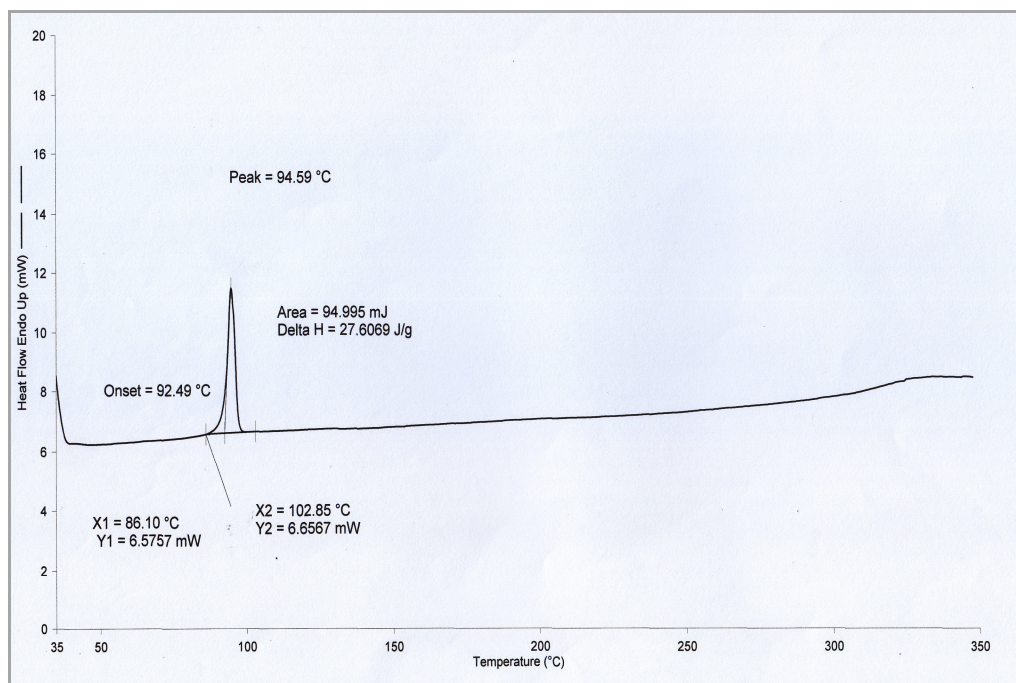


Figure 4.94 : DSC plot of  $[\text{Dmae}]^{2+} \cdot 2[\text{NTf}_2]^-$

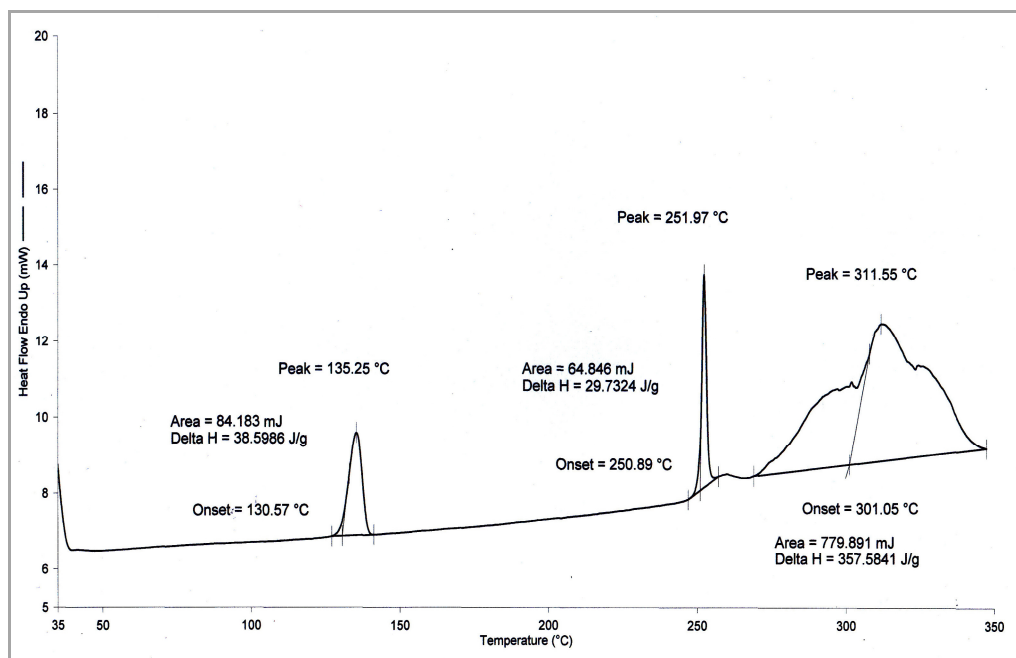
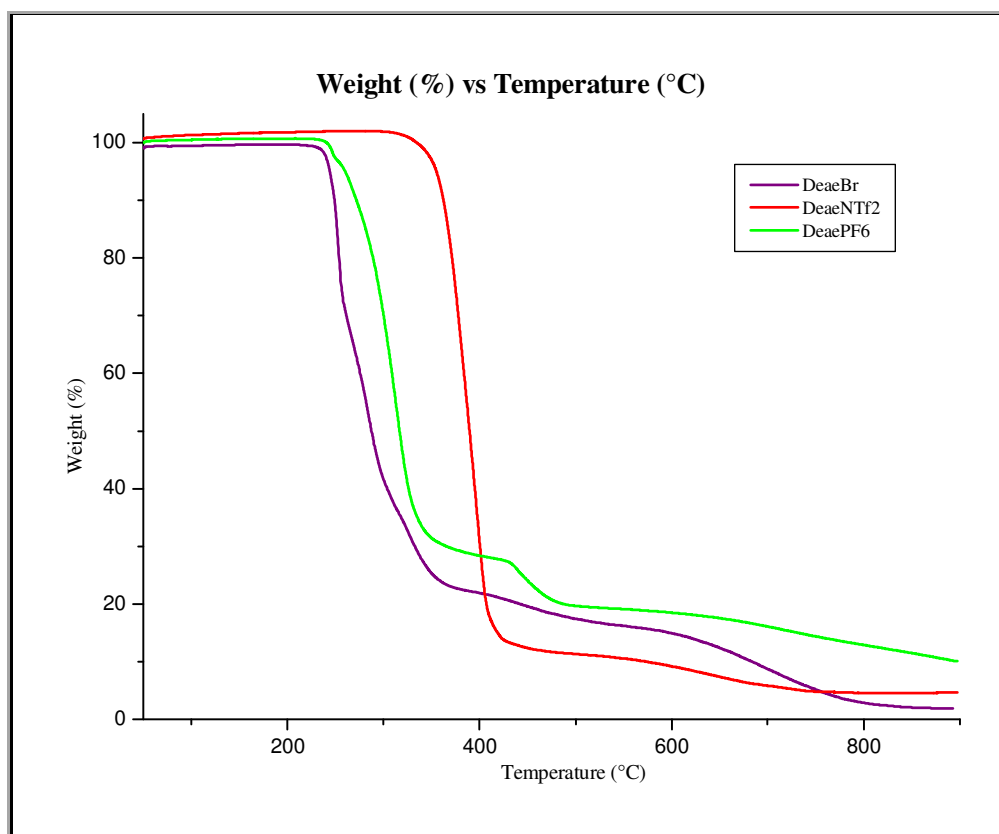


Figure 4.95 : DSC plot of  $[\text{Dmae}]^{2+} \cdot 2[\text{PF}_6]^-$

#### 4.9.8 : Thermal properties of [Deae] series

The TG curves (Figure 4.96) displayed the PF<sub>6</sub> and Br salts were degrading at 236 °C and 225 °C respectively. However, the NTf<sub>2</sub> salt has the highest thermal stability than the other two salts which was started to decompose at 304 °C.

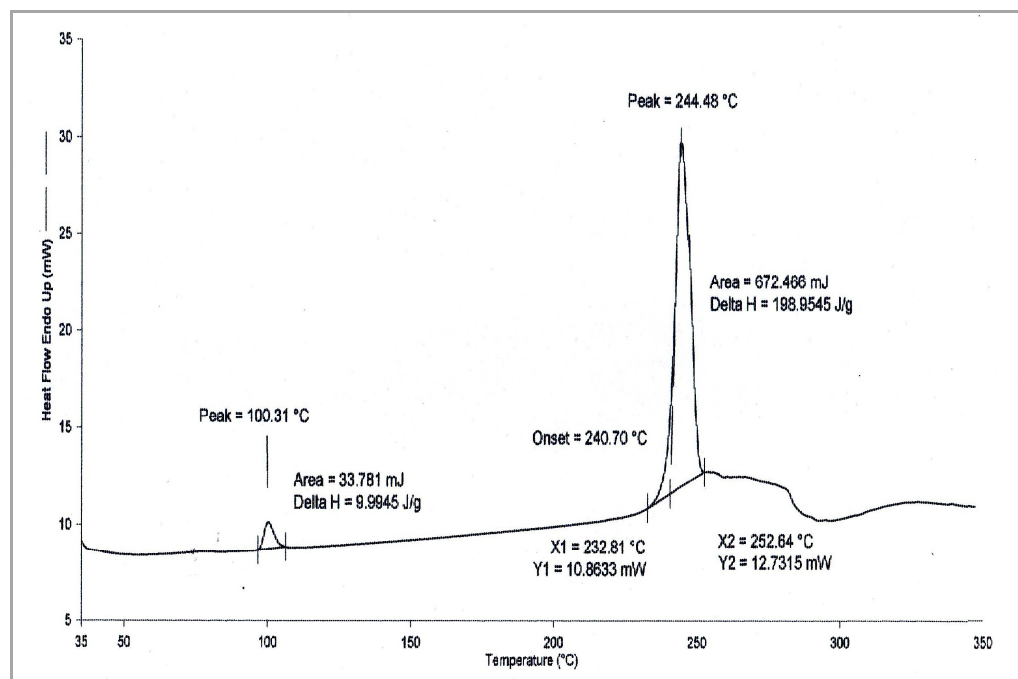
The plot of weight percent loss versus temperature below represents the thermal decomposition of three dicationic ionic liquids for [Deae] series. The experiments were run from 40 °C until 900 °C at heating rate 10 °C/min.



**Figure 4.96 :** TGA curves of *N,N'*-[1,4-phenylenebis(methylene)]bis-(*N,N*-dibutyl-(2-hydroxy) ethanaminium) series; Br, NTf<sub>2</sub> and PF<sub>6</sub>.



DSC experiments illustrate only one phase transition for NTf<sub>2</sub> salt (Figure 4.98) that is melting temperature (T<sub>m</sub>) which was recorded at 89.73 °C. The cation and anion molecules were large thus affect the arrangement of the molecules in a crystal system. This might explained why the NTf<sub>2</sub> salt melts at lower temperature compared to Br and PF<sub>6</sub> salts which were tend to decompose without undergo melting phase. In the DSC plot of Br salt (Figure 4.97), the peak at 100.31 °C was due to the evaporation of water while at 244.48 °C the decomposition temperature of dicationic ionic liquid was observed. Meanwhile, DSC plot of PF<sub>6</sub> salt (Figure 4.99) does not recorded any melting temperature except the compound was decomposing at temperature above 260 °C.



**Figure 4.97** : DSC plot of [Deae]<sup>2+</sup>.2[Br]<sup>-</sup>

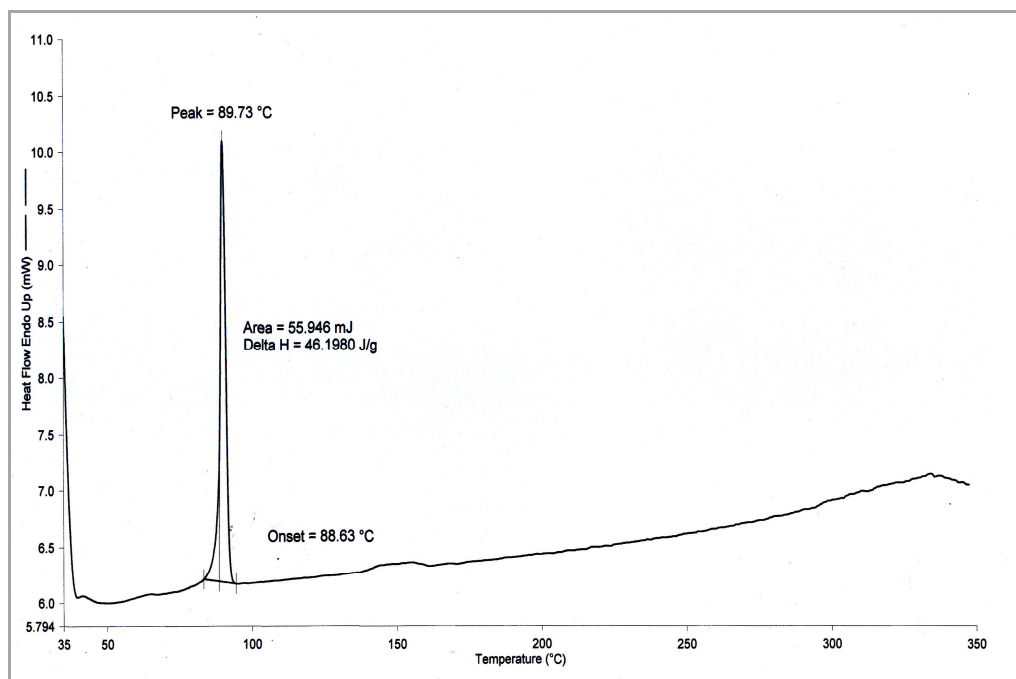


Figure 4.98 : DSC plot of [Deae]<sup>2+</sup>·2[NTf<sub>2</sub>]

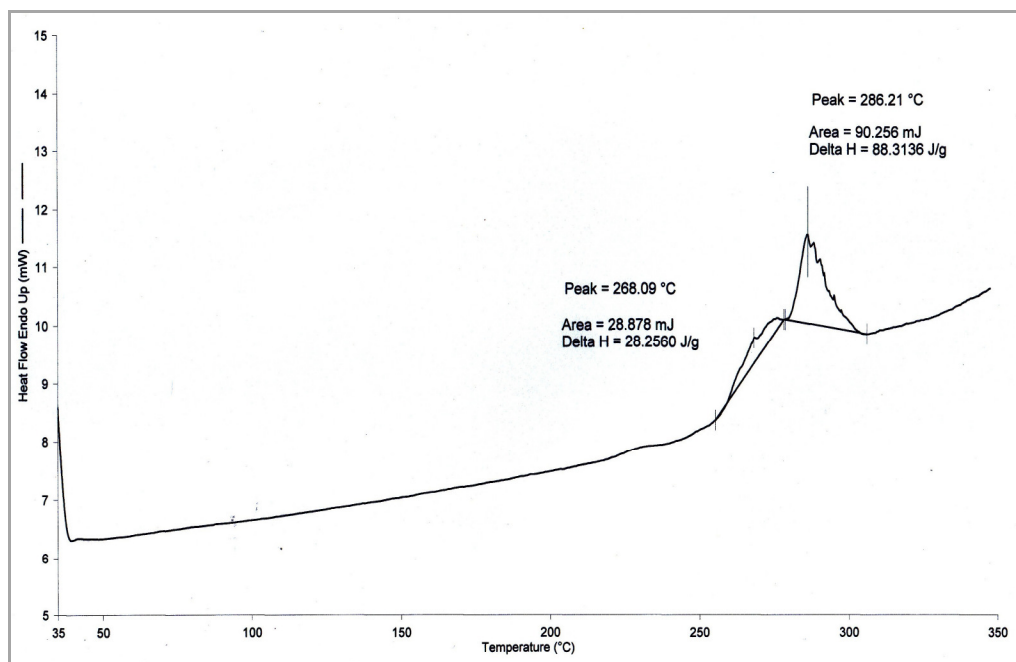


Figure 4.99 : DSC plot of [Deae]<sup>2+</sup>·2[PF<sub>6</sub>]



**Table 4.23** : Melting temperature ( $T_m$ ) and decomposition temperature ( $T_d$ ) of synthesized dicationic ionic liquids. (n.o. denotes not observed)

Dicationic ILs	Molecular weight (g/mol)	Phase transition		
		$T_m$ (°C)	$T_g$ (°C)	$T_d$ (°C)
[Pyr] <sup>2+</sup> .2[Br] <sup>-</sup>	422.162	n.o.	n.o.	252.60
[Tea] <sup>2+</sup> .2[Br] <sup>-</sup>	466.343	n.o.	n.o.	226.69
[Mpyl] <sup>2+</sup> .2[Br] <sup>-</sup>	434.258	n.o.	n.o.	238.36
[Bpyl] <sup>2+</sup> .2[Br] <sup>-</sup>	518.419	n.o.	n.o.	213.06
[Nmpp] <sup>2+</sup> .2[Br] <sup>-</sup>	462.311	n.o.	n.o.	237.47
[Mmorp] <sup>2+</sup> .2[Br] <sup>-</sup>	466.256	n.o.	n.o.	223.65
[Dmae] <sup>2+</sup> .2[Br] <sup>-</sup>	442.234	n.o.	n.o.	229.58
[Deae] <sup>2+</sup> .2[Br] <sup>-</sup>	498.342	n.o.	n.o.	224.64
[Pyr] <sup>2+</sup> .2[NTf <sub>2</sub> ] <sup>-</sup>	822.646	154.75	n.o.	375.06
[Tea] <sup>2+</sup> .2[NTf <sub>2</sub> ] <sup>-</sup>	866.828	122.59	n.o.	320.50
[Mpyl] <sup>2+</sup> .2[NTf <sub>2</sub> ] <sup>-</sup>	834.742	91.56	n.o.	365.21
[Bpyl] <sup>2+</sup> .2[NTf <sub>2</sub> ] <sup>-</sup>	900.760	94.52	n.o.	309.93
[Nmpp] <sup>2+</sup> .2[NTf <sub>2</sub> ] <sup>-</sup>	862.796	129.35	n.o.	334.30
[Mmorp] <sup>2+</sup> .2[NTf <sub>2</sub> ] <sup>-</sup>	866.740	171.87	n.o.	293.31
[Dmae] <sup>2+</sup> .2[NTf <sub>2</sub> ] <sup>-</sup>	842.718	94.59	n.o.	295.71
[Deae] <sup>2+</sup> .2[NTf <sub>2</sub> ] <sup>-</sup>	898.826	89.73	n.o.	303.63
[Pyr] <sup>2+</sup> .2[PF <sub>6</sub> ] <sup>-</sup>	552.284	n.o.	n.o.	291.54
[Tea] <sup>2+</sup> .2[PF <sub>6</sub> ] <sup>-</sup>	596.466	n.o.	n.o.	319.38
[Mpyl] <sup>2+</sup> .2[PF <sub>6</sub> ] <sup>-</sup>	564.380	n.o.	n.o.	336.21
[Bpyl] <sup>2+</sup> .2[PF <sub>6</sub> ] <sup>-</sup>	648.542	177.74	n.o.	277.44
[Nmpp] <sup>2+</sup> .2[PF <sub>6</sub> ] <sup>-</sup>	592.434	n.o.	n.o.	278.45
[Mmorp] <sup>2+</sup> .2[PF <sub>6</sub> ] <sup>-</sup>	596.378	161.80	n.o.	271.04
[Dmae] <sup>2+</sup> .2[PF <sub>6</sub> ] <sup>-</sup>	572.356	135.25	n.o.	255.10
[Deae] <sup>2+</sup> .2[PF <sub>6</sub> ] <sup>-</sup>	628.464	n.o.	n.o.	235.94

#### 4.9.9 : Thermal Properties based on Anion Moiety

##### 1. Bromide moiety

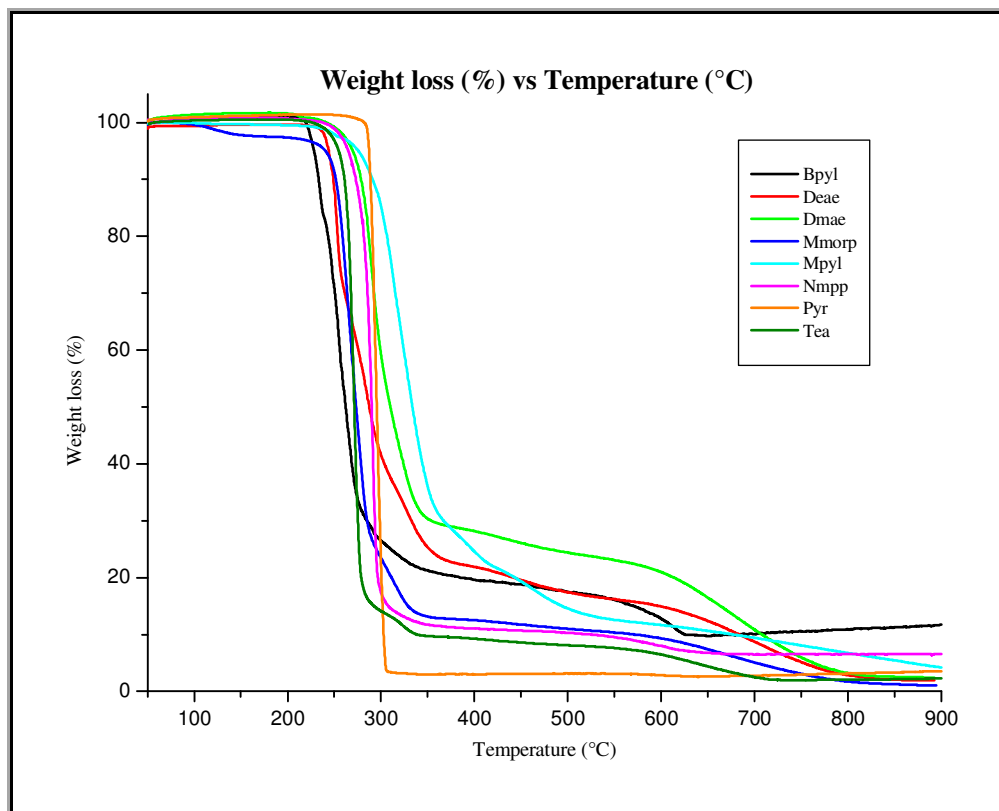
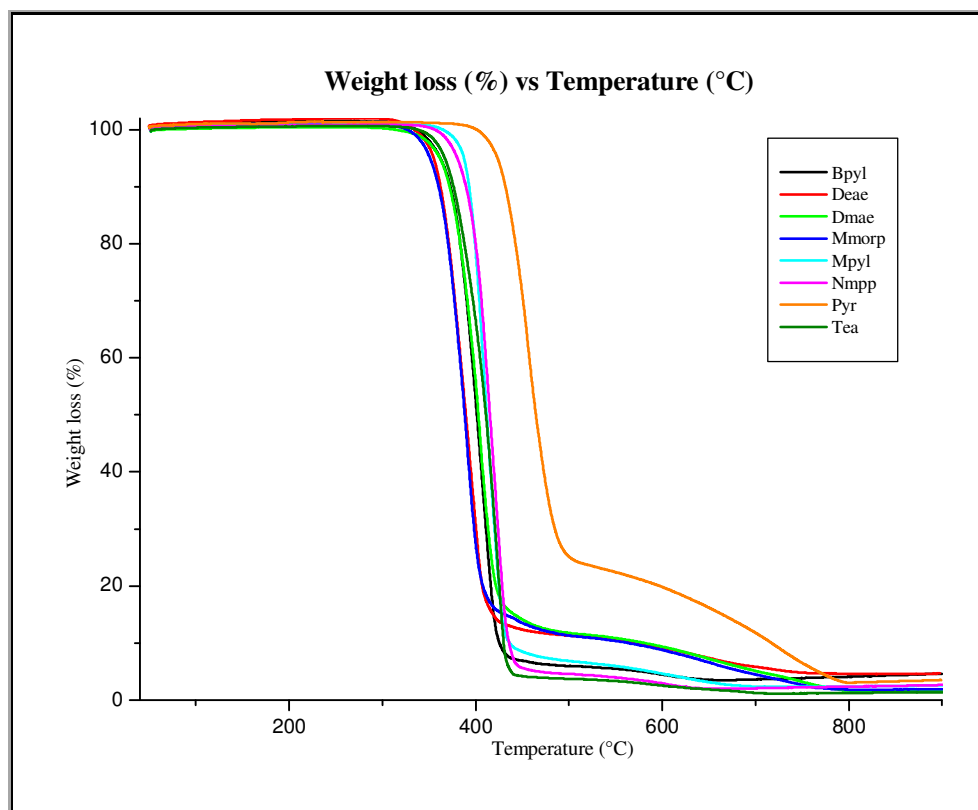


Figure 4.100 : TGA curves of bromide salts moieties.

Figure 4.100 shows TGA curves for bromide salts moiety. It was observed that thermal stability of bromide moiety is the lowest compared to hexafluorophosphate moiety and bis(trifluoromethanesulfonyl)imide moiety which is within the temperature range 220-250 °C. The lowest reading was observed for compound  $[\text{Mmorp}]^{2+} \cdot 2[\text{Br}]^-$  while the highest reading was recorded for compound  $[\text{Pyr}]^{2+} \cdot 2[\text{Br}]^-$ . Therefore, the bromide salts do not melt instead of decomposing. In addition, from the TGA curves, it was observed  $[\text{Mmorp}]^{2+} \cdot 2[\text{Br}]^-$  contained 2 % of water. Based on DSC analysis, it was found that Br salts do not show melting transition and thus only decomposition peak.

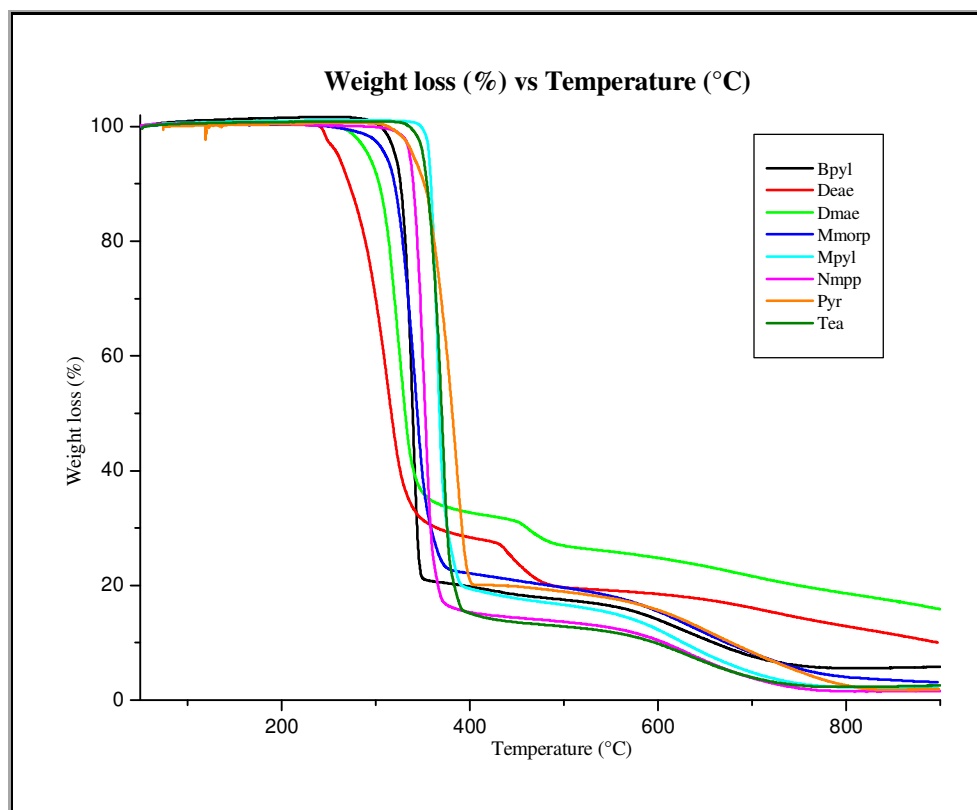
## 2. Bis(trifluoromethanesulfonyl)imide moiety



**Figure 4.101** : TGA curves of bis(trifluoromethanesulfonyl)imide salts moieties.

**Figure 4.101** shows TGA curves for bis(trifluoromethanesulfonyl)imide salts moieties. It was found that thermal stability of bis(trifluoromethanesulfonyl)imide moieties is the highest amongst hexafluorophosphate moieties and bromide moieties which is within the temperature range 300-375°C. Based on the results,  $[\text{Pyr}]^{2+} \cdot 2[\text{NTf}_2]^-$  is considered the most stable dicationic ionic liquid even though it has high melting temperature, while the least stable was  $[\text{Mmorp}]^{2+} \cdot 2[\text{NTf}_2]^-$  salts. Unlike most of the bromide salts, bis(trifluoromethanesulfonyl)imide salts melt at certain temperature. The lowest melting temperature was recorded for  $[\text{Deae}]^{2+} \cdot 2[\text{NTf}_2]^-$  (m.p 90 °C) while compounds  $[\text{Mpyl}]^{2+} \cdot 2[\text{NTf}_2]^-$ ,  $[\text{Bpyl}]^{2+} \cdot 2[\text{NTf}_2]^-$  and  $[\text{Dmae}]^{2+} \cdot 2[\text{NTf}_2]^-$  melts at temperature below 100 °C.

### 3. Hexafluorophosphate moiety



**Figure 4.102** : TGA curves of hexafluorophosphate salts moieties.

**Figure 4.102** shows TGA curves for hexafluorophosphate salts moiety. The results proved that thermal stability of hexafluorophosphate moiety is somehow moderate which lies between bis(trifluoromethanesulfonyl)imide salt moiety and bromide salts moiety. The highest thermal stability is owned by  $[\text{Mpyl}]^{2+} \cdot 2[\text{PF}_6]^-$  which decomposed at  $336.21^\circ\text{C}$  while the least stable is  $[\text{Deae}]^{2+} \cdot 2[\text{PF}_6]^-$  which was decomposed at  $235.94^\circ\text{C}$ . From the DSC plot, some of the synthesized dicationic ionic liquids do not show any melting transition and thus show only decomposition peak. Meanwhile,  $[\text{Dmae}]^{2+} \cdot 2[\text{PF}_6]^-$ ,  $[\text{Mmorp}]^{2+} \cdot 2[\text{PF}_6]^-$  and  $[\text{Bpyl}]^{2+} \cdot 2[\text{PF}_6]^-$  were melted at  $135.25^\circ\text{C}$ ,  $161.80^\circ\text{C}$  and  $177.74^\circ\text{C}$  respectively.

#### **4.10 : Fourier-Transform Infra-Red Spectroscopy**

The significant vibrations observed in the IR spectra of all synthesized ionic liquids were tabulated in the **Table 4.24**.

**Table 4.24** : IR spectral data of synthesized dicationic ionic liquids

Dicationic ionic liquids		Wavenumber (cm <sup>-1</sup> )				
		S=O sulfoxide	C-N stretching	-CF <sub>3</sub>	O-H stretching	PF <sub>6</sub>
Pyr	Br <sup>-</sup>	-	-	-	-	-
	NTf <sub>2</sub> <sup>-</sup>	1056.72 (vs)	1140.05 (vs),	1358.92 (s)	-	-
	PF <sub>6</sub> <sup>-</sup>	-	1186.86 (vs) -	-	-	835.16 (vs), 556.99 (vs)
Tea	Br <sup>-</sup>	-	-	-	-	-
	NTf <sub>2</sub> <sup>-</sup>	1049.01 (vs)	1138.23 (vs),	1354.12 (s)	-	-
	PF <sub>6</sub> <sup>-</sup>	-	1180.90 (vs) -	-	-	838.63 (vs), 558.18 (vs)
Mpyl	Br <sup>-</sup>	-	-	-	3403-3460 (H <sub>2</sub> O)	-
	NTf <sub>2</sub> <sup>-</sup>	1054.17 (vs)	1140.10 (vs),	1354.27 (s)	-	-
	PF <sub>6</sub> <sup>-</sup>	-	1201.50 (vs) -	-	-	827.78 (vs), 556.16 (vs)
Bpyl	Br <sup>-</sup>	-	-	-	3398-3462 (H <sub>2</sub> O)	-
	NTf <sub>2</sub> <sup>-</sup>	1054.72 (vs)	1142.74 (vs),	1351.49 (s)	-	-
	PF <sub>6</sub> <sup>-</sup>	-	1197.11 (vs) -	-	-	824.60 (vs), 554.84 (vs)
Nmpp	Br <sup>-</sup>	-	-	-	3371 (H <sub>2</sub> O)	-
	NTf <sub>2</sub> <sup>-</sup>	1055.21 (vs)	1143.36 (vs),	1351.51 (s)	-	-
	PF <sub>6</sub> <sup>-</sup>	-	1194.17 (vs) -	-	-	827.18 (vs), 555.30 (vs)

Mmorp	Br <sup>-</sup>	-	-	-	3377 (H <sub>2</sub> O)	-
	NTf <sub>2</sub> <sup>-</sup>	1057.19 (vs)	1128.29 (vs),	1356.63 (s)	-	-
	PF <sub>6</sub> <sup>-</sup>	-	1209.67 (vs) -	-	-	816.91 (vs), 554.55 (vs)
Dmae	Br <sup>-</sup>	-	-	-	3259.29 (s)	-
	NTf <sub>2</sub> <sup>-</sup>	1046.31 (vs)	1135.37 (vs),	1344.11 (s)	3502.42	-
	PF <sub>6</sub> <sup>-</sup>	-	1186.71 (vs) -	-	(w) 3586.95 (m)	824.23 (vs), 555.68 (vs)
Deae	Br <sup>-</sup>	-	-	-	3291.52 (s)	-
	NTf <sub>2</sub> <sup>-</sup>	1049.66 (vs)	1136.92 (vs),	1344.18 (s)	3517.92	-
	PF <sub>6</sub> <sup>-</sup>	-	1187.70 (vs) -	-	(w) 3602.53 (w)	827.70 (vs), 556.02 (vs)

#### **4.11 : Elemental Analyses**

The percentage of carbon, hydrogen, nitrogen and sulphur in synthesized dicationic organic salts were determined and the data of analyses are accordance to the expected compositions and structures. However, the percentage of these elements in bromide salts might deviate slightly from the theoretical values since the compounds were very hygroscopic, therefore water might be presence in a small percentage. The complete results of the elemental analyses were tabulated in the **Table 4.25**.



**Table 4.25** : Elemental Analysis

Dicationic ILs	Molecular formula	Results	C (%)	H (%)	N (%)	S (%)
[Pyr] <sup>+</sup> .2[Br] <sup>-</sup>	C <sub>18</sub> H <sub>18</sub> N <sub>2</sub> Br <sub>2</sub>	Calculated	51.21	4.30	6.64	-
		Found	51.02	4.51	6.58	-
[Tea] <sup>+</sup> .2[Br] <sup>-</sup>	C <sub>20</sub> H <sub>38</sub> N <sub>2</sub> Br <sub>2</sub>	Calculated	51.51	8.21	6.01	-
		Found	50.97	8.74	5.97	-
[Mpyl] <sup>+</sup> .2[Br] <sup>-</sup>	C <sub>18</sub> H <sub>30</sub> N <sub>2</sub> Br <sub>2</sub>	Calculated	49.79	6.96	6.45	-
		Found	49.98	7.13	6.06	-
[Bpyl] <sup>+</sup> .2[Br] <sup>-</sup>	C <sub>24</sub> H <sub>42</sub> N <sub>2</sub> Br <sub>2</sub>	Calculated	55.60	8.17	5.40	-
		Found	55.83	9.73	5.39	-
[Nmpp] <sup>+</sup> .2[Br] <sup>-</sup>	C <sub>20</sub> H <sub>34</sub> N <sub>2</sub> Br <sub>2</sub>	Calculated	51.96	7.41	6.06	-
		Found	51.29	8.61	5.98	-
[Mmorp] <sup>+</sup> .2[Br] <sup>-</sup>	C <sub>18</sub> H <sub>30</sub> N <sub>2</sub> O <sub>2</sub> Br <sub>2</sub>	Calculated	46.37	6.49	6.01	-
		Found	45.77	7.68	5.93	-
[Dmae] <sup>+</sup> .2[Br] <sup>-</sup>	C <sub>16</sub> H <sub>30</sub> N <sub>2</sub> O <sub>2</sub> Br <sub>2</sub>	Calculated	43.46	6.84	6.33	-
		Found	43.45	7.30	6.26	-
[Deae] <sup>+</sup> .2[Br] <sup>-</sup>	C <sub>20</sub> H <sub>38</sub> N <sub>2</sub> O <sub>2</sub> Br <sub>2</sub>	Calculated	48.20	7.69	5.62	-
		Found	47.87	8.59	5.54	-
[Pyr] <sup>+</sup> .2[NTf <sub>2</sub> ] <sup>-</sup>	C <sub>22</sub> H <sub>18</sub> N <sub>4</sub> F <sub>12</sub> O <sub>8</sub> S <sub>4</sub>	Calculated	32.12	2.21	6.81	15.59
		Found	32.37	2.12	7.24	16.23
[Tea] <sup>+</sup> .2[NTf <sub>2</sub> ] <sup>-</sup>	C <sub>24</sub> H <sub>38</sub> N <sub>4</sub> F <sub>12</sub> O <sub>8</sub> S <sub>4</sub>	Calculated	33.25	4.42	6.46	14.48
		Found	33.51	4.29	6.58	14.89
[Mpyl] <sup>+</sup> .2[NTf <sub>2</sub> ] <sup>-</sup>	C <sub>22</sub> H <sub>30</sub> N <sub>4</sub> F <sub>12</sub> O <sub>8</sub> S <sub>4</sub>	Calculated	31.65	3.62	6.71	15.37
		Found	31.81	3.18	6.90	14.97
[Bpyl] <sup>+</sup> .2[NTf <sub>2</sub> ] <sup>-</sup>	C <sub>28</sub> H <sub>42</sub> N <sub>4</sub> F <sub>12</sub> O <sub>8</sub> S <sub>4</sub>	Calculated	36.60	4.61	6.10	13.96
		Found	36.99	4.30	6.40	14.37
[Nmpp] <sup>+</sup> .2[NTf <sub>2</sub> ] <sup>-</sup>	C <sub>24</sub> H <sub>34</sub> N <sub>4</sub> F <sub>12</sub> O <sub>8</sub> S <sub>4</sub>	Calculated	33.41	3.97	6.49	14.87
		Found	33.71	3.92	6.61	14.34
[Mmorp] <sup>+</sup> .2[NTf <sub>2</sub> ] <sup>-</sup>	C <sub>22</sub> H <sub>30</sub> N <sub>4</sub> F <sub>12</sub> O <sub>10</sub> S <sub>4</sub>	Calculated	30.49	3.49	6.46	14.80

		Found	30.30	3.13	6.25	15.88
[Dmae] <sup>+</sup> .2[NTf <sub>2</sub> ] <sup>-</sup>	C <sub>20</sub> H <sub>30</sub> N <sub>4</sub> F <sub>12</sub> O <sub>10</sub> S <sub>4</sub>	Calculated	28.50	3.59	6.65	15.22
		Found	28.89	3.51	6.89	15.41
[Deae] <sup>+</sup> .2[NTf <sub>2</sub> ] <sup>-</sup>	C <sub>24</sub> H <sub>38</sub> N <sub>4</sub> F <sub>12</sub> O <sub>10</sub> S <sub>4</sub>	Calculated	32.07	4.26	6.23	14.27
		Found	31.96	4.38	6.44	14.71
[Pyr] <sup>+</sup> .2[PF <sub>6</sub> ] <sup>-</sup>	C <sub>18</sub> H <sub>18</sub> N <sub>2</sub> F <sub>12</sub> P <sub>2</sub>	Calculated	39.15	3.28	5.07	-
		Found	38.71	2.89	5.06	-
[Tea] <sup>+</sup> .2[PF <sub>6</sub> ] <sup>-</sup>	C <sub>20</sub> H <sub>38</sub> N <sub>2</sub> F <sub>12</sub> P <sub>2</sub>	Calculated	40.27	6.42	4.70	-
		Found	39.65	6.23	4.50	-
[Mpyl] <sup>+</sup> .2[PF <sub>6</sub> ] <sup>-</sup>	C <sub>18</sub> H <sub>30</sub> N <sub>2</sub> F <sub>12</sub> P <sub>2</sub>	Calculated	38.31	5.36	4.96	-
		Found	38.27	5.14	5.02	-
[Bpyl] <sup>+</sup> .2[PF <sub>6</sub> ] <sup>-</sup>	C <sub>24</sub> H <sub>42</sub> N <sub>2</sub> F <sub>12</sub> P <sub>2</sub>	Calculated	44.45	6.53	4.32	-
		Found	43.96	6.29	4.51	-
[Nmpp] <sup>+</sup> .2[PF <sub>6</sub> ] <sup>-</sup>	C <sub>20</sub> H <sub>34</sub> N <sub>2</sub> F <sub>12</sub> P <sub>2</sub>	Calculated	40.55	5.78	4.73	-
		Found	40.80	5.35	4.79	-
[Mmorp] <sup>+</sup> .2[PF <sub>6</sub> ] <sup>-</sup>	C <sub>18</sub> H <sub>30</sub> N <sub>2</sub> O <sub>2</sub> F <sub>12</sub> P <sub>2</sub>	Calculated	36.25	5.07	4.70	-
		Found	36.20	4.95	4.74	-
[Dmae] <sup>+</sup> .2[PF <sub>6</sub> ] <sup>-</sup>	C <sub>16</sub> H <sub>30</sub> N <sub>2</sub> F <sub>12</sub> O <sub>2</sub> P <sub>2</sub>	Calculated	33.58	5.28	4.89	-
		Found	33.56	4.87	4.86	-
[Deae] <sup>+</sup> .2[PF <sub>6</sub> ] <sup>-</sup>	C <sub>20</sub> H <sub>38</sub> N <sub>2</sub> F <sub>12</sub> O <sub>2</sub> P <sub>2</sub>	Calculated	38.22	6.09	4.46	-
		Found	38.32	6.12	4.48	-

---

#### 4.12 : Halides Analysis

The bis(trifluoromethanesulfonyl)imide and hexafluorophosphate dicationic ionic liquids were obtained from the metathesis of bromide dicationic ionic liquids with lithium bis(trifluoromethanesulfonyl)imide and ammonium hexafluorophosphate. The ion chromatography technique was used to determine the halides content of synthesized dicationic ionic liquids.

It was observed that the chromatographic analysis of bromide level in bis(trifluoromethanesulfonyl)imide dicationic ionic liquids was below the detection limit. On the other hand, the concentration of bromide in hexafluorophosphate dicationic ionic liquids was below 2 ppm. Meanwhile, the purity of all synthesized dicationic ionic liquids was above 99 %. The data on the retention time and concentration of particular anions for bis(trifluoromethanesulfonyl)imide and hexafluorophosphate moieties was summarized in the **Table 4.26** below:

**Table 4.26** : Chromatographic analysis data of NTf<sub>2</sub> and PF<sub>6</sub> moieties.

Dicationic ionic liquids	Anions	Sample weight (mg)	Concentration (ppm)	Retention time (min)	Purity (%)
[Pyr] <sup>+</sup> .2[NTf <sub>2</sub> ] <sup>-</sup>	Br	9.5	-	-	99.99
	NTf <sub>2</sub>		892.575	9.03	
[Tea] <sup>+</sup> .2[NTf <sub>2</sub> ] <sup>-</sup>	Br	10.5	-	-	99.99
	NTf <sub>2</sub>		918.999	9.04	
[Mpyl] <sup>+</sup> .2[NTf <sub>2</sub> ] <sup>-</sup>	Br	9.8	-	-	99.99
	NTf <sub>2</sub>		930.051	9.04	
[Bpyl] <sup>+</sup> .2[NTf <sub>2</sub> ] <sup>-</sup>	Br	9.6	-	-	99.99
	NTf <sub>2</sub>		773.217	9.08	

[Nmpp] <sup>+</sup> .2[NTf <sub>2</sub> ] <sup>-</sup>	Br	9.9	-	-	99.99
	NTf <sub>2</sub>		700.577	9.08	
[Mmorp] <sup>+</sup> .2[NTf <sub>2</sub> ] <sup>-</sup>	Br	9.5	-	-	99.99
	NTf <sub>2</sub>		719.968	9.03	
[Dmae] <sup>+</sup> .2[NTf <sub>2</sub> ] <sup>-</sup>	Br	10.2	-	-	99.99
	NTf <sub>2</sub>		821.845	9.04	
[Deae] <sup>+</sup> .2[NTf <sub>2</sub> ] <sup>-</sup>	Br	10.4	-	-	99.99
	NTf <sub>2</sub>		977.372	9.02	
[Pyr] <sup>+</sup> .2[PF <sub>6</sub> ] <sup>-</sup>	Br	9.7	0.462	5.00	99.93
	PF <sub>6</sub>		618.439	13.82	
[Tea] <sup>+</sup> .2[PF <sub>6</sub> ] <sup>-</sup>	Br	9.7	0.066	5.07	99.98
	PF <sub>6</sub>		509.479	14.11	
[Mpyl] <sup>+</sup> .2[PF <sub>6</sub> ] <sup>-</sup>	Br	10.0	0.179	5.08	99.97
	PF <sub>6</sub>		678.335	13.80	
[Bpyl] <sup>+</sup> .2[PF <sub>6</sub> ] <sup>-</sup>	Br	10.0	0.255	5.10	99.95
	PF <sub>6</sub>		525.591	13.96	
[Nmpp] <sup>+</sup> .2[PF <sub>6</sub> ] <sup>-</sup>	Br	9.9	0.226	5.01	99.96
	PF <sub>6</sub>		600.249	13.97	
[Mmorp] <sup>+</sup> .2[PF <sub>6</sub> ] <sup>-</sup>	Br	9.3	0.896	5.01	99.84
	PF <sub>6</sub>		543.216	13.98	
[Dmae] <sup>+</sup> .2[PF <sub>6</sub> ] <sup>-</sup>	Br	10.4	0.321	5.10	99.95
	PF <sub>6</sub>		658.989	13.78	
[Deae] <sup>+</sup> .2[PF <sub>6</sub> ] <sup>-</sup>	Br	10.4	1.717	4.98	99.71
	PF <sub>6</sub>		583.389	13.85	

#### 4.13 : Solubility in Solvents

The solubility of these ionic liquids was tested in some common organic solvents and water at ambient temperature. Based on the tabulated results, those bromide salts demonstrate hydrophilic nature as they possessed excellent solubility in polar solvent such as water, methanol and DMSO. The hydrophobic NTf<sub>2</sub><sup>-</sup> salts have a wide solubility in medium polarity organic solvents while immiscible in water and non polar solvent such as ether. On the other hand, it was observed that the PF<sub>6</sub><sup>-</sup> salts dissolved in certain medium polar organic solvents but immiscible in water. This is probably because of hydrophilicity/hydrophobicity nature of these organic salts lies in the medium polarity. The presence of hydroxyl functionality does not affect the solubility of organic salt in particular solvent. Furthermore, all dicationic organic salts were miscible in DMSO but immiscible in ether. In conclusion, the order of increasing polarity of these organic salts can be written as follows: NTf<sub>2</sub><sup>-</sup> < PF<sub>6</sub><sup>-</sup> < bromide.

The results were summarised in the **Table 4.27** as follows:

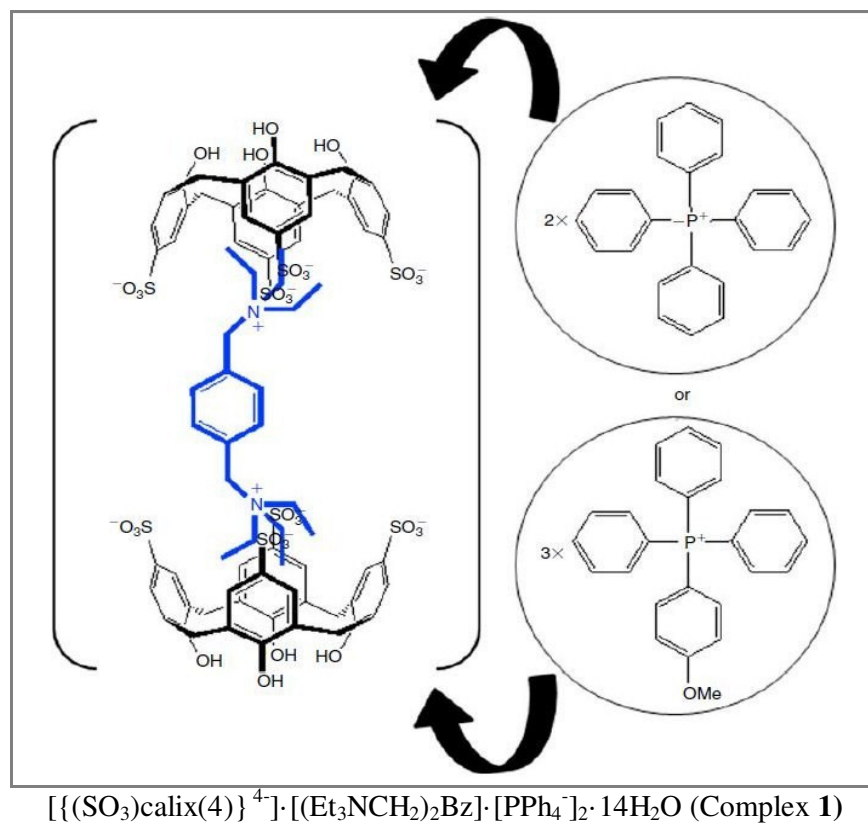
**Table 4.27** : Solubility behaviour of ionic liquids in water and common organic solvents

Dicationic ILs	Solvents							
	DMSO	H <sub>2</sub> O	MeOH	EtOH	CH <sub>3</sub> CN	EA	Acetone	Ether
[Pyr] <sup>+</sup> .2[Br] <sup>-</sup>	m	m	m	im	im	im	im	im
[Tea] <sup>2+</sup> .2[Br] <sup>-</sup>	m	m	m	m	im	im	im	im
[Mpyl] <sup>2+</sup> .2[Br] <sup>-</sup>	m	m	m	m	im	im	im	im
[Bpyl] <sup>2+</sup> .2[Br] <sup>-</sup>	m	m	m	m	im	im	im	im
[Nmpp] <sup>2+</sup> .2[Br] <sup>-</sup>	m	m	m	m	im	im	im	im
[Mmorp] <sup>2+</sup> .2[Br] <sup>-</sup>	m	m	m	m	im	im	im	im
[Dmae] <sup>2+</sup> .2[Br] <sup>-</sup>	m	m	m	m	im	im	im	im
[Deae] <sup>2+</sup> .2[Br] <sup>-</sup>	m	m	m	m	im	im	im	im
[Pyr] <sup>2+</sup> .2[NTf <sub>2</sub> ] <sup>-</sup>	m	im	m	m	m	m	m	im
[Tea] <sup>2+</sup> .2[NTf <sub>2</sub> ] <sup>-</sup>	m	im	m	m	m	m	m	im
[Mpyl] <sup>2+</sup> .2[NTf <sub>2</sub> ] <sup>-</sup>	m	im	m	m	m	m	m	im
[Bpyl] <sup>2+</sup> .2[NTf <sub>2</sub> ] <sup>-</sup>	m	im	m	m	m	m	m	im
[Nmpp] <sup>2+</sup> .2[NTf <sub>2</sub> ] <sup>-</sup>	m	im	m	m	m	m	m	im
[Mmorp] <sup>2+</sup> .2[NTf <sub>2</sub> ] <sup>-</sup>	m	im	m	m	m	m	m	im
[Dmae] <sup>2+</sup> .2[NTf <sub>2</sub> ] <sup>-</sup>	m	im	m	m	m	m	m	im
[Deae] <sup>2+</sup> .2[NTf <sub>2</sub> ] <sup>-</sup>	m	im	m	m	m	m	m	im
[Pyr] <sup>2+</sup> .2[PF <sub>6</sub> ] <sup>-</sup>	m	im	im	im	m	im	im	im
[Tea] <sup>2+</sup> .2[PF <sub>6</sub> ] <sup>-</sup>	m	im	im	im	m	im	im	im
[Mpyl] <sup>2+</sup> .2[PF <sub>6</sub> ] <sup>-</sup>	m	im	im	im	m	im	im	im
[Bpyl] <sup>2+</sup> .2[PF <sub>6</sub> ] <sup>-</sup>	m	im	im	im	m	im	im	im
[Nmpp] <sup>2+</sup> .2[PF <sub>6</sub> ] <sup>-</sup>	m	im	im	im	m	im	im	im
[Mmorp] <sup>2+</sup> .2[PF <sub>6</sub> ] <sup>-</sup>	m	im	im	im	m	im	im	im
[Dmae] <sup>2+</sup> .2[PF <sub>6</sub> ] <sup>-</sup>	m	im	im	im	m	im	im	im
[Deae] <sup>2+</sup> .2[PF <sub>6</sub> ] <sup>-</sup>	m	im	im	im	m	im	im	im

m - miscible, im - immiscible

#### 4.14 : Application : Self-Assembly Chemistry of [Tea]<sup>2+</sup>.2[Br] with *p*-Sulfonatocalix[4]arene

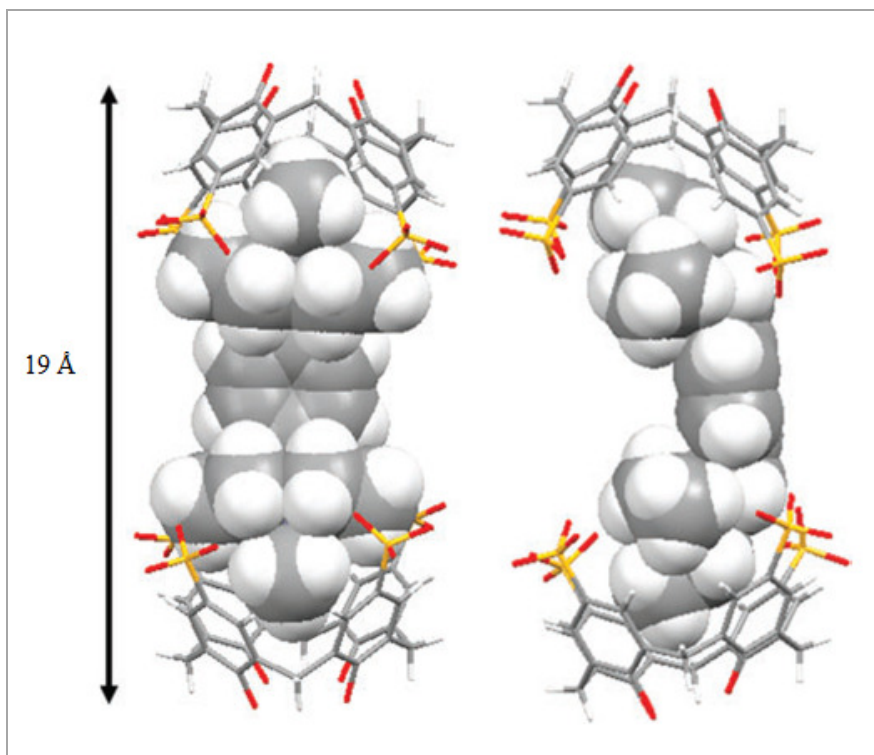
Several attempts had been made on the synthesized dicationic ionic liquids for molecular self-assembly application. Only [Tea]<sup>2+</sup>.2[Br] was successful in forming complex with *p*-sulfonatocalix[4]arene.



**Figure 4.103 :** The components and ‘molecular capsule’ arrangement in complex 1 and 2.

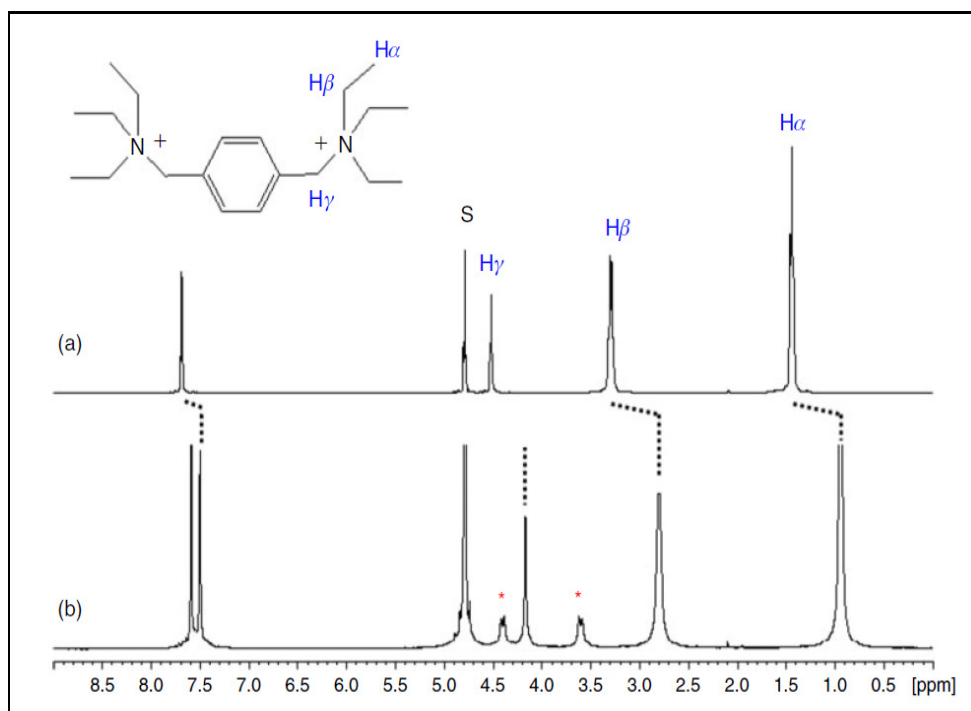
In this study, the utility of the *N,N'*-[1,4-phenylenebis(methylene)]bis-(*N,N*-diethylethanaminium) ([Tea]) cation as a versatile building component in forming multicomponent materials with water-soluble *p*-sulfonatocalix[4]arene, and the mono-phosphonium cation has been established. Complex 1 and 2 consist of a [Tea] cation being capped at both end with two molecules of calix[4]arene anions (taking on a -4 charge and -5 charge for complex 1 and 2 respectively)

forming ‘molecular capsules’. Both complexes were  $\sim 19$  Å in length with the central aromatic ring of the cation aligned close to the principal axes of the calixarenes (Figure 4.104). The size of the [Tea] cation was comparable to the previously reported structure based on the bis-imidazolium cations having either a methyl or butyl terminus,<sup>79-81</sup> whereby the termini of the [Tea] cation embedded in a cavity of a calixarene. The capsules themselves are arranged in a scaffold network in the presence of mono-phosphonium cations.<sup>82</sup>



**Figure 4.104:** Front and side view of the [Tea] cation (space filling) shrouded at the termini by two *p*-sulfonatocalix[4]arenes.





**Figure 4.105** :  $^1\text{H}$  NMR spectra for (a) [Tea], and (b) [Tea] in *p*-sulfonatocalix[4]arene (1:2), measured in  $\text{D}_2\text{O}$ .

The formation of the molecular capsule of calixarene and [Tea] cation was validated by performing  $^1\text{H}$  NMR experiment in  $\text{D}_2\text{O}$  at  $25^\circ\text{C}$  whereby two groups of triethylamine terminus were accommodating in the cavity of the calixarene. The experiment provides information on how the [Tea] cations interact with calixarenes. Based on the data from **figure 4.105**, the aliphatic protons  $\text{H}_\alpha$  and  $\text{H}_\beta$  experienced a slight shifting ( $\sim 0.7$  ppm) towards upper field which was caused by the shielding of triethylamine terminus in the calixarene cavity. Meanwhile, the methylene bridge protons  $\text{H}_\gamma$  and the benzene ring protons experienced the slightest shifting ( $\sim 0.2$ - $0.5$  ppm) towards upfield region. Furthermore, noted the appearance of signals at 3.0 to 4.5 ppm (asterisks) which were due to the methylene protons of [Tea] cation, proves that the calixarenes adapt the conical conformation.

## CHAPTER 5

### Conclusion

In conclusion, phenylene-based dicationic ionic liquids were successfully synthesized by implementing the conventional method of synthesis namely alkylation and anion exchange reactions producing 24 kinds of dicationic ionic liquids consisting bromide, bis(trifluoromethanesulfonyl)imide (NTf<sub>2</sub>) and hexafluorophosphate (PF<sub>6</sub>) moieties. The purification of these new dicationic ionic liquids was accomplished via recrystallization techniques. The characterizations of dicationic ionic liquids were carried out through spectroscopic techniques such as NMR and FT-IR spectroscopy as well as single crystal X-ray diffraction techniques. The physical properties of these dicationic ionic liquids such as thermal properties, halides content and solubility behavior were investigated, reported and discussed. Thermal stability of the synthesized ionic liquids varies depending on the type of counter-anions. Bis(trifluoromethanesulfonyl)imide moieties were the most thermally stable decomposing at temperature range of 300-380°C, followed by hexafluorophosphate moieties and bromide moieties. Furthermore, NTf<sub>2</sub> moieties have the lowest melting temperature compared with other moieties. Some of them melted at temperature below 100°C, in agreement with the ionic liquids' definition. Upon recrystallization, nine compounds were suitable for single crystal X-ray diffraction studies, the molecular structures of these dicationic ionic liquids were authenticated with the proposed structures. On the other hand, chromatographic analysis proved that, the purity level of NTf<sub>2</sub> moieties and PF<sub>6</sub> moieties are above 99%. In addition, the water content was extremely low for NTf<sub>2</sub> and PF<sub>6</sub> moieties while 2% of water was detected in [Mmorp]<sup>2+</sup>.2[Br]<sup>-</sup>. Besides, the synthesis of dicationic ionic liquids was successful

in producing highly pure ionic liquids with an excellent yield above 85% each. Finally, the utility of [Tea] cation was established as a versatile building component in end-capped ‘molecular capsules’ *i.e.* water-soluble *p*-sulfonatocalix[4]arene and in the presence of mono-phosphonium cations.

#### **Further works on the application of the synthesized dicationic ionic liquids:**

Throughout this research, the characterization of synthesized dicationic ionic liquids was accomplished by performing elemental and spectroscopic analyses as well as thermal experiments. Therefore, it will be more meaningful and beneficial to investigate the electrochemical profile of dicationic ionic liquids by carrying out the cyclic-voltammetry experiment. This technique will provide the information on electrochemical window which can be related to the purity and electrochemical stability of the synthesized dicationic ionic liquids towards oxidative and reductive decompositions. In addition, the electrochemical window is a crucial design criterion for electrochemical applications.

## REFERENCES

- 1 Peter Wasserscheid and Thomas Welton, *Ionic Liquids in Synthesis / Edited by P. Wasserscheid and T. Welton.* ed. by Peter Wasserscheid and Thomas Welton. 2nd edn, *Ionic Liquids in Synthesis* (Weinheim: Wiley-VCH, 2008), p. 721.
- 2 Maciej Galiński, Andrzej Lewandowski, and Izabela Stępnia, 'Ionic Liquids as Electrolytes', *Electrochimica Acta*, 51 (2006), 5567-5580.
- 3 Anja-Verena Mudring, Arash Babai, Sven Arenz, Ralf Giernoth, K. Binnemans, Kris Driesen, and Peter Nockemann, 'Strong Luminescence of Rare Earth Compounds in Ionic Liquids: Luminescent Properties of Lanthanide(III) Iodides in the Ionic Liquid 1-Dodecyl-3-Methylimidazolium Bis(Trifluoromethanesulfonyl)Imide', *Journal of Alloys and Compounds*, 418 (2006), 204-208
- 4 Dana Bejan, Nikolai Ignat'ev, and Helge Willner, 'New Ionic Liquids with the Bis[Bis(Pentafluoroethyl)Phosphinyl]Imide Anion, [(C<sub>2</sub>F<sub>5</sub>)<sub>2</sub>P(O)]<sub>2</sub>N–Synthesis and Characterization', *Journal of Fluorine Chemistry*, 131 (2010), 325-332.
- 5 N. V. Ignat'ev, U. Welz-Biermann, A. Kucheryna, G. Bissky, and H. Willner, 'New Ionic Liquids with Tris(Perfluoroalkyl)Trifluorophosphate (FAP) Anions', *Journal of Fluorine Chemistry*, 126 (2005), 1150-1159.
- 6 Jui-Cheng Chang, Wen-Yueh Ho, I. Wen Sun, Yung-Liang Tung, Meng-Chin Tsui, Tzi-Yi Wu, and Shih-Shin Liang, 'Synthesis and Characterization of Dicationic Ionic Liquids That Contain Both Hydrophilic and Hydrophobic Anions', *Tetrahedron*, 66 (2010), 6150-6155.
- 7 Hao Geng, Ling-hua Zhuang, Jian Zhang, Guo-wei Wang, and Ai-lin Yuan, '3,3'-Dimethyl-1,1'-(Butane-1,4-Diyl)Diimidazolium Bis(Tetrafluoroborate)', *Acta Crystallographica Section E*, 66 (2010), o1267.
- 8 Xinxin Han, and Daniel W. Armstrong, 'Using Geminal Dicationic Ionic Liquids as Solvents for High-Temperature Organic Reactions', *Organic Letters*, 7 (2005), 4205-4208.
- 9 Hui Sun, Juan Li, Xiao Chen Cai, Dong Jiang, and Li Yi Dai, 'Ionic Liquids as Efficient Phase-Transfer Catalysts for the Solid Base-Promoted Monoalkylation of Diethyl Malonate', *Chinese Chemical Letters*, 18 (2007), 279-282.
- 10 Yun Sheng Ding, Min Zha, Jun Zhang, and Seng Shan Wang, 'Synthesis of a Kind of Geminal Imidazolium Ionic Liquid with Long Aliphatic Chains', *Chinese Chemical Letters*, 18 (2007), 48-50.
- 11 Zhengxi Zhang, Li Yang, Shichun Luo, Miao Tian, Kazuhiro Tachibana, and Kouichi Kamijima, 'Ionic Liquids Based on Aliphatic

- Tetraalkylammonium Dications and Tfsi Anion as Potential Electrolytes', *Journal of Power Sources*, 167 (2007), 217-222.
- 12 ZhengXi Zhang, HongYan Zhou, Li Yang, Kazuhiro Tachibana, Kouichi Kamijima, and Jian Xu, 'Asymmetrical Dicationic Ionic Liquids Based on Both Imidazolium and Aliphatic Ammonium as Potential Electrolyte Additives Applied to Lithium Secondary Batteries', *Electrochimica Acta*, 53 (2008), 4833-4838.
  - 13 Zhuo Zeng, Benjamin S. Phillips, Ji-Chang Xiao, and Jean'ne M. Shreeve, 'Polyfluoroalkyl, Polyethylene Glycol, 1,4-Bismethylenebenzene, or 1,4-Bismethylene-2,3,5,6-Tetrafluorobenzene Bridged Functionalized Dicationic Ionic Liquids : Synthesis and Properties as High Temperature Lubricants', 20 (2008), 8.
  - 14 Jared L. Anderson, and Daniel W. Armstrong, 'High-Stability Ionic Liquids. A New Class of Stationary Phases for Gas Chromatography', *Analytical Chemistry*, 75 (2003), 4851-4858.
  - 15 Yun-Sheng Ding, Min Zha, Jun Zhang, and Seng-Shan Wang, 'Synthesis, Characterization and Properties of Geminal Imidazolium Ionic Liquids', *Colloids and Surfaces A: Physicochemical and Engineering Aspects*, 298 (2007), 201-205.
  - 16 Sengodagounder Muthusamy, and Boopathy Gnanaprakasam, 'Imidazolium Salts as Phase Transfer Catalysts for the Dialkylation and Cycloalkylation of Active Methylene Compounds', *Tetrahedron Letters*, 46 (2005), 635-638.
  - 17 Peter Wasserscheid and Thomas Welton, *Ionic Liquids in Synthesis / Edited by P. Wasserscheid and T. Welton.* ed. by Peter Wasserscheid and Thomas Welton. 2<sup>nd</sup> edition, *Ionic Liquids in Synthesis* (Weinheim: Wiley-VCH, 2008), p. 721.
  - 18 A. Fernicola, B. Scrosati, and H. Ohno, 'Potentialities of Ionic Liquids as New Electrolyte Media in Advanced Electrochemical Devices', *Ionics*, 12 (2006), 95-102.
  - 19 Xinxin Han and Daniel W. Armstrong, 'Using Geminal Dicationic Ionic Liquids as Solvents for High-Temperature Organic Reactions', *Organic Letters*, 7 (2005), 4205-4208.
  - 20 Amutha Chinnappan, and Hern Kim, 'Environmentally Benign Catalyst: Synthesis, Characterization, and Properties of Pyridinium Dicationic Molten Salts (Ionic Liquids) and Use of Application in Esterification', *Chemical Engineering Journal*.
  - 21 Jairton Dupont, Roberto F. de Souza, and Paulo A. Z. Suarez, 'Ionic Liquid (Molten Salt) Phase Organometallic Catalysis', *Chemical Reviews*, 102 (2002), 3667-3692.

- 22 Neeraj Gupta, Goverdhan L. Kad, and Jasvinder Singh, 'Enhancing Nucleophilicity in Ionic Liquid [Bmim]HSO<sub>4</sub>: A Recyclable Media and Catalyst for the Halogenation of Alcohols', *Journal of Molecular Catalysis A: Chemical*, 302 (2009), 11-14.
- 23 P. Wasserscheid, and W. Keim, 'Ionic Liquids-New "Solutions" for Transition Metal Catalysis', *Angewandte Chemie (International ed. in English)*, 39 (2000), 3772-3789.
- 24 Jun Young Kim, Tae Ho Kim, Dong Young Kim, Nam-Gyu Park, and Kwang-Duk Ahn, 'Novel Thixotropic Gel Electrolytes Based on Dicationic Bis-Imidazolium Salts for Quasi-Solid-State Dye-Sensitized Solar Cells', *Journal of Power Sources*, 175 (2008), 692-697.
- 25 Zhengjian Chen, Shimin Liu, Zuopeng Li, Qinghua Zhang, and Youquan Deng, 'Dialkoxy Functionalized Quaternary Ammonium Ionic Liquids as Potential Electrolytes and Cellulose Solvents', *New Journal of Chemistry*, 35 (2011).
- 26 Maw-Ling Wang, Ze-Fa Lee, and Feng-Sheng Wang, 'Synthesis of Novel Multi-Site Phase-Transfer Catalyst and Its Application in the Reaction of 4,4'-Bis(Chloromethyl)-1,1'-Biphenyl with 1-Butanol', *Journal of Molecular Catalysis A: Chemical*, 229 (2005), 259-269.
- 27 Jason E. Bara, Evan S. Hatakeyama, Christopher J. Gabriel, Xiaohui Zeng, Sonja Lessmann, Douglas L. Gin, and Richard D. Noble, 'Synthesis and Light Gas Separations in Cross-Linked Gemini Room Temperature Ionic Liquid Polymer Membranes', *Journal of Membrane Science*, 316 (2008), 186-191.
- 28 John D. Holbrey, Ann E. Visser, Scott K. Spear, W. Matthew Reichert, Richard P. Swatloski, Grant A. Broker, and Robin D. Rogers, 'Mercury(II) Partitioning from Aqueous Solutions with a New, Hydrophobic Ethylene-Glycol Functionalized Bis-Imidazolium Ionic Liquid', *Green Chemistry*, 5 (2003).
- 29 Xueqin Li, Ruili Guo, Xiaopeng Zhang, and Xiaoyue Li, 'Extraction of Glabridin Using Imidazolium-Based Ionic Liquids', *Separation and Purification Technology*, 88 (2012), 146-150.
- 30 C. Yao, W. R. Pitner, and J. L. Anderson, 'Ionic Liquids Containing the Tris(Pentafluoroethyl)Trifluorophosphate Anion: A New Class of Highly Selective and Ultra Hydrophobic Solvents for the Extraction of Polycyclic Aromatic Hydrocarbons Using Single Drop Microextraction', *Anal. Chem.*, 81 (2009), 5054-5063.
- 31 Peter Nockemann, Koen Binnemans, and Kris Driesen, 'Purification of Imidazolium Ionic Liquids for Spectroscopic Applications', *Chemical Physics Letters*, 415 (2005), 131-136.

- 32 Pierre Bonhôte, Ana-Paula Dias, Nicholas Papageorgiou, Kuppaswamy Kalyanasundaram, and Michael Grätzel, 'Hydrophobic, Highly Conductive Ambient-Temperature Molten Salts†', *Inorganic Chemistry*, 35 (1996), 1168-1178.
- 33 Richard P. Swatloski, John D. Holbrey, and Robin D. Rogers, 'Ionic Liquids Are Not Always Green: Hydrolysis of 1-Butyl-3-Methylimidazolium Hexafluorophosphate', *Green Chemistry*, 5 (2003), 361-363.
- 34 K.R. Seddon, A. Stark, and M.J. Torres, 'Influence of Chloride, Water, and Organic Solvents on the Physical Properties of Ionic Liquids', *Pure Appl. Chem*, 72 (2000), 2275--2287.
- 35 Zhi-Bin Zhou, Masayuki Takeda, and Makoto Ue, 'New Hydrophobic Ionic Liquids Based on Perfluoroalkyltrifluoroborate Anions', *Journal of Fluorine Chemistry*, 125 (2004), 471-476.
- 36 Zuopeng Li, Zhengyin Du, Yanlong Gu, Laiying Zhu, Xiaoping Zhang, and Youquan Deng, 'Environmentally Friendly and Effective Removal of Br<sup>-</sup> and Cl<sup>-</sup> Impurities in Hydrophilic Ionic Liquids by Electrolysis and Reaction', *Electrochemistry Communications*, 8 (2006), 1270-1274.
- 37 Sun-Hwa Yeon, Ki-Sub Kim, Sukjeong Choi, Huen Lee, Hoon Sik Kim, and Honggon Kim, 'Physical and Electrochemical Properties of 1-(2-Hydroxyethyl)-3-Methyl Imidazolium and N-(2-Hydroxyethyl)-N-Methyl Morpholinium Ionic Liquids', *Electrochimica Acta*, 50 (2005), 5399-5407.
- 38 Kenta Fukumoto, Masahiro Yoshizawa, and Hiroyuki Ohno, 'Room Temperature Ionic Liquids from 20 Natural Amino Acids', *Journal of the American Chemical Society*, 127 (2005), 2398-2399.
- 39 S. Himmler, A. König, and P. Wasserscheid, 'Synthesis of [Emim]OH Via Bipolar Membrane Electrodialysis - Precursor Production for the Combinatorial Synthesis of [Emim]-Based Ionic Liquids', *Green Chemistry*, 9 (2007), 935-942.
- 40 Hong Yu, You-Ting Wu, Ying-Ying Jiang, Zheng Zhou, and Zhi-Bing Zhang, 'Low Viscosity Amino Acid Ionic Liquids with Asymmetric Tetraalkylammonium Cations for Fast Absorption of Co<sub>2</sub>', *New Journal of Chemistry*, 33 (2009).
- 41 Huanrong Li, Dan Li, Yige Wang, and Qiaorong Ru, 'A Series of Carboxylic-Functionalized Ionic Liquids and Their Solubility for Lanthanide Oxides', *Chemistry – An Asian Journal*, 6 (2011), 1443-1449.
- 42 Peter Nockemann, Ben Thijs, Tatjana N. Parac-Vogt, Kristof Van Hecke, Luc Van Meervelt, Bernard Tinant, Ingo Hartenbach, Thomas Schleid, Vu Thi Ngan, Minh Tho Nguyen, and Koen Binnemans, 'Carboxyl-Functionalized Task-Specific Ionic Liquids for Solubilizing Metal Oxides', *Inorganic Chemistry*, 47 (2008), 9987-9999.

- 43 Jafar Akbari, Akbar Heydari, Hamid Reza Kalhor, and Sirus Azizian Kohan, 'Sulfonic Acid Functionalized Ionic Liquid in Combinatorial Approach, a Recyclable and Water Tolerant-Acidic Catalyst for One-Pot Friedlander Quinoline Synthesis', *Journal of Combinatorial Chemistry*, 12 (2009), 137-140.
- 44 Luís C. Branco, João N. Rosa, Joaquim J. Moura Ramos, and Carlos A. M. Afonso, 'Preparation and Characterization of New Room Temperature Ionic Liquids', *Chemistry – A European Journal*, 8 (2002), 3671-3677.
- 45 Josh Y. Z. Chiou, J. N. Chen, J. S. Lei, and Ivan J. B. Lin, 'Ionic Liquid Crystals of Imidazolium Salts with a Pendant Hydroxyl Group', *Journal of Materials Chemistry*, 16 (2006).
- 46 Amal I. Siriwardana, Angel A. J. Torriero, Juan M. Reyna-González, Iko M. Burgar, Noel F. Dunlop, Alan M. Bond, Glen B. Deacon, and Douglas R. MacFarlane, 'Nitrile Functionalized Methimazole-Based Ionic Liquids', *The Journal of Organic Chemistry*, 75 (2010), 8376-8382.
- 47 Guozhen Fang, Jia Zhang, Jinping Lu, Ligai Ma, and Shuo Wang, 'Preparation, Characterization, and Application of a New Thiol-Functionalized Ionic Liquid for Highly Selective Extraction of Cd(II)', *Microchimica Acta*, 171 (2010), 305-311.
- 48 Kilivelu Ganesan, Yatimah Alias, and Seik Weng Ng, 'Imidazolium-Based Ionic Liquid Salts: 3,3'-Dimethyl-1,1'-(1,4-Phenylenedimethylene)Diimidazolium Bis(Tetrafluoroborate) and 3,3'-Di-N-Butyl-1,1'-(1,4-Phenylenedimethylene)Diimidazolium Bis(Trifluoromethanesulfonate)', *Acta Crystallographica Section C*, 64 (2008), o478-o80.
- 49 Hao Geng, Ling-hua Zhuang, Jian Zhang, Guo-wei Wang, and Ai-lin Yuan, '3,3'-Dimethyl-1,1'-(Butane-1,4-Diyl)Diimidazolium Bis(Tetrafluoroborate)', *Acta Crystallographica Section E*, 66 (2010), o1267.
- 50 Zhuo Zeng, Benjamin S. Phillips, Ji-Chang Xiao, and Jean'ne M. Shreeve, 'Polyfluoroalkyl, Polyethylene Glycol, 1,4-Bismethylenebenzene, or 1,4-Bismethylene-2,3,5,6-Tetrafluorobenzene Bridged Functionalized Dicationic Ionic Liquids : Synthesis and Properties as High Temperature Lubricants', 20 (2008), 8.
- 51 Jared L. Anderson, Rongfang Ding, Arkady Ellern, and Daniel W. Armstrong, 'Structure and Properties of High Stability Geminal Dicationic Ionic Liquids', *Journal of the American Chemical Society*, 127 (2004), 593-604.
- 52 Jingyi An, Laurence Bagnell, Teresa Cablewski, Christopher R. Strauss, and Robert W. Trainor, 'Applications of High-Temperature Aqueous Media for Synthetic Organic Reactions', *The Journal of Organic Chemistry*, 62 (1997), 2505-2511.



- 53 Wikipedia contributors, 'Surfactant', *Wikipedia, The Free Encyclopedia*, 25 January 2012, 18:26 UTC, <<http://en.wikipedia.org/w/index.php?title=Surfactant&oldid=473195506>> [accessed 9 February 2012].
- 54 Yun-Sheng Ding, Min Zha, Jun Zhang, and Seng-Shan Wang, 'Synthesis, Characterization and Properties of Geminal Imidazolium Ionic Liquids', *Colloids and Surfaces A: Physicochemical and Engineering Aspects*, 298 (2007), 201-205.
- 55 Fredric M. Menger, and Jason S. Keiper, 'Gemini Surfactants', *Angewandte Chemie International Edition*, 39 (2000), 1906-1920.
- 56 Verónica Pino, Quinner Q. Baltazar, and Jared L. Anderson, 'Examination of Analyte Partitioning to Monocationic and Dicationic Imidazolium-Based Ionic Liquid Aggregates Using Solid-Phase Microextraction–Gas Chromatography', *Journal of Chromatography A*, 1148 (2007), 92-99.
- 57 Quinner Q. Baltazar, Janaki Chandawalla, Keahna Sawyer, and Jared L. Anderson, 'Interfacial and Micellar Properties of Imidazolium-Based Monocationic and Dicationic Ionic Liquids', *Colloids and Surfaces A: Physicochemical and Engineering Aspects*, 302 (2007), 150-156.
- 58 Chuan-Ming Jin, Chengfeng Ye, Benjamin S. Phillips, Jeffery S. Zabinski, Xuqing Liu, Weimin Liu, and Jean'ne M. Shreeve, 'Polyethylene Glycol Functionalized Dicationic Ionic Liquids with Alkyl or Polyfluoroalkyl Substituents as High Temperature Lubricants', *Journal of Materials Chemistry*, 16 (2006).
- 59 Meihuan Yao, Yongmin Liang, Yanqiu Xia, and Feng Zhou, 'Bisimidazolium Ionic Liquids as the High-Performance Antiwear Additives in Poly(Ethylene Glycol) for Steel–Steel Contacts', *ACS Applied Materials & Interfaces*, 1 (2009), 467-471.
- 60 B. S. Phillips, G. John, and J. S. Zabinski, 'Surface Chemistry of Fluorine Containing Ionic Liquids on Steel Substrates at Elevated Temperature Using Mössbauer Spectroscopy', *Tribology Letters*, 26 (2007), 85-91.
- 61 Qing-Xiang Liu, Jie Yu, Xiao-Jun Zhao, Shu-Weng Liu, Xiao-Qiong Yang, Kang-Ying Li, and Xiu-Guang Wang, 'Mercury(II), Copper(II) and Silver(I) Complexes with Ether or Diether Functionalized Bis-Nhc Ligands: Synthesis and Structural Studies', *CrystEngComm*, 13 (2011).
- 62 Jared L. Anderson, and Daniel W. Armstrong, 'High-Stability Ionic Liquids. A New Class of Stationary Phases for Gas Chromatography', *Analytical Chemistry*, 75 (2003), 4851-4858.
- 63 Tharanga Payagala, Junmin Huang, Zachary S. Breitbach, Pritesh S. Sharma, and Daniel W. Armstrong, 'Unsymmetrical Dicationic Ionic Liquids: Manipulation of Physicochemical Properties Using Specific Structural Architectures', *Chemistry of Materials*, 19 (2007), 5848-5850.

- 64 Tharanga Payagala, Ying Zhang, Eranda Wanigasekara, Ke Huang, Zachary S. Breitbach, Pritesh S. Sharma, Leonard M. Sidisky, and Daniel W. Armstrong, 'Trigonal Tricationic Ionic Liquids: A Generation of Gas Chromatographic Stationary Phases', *Analytical Chemistry*, 81 (2008), 160-173.
- 65 Xinxin Han, and Daniel W. Armstrong, 'Ionic Liquids in Separations', *Accounts of Chemical Research*, 40 (2007), 1079-1086.
- 66 Arvind H. Jadhav, and Hern Kim, 'Efficient Selective Dehydration of Fructose and Sucrose into 5-Hydroxymethylfurfural (HMF) Using Dicationic Room Temperature Ionic Liquids as a Catalyst', *Catalysis Communications*.
- 67 Quan Cao, Xingcui Guo, Shengxi Yao, Jing Guan, Xiaoyan Wang, Xindong Mu, and Dongke Zhang, 'Conversion of Hexose into 5-Hydroxymethylfurfural in Imidazolium Ionic Liquids with and without a Catalyst', *Carbohydrate Research*, 346 (2011), 956-959.
- 68 Brian O'Regan, and Michael Gratzel, 'A Low-Cost, High-Efficiency Solar Cell Based on Dye-Sensitized Colloidal Tio<sub>2</sub> Films', *Nature*, 353 (1991), 737-740.
- 69 Wikipedia contributors, 'Dye-sensitized solar cell', *Wikipedia, The Free Encyclopedia*, 27 January 2012, 22:55 UTC, <[http://en.wikipedia.org/w/index.php?title=Dye-sensitized\\_solar\\_cell&oldid=473593318](http://en.wikipedia.org/w/index.php?title=Dye-sensitized_solar_cell&oldid=473593318)> [accessed 15 February 2012].
- 70 Peng Wang, Shaik M. Zakeeruddin, Jacques- E. Moser, and Michael Grätzel, 'A New Ionic Liquid Electrolyte Enhances the Conversion Efficiency of Dye-Sensitized Solar Cells', *The Journal of Physical Chemistry B*, 107 (2003), 13280-13285.
- 71 Mir Wais Hosseini, 'Self-Assembly and Generation of Complexity', *Chemical Communications* (2005), 5825-5829.
- 72 C. D. Gutsche, 'Chapter 1 from Resinous Tar to Molecular Baskets', in *Calixarenes: An Introduction*, The Royal Society of Chemistry, (2008), 1-26.
- 73 Irene Ling, Yatimah Alias, Alexandre N. Sobolev, and Colin L. Raston, 'Multi-Component Bi-Layers Featuring [1-Octyl-2,3-Dimethylimidazolium [Intersection] P-Sulfonatocalix[4]Arene] Supermolecules', *New Journal of Chemistry*, 34 (2010), 414-419.
- 74 Irene Ling, Yatimah Alias, Alexandre N. Sobolev, and Colin L. Raston, 'Constructing Multicomponent Materials Containing Cavitands, and Phosphonium and Imidazolium Cations', *Crystal Growth & Design*, 9 (2009), 4497-4503.

- 75 Irene Ling, Yatimah Alias, and Colin L. Raston, 'Structural Diversity of Multi-Component Self-Assembled Systems Incorporating P-Sulfonatocalix[4]Arene', *New Journal of Chemistry*, 34 (2010), 1802-1811.
- 76 Irene Ling, Yatimah Alias, Alexandre N. Sobolev, Lindsay T. Byrne, and Colin L. Raston, 'Supramolecular Architecture Containing End-Capping Bis-Imidazolium Cations', *CrystEngComm*, 13 (2011), 787-793.
- 77 Irene Ling, Yatimah Alias, Alexandre N. Sobolev, and Colin L. Raston, 'Calixarene C8-Imidazolium Interplay as a Design Strategy for Penetrating Organic Bi-Layers', *CrystEngComm*, 12 (2010), 573-578.
- 78 Irene Ling, Yatimah Alias, Alexandre N. Sobolev, and Colin L. Raston, 'Constructing Multicomponent Materials Containing Cavitands, and Phosphonium and Imidazolium Cations', *Crystal Growth & Design*, 9 (2009), 4497-4503.
- 79 Irene Ling, Yatimah Alias, Munirah Sufiyah Abdul Rahim, Brian W. Skelton, Lindsay T. Byrne, and Colin L. Raston, 'Axially Aligned Confinement of 1,4-Bis(Triethylammoniomethyl)Benzene by Two P-Sulfonatocalix[4]Arenes', *Australian Journal of Chemistry* (2012).

## LIST OF PUBLICATIONS :

- 1      Munirah Sufiyah Abdul Rahim, Yatimah Alias, and Seik Weng Ng, '1,1'-(p-Phenylenedimethylene)dipyridinium bis(hexafluoridophosphate)', *Acta Crystallographica Section E*, 66 (2010), o2653.
- 2      Munirah Sufiyah Abdul Rahim, Yatimah Alias and Seik Weng Ng, '1,1',2,2'-Tetramethyl-3,3'-(p-phenylenedimethylene)diimidazolium bis[bis(trifluoromethylsulfonyl)imide]', *Acta Crystallographica Section E*, 66 (2010), o2668.
- 3      Munirah Sufiyah Abdul Rahim, Hamid Khaledi, Yatimah Alias, and Urs Welz-Biermann, 'N,N'-[1,4-Phenylenebis(methylene)]bis(N,N-diethylethanaminium) dibromide', *Acta Crystallographica Section E*, 68 (2012), o369.
- 4      Irene Ling, Yatimah Alias, Munirah Sufiyah Abdul Rahim, Brian W. Skelton, Lindsay T. Byrne, and Colin L. Raston, 'Axially Aligned Confinement of 1,4-Bis(Triethylammoniomethyl)Benzene by Two P-Sulfonatocalix[4]Arenes', *Australian Journal of Chemistry* (2012).

## CONFERENCES AND PROCEEDINGS.

1. Abd Rahim, Munirah Sufiyah, Subramaniam, Puvaneswary, Alias, Yatimah, and Welz-Bermann, Urs. *Purification methods of bis-imidazolium ionic liquids. 2<sup>nd</sup> Asian Pacific Conference on Ionic Liquids and Green Processes (APCIL-2)*. September 7-10<sup>th</sup>, 2010, Dalian, China.
2. Abd Rahim, Munirah Sufiyah, Abdul Halim, Siti Nadiah, Yatimah, and Welz-Bermann, Urs. *Synthesis and characterization of bistriflamide ionic liquids. 7<sup>th</sup> Mathematic and Physical Sciences Graduate Congress (7<sup>th</sup> MPSGC)*. December 12-14<sup>th</sup>, 2011, National University of Singapore (NUS), Singapore.

# Appendices

- IR spectra of the synthesized dicationic ionic liquids.
- Publications